

University of Southampton Research Repository ePrints Soton

Copyright © and Moral Rights for this thesis are retained by the author and/or other copyright owners. A copy can be downloaded for personal non-commercial research or study, without prior permission or charge. This thesis cannot be reproduced or quoted extensively from without first obtaining permission in writing from the copyright holder/s. The content must not be changed in any way or sold commercially in any format or medium without the formal permission of the copyright holders.

When referring to this work, full bibliographic details including the author, title, awarding institution and date of the thesis must be given e.g.

AUTHOR (year of submission) "Full thesis title", University of Southampton, name of the University School or Department, PhD Thesis, pagination

UNIVERSITY OF SOUTHAMPTON

FACULTY OF MEDICINE, HEALTH AND LIFE SCIENCES

School of Medicine

**INVESTIGATION OF CD20-DIRECTED
IMMUNOTHERAPY IN B-CELL MALIGNANCIES**

Sean Hua Lim MBChB MRCP

**Thesis for the degree of Doctor of Philosophy
October 2011**

UNIVERSITY OF SOUTHAMPTON
ABSTRACT

FACULTY OF MEDICINE, HEALTH AND LIFE SCIENCES
School of Medicine

Doctor of Philosophy

Investigation of CD20-directed immunotherapy in B-cell malignancies

Sean Hua Lim

Monoclonal antibodies (mAb) are now invaluable in anti-cancer therapy, and the targeting of CD20 by rituximab in B-cell malignancies is a good example of this. However not all CD20⁺ B-cell malignancies are responsive and the reasons for resistance are unclear. Using primary tumour material and in vitro flow cytometry-based assays, this project examines the internalisation of rituximab from the surface of target B cells as a likely explanation for mAb resistance. Anti-CD20 mAb can be characterised as type I (rituximab, ofatumumab) or type II (tositumomab (mIgG2a), GA101) based on different effects in vitro assays. Here, the results show that type I mAb were internalised from the surface of B cells, unlike type II mAb which showed far less internalisation. However, the internalisation of type I mAb was variable, even within the same subtypes of B cells. Further investigations showed that FcγRIIb expression levels on target B cells correlated strongly with the rate of internalisation of rituximab regardless of the disease subtype. Rituximab was observed to co-ligate CD20 and FcγRIIb on the same cell. Furthermore, FcγRIIb was activated in the process, and the resultant rituximab:CD20:FcγRIIb complexes were seen to co-localise into endosomes/lysosomes. These in vitro findings are supported by clinical data demonstrating that FcγRIIb expression was able to predict responses to rituximab-containing regimens in a small cohort of patients with mantle cell lymphoma. In summary, these investigations provide a plausible explanation for cases of rituximab resistance and indicate that responses can be augmented by bypassing this mechanism of resistance.

Table of Contents

Table of Contents	3
Index of Figures	7
Index of Tables	9
Declaration of Authorship	10
Acknowledgements	12
Abbreviations	13
<u>1 Introduction</u>	<u>16</u>
1.1 Cancer immunotherapy	16
1.2 mAb therapy	20
1.2.1 Current mAb in clinical trials	24
1.3 B-cell malignancies and their association to normal development	28
1.3.1 B-cell development	29
1.3.2 B-cell lymphomas	40
1.3.3 Chronic lymphocytic leukaemia	42
1.4 Anti-CD20 mAb	49
1.4.1 Clinical applications of anti-CD20 mAb	49
1.4.2 The CD20 antigen	50
1.5 Effects of anti-CD20 mAb	52
1.5.1 Ab-dependent cellular cytotoxicity (ADCC)	55
1.5.2 Complement-dependent cytotoxicity	63
1.5.3 Direct cell death induction	68
1.5.4 Induction of T-cell mediated immunity	71
1.6 Mechanisms of resistance to anti-CD20 therapy	73

2	Project Outline	78
3	Materials and Methods	79
3.1	Cell lines	79
3.2	Healthy human B cells and monocytes	79
3.2.1	Peripheral blood mononuclear cell isolation	79
3.2.2	B cell isolation	80
3.2.3	Monocyte isolation	81
3.3	Clinical samples	81
3.4	Cell quantitation	82
3.5	Characterisation of prognostic markers in CLL samples	82
3.6	RT-PCR	83
3.6.1	RNA extraction	84
3.6.2	cDNA synthesis	84
3.6.3	PCR and visualisation by agarose gel electrophoresis	84
3.7	Ab and reagents	85
3.8	Labelling of mAb with fluorochromes	89
3.9	Flow cytometry	90
3.10	Viability assay	91
3.11	Quenching assay	91
3.12	Phagocytosis assay	93
3.13	PKH26 cell labelling	94
3.14	CDC assay	95
3.15	Western blotting	95
3.16	Light microscopy	97
3.17	Confocal microscopy	97
3.18	May-Grünwald-Giemsa (MGG) staining	99
3.19	Immunohistochemistry (IHC) and collection of clinical data	99
3.20	Statistical analysis	100

4	<u>Internalisation of anti-CD20 mAb in different B cell-types</u>	101
4.1	Introduction	101
4.2	Results	102
4.2.1	Internalisation of anti-CD20 mAb in human lymphoma cell lines	102
4.2.2	Internalisation of anti-CD20 mAb in normal human B cells	105
4.2.3	Validation of the quenching assay	109
4.2.4	Internalisation of anti-CD20 mAb in primary neoplastic B cells	111
4.2.5	Potential modulators of internalisation of rituximab	114
4.3	Discussion	121
5	<u>The role of FcγRIIb in the internalisation of anti-CD20 mAb</u>	126
5.1	Introduction	126
5.2	Results	127
5.2.1	The influence of the Fc domain on the internalisation of rituximab	127
5.2.2	Characterisation of FcγR expression on B cells	127
5.2.3	The influence of target cell FcγRIIb expression on the internalisation of rituximab	132
5.2.4	The binding orientation of rituximab to FcγRIIb	137
5.2.5	Activation of FcγRIIb by anti-CD20	141
5.2.6	Intracellular trafficking of anti-CD20:CD20:FcγRIIb complexes	143
5.2.7	The effect of internalisation of anti-CD20 on engagement of immune effector cells	147
5.3	Discussion	150
6	<u>Validation of FcγRIIb as a prognostic marker in patients</u>	155
6.1	Introduction	155
6.2	Results	156
6.2.1	FcγRIIb expression of B-NHL by immunohistochemistry (IHC)	156

6.2.2	Treatment outcomes of B-NHL patients according to FcγRIIb expression	158
6.2.3	The correlation between FcγRIIb expression by IHC and flow cytometry	165
6.3	Discussion	166
7	<u>The activity of new anti-CD20 mAb in CLL with del(17p)</u>	169
7.1	Introduction	169
7.2	Results	170
7.2.1	The effect of del(17p) on anti-CD20 mAb-mediated direct cell death in CLL	170
7.2.2	Internalisation of anti-CD20 mAb in normal 17p and del(17p) CLL cases	174
7.2.3	The impact of del(17p) on anti-CD20 mediated CDC in CLL	176
7.3	Discussion	180
8	<u>Final discussion and future work</u>	183
9	<u>References</u>	192
	<u>Appendix 1</u>	226
	<u>Appendix 2</u>	227
	<u>Appendix 3</u>	228
	<u>Appendix 4</u>	242
	<u>Appendix 5</u>	243

Index of Figures

Figure 1: The structure of an Ig molecule	22
Figure 2: History of anti-CD20 mAb in clinical translation	24
Figure 3: Overview of haematopoiesis	30
Figure 4: B-cell development.....	39
Figure 5: The effector mechanisms of anti-CD20 mAb.....	54
Figure 6: The classical complement pathway.....	65
Figure 7: Illustration of the CD20 molecule and anti-CD20 mAb binding sites...	68
Figure 8: Illustration of the basic principle of the quenching assay	92
Figure 9: Internalisation of anti-CD20 mAb in human lymphoma cell lines	104
Figure 10: Internalisation of rituximab in whole blood and purified B cells.....	106
Figure 11: Internalisation of anti-CD20 in human B cells purified from healthy volunteers	108
Figure 12: Validation of the quenching assay	110
Figure 13: Type I mAb internalise from the cell surface of normal and malignant human B-cells	112
Figure 14: Type I mAb internalise from the cell surface of normal and malignant human B cells	113
Figure 15: Correlation between internalisation of rituximab and CLL phenotypic and prognostic markers	115
Figure 16: The effect of CD38 variability and rituximab internalisation.....	116
Figure 17: Correlation between internalisation of rituximab and ATM loss in CLL	117
Figure 18: Correlation between internalisation of rituximab and del(11q) in CLL	118
Figure 19: Changes in sIg expression of CLL cells after anti-CD20 cross-linking	120
Figure 20: Investigation of co-localisation of BCR and rituximab	121
Figure 21: The Fc-dependency of internalisation of rituximab.....	127
Figure 22: FcγRIIIa and FcγRIIb1/2 expression on different primary B cell subtypes.....	129

Figure 23: Confirmation of FcγRIIa and FcγRIIb expression on Ramos transfectants by flow cytometry	130
Figure 24: FcγRIIa and FcγRIIb expression on different primary B cell subtypes using specific mAb.....	131
Figure 25: FcγRIIb inhibition reduces internalisation of rituximab	132
Figure 26: FcγRIIb expression on normal and malignant B cells	134
Figure 27: The correlation between FcγRIIb expression on B cell targets and the internalisation of rituximab	136
Figure 28: Effect of FcγRIIb expression level on internalisation of rituximab. .	137
Figure 29: The effect of co-culturing with different FcγRIIb-expressing cells on rituximab internalisation	139
Figure 30: The effect of varying cell concentrations on rituximab internalisation	140
Figure 31: Type I and not type II anti-CD20 mAb phosphorylated FcγRIIb.....	141
Figure 32: FcγRIIb phosphorylation and CD20 degradation following mAb stimulation of CLL cells	142
Figure 33: FcγRIIb expression is reduced over time in rituximab-treated CLL cells	144
Figure 34: Rituximab: CD20: FcγRIIb complexes are internalised together into lysosomes	146
Figure 35: The effect of anti-CD20 internalisation on macrophage phagocytosis	149
Figure 36: The effect of FcγRIIb inhibition on B cells on macrophage phagocytosis	150
Figure 37: Confirmation of specificity of anti-FcγRIIb mAb used in IHC.....	157
Figure 38: Anti-FcγRIIb staining of primary tumour material by IHC	158
Figure 39: The role of FcγRIIb in predicting PFS of RCVP-treated FL patients ..	163
Figure 40: Stratification of FcγRIIb as a biomarker of response in rituximab-treated MCL patients.....	165
Figure 41: Comparison of FcγRIIb expression by IHC and flow cytometry	166
Figure 42: Fludarabine-induced cell death in normal and del(17p) CLL.....	171

Figure 43: mAb-mediated direct cell death in normal and del(17p) CLL..... 172

Figure 44: Correlation between CD52 expression and sensitivity to mAb-induced cell death..... 173

Figure 45: Induction of direct cell death in normal and del(17p) CLL 174

Figure 46: Internalisation of anti-CD20 mAb in del(17p) and normal 17p patients 175

Figure 47: Confirmation of CDC activity of in-house produced GA101_{gly} and ofatumumab..... 177

Figure 48: Expression of complement defence molecules in CLL cases with or without del(17p)..... 178

Figure 49: mAb-mediated CDC activity in CLL with or without del(17p) 179

Figure 50: Correlation between CD59 expression and ofatumumab-mediated CDC 179

Index of Tables

Table 1: Examples of non-CD20 mAb currently in clinical development for B-NHL 28

Table 2: The Rai and Binet clinical staging systems for CLL 43

Table 3: The frequency and impact of prognostic markers in CLL 46

Table 4: Affinity, allelic variants and distribution of human and mouse FcγRs .. 56

Table 5: The list of PCR primer pairs used in the investigations. 85

Table 6: List of Ab used in the investigations 88

Table 7: Primary and secondary Ab used in Western blots 97

Table 8: Demographic and clinical characteristics of FcγRIIb-phenotyped B-NHL patients 161

Table 9: Baseline characteristics of FcγRIIb^{+/-} FL patients treated with front-line RCVP 162

Table 10: Baseline characteristics of MCL patients 164

Table 11: FcγRIIb expression in different subtypes of B-cell malignancies..... 166

DECLARATION OF AUTHORSHIP

I Sean Hua Lim declare that the thesis entitled 'Investigation of CD20-directed immunotherapy in B-cell malignancies' and the work presented in the thesis are both my own, and have been generated by me as the result of my own original research. I confirm that:

- **this work was done wholly or mainly while in candidature for a research degree at this University;**
- **where any part of this thesis has previously been submitted for a degree or any other qualification at this University or any other institution, this has been clearly stated;**
- **where I have consulted the published work of others, this is always clearly attributed;**
- **where I have quoted from the work of others, the source is always given. With the exception of such quotations, this thesis is entirely my own work;**
- **I have acknowledged all main sources of help;**
- **where the thesis is based on work done by myself jointly with others, I have made clear exactly what was done by others and what I have contributed myself;**
- **part of this work has been/is being published before submission in the following publications:**

Lim S.H., Vaughan A.T., Ashton-Key M., Williams E.L., Dixon S.V., Chan H.T., Beers S.A., French R.R., Cox K.L., Davies A.J., Potter N.K., Mockridge I., Oscier D.G., Johnson P.W.M., Cragg M.S., Glennie M.J. Fc gamma Receptor IIb on target B cells promotes rituximab internalization and reduces clinical efficacy. *Blood* 2011 Sept; 118(9):2530-40.

Alduaij W.A., Ivanov A., Honeychurch J., Cheadle E., Potluri S., Lim S.H., Shimada K., Chan C.H.T., Tutt A., Beers S.A., Glennie M.J., Cragg M.S., Illidge T.M. Novel type II anti-CD20 monoclonal antibody (GA101) evokes homotypic adhesion and actin-dependent, lysosome-mediated cell death in B-cell malignancies. *Blood* 2011 Mar; 117(17):4529-29.

Beers S.A., French R.R., Chan H.T., Lim S.H., Jarrett J.C., Vidal R.M., Wijayaweera S.S., Dixon S.V., Kim H.J., Cox K.L., Kerr J.P., Johnston D.A., Johnson P.W.M.,

Verbeek J.S., Glennie M.J., Cragg M.S. Antigenic modulation limits the efficacy of anti-CD20 antibodies. Blood 2010 Jun; 115(25): 5191-201.

Lim S.H., Beers S.A., French R.R., Johnson P.W., Glennie M.J., Cragg M.S. Anti-CD20 monoclonal antibodies: historical and future perspectives. Haematologica. 2010 Jan; 95(1):135-43.

Signed:

Date:.....

Acknowledgements

I am wholly grateful to Professor Peter Johnson for having guided and given me the opportunity to undertake this fellowship in the first place. His mentorship and support has been unsurpassable.

Professor Mark Cragg is simply an outstanding scientific supervisor. His breadth of knowledge and unending enthusiasm is inspirational. I am deeply appreciative of his forbearance of the dreadful combination that is my impatience and initial limited scientific background.

To everyone in Tenovus research laboratory who has made this experience enjoyable; Professor Martin Glennie for his enthusiasm in the project and career advice; Mrs Christine Penfold and Ms Snita Bansal for equally important unscientific support; Dr Claude Chan and his molecular magic wand; Dr Sandie Dixon and Sonya James for their assistance with confocal microscopy; Ms Kerry Cox, for the instances when multi-tasking goes askew and Mr Matthew Carter, for his technical advice.

I am also grateful to the CLL Bank (Kathy Potter and Isla Henderson) and the ECMC Human Tissue Bank staff for providing the primary tumour material.

To collaborators outside of Tenovus, Professor David Oscier, for providing tumour material within the blink of an eye; Dr Sheila Barton for her statistical expertise; Dr Andrew Davies, for the long hours spent in collecting clinical data; Dr Meg Ashton-Key, for the immunohistochemistry data; and Dr Jonathan Strefford, for the del(11q) data.

Finally, I am indebted to the Medical Research Council for funding this fellowship.

Abbreviations

Ab	Antibody
ABC	Activated B-cell like
ADCC	Antibody directed cellular cytotoxicity
AID	Activation-induced deaminase
ALL	Acute lymphoblastic leukaemia
APC	Antigen-presenting cells
APC	Allophycocyanin
ATM	Ataxia telangiectasia mutated
ATR	Ataxia telangiectasia related
β 2M	Beta 2 microglobulin
BAFF	B-cell activating factor
BCL-2	B-cell lymphoma-2
BCL-xL	B-cell lymphoma-extra long
BCR	B-cell receptor
BiTE	Bispecific T-cell engager
Blimp-1	B-lymphocyte induced maturation protein-1
bp	Base pair
BSA	Bovine serum albumin
BTK	Bruton's tyrosine kinase
C1 Inh	C1 esterase inhibitor
CDC	Complement-mediated cytotoxicity
cDNA	Complementary DNA
CDR	Complementarity determining region
CFSE	Carboxyfluorescein succinimidyl ester
CH/L	Constant region of heavy chain
CHO	Chinese hamster ovary
CHOP	Cyclophosphamide, doxorubicin, vincristine, prednisolone
CLL	Chronic lymphocytic leukaemia
CLP	Common lymphoid progenitor
CMP	Common myeloid progenitor
CSR	Class-switch recombination
CTL	Cytotoxic T-cell
CTLA-4	Cytotoxic T-lymphocyte antigen 4
CVP	Cyclophosphamide, vincristine and prednisolone
DC	Dendritic cells
DLBCL	Diffuse large B-cell lymphoma
DMEM	Dubelcco's modified eagle medium
DMSO	Dimethyl sulfoxide
EBF1	Early B-cell Factor 1
EBV	Epstein Barr virus
EDTA	Ethylenediaminetetraacetic acid
Fab	Fragment antigen-binding
FACS	Fluorescent-activated cell sorter
Fc	Fragment crystallisable
FC	Fludarabine and cyclophosphamide
Fc γ R	Fc gamma receptors
FCR	Fludarabine, cyclophosphamide and rituximab
FCS	Foetal calf serum
FDC	Follicular dendritic cells

FDX1	Ferredoxin 1
FISH	Fluorescent in situ hybridisation
FITC	Fluorescein isothiocyanate
FL	Follicular lymphoma
Flt-3	Fms-like tyrosine kinase-3
FOXO	Forkhead box class O
FRET	Fluorescence resonance energy transfer
G	Relative centrifugal force
GA101(gly)	GA101 with unmodified Fc region
GAPDH	Glyceraldehyde 3-phosphate dehydrogenase
GC	Germinal centres
Geo MFI	Geographic mean fluorescence intensity
GM-CSF	Granulocyte macrophage colony stimulating factor
GMP	Granulocyte monocyte progenitor
h	Hours
HAMA	Human anti-mouse antibodies
HGPRT	Hypoxanthine guanine phosphoribosyl transferase
HMGB1	High mobility group box 1 protein
HPLC	High performance liquid chromatography
HSC	Haematopoietic stem cell
ICOS	Inducible co-stimulator
Ig	Immunoglobulin
IHC	Immunohistochemistry
IL	Interleukin
IRF	Interferon regulatory factor
ITAM	Immunoreceptor tyrosine-based activation motif
ITIM	Immunoreceptor tyrosine-based inhibitory motif
IVIg	Intravenous immunoglobulin
LDH	Lactate dehydrogenase
LDT	Lymphocyte doubling time
LPL	Lymphoplasmacytic lymphoma
mAb	Monoclonal antibodies
MAC	Membrane attack complex
MAPK	Mitogen-activated protein kinase
MBL	Mannose-binding lectin
MCL	Mantle cell lymphoma
MCL-1	Myeloid cell leukaemia sequence 1
M-CSF	Monocyte colony stimulating factor
MDM2	Murine double minute 2
MEP	Megakaryocyte erythroid progenitor
MGG	May-Grünwald-Giemsa
MHC	Major histocompatibility
Mins	Minutes
miR	microRNA
MRD	Minimal residual disease
mRNA	Messenger RNA
MZ	Marginal zone
MZL	Marginal zone lymphoma
NHL	Non-Hodgkin's lymphoma
NK	Natural killer
NQ	Non-quenched
Ofatum	Ofatumumab

OS	Overall survival
Pax5	Paired box protein 5
PBMC	Peripheral blood mononuclear cells
PBS	Phosphate-buffered saline
PCD	Programmed cell death
PE	Phycoerythrin
PFH	Preservative-free heparin
PFS	Progression-free survival
PI	Propidium iodide
PI3K	Phosphoinositide 3 kinase
PIP3	Phosphatidylinositol 3,4,5 triphosphate
PLC γ	Phospholipase C gamma
PVDF	Polyvinylidene fluoride
Q	Quenched
RA	Rheumatoid arthritis
RAG	Recombinant activating gene
RCHOP	Rituximab-CHOP
RDX	Radixin
Ritux	Rituximab
RPMI	Roswell Park Memorial Institute 1640 medium
RT	Room temperature
RT-PCR	Reverse transcriptase polymerase chain reaction
s	Seconds
SAP	SH2 domain intracellular signalling protein
SD	Standard deviation
SHIP	SH2-containing inositol polyphosphate 5-phosphatase
SHM	Somatic hypermutation
SLC	Surrogate light chain
SLE	Systemic lupus erythematosus
SLL	Small lymphocytic lymphoma
SOS	Son of sevenless homologue
TAE	Tris base, acetic acid and EDTA
TBS-T	Tris-buffered saline with 0.5% v/v Tween-20
TCR	T-cell receptor
TD	T-cell dependent
Tdt	Terminal deoxyribonucleotidyl transferase
Tfh cells	Follicular helper CD4 T cells
Tg	Transgenic
TI	T-cell independent
TLR	Toll-like receptor
TNF	Tumour necrosis factor
Tosit	Tositumomab
Tris	Tris(hydroxymethyl)aminomethane
TTP	Time to progression
VH/L	Variable region of heavy or light immunoglobulin chain
WAF1	Wild type p53-activated fragment 1
ZAP-70	Zeta associated protein 70 kDa

1 Introduction

1.1 Cancer immunotherapy

Cancer immunotherapy can be broadly described as the manipulation of the host immune system to recognise and destroy tumours. This concept was developed from the hypothesis of 'immunosurveillance', proposed in 1957 by Burnet and Thomas, which suggested that the host immune system is capable of eliminating spontaneously-occurring tumours (reviewed in¹). The first supportive evidence for the ability of the immune system to recognise tumour-specific antigens arose from work demonstrating that mice could be immunised against transplanted syngeneic tumours (reviewed in²). However it was not until the 1990s when the concept of immunosurveillance was substantiated. A crucial piece of evidence arose with the generation of recombinant activating gene-2 (RAG-2) deficient mice. RAG-2 is an enzyme expressed exclusively on lymphoid precursors and is essential for immunoglobulin (Ig) or T-cell receptor (TCR) gene rearrangement. RAG-2 $-/-$ mice therefore lack NKT, T and B cells and have a severe combined immunodeficiency phenotype but with preservation of other cell types.³ In accordance with immunosurveillance, RAG-2 $-/-$ mice were more susceptible in developing carcinogen-induced sarcomas and spontaneous epithelial tumours, compared to their wild type counterparts.⁴ Since then, the immunosurveillance hypothesis has been further revised into 'immunoediting', which also takes into account the dynamic interactions between the host and the tumour, including the possible promotion of tumour growth by the host itself.¹ Immunoediting can be separated into three broad but distinct phases. The first is 'elimination', which is similar to the principles of immunosurveillance that is, the immune system has the ability to destroy a tumour. However if the tumour cells succeed in surviving the elimination phase, they enter into an 'equilibrium' phase with the host, whereby the immune system is able to control but not fully eliminate the tumour. During this stage, the immune system inadvertently selects for resistant tumours capable of surviving the continued immune attack. Finally during the 'escape' phase, the evolved

tumour overcomes the immune system and grows in an uncontrolled manner. Thus, tumour development hinges on the failure of the host immune system to eliminate and suppress it. Therefore it is reasonable to suggest that augmentation and re-engagement of the immune system could overcome tumour progression.

Immunotherapy serves to augment host immunity. The approaches are diverse and will be described here sequentially. Broadly, immunotherapy can be defined as either active or passive. The effects of passive immunotherapy are generally short-lived as immunologic memory is not elicited (see **Section 1.3.1**). Passive immunotherapy can be achieved via transfer of direct cancer-targeting antibodies (Ab) (e.g. anti-CD20 for lymphoma and anti-HER2 for breast cancer) or cellular immunotherapy, i.e. transfer of immune effector cells (e.g. T, NK or dendritic cells) capable of directly destroying tumour cells. The use of mAb will be discussed in more detail later. The idea of cellular immunotherapy stems from early observations demonstrating that established tumours in murine models completely regressed after transfer of leucocytes.^{5,6} However, early studies involving transfer of allogeneic leucocytes in cancer patients were less successful.^{7,8} Approaches in cellular immunotherapy have been honed and improved since. In general, autologous leucocytes are first isolated from patients, and then the cells are activated, expanded in vitro and re-administered back to the patient. The transferred cells only have a limited period of viability and may not be functionally optimal owing to the physical manipulation and microenvironmental changes. In order to induce proliferation and augment the anti-tumour function, priming regimens containing cytokines or chemotherapy are also administered to the patient (reviewed in⁹). As an example, concomitant interleukin-2 (IL-2) administration increased the median survival of transferred CD8⁺ T cells from 6.7 to 17 days in a clinical trial for treatment of metastatic malignant melanoma.¹⁰ Persistence of transferred CD8⁺ T cells has been variable from study to study, ranging from a week, to up to 4 months in one another study of melanoma.¹¹ The reason for this variation is not known. At present, patients with melanoma have seen the most benefit from cellular

immunotherapy. Depending on the specific approach employed, transfer of cytotoxic T-cells or tumour-infiltrating lymphocytes has produced objective responses of up to 70% in previously refractory metastatic melanoma.^{10,12,13} It is not entirely clear if immunologic memory is generated in these cases as it has not been measured in these trials. However, in post-transplant lymphoproliferative disease, Epstein Barr virus (EBV)-specific T-cell memory is clearly documented and associated with long-term responses after transfer of EBV-specific T cells from the allogeneic donor.¹⁴ Therefore the generation of immunologic memory may be dependent on the immunogenicity of the tumour.

Active immunotherapy aims to elicit tumour destruction followed by the establishment of long-lasting anti-tumour immunologic memory. This can be achieved by administering a cancer vaccine which contains an immunogen that is taken up by antigen presenting cells (APC) for presentation to T cells and subsequent stimulation of cell-mediated immunity. The immunogens which make up cancer vaccines are varied and early efforts were focused on tumour-specific markers (e.g. idiotypic antigens of B-cell tumours) or common tumour-associated antigens (e.g. carcinoembryonic antigen and prostate-specific membrane antigen)(reviewed in¹⁵). Idiotype refers to the unique epitopes formed by the variable regions of the Ig molecule (see **Section 1.2**) and is therefore theoretically an ideal target, being unique to the tumour.¹⁶ The idiotypic antigen is only weakly immunogenic and therefore an immunogenic adjuvant carrier is typically added. Early efforts were focused on follicular lymphoma (FL) due to its indolent behaviour and therefore the lack of need for urgent and aggressive therapies, the availability of an idiotypic antigen, and promising idiotypic immune responses in a small initial trial.¹⁷ Most significantly, development of the vaccine-specific responses correlated with improved overall survival (OS).¹⁸ However, significant survival benefit was not demonstrated in larger phase II/III trials (reviewed in¹⁹). The lack of success encountered by this approach has been attributed to, first, the presence of regulatory T cells in tumour infiltrates, which dampen immune activation,²⁰ and second, the ability of tumour cells to down-regulate surface expression of target

antigens as well as secrete defensive immunosuppressive molecules.²¹ DNA fusion vaccines are able to overcome some of these problems by allowing the incorporation of immunostimulatory genes of co-stimulatory molecules, chemokines to attract APC or sequences from foreign antigens such as tetanus toxin to stimulate innate immunity and engage T-cell help (reviewed in¹⁵). Structurally, DNA vaccines normally comprise a bacterial plasmid backbone into which desired sequences are added alongside with a promoter sequence to ensure high transcriptional activity. DNA vaccines are usually administered via intradermal or intramuscular routes or, more recently, via electroporation, to induce local inflammation and increase recruitment of dendritic cells (DC), macrophages and lymphocytes to the site.^{22,23} Once administered, the expressed antigen is taken up by either non-professional APC and transferred to professional APC (e.g. DC) for cross-priming, or taken up directly by APC for direct priming of T cells. A variety of different DNA vaccines have entered early phase clinical trials for melanoma,^{24,25} prostate cancer,²⁶ and follicular lymphoma.²⁷

The other approach of cancer vaccination is through the use of DC vaccines. Amongst all the professional APC, DC are the most efficient in antigen uptake, processing and presentation and are therefore crucial regulators of the adaptive immune system.²⁸ As a more direct approach to cancer vaccination, autologous DC are primed with tumour antigen *ex vivo* and then administered to the patient. Like DNA vaccines, studies have shown that most DC vaccines are capable of inducing immunologic responses but once again clinical responses have only been observed in a minority of patients (reviewed in²⁹). Perhaps the exception to the rule is sipuleucel-T in prostate cancer. Sipuleucel-T consists of autologous peripheral blood mononuclear cells primed *in vitro* with PA2024 (a recombinant fusion protein composed of the tumour-associated antigen, prostatic acid phosphatase and granulocyte macrophage colony stimulating factor (GM-CSF) for immunostimulation).³⁰ Two randomised, double-blinded, placebo-controlled phase III trials have demonstrated a survival benefit in 225 patients with advanced, hormone-refractory prostate cancer,³⁰ and sipuleucel-T

is the first therapeutic cancer vaccine to be licensed by the US FDA for clinical use in September 2010. However, to date passive immunotherapeutic approaches, particularly mAb, have been far more successful.

1.2 mAb therapy

Ab are produced by terminally differentiated B cells known as plasma cells as part of the adaptive immune response.³¹ Each plasma cell clone produces Ab with a single specificity (i.e. the antigen-binding site only recognises a single epitope on an antigen). However, when B cells are stimulated by an antigen, multiple B cell clones respond leading to multiple plasma cells being produced and the resultant Ab have diverse specificity for the antigen (polyclonal response). This section focuses on Ab alone whilst **Section 1.3.1** describes the associated B-cell development.

The basic structure of an Ab or Ig monomer is a heterodimeric glycoprotein comprising two large identical polypeptides (heavy chains (H), ~55,000 Da) and two smaller identical polypeptides (light chains (L), ~22,000 Da) (**Fig. 1**) (reviewed in³²). Each heavy chain is bound to a light chain by a disulphide bond and both chains are also linked by disulphide bonds to form a heterodimer. Heavy and light chains possess variable (V) or constant (C) regions depending on the diversity of the amino acid sequence.³³ The variable region is formed by the first ~110 amino acids of the NH_3^+ terminal of heavy and light chains (V_H and V_L respectively), and within it are further hypervariable regions called complementarity-determining regions (CDR).³⁴ The antigen-binding surface is formed by these CDR, three each from V_H and V_L chains. Despite crystallography data demonstrating that side chains from all CDR come into contact with cognate antigen (reviewed in³⁵), antigen specificity is primarily determined by V_H CDR3 sequence diversity.³⁶ In contrast, the other CDR have only a small repertoire of chain conformations³⁴ which help provide stability to the binding

site.³⁶ Changes in binding affinity are achieved by somatic hypermutation (SHM) (discussed in detail in **Section 1.3.1**).

The L and H chains can be further subdivided based on differences in the amino acid sequences of the C regions. There are two types of light chain (either κ or λ) and five types of heavy chain ($\gamma, \alpha, \mu, \delta$ and ϵ)(reviewed in³³). The heavy chain of an Ig determines its isotype or class (i.e. IgG, IgA, IgM, IgD and IgE, respectively).³⁷ IgG molecules can also be further subdivided into IgG1, IgG2, IgG3 and IgG4, and IgA into IgA1 and IgA2 based on subtle differences in the amino acid sequences. Isotype and subclass variation allows the Ab to mediate different effector functions.

Through papain digestion of peptide bonds, an Ig molecule can be separated into two antigen-binding fragments (Fab) and a further fragment which crystallises in the cold (Fragment, crystallisable or Fc).³⁸ The Fab fragments possess the CDR whilst the Fc fragment possesses only C_H domains and hence has no antigen-binding capability. Instead, the Fc mediates the Ab's effector functions by binding to Fc receptors or complement components such as C1q.³⁹ Essential to Fc function are glycan domains which are linked to the heavy chains.³² The precise location and number of glycan groups depend on the isotype of the Ig. In an IgG molecule, there is a single N-linked glycan which covalently links to an asparagine residue of the C_{H2} domain. The Fc glycan is important for maintaining the Fc heavy chains in an open conformation, required for optimal binding with Fc gamma receptors (Fc γ R)⁴⁰ and maintaining solubility.⁴¹ As such, modification of specific sugar moieties on the glycan can alter Fc γ R binding affinity (see **Section 1.5**). For example, it has been suggested that defucosylation of the Fc glycan leads to a wider structural change of the Fc domain which allows improved formation of non-covalent interactions with Fc γ RIIIa, and thus increased binding affinity to this Fc receptor.⁴²

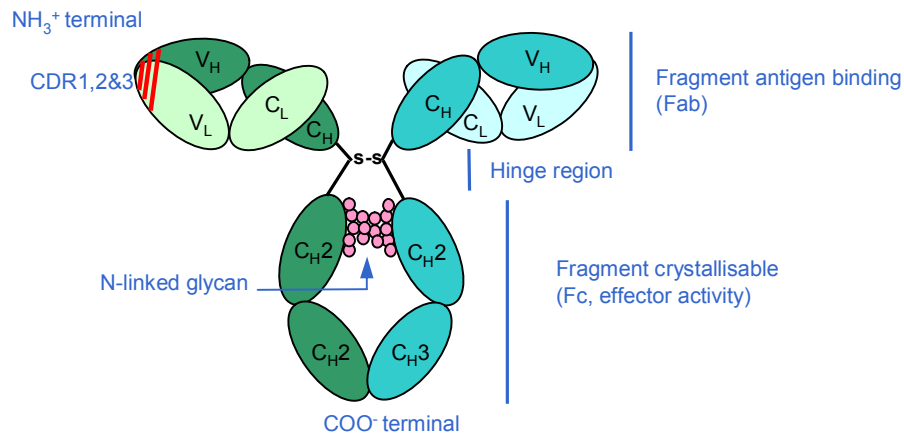


Figure 1: The structure of an IgG molecule

The above illustration is an example of an IgG molecule, which comprises two identical light chains (lighter colours) and two identical heavy chains (darker colours). IgG, IgD and IgE exist in monomeric forms, whereas IgA and IgM exist as a dimer and pentamer, respectively. Different colours are used to allow distinction of the chains. Each domain is labelled according to whether they are a variable (V) or constant (C) region and the subscript shows whether it is a light (L) or heavy (H) chain. Both pairs of chains are linked together by a disulphide bond (s-s). Within the Fc domain, there is an N-linked glycan situated beneath the hinge region, which is covalently linked to the C_H2 domains. The antigen binding site is formed by six CDR, and the first three are illustrated in red as an example.

As mentioned earlier, antigen stimulation of B cells leads to production of Ab of heterogeneous specificity. Such polyclonal reagents are problematic in the clinical setting as responses may be non-specific and ill-defined. Moreover, each batch of Ab would be variable. The pioneering of mAb production by Köhler and Milstein⁴³ in 1975 marked a momentous step forward for the advancement of this type of immunotherapy. In this procedure, mice are exposed to a specific antigen multiple times over the course of several weeks to drive a B-cell mediated Ab response. B cells isolated from the spleens of immunised mice are then fused with immortal non-Ig producing myeloma cell lines (originally derived from myeloma patients) using polyethylene glycol. To select for fused cells (hybridoma), the cultures are grown in hypoxanthine aminopterin thymidine medium, which blocks nucleic acid synthesis via the de novo pathway. This automatically triggers nucleic acid synthesis via hypoxanthine guanine phosphoribosyl transferase (HGPRT)-dependent salvage

pathway. The myeloma cells will die unless they have inherited HGPRT from the fused B cell component. The hybridoma cells are then diluted to a single cell level so that only one hybridoma cell produces a single mAb in each well. Supernatant from each clone is screened for the desired mAb reactivity, and the chosen hybridomas expanded.

mAb were envisaged to be the “magic bullets” of cancer therapy because of their high specificity for targets.⁴⁴ However it was not until two decades later that the first therapeutically successful mAb, anti-GPIIb/IIIa (platelet receptor) abciximab and anti-CD20 rituximab were approved for clinical use. The first, less commercially successful US FDA-approved mAb was muromonab, a murine anti-CD3 mAb, approved in 1986.⁴⁵ Although it is still currently licensed for use in prevention of acute rejection post renal transplantation and other solid organ transplants, its use is limited by the relatively high risk of severe reactions⁴⁶ probably caused by its murine components. Therefore one of the problems associated with the early progress of mAb was the development of human anti-mouse Ab (HAMA) against the murine components which reduced the therapeutic efficacy, increased Ab clearance^{47,48} and posed potential side effects, although no ‘serious’ events have been formally documented.⁴⁹ Later, advancement in DNA recombinant technology allowed the creation of chimeric mAb which comprise murine variable and human constant regions.⁵⁰ Chimeric mAb still possess 33% murine regions and thus, theoretical risk of HAMA. Jones et al.⁵¹ discovered that it was possible to further humanise mAb, yet retain their specificity by grafting the bare minimum critical murine sequences i.e. the CDR into a human framework. By the mid-1990s, successful development of fully human mAb was achieved either through the use of phage display technology⁵² or human transgenic (Tg) mice.⁵³ **Fig. 2** provides a timeline of this progress with examples in the development of anti-CD20 mAb.⁵⁴

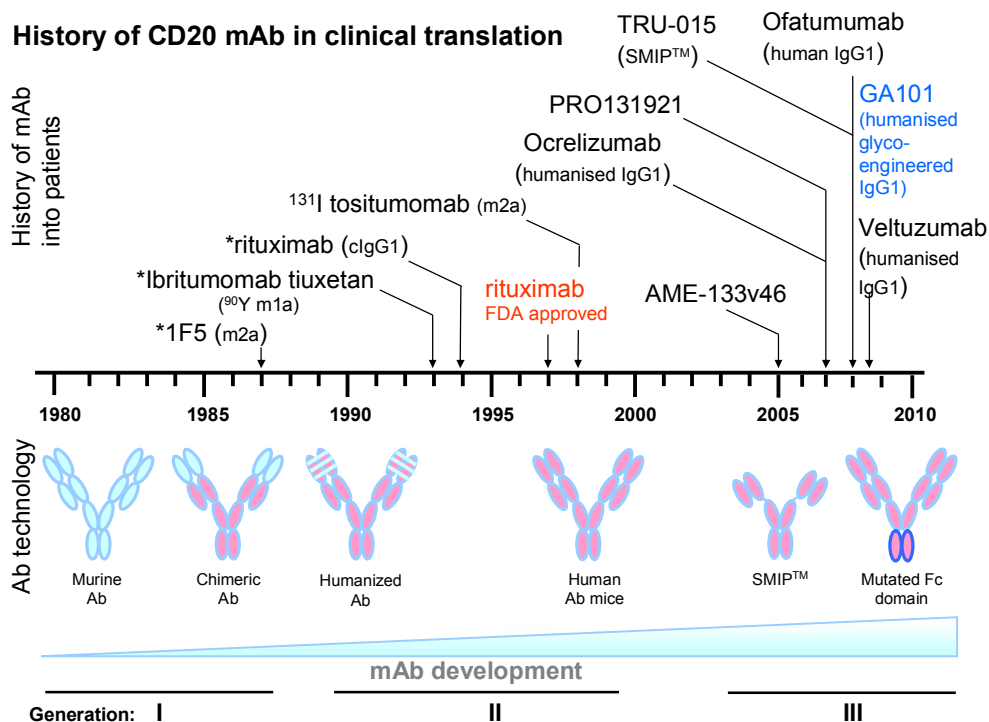


Figure 2: History of anti-CD20 mAb in clinical translation

The timeline illustrates the chronological introduction of respective anti-CD20 mAb in human trials and corresponding progressing in Ab. First generation Ab are murine or human/mouse chimeras, second generation Ab are humanised or fully human and third generation Ab have further modification to the basic Ab structure e.g. defucosylation of the Fc domain for enhanced recruitment of Fc-bearing immune effector cells. Figure taken from Lim et al.⁵⁴

1.2.1 Current mAb in clinical trials

Since the introduction of chemotherapy in the 1970s, no other drug has succeeded in improving the OS of patients with the commonest subtypes of B-cell lymphoma until the incorporation of rituximab. The success of rituximab has encouraged the development of mAb to other targets. **Table 1** describes some of those mAb currently in development for lymphoma. Most of these mAb share similar features to anti-CD20 mAb in that the target is commonly expressed by tumour cells, and tumour destruction is apparently a result of direct cytotoxic mechanisms such as complement-dependent cytotoxicity (CDC), Ab-dependent cellular cytotoxicity (ADCC) or induction of direct cell death, as will be discussed in detail in **Section 1.5**. A further class of mAb, e.g. anti-CD40

mAb, are distinct in that they target components of the host immune system as opposed to tumour cells directly.⁵⁵ In the case of anti-CD40 mAb, these agonistic mAb mimic CD40 ligand (CD40L or CD154) to induce maturation of DC. Mature DC are then able to induce an effective anti-tumour cytotoxic T-cell (CTL) response. As such, anti-CD40 also has activity against CD40-negative T cell tumours in mouse models. The findings of a phase I trial using humanised anti-CD40 mAb, dacetuzumab (SGN-40) was recently published.⁵⁶ Of 50 patients with relapsed/refractory B-cell lymphoma, 6 patients demonstrated objective responses, and a further 13 had stable disease. Encouragingly, one of the responding patients with aggressive lymphoma demonstrated continued remission lasting over 62 weeks. Whether the responses seen are due to dacetuzumab's direct cytotoxicity or immune modulation, is unknown. No correlation was found between CD40 expression and clinical responses but the study may have been under-powered to detect one. As a further example of this kind, anti-cytotoxic T-lymphocyte antigen-4 (CTLA-4) mAb, ipilimumab inhibits negative feedback signalling of T-cell activation, and hence can potentiate an anti-tumour T-cell response (reviewed in⁵⁷). A recent phase III trial in patients with advanced melanoma demonstrated that ipilimumab, regardless of concomitant glycoprotein-100 peptide vaccine administration, was able to prolong the OS of these patients.⁵⁸ Whilst the improvement was modest (median survival 10 months versus 6.4 months), the results suggest that immune modulation by mAb targeting has therapeutic potential.

The other approach for mAb use is conjugation to a toxin, drug or radioactive nuclide. Development of a targeted immunotoxin can be complex as the toxin can be immunogenic, triggering a HAMA-like response and potentially causing damage to adjacent non-target cells.⁵⁹ Examples of mAb used as targeted immunotoxins are anti-CD33 (gemtuzumab ozogomicin, for acute myeloid leukaemia),⁶⁰ anti-CD22 (inotuzumab ozogomicin, CMC-544 for B-cell non-Hodgkin's lymphoma (NHL),^{56,61} and anti-CD30 (brentuximab vedotin, SGN35) for Hodgkin's lymphoma and anaplastic large cell lymphoma.⁶² The first two mAb are conjugated to a potent antibiotic, calicheamicin, which causes double-

strand DNA breaks and subsequent apoptosis in target cells. Brentuximab is an anti-CD30 mAb conjugated to monomethylauristatin E, an anti-tubulin agent.⁶³ Once internalised into lysosomes, the anti-tubulin agent is cleaved and it binds to tubulin and induces growth arrest and cell death in CD30⁺ cells. The drug is now in clinical development⁶² and a phase II trial of 102 patients with relapsed/refractory Hodgkin's lymphoma reported a promising results with 95% of patients have a reduction in tumour size.⁶⁴ The final results of the trial are still awaited.

Conjugation of a mAb to a radioactive nuclide e.g. anti-CD20 Bexxar (¹³¹I-labelled tositumomab) and Zevalin (⁹⁰Y-labelled ibritumomab tiuxetan), allows delivery of targeted radiotherapy to CD20⁺ and adjacent cells. Both produce good durable overall response rates in FL but no trials have directly compared their efficacy.^{65,66} Zevalin is licensed in the European market for relapsed and refractory low grade B-cell non-Hodgkin's lymphoma (B-NHL) and for consolidation of first remission in FL whilst Bexxar is licensed in the US for treatment of relapsed and refractory low-grade B-NHL or high-grade transformation.⁶⁷ Unlike rituximab, radioimmunoconjugates only require a single administration, and are therefore ideal for reducing hospital visits. However, there are clinical and logistical issues associated with radioimmunoconjugates. Radioimmunotherapy can cause severe and prolonged myelosuppression, and is therefore generally avoided in patients with >25% marrow infiltration.⁶⁸ As a precautionary measure, patients also require weekly full blood count testing for 6 weeks after administration,⁶⁹ and there is a risk of radiation exposure to medical staff and surrounding persons depending on the radionuclide utilised. Hence these treatments need to be given in a nuclear medicine facility by qualified personnel and sufficient advice given to patients with regards to personal contact and disposal of bodily fluids. It is likely that all these practical issues have dissuaded the widespread use of radioimmunoconjugates compared to unlabelled mAb even in light of good clinical responses.

The bispecific T-cell engager (BiTE) represents another type of novel immunomodulatory Ab modality. Conventional mAb are not able to directly engage T cells since they lack Fc receptors (see **Section 1.5**). BiTE is designed to engage cellular-mediated immunity by directly engaging T cells and bringing them into contact with the tumour target cell. Blinatumomab is the most clinically advanced BiTE in development and has specificity for the pan B-cell marker, CD19, and the pan T-cell marker CD3, thus enabling direct linkage of B cell tumours to CTL.⁷⁰ CTL activation leads to direct tumour cell lysis and is independent of T-cell co-stimulation. Pre-clinical studies suggest that blinatumomab has far more potent cytotoxic activity than rituximab.⁷¹ Furthermore, two clinical trials, the first in relapsed/refractory B-NHL, has demonstrated sustained responses in 5/7 patients,⁷² whilst in the second, blinatumomab was able to eradicate residual disease in 13/16 minimal residual disease (MRD) positive B-cell acute lymphoblastic leukaemia/lymphoma (B-ALL) patients.⁷³

Specificity	Drug	Stage of Development	Dominant mechanisms of action
CD22	Epratuzumab	Phase II FL (in combination with rituximab) ⁷⁴	Moderate ADCC
CD22	Inotuzumab ozogamicin (CMC-544)	Phase I B-NHL ⁷⁵	Immunotoxin; conjugated to calicheamicin
CD23	Lumiliximab	Phase I CLL ⁷⁶	Apoptosis (down regulation of anti-apoptotic proteins)
CD40	Dacetuzumab	Phase I CLL ⁷⁷ Phase I B-NHL ⁵⁶	Apoptosis (activate pro-apoptotic signals) ADCC
	HCD122	Phase I B-NHL ⁷⁸	ADCC Growth inhibition
CD52	Alemtuzumab	Approved for CLL and T cell lymphoma	Complement ADCC
CD70 (CD27L)	SGN-70	Pre-clinical phase ⁷⁹	ADCC, particularly phagocytosis
CD80	Galiximab	Phase I/II FL (with rituximab) ⁸⁰	ADCC Upregulation of apoptotic molecules
Bispecific	Blinatumomab (CD9/CD3)	Phase I (B-NHL) ⁷²	T-cell cytotoxicity

CLL = chronic lymphocytic leukaemia

Table 1: Examples of non-CD20 mAb currently in clinical development for B-NHL

The table describes some of the current mAb under clinical investigation, the published level of clinical development in B-cell neoplasms and their reported mode of action.

1.3 B-cell malignancies and their association to normal development

Approximately 8000 cases of B-cell malignancy were diagnosed in the United Kingdom in 2007⁸¹ and worldwide, this group accounts for 4% of new cancers diagnosed per year.⁸² The diseases that make up this group are diverse and are classified according to the World Health Organisation's recommendations (**Appendix 1**). This classification is based on a combination of clinical, morphologic, immunophenotypic and genetic characteristics. In general, an attempt is made to link individual B-cell diseases to their normal cellular

counterparts. In order to fully appreciate the differences between each disease, an understanding of normal B-cell development is necessary.

1.3.1 B-cell development

Much of the current understanding on the development of human B cells is based on murine studies. Many similarities have been identified between the B-cell subsets of both species, thus it is generally accepted that findings from mouse studies can be broadly extrapolated to humans, albeit with certain exceptions. All haematopoietic cells are derived from pluripotent haematopoietic stem cells (HSC) (reviewed in⁸³) (**Fig. 3**). The stem cell resides in the bone marrow and is unique in that it has self-renewing capacity and is able to regenerate into haematopoietic cells of any lineage.^{84,85} Phenotypically, HSC can be identified by high levels of the stem cell factor receptor (c-kit or CD117) and the absence of lineage-specific markers. Under the regulation of lineage-specific transcription factors, HSC mature and commit into early lymphoid⁸⁶ or myeloid⁸⁷ progenitors. The development of HSC into lymphoid precursors is dependent on the timely expression of PU.1 and Ikaros transcription factors, which regulate expression of c-kit, Fms-like tyrosine kinase-3 (Flt-3) and interleukin-7 receptor α chain (IL-7R α) (reviewed in⁸⁸). Thereafter, E box binding protein 2A (E2A), early B-cell factor 1 (EBF1) and paired box protein 5 (Pax5) transcription factors are critical in the differentiation of the common lymphoid precursors into early B cells (**Fig. 3**). E2A and EBF are both critical for initiating gene rearrangements, and Pax5 maintains B-lineage commitment as well as induces expression of the B-lineage restriction marker, CD19. Mouse models lacking any one of these transcription factors have impaired B-cell development (reviewed in⁸³).

Several growth factors have been implicated in the control of B-cell development, and of these, Flt-3 and IL-7R α are thought to be most crucial in murine studies.⁸⁹ Although mice deficient in Flt3 alone had only marginally

lower mature B cell numbers, combined loss of Flt3 and IL-7R α resulted in complete absence of mature IgM⁺ B cells.⁸⁹ In contrast, in humans, IL-7R α is thought to be far less crucial, as patients lacking components of the IL-7R signalling pathway have relatively normal numbers of circulating B cells.⁹⁰ The role of Flt3 in human B cell development has not yet been ascertained.

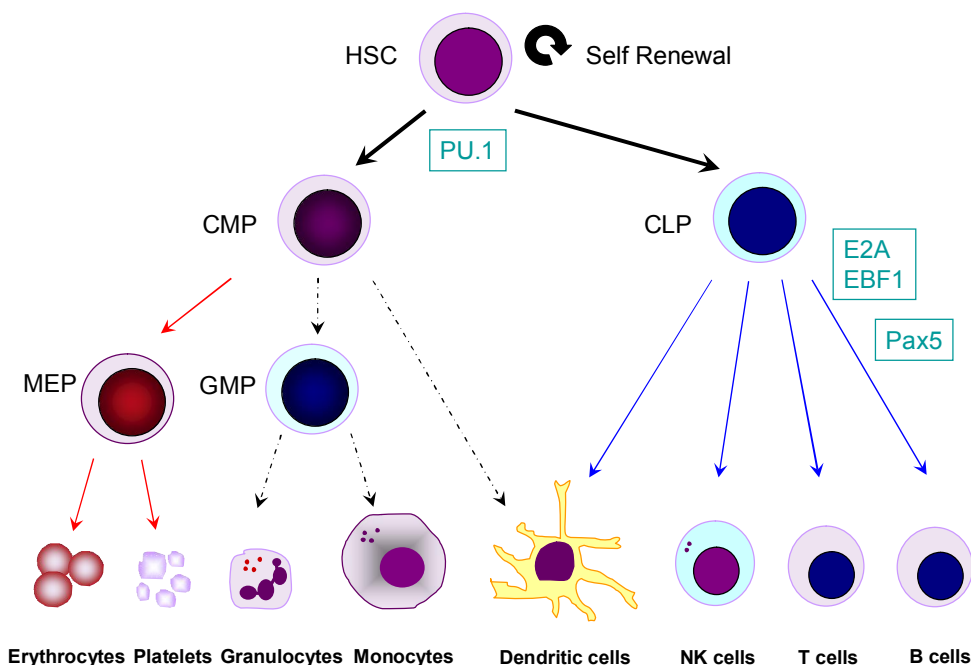


Figure 3: Overview of haematopoiesis

Self-renewing HSC give rise to multipotent progenitors which generate common lymphoid progenitors (CLP) or common myeloid progenitors (CMP), under the control of PU.1, an Ets family transcription factor. CMP further generate megakaryocyte-erythroid progenitors (MEP) and granulocyte-monocyte progenitors (GMP) which give rise to the mature effectors erythrocytes and platelets, and granulocytes and monocytes respectively. Similarly CLP generates DC, natural killer (NK) cells, T cells and B cells. The origin of human DC are unclear in part due to their low frequency in the peripheral blood. E2A and EBF1 transcription factors are crucial in directing CLP into B cell development whilst Pax5 is needed to maintain commitment to the B-lineage commitment (reviewed in⁸³).

B-cell development begins in the bone marrow and can be divided into antigen-independent and antigen-dependent stages (**Fig. 4**). The differentiation pathway is well-described in mice, where early B-cells differentiate from pre-pro-B into pro-B and then pre-B cell stages, and are marked by varying expression of CD19, CD43, and CD24 surface expression levels.⁸³ In humans,

pro-B and pre-B cell subsets have been identified but earlier B-cell precursors remain less well-defined. It is generally agreed that each of these human B-cell subsets can be identified using the following immunophenotypes; early B (CD34⁺CD19⁻CD10⁺), pro-B (CD34⁺CD19⁺CD10⁺ and terminal deoxyribonucleotidyl transferase (Tdt)⁺) and pre-B (CD34⁺Tdt⁻CD19⁺CD10⁺ and cytoplasmic μ heavy chain expression) (reviewed in ⁹¹).

As Igs are the primary product of B cells, B-cell maturation can also be described through the prism of Ig rearrangements and expression patterns. Pro-B cells are marked by the initiation of heavy chain gene rearrangement (D_H to J_H , then V_H to D_HJ_H).⁹² This process is mediated by RAG-1/RAG-2 enzymes, which catalyse double-strand DNA breaks at specific regions called recombination signal sequences.^{93,94} Cleaved DNA ends are rejoined in a non-homologous manner by a set of ubiquitously expressed proteins such as DNA protein kinases (reviewed in⁹⁵). As a means of further expansion of the Ab repertoire, Tdt catalyses the addition of random nucleotides at rearranging gene segment junctions.⁹⁶ The completion of heavy chain rearrangement marks the transition from the pro-B to the pre-B cell stage⁹² and formation of a pre-B-cell receptor (pre-BCR).⁹¹ The pre-B-cell receptor consists of a membrane μ heavy chain that is covalently linked to a germline-encoded surrogate light chain (SLC), itself consisting of V_{pre-B} and $\lambda 5$ molecules, along with a signalling heterodimer of Ig- α (CD79a) and Ig- β (CD79b). The production of a functional pre-BCR signifies that heavy chain gene rearrangement was successful, and provides a critical developmental checkpoint. Its formation is associated with suppression of RAG-1/RAG-2 expression, thereby ensuring allelic exclusion at the μ heavy chain locus, and is followed by proliferation of pre-BCR-expressing cells and finally, re-expression of RAG-1/RAG-2, required for light chain gene rearrangement. That the pre-BCR is equivalently important in human and mouse B-cell development is reflected in various studies (reviewed in⁹¹). Selective targeted deletion of any of the components of the pre-BCR complex in mouse models leads to a developmental block beyond the pro-B cell stage. Knockouts of the SLC components appeared

to produce only a partial block in mouse models, but the report of an agammaglobulinaemic patient with biallelic loss of $\lambda 5$ ⁹⁷ suggests that both the expression and signalling components of the pre-BCR are required for continued B-cell maturation in humans.

V_L to J_L gene rearrangement occurs during the pre-B cell stage.⁹² The κ gene locus is rearranged first, and if it fails, rearrangement then takes place in the λ locus. This light chain restriction provides a means by which clonality of cells can be determined. The next critical step in B-cell development is the maturation of the pre-BCR into a B-cell receptor (BCR).⁹⁸ This requires the effective pairing of rearranged light chains with rearranged heavy chains, and presents the transition of a pre-B cell into an immature B cell. The BCR consists of an antigen-detecting component, surface immunoglobulin M (sIgM) and a signalling component similar to the pre-BCR i.e. Ig- α and Ig- β .⁹⁹

V(D)J recombination produces a diverse Ig repertoire, essential for host defence, but a drawback is that the specificity is generated randomly and so some of the Ig will be reactive against self-antigens. As a result, tolerance mechanisms are required to prevent auto-immunity. Unlike mature B cells, cross-linking of the surface Ig on immature B cells does not result in cellular proliferation.¹⁰⁰ Instead, deletion, anergy (a process whereby self-tolerance is generated through reduced BCR expression and signalling)¹⁰¹ or receptor editing^{102,103} occurs (reviewed in¹⁰⁴). Receptor editing is a process by which the RAG enzymes continue to catalyse light chain rearrangement until a non-self-reactive BCR results.^{102,103}

The non-autoreactive, naïve and immature B cells (also identified as transitional B cells) migrate into the peripheral blood and then localise into the follicular regions of the secondary lymphoid organs, where they are termed follicular B cells.⁸³ The survival of these B cells is entirely reliant on the BCR.⁹⁸ Lam et al.⁹⁸ initially demonstrated that BCR-deficient murine B-cells, achieved through deletion of the V region genes, resulted in a block in B-cell development. Kraus

et al.¹⁰⁵ further demonstrated that BCR expression alone was insufficient to maintain B-cell survival, but that the signalling component Ig α and Ig β , transmitted essential 'basal signalling' required for survival. However, it is still contentious whether this 'tonic' or basal signalling occurs independently of antigen-binding or is the result of low-affinity self-reactive antigen stimulation (reviewed in¹⁰⁶). More recently, the tumour necrosis factor (TNF)-like ligand, B-cell activating factor (BAFF), and forkhead box class O (FOXO) proteins have also been shown to be vital for the survival of peripheral B cells.¹⁰⁶ BAFF receptor expression is first induced on immature B cells by the expression of a functional BCR, and its signalling promotes the expression of pro-survival proteins such as B-cell lymphoma 2 (BCL-2), BCL-xL (BCL-extra long) and myeloid cell leukaemia sequence 1 (MCL-1). Furthermore, BCR-signalling, via phosphoinositide-3 kinase (PI3K) also down-regulates FOXO transcription factors, which target and drive pro-apoptotic and anti-proliferative proteins. Thus, BCR and BAFF cooperate to maintain survival of peripheral B cells.

The majority of B cells produced in this pathway have been characterised as B-2, or 'conventional' B cells.¹⁰⁷ Another smaller subset of cells, defined as B-1, differs in phenotype, anatomical distribution, self-renewing capacity and function.¹⁰⁸ B-1 cells are CD5⁺, preferentially found in the peritoneal and pleural cavities (in mice) and are capable of providing an immediate and short-lived response to pathogen invasion. These B-cell subsets have been characterised primarily in mice, and until recently, it was uncertain if the same differentiation could be applied to human B cells. However, Rothstein's group recently demonstrated that a subset of B cells, found both in human umbilical cord and adult peripheral blood, and defined by CD20⁺, CD27⁺ and CD43⁺ were functionally comparable to murine B-1 cells.¹⁰⁹ Like murine B-1 cells, this human subset secreted IgM spontaneously, displayed evidence of tonic signalling, and was an efficient antigen-presenter to T cells. Whilst murine B-1 cells are defined by CD5 cell surface expression, most (75%) but not all human B-1 cells were found to be CD5⁺.

Within the follicles of the spleen or lymph nodes, the naïve follicular B cells will encounter cognate antigen complexed on the surface of complement receptors of primary follicular dendritic cells (FDC) and then migrate to the T:B border (reviewed in¹¹⁰). While B cells can be activated by soluble antigen, the affinity for BCR is generally low. In contrast, membrane-bound antigens are able to tether B cells more strongly and enhance BCR signalling through co-stimulation by other surface receptors such as VLA-4/VCAM-1.¹¹¹ Lymphocytes enter the secondary lymphoid organs via afferent lymphatics or arterioles and are attracted into the different areas in a chemokine-dependent manner. For instance, the chemokines ligand, CXCL13 attracts CXCR5-bearing B cells into B-cell follicles, whereas the chemokines ligands, CCL19 and CCL21 attracts CCR7-bearing T cells into the T-cell zone (also known as the periarteriolar lymphatic sheath (PALS)).¹¹⁰ Mature, naïve B cells are activated on antigen encounter either through a T-cell independent (TI) or a T-cell dependent (TD) pathways.¹¹⁰ TI antigens can themselves be further subdivided into either TI-1 or TI-2 types: TI-1 antigens stimulate B cells independently of BCR signalling, whereas TI-2 antigens require BCR signalling and additional co-stimulation of pathogen-associated molecular pattern receptors such as the Toll-like receptors (TLR).¹¹⁰ Examples of these antigens are lipopolysaccharide and TLR4 agonists (TI-1), and polysaccharides from the cell wall of encapsulated bacteria and Ficoll- or dextran-conjugated haptens (TI-2). Whilst any B cell subset can be stimulated by TI-1 antigens, only B-1 cells and marginal zone (MZ) B cells react to TI-2 antigens.¹¹² MZ B cells are a distinct subset of B cells which reside in an anatomically-defined MZ area of the spleen. These cells are classically CD27⁺IgM⁺IgD⁺ in humans, and are thought to developmentally derive from either transitional B cells, mature naïve IgM⁺CD27⁻ B cells, or pre-mutated germinal centre-derived B cells (reviewed in¹¹³). All TI-activated B cells undergo intense proliferation in the extrafollicular regions and differentiate to become IgM-secreting plasmablasts.¹¹⁴ This relatively weak and rapid response serves to provide an initial protective immune response, and but is only transient. In general, these plasmablasts apoptose after 3 days,¹¹⁵ although B1-derived plasmablasts appear to survive for far longer periods.¹¹⁶

After encountering antigen and migration to the T:B cell zone border where B cells receive T-cell help, B cells undergo intense proliferation to form germinal centres (GC).¹¹⁷ GC formation is essential for the development of secondary immune responses and immunologic memory.¹¹⁸ TI responses can also result in GC formation but they only exist transiently (several days), unlike TD-stimulated GC which last for weeks.¹¹⁹ Within the GC, two distinct diversification processes occur at the immunoglobulin loci, SHM and class-switch recombination (CSR) (reviewed in ¹²⁰). SHM increases the affinity of the antigen-binding domain of the Ig whereas CSR allows a switch between the variable and constant regions, thereby allowing the Ig to vary its effector function. Despite being distinctly different processes, both are dependent on the enzymatic activity of activation-induced deaminase (AID), as evidenced by the lack of either CSR or SHM in both mice and humans lacking AID.^{121,122} In SHM, AID catalyses the deamination of cytidine residues¹²³ in particular hotspot motifs within a 2 kb region, downstream of the transcription start site of the Ig variable gene, leading to the introduction of non-random point mutations.¹²⁰ For CSR, AID induces double-strand breaks within switch regions (guanine-rich tandem repeats that are situated upstream of each heavy chain constant region), leading to subsequent recombination in a non-homologous manner.¹²⁰

Despite the fundamental need for V(D)J recombination, SHM and CSR, errors during these processes are potentially pathological. Indeed, reciprocal chromosomal translocations which juxtapose a proto-oncogene next to an immunoglobulin regulatory locus, are one of the hallmarks of B-cell lymphomas (reviewed in¹²⁴). Examples of these include c-myc in Burkitt's lymphoma, BCL-2 in FL, BCL-6 in diffuse large B-cell lymphoma (DLBCL) and BCL-1 (resulting in cyclin D1 overexpression) in mantle cell lymphoma (MCL). Aside from chromosomal translocations, mis-targeting by AID can also contribute to dysregulation of proto-oncogenes and tumour suppressor genes, as in the case of BCL-6¹²⁵ and the death receptor, CD95.¹²⁶

To summarise B-cell development so far, the GC B-cell enters cell cycle and undergoes intense proliferation, thereby generating centroblasts in which SHM occurs. Mutated centroblasts then exit the cell cycle (becoming centrocytes) and gradually migrate to the edge to form the morphologically-described “light zone”. In order to achieve sufficient numbers of high affinity mutations per mutated B-cell, centrocytes re-enter cell cycle and undergo SHM repeatedly (reviewed in¹²⁷). Throughout this stage, both centroblasts and centrocytes which express high-affinity Ig receptors are selected for survival, in a process known as affinity maturation.¹²⁷ A multitude of inter-dependent factors are involved in the GC reaction, with the crucial cellular components being the FDC and the follicular helper CD4 T cells (Tfh cells).

FDC can be differentiated into primary FDC (found within the primary follicle) or secondary FDC (found within the GC), and they have different surface receptor expression, as will be discussed later.¹²⁷ FDC specialise in trapping antigen from macrophages or non-cognate B cells for presentation as immune complexes to B cells. Immune complexes on primary FDC are only presented on complement receptors, whereas on secondary FDC, immune complexes are presented on both complement receptors and FcγRIIb receptors (see **Section 1.5.1.1**). Aside from this, FDC also produce a high concentration of CXCL13, which attracts CXCL5-expressing B and T cells to the follicle.¹²⁷ FDC have been shown to be crucial in promoting B-cell survival and assisting in affinity maturation through various means. First, FDC deliver co-stimulatory survival signals to the B cells via interaction with complement products, and CD21 (C3 receptor)¹²⁸ or CD40 (C4bp receptor)¹²⁹ on B cells. Second, the high concentration of FcγRIIb on secondary DC results in preferential binding of Fc fragments of immune complexes to DC, thus prevents a negative, inhibitory signal to the B cell.¹³⁰ Finally, the delivery of integrin- and Notch-mediate signals to B cells, which are necessary for survival, but the mechanism by which this happens remains poorly understood.¹²⁷

Tfh cells are the crucial subset of CD4 T cells involved in B-cell help as evidenced in experiments demonstrating that chimeric mice which lack BCL-6 in T cells, thereby lacked Tfh cells but had abundant Th1, Th2 and Th17 cells, failed to form GC.^{131,132} Murine Tfh cells can be characterised by expression of CXCR5, SH2-domain intracellular signalling protein (SAP), inducible co-stimulator (ICOS), secretion of IL-21 and lack B-lymphocyte inducible maturation protein-1 (Blimp-1) (reviewed in¹³³). As suggested earlier, the differentiation of naïve CD4 T cells into Tfh cells is regulated by BCL-6 – an antagonist of Blimp-1, which itself promotes differentiation of non-Tfh subsets. BCL-6 is also vital in promoting B-cell proliferation in the GC and suppression of B-cell differentiation,^{134,135} but its effects on T and B cells are thought to be distinct.¹³³ As mentioned earlier, CXCR5-expressing Tfh cells are attracted into the follicles by the CXCL13, thus allowing co-localisation of Tfh and B cells. TD B-cell activation is dependent on encounter with a cognate antigen as well as CD40 co-stimulation on the B cell via interaction with CD40L on activated Tfh cells.¹³⁶ Key amongst the molecular interactions is that between CD40L and CD40 which serves to maintain the GC. Loss of CD40L results in rapid disappearance of pre-formed GC in mice¹³⁷ and patients with genetic deficiencies of either CD40L or CD40 fails to form GC.¹³⁸ It is suggested that CD40 signalling allows the repeated recycling of centrocytes into centroblasts, thus allowing renewal of proliferating cells.¹³⁹ Furthermore, GC B cells express constitutively high levels of Fas. Without pro-survival stimulation by CD40L amongst other interactions, the GC B cells will die via Fas-Fas ligand (on T cells) stimulation.¹³³ The other crucial co-stimulatory molecule is ICOS.¹⁴⁰ ICOS is upregulated on most subsets of activated CD4⁺ T cells, including Tfh.¹⁴¹ Both ICOS-deficient mice and humans have impaired GC formation and reduced CSR to IgG, IgA and IgE isotypes.^{140,142,143} Furthermore, ICOS has also been shown to maintain CD40L expression on T cells.¹⁴⁴

The maturation of an immune response is associated with CSR leading to Ab isotype changes through further rearrangement of the C_H segments.¹⁴⁵ As the C_H segments have different effector capacity, CSR allows the activated B cell to produce Ab capable of engaging different immune effectors without changes in

antigenic specificity. The isotype generated is dependent on environmental stimulation e.g. IL-10 directs switching to IgA,¹⁴⁶ and IL-13, towards IgG4 and IgE.¹⁴⁷ Selected and class-switched B cells differentiate into either long-live Ig-secreting plasma cells or memory B cells.¹⁴⁸ The transcription factor, Blimp-1 is crucial in regulating plasma cell differentiation.¹⁴⁹ In concert with the interferon regulatory factor-4 (IRF-4), both transcription factors suppress Pax5 and BCL-6 to induce plasma cell differentiation.¹⁵⁰ Plasmablasts leave the GC to mature into terminally differentiated plasma cells, which in humans are classically CD38⁺ and CD20⁻.¹⁵¹ Memory B cells do not secrete Ab and are phenotypically defined as CD27⁺ and IgD⁻ in humans.¹⁵² They are long-lived despite the absence of antigenic stimulation.¹⁵³ Upon re-stimulation by cognate antigen, rapid and massive clonal proliferation occurs, generating up to 10-fold more plasma cells than in the primary response.¹⁵⁴

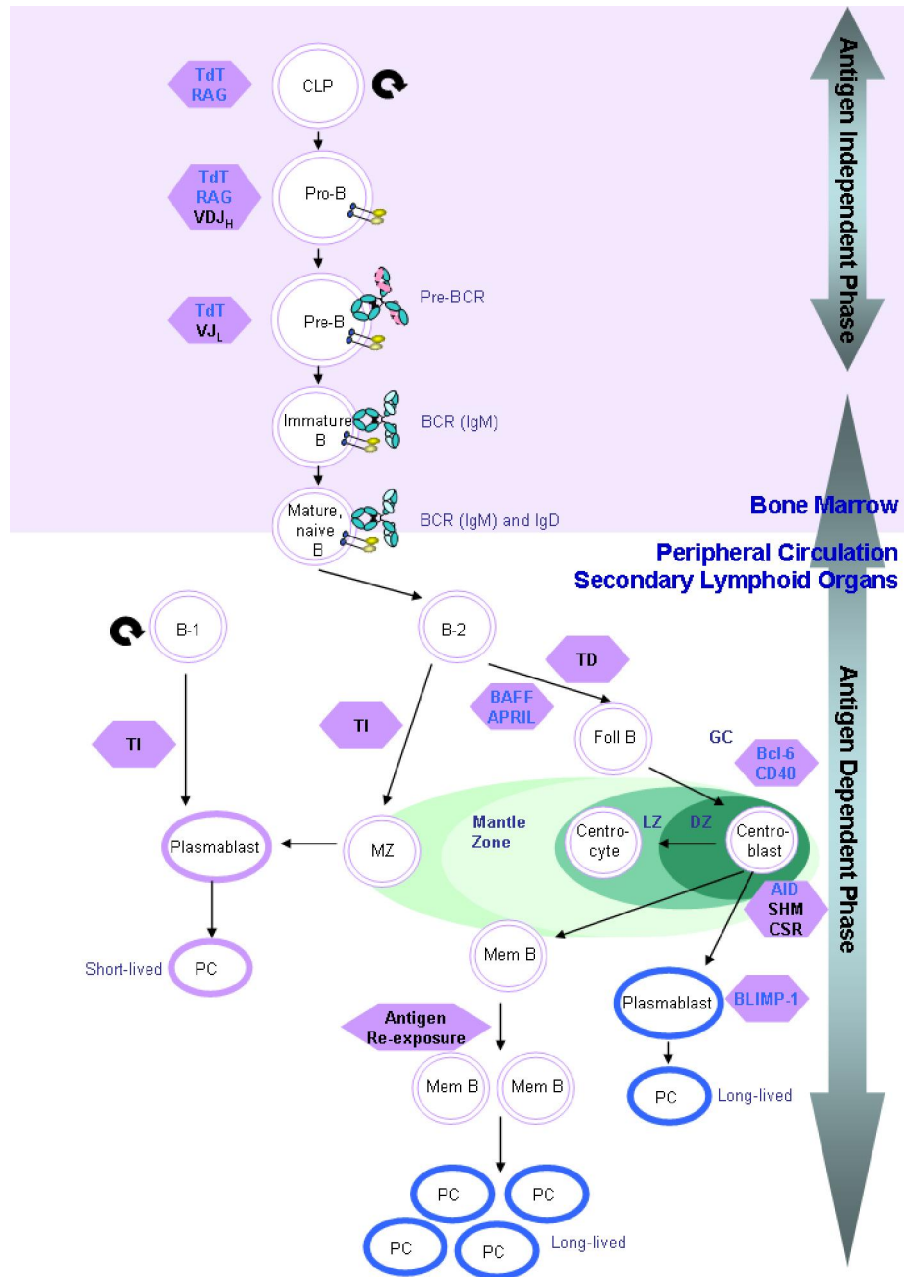


Figure 4: B-cell development

The key transcription factors and steps in B-cell development are summarised here. The antigen-independent phase of B-cell development takes place in the bone marrow. During this phase, mature but naïve B cells expressing BCR are produced. The cells then enter the peripheral circulation and upon antigen-encounter, are stimulated via TI or TD pathways. TD-stimulated cells migrate to the GC where SHM and CSR take place. Proliferating and non-proliferating B-cells are known as centroblasts and centrocytes, respectively. Centrocytes will apoptose, unless they receive rescue signals from CD40-CD40L interaction on T cells, and further differentiate into either plasma cells (under control of Blimp-1) or memory B cells. Self-renewing B-1 cells and MZ B cells are stimulated via TI pathways and produce a rapid but transient Ab response.

1.3.2 B-cell lymphomas

Lymphoid neoplasms can be broadly divided into leukaemias or lymphomas depending on whether they predominate in the blood or lymphoid tissues. DLBCL and FL, comprise 31% and 22% of cases respectively, and so account for the majority of all lymphomas.¹⁵⁵ DLBCL is an aggressive disease which can develop de novo or secondary to an indolent lymphoma such as FL or CLL. Immunophenotypically, DLBCL express pan B-cell markers such as CD20, CD19 and CD79a and often show high Ki67 staining, indicative of a high proliferative capacity.¹⁵⁶ It is suggested that DLBCL can be divided into two subgroups based on gene expression profiling i.e. GC B- cell like, and activated B cell-like (ABC) subtypes, which show gene expression profiles similar to GC and in vitro activated peripheral B cells, respectively.¹⁵⁷ DLBCL GC subtype patients were shown to have significantly better OS than the ABC subtype in a retrospective study of patients treated with CHOP chemotherapy +/- rituximab.^{157,158} In another gene expression profiling study of DLBCL, Shipp et al. devised a 13-gene model capable of accurately predicting outcome in DLBCL.¹⁵⁹ When the same cohort of patients was examined using the gene signature proposed from the first study, no correlation with outcomes was seen.¹⁵⁷ Thus, although the subtyping of DLBCL into GC and ABC subtypes has been widely adopted, Alizadeh et al.'s model requires further confirmation, ideally in a more robust prospective study. Furthermore, due to the requirement of fresh-frozen material for gene expression profiling and the failure to confirm representative surrogate markers for paraffin-embedded tissue,^{160,161} the importance of subtyping of DLBCL is still somewhat contentious.

In contrast to DLBCL, FL is an indolent lymphoma of GC B cells. The tumour cells usually express pan B-cell markers, surface Ig, CD10, BCL-2 and BCL-6.⁸² The disease is graded from 1 to 3 depending on the number of centroblasts (morphologically defined as large immature cells with multiple distinct nucleoli) seen per high-power field by microscopy.⁸² Grade 3 is further subdivided into A or B depending on whether centrocytes are present (3A), or absent and associated with solid sheets of centroblasts (3B). Grade 3B FL is clinically

managed like DLBCL i.e. treatment with RCHOP, and not RCVP chemotherapy. Genetically, the disease is characterised by the translocation t(14;18)(q32;q21) involving the BCL-2 gene, which encodes an anti-apoptotic protein.¹⁶² The translocation t(14;18) places BCL-2 under the control of the IgH enhancer, resulting in BCL-2 over-expression and hence resistance to apoptosis. However, BCL-2 over-expression is in itself insufficient to induce FL as clonal BCL-2-Ig rearrangement products can be detected in normal B cells.¹⁶³ Furthermore, BCL-2 Tg mice carry a very low incidence of FL, indicating further mutations are required for the disease to develop.¹⁶⁴ About a quarter of patients with FL progress into a high grade lymphoma, usually DLBCL, after a median of 10 years from diagnosis, and this transformation is usually associated with treatment refractoriness and poor clinical outcome.¹⁶⁵

MCL is classified by the WHO as a disease of intermediate grade.¹⁵⁵ It is much less common than DLBCL and FL and accounts for only approximately 6% of all NHL.¹⁵⁵ In comparison to DLBCL and FL, MCL patients have a far poorer median OS of 3-4 years.(reviewed in¹⁶⁶) However, a small subset of patients have indolent disease and do not require immediate treatment.¹⁶⁷ The postulated normal counterpart of MCL is the B cell of the inner mantle zone, which comprise mostly of pre-GC cells. The translocation t(11;14)(q13;q32) between IgH and cyclin D1 genes which results in deregulation of cyclin D1 is characteristic of MCL and thought to be the primary initiating event.¹⁶⁸ Cyclin D1 is not expressed in normal B cells, and regulates the cell cycle transition from G1 to S phase by promoting phosphorylation of the cell cycle suppressor, retinoblastoma protein.¹⁶⁹ The other commonly observed mutations in MCL are inactivating mutations of the ataxia telangiectasia mutation (ATM) gene which are present in up to 75% of cases.¹⁷⁰ Like other B-cell lymphomas, MCL typically expresses pan B-cell markers such as CD19 and CD79a but it is unusual in that it is also CD5⁺ like CLL.

1.3.3 Chronic lymphocytic leukaemia

CLL is the most common leukaemia in Western countries. The incidence is approximately 2-6/100,000 persons/year and increases with age.⁸² Unlike lymphomas, CLL presents in the blood, although associated lymphadenopathy is very common. If patients present primarily with lymphadenopathy and have no detectable circulating tumour cells, a diagnosis of small lymphocytic lymphoma (SLL) is made. Differences in the expression of the adhesion molecule, lymphocyte function-associated antigen-1 (LFA-1) have been reported between both diseases, with SLL tending to show higher expression of LFA-1.^{171,172} Apart from this, there is no evidence to support other differences between SLL and CLL in terms of phenotype, biology, time to progression or response to treatment.^{82,173}

Amongst all of the B-cell neoplasms, CLL is perhaps the best characterised in terms of biology, diagnosis and prognostic markers. In part, this is likely to be due to the relatively high frequency of the disease and the ease of obtaining tumour material from the peripheral blood. To differentiate CLL from other B-cell leukaemias, an immunophenotypic scoring system is employed.¹⁷⁴ Classically, CLL cells demonstrate weak surface IgM/D, weak or negative CD79b, negative FMC7 and are positive for CD5 and CD23. Expression of each marker equates with a score of 1 and a total score of 4-5 strongly supports a diagnosis of CLL.

1.3.3.1 Prognostic markers in CLL

Despite being an indolent disease with a median survival of 10 years, individual prognosis in CLL is highly heterogeneous (reviewed in¹⁷⁵). Identification of markers that predict disease progression could assist clinicians in managing patients by allowing appropriate follow-up times and recruitment of high-risk patients into clinical trials. However, it is unknown if early treatment of selected patients as opposed to current 'expectant management' (i.e. treatment on development of symptoms or disease complications) improves overall

outcomes. The Rai and Binet clinical staging systems were first used as predictors of patient survival (**Table 2**).^{176,177} Both systems divided patients into stages of progression based on assessment of tumour mass. However, significant heterogeneity remained within each stage and both systems were unable to predict the rate of progression of patients in Rai stage 0 and Binet stage A despite the majority of patients presenting in these early stages (reviewed in¹⁷⁸).

Classification	Stage (Risk)	Minimum Criteria	Median survival (months)
Rai	0 (Low)	Lymphocytosis ¹ only	> 150
	I (Intermediate)	Lymphocytosis + lymphadenopathy	101
	II (Intermediate)	Lymphocytosis + splenomegaly or hepatomegaly	71
	III (High)	Lymphocytosis + anaemia ²	19
	IV (High)	Lymphocytosis + thrombocytopenia ³	19
Binet	A (Low)	<3 nodal sites involved ⁴	Not reached
	B (Intermediate)	≥ 3 nodal sites involved	84
	C (High)	Anaemia ⁵ and/or thrombocytopenia ⁶	24

¹Absolute lymphocyte count > 5 x 10⁹/L, ²Haemoglobin (Hb) < 110 g/L, ³Platelets < 100 x 10⁹/L, ⁴The 5 possible nodal sites are cervical, axillary, inguinal, spleen and liver, ⁵Hb < 100 g/L

Table 2: The Rai and Binet clinical staging systems for CLL

The table describes the minimum required criteria for staging of CLL under the Rai and Binet system, and associated median survival times.^{176,177}

A number of easily obtainable markers that reflected tumour mass and cellular proliferation were also found to be predictive of prognosis in CLL. Lymphocyte doubling time (LDT, i.e. the number of months required for the absolute lymphocyte count to double),¹⁷⁹ serum lactate dehydrogenase level (LDH, which reflects cell turnover and is raised in a number of malignant disorders), serum beta 2 microglobulin (β2m, a nucleated cell membrane protein associated with the α-chain of class I major histocompatibility complex (MHC))¹⁸⁰ and soluble CD23 (an unstable transmembrane low affinity IgE receptor found on lymphoblastoid B-cells)¹⁸¹ are also established prognostic markers.

Chromosomal abnormalities, identifiable in 80% of CLL cases by fluorescent in-situ hybridisation (FISH), are important prognostic markers of the disease.¹⁸²

This sensitive technique allows visual detection of the location and presence or absence of specific DNA sequences in interphase cells by using fluorescent DNA probes. This property is particularly important as CLL cells have low mitotic activity, and earlier techniques such as chromosomal banding analysis, which required cells to be in metaphase growth, only had a sensitivity of 40-50% compared to 80% with FISH.¹⁸² Most of the chromosomal abnormalities in CLL can be largely accounted for by the four abnormalities described in **Table 3**. The genes implicated in the deletion of 17p (del(17p)) and 11q (del(11q)) are well-delineated and are discussed separately in **Section 1.3.3.2**. The pathogenic genes involved in the other two chromosomal abnormalities, del(13q14) and trisomy 12, are less clear. Two specific micro-RNA genes (miR, non-coding genes involved in post-transcriptional regulation) i.e. miR15 and miR16 have been located within del(13q14)¹⁸³ and were initially reported to negatively regulate the expression of anti-apoptotic BCL-2¹⁸⁴ although this was contradicted in later investigations by another group.¹⁸⁵ Furthermore, contradictory to the initial evidence, patients with isolated del(13q14) show longer survival than patients with normal karyotype.¹⁸⁶ With trisomy 12, four candidate genes have recently been identified, although the significance of these findings is yet to be determined.¹⁸⁷ Microarray analysis and reverse transcriptase polymerase chain reaction (RT-PCR) revealed two over-expressed genes on chromosome 12 (Huntingtin interacting protein-1 related, HIP1R and myogenic factor 6, MYF6) and two under-expressed genes on chromosome 3 (purinergic receptor P2Y G-protein coupled 14, P2RY14 and CD200).

A key milestone in the understanding of CLL biology and prognostication was made when two independent groups identified the prognostic importance of the degree of SHM of the variable region of the IgH.^{188,189} Initial studies had shown that CLL cells were in germline configuration,^{190,191} corresponding to naïve B-cell V_H gene sequences, but these findings were subsequently refuted^{188,189,192} and two independent groups showed that CLL could be divided into mutated and unmutated groups based on the percentage of SHM incurred in the V_H genes, in comparison to germline sequences. Taking into account

naturally-occurring polymorphisms, a 98% cut-off value was chosen to distinguish between the two groups.^{189,193} Critically, unmutated CLL had a significantly worse outcome than mutated CLL, with a median survival of 9.8 years compared to 24.4 years ($p=0.001$).¹⁸⁹

Although useful, determination of IgV_H gene mutation status requires RT-PCR, DNA sequencing and analysis, which is technically time-consuming and expensive in routine clinical practice. Moreover, an optimal cut-off value is not known.¹⁹⁴ Therefore a surrogate marker for IgV_H mutational status was sought. Comparative genome-wide microarray profiles of mutated and unmutated CLL cases revealed that despite an overwhelming similarity between both groups, expression of several genes differed. Amongst them, 70 kDa zeta-associated protein (ZAP-70), a tyrosine kinase usually found in T cells but not in normal circulating B cells, was identified as a reliable surrogate marker for V_H gene mutation status.^{194,195} ZAP-70 expression correlates with unmutated V_H genes, and is also an independent prognostic marker.¹⁹⁴⁻¹⁹⁶ Although easily performed by flow cytometry, ZAP-70 is yet to be incorporated into routine clinical practice largely because a common assay and cut-off value to determine positive or negative expression has yet to be agreed.

CD38 is expressed widely as a signalling molecule and exists both as a transmembrane molecule and a soluble protein (reviewed in¹⁹⁷). Its precise role in signalling depends on the cell it resides in. In mature B cells, it is thought to up-regulate BCL-2 expression and hence rescues cells from apoptosis.¹⁹⁷ It was also initially thought that CD38 expression was a surrogate marker for IgV_H mutation status¹⁸⁸ but this has not been confirmed in further studies.^{198,199} However, it remains an independent prognostic marker, although weaker than IgV_H genes and ZAP-70 status.^{188,200} Furthermore, unlike ZAP-70 which is stable over time, CD38 expression varies throughout the course of the disease.²⁰¹

Marker	Prevalence in CLL (%)	Median TTP/Median OS (months)	References
Del(11q22-23)	8-18	13	186,202
Del(13q14)	10-55	92	
Trisomy 12	16-19	33	
Del(17p13)	4-7	9	
IgV _H genes	32-51 (unmutated) 49-68 (mutated)	108-109 (unmutated) vs 204- 293 (mutated)	188,189,196
ZAP-70	31 (positive) 69 (negative)	112 (positive) vs 294 (negative)	194-196
CD38	36-47 (positive) 53-64 (negative)	120-163 (positive) vs 288 – not reached (negative)	188,196,201

Table 3: The frequency and impact of prognostic markers in CLL

The table describes some of the most well-established prognostic markers in CLL, their frequency, and associated impact on survival, expressed as either time to progression (TTP) or OS.

1.3.3.2 17p and 11q deletion in CLL

Amongst all of the common chromosomal abnormalities identified, deletion of a region of 17p (del(17p)) has the most deleterious effect because the deleted region harbours the p53 tumour suppressor gene. p53 is a commonly mutated gene implicated in cancer, being described in ~50% of human malignancies.²⁰³ Within B-cell malignancies its frequency varies, with the mutation commonest in CLL (6/40 cases) and Burkitt's lymphoma (9/27 cases),²⁰⁴ but is rare in ALL,²⁰⁵ and FL.²⁰⁶ In CLL, p53 is usually inactivated through del(17p) on one allele and a missense mutation in the remaining allele.²⁰⁷ In a third of the CLL cases investigated, only one allele was affected by an isolated mutation. Both monoallelic and biallelic p53 defects are associated with an inferior survival compared to p53 wild-type cases.^{207,208}

In resting cells, p53 is inactivated by murine double minute 2 (MDM2), which binds to and blocks the transport of p53 from the cytosol to the nucleus (reviewed in²⁰⁹). MDM2 also has E3 ligase activity which ubiquitinates and promotes proteasomal degradation of p53. When single-stranded DNA damage, double-stranded DNA damage or oncogenic signals are induced, AT-related (ATR), ATM and p14ARF,²¹⁰ respectively, phosphorylate and disrupt MDM2-p53 binding. Through wild-type p53 activated fragment-1 (WAF1), p53

inhibits cyclin dependent kinase-2 and induces cell cycle arrest.²¹¹ This is proceeded by DNA repair but if the damage is irreparable, p53 induces mitochondrial-dependent apoptosis through down-regulation and up-regulation of anti-apoptotic (e.g. BCL-2) and pro-apoptotic genes (e.g. Puma), respectively.^{212,213}

Alkylating agents (e.g. chlorambucil) and purine analogues (e.g. fludarabine) are at least partially dependent on the p53 pathway for cell-killing. Thus, CLL patients with dysfunctional or deleted p53 are refractory to these agents.^{214,215} For this reason, alemtuzumab (Campath, anti-CD52 mAb) and corticosteroids are often the first-line choice in del(17p) patients (reviewed in²¹⁶). In a sub-analysis of a clinical trial which tested the safety and efficacy of alemtuzumab in fludarabine-refractory CLL patients, alemtuzumab was found to be efficacious irrespective of p53 mutation status.²¹⁷ However, the median survival in fludarabine-refractory patients was generally poorer regardless of the p53 mutational status.

Deletions in 11q are relatively common in CLL (8-18% of cases, see **Table 3**), and this region harbours the ATM gene. 11q deletion is an independent poor prognostic marker in CLL.^{218,219} CLL patients with del(11q) tend to be young and male, with more prominent constitutional symptoms, bulky lymphadenopathy and rapid disease progression. Nevertheless, a recent randomised control trial suggests that this genetic subgroup might actually be more responsive to chemo-immunotherapy than previously thought. For instance, in the recent German CLL8 trial comparing first line therapy of FCR (fludarabine, cyclophosphamide and rituximab) vs FC in 817 patients, most benefit in OS was seen with addition of rituximab in the 11q del group.²²⁰ The reasons for this particular sensitivity are currently unclear.

Interestingly, ATM mutations are not specific to CLL, and have been described in other B-cell tumours including the majority of MCL cases.^{221,222} Detailed analysis of the region (11q21-923) in 43 patients (40 with CLL, 3 with MCL) using FISH

and overlapping yeast artificial chromosome clones showed a common minimally deleted region encompassing 2-3 Mb in 11q22.3-23.1.²²³ Three genes were encoded within this minimally deleted region; RDX, FDX1 and ATM. Radixin (RDX) encodes a cytoskeletal protein important in linking actin filaments and adhesion proteins,²²⁴ and is also homologous to the NF2 tumour suppressor gene product whilst FDX1 encodes for ferredoxin-1, an iron-sulphur protein necessary for mitochondrial electron transport.²²⁵ Of the three genes, ATM is thought most likely to be responsible for disease progression in CLL due to its known association with malignancy.^{221,226,227} Ataxia telangiectasia is an autosomal recessive neurodegenerative disease characterised by absent ATM protein due to biallelic truncating ATM mutations.²²⁸ The risk of malignancy, including lymphoma is elevated in these patients.

ATM encodes a 350 kDa nuclear protein kinase which contains a PI3K-like domain in the C-terminus.²²⁹ Like several other PI3K-related proteins, ATM is involved in DNA repair.^{230,231} Double-stranded DNA breaks (e.g. induced by ionising radiation or topoisomerase II inhibitors) cause autophosphorylation of ATM and activation of the p53 pathway as described earlier.^{232,233} Therefore, ATM dysfunction is an indirect route towards p53 dysfunction.²³⁴

Differences in cell surface expression have also been observed between del(11q) and non-del(11q) subsets of CLL. However the relatively low frequency of del(11q) and hence small number of cases means that findings have been inconsistent and clear statistical significance difficult to obtain. Sembries et al.²³⁵ had a cohort of 19 del(11q) patients who demonstrated lower expression of 12/57 antigens tested. Amongst them, CD6, CD11a, CD11c, CD18, CD31, CD35, CD39, CD45, CD48, CD58, and in a few cases, CD62L and CD71 expression was reduced. All these antigens shared a common function in mediating cellular adhesion. The authors suggested that a defect in cell adhesion explained the tendency of CLL patients with del(11q) to present with widespread bulky disease. When comparing CD20 expression across all genetic subtypes, Tam et al.²³⁶ also observed that the del(11q) subgroup had the lowest CD20 expression.

The reason for this is unclear as the gene locus for CD20 (chromosome 11 at position q12-q13)²³⁷ lies outside the minimally deleted region. Although it is possible that long distance transcriptional regulators or other epigenetic factors may lie within the del(11q) region, definitive proof for of this is lacking. However it remains interesting that despite the weaker CD20 expression in the del(17q) cohort, this subset of patients might still benefit more from the addition of rituximab to standard fludarabine and cyclophosphamide (FC) chemotherapy.^{220,238}

1.4 Anti-CD20 mAb

1.4.1 Clinical applications of anti-CD20 mAb

Approval of the anti-CD20 mAb rituximab by the US FDA in 1997 has resulted in a marked improvement in the survival of a subset of B-cell malignancies.²³⁹ Whilst rituximab is efficacious as a single agent, most sustained benefit is obtained when it is used in combination with chemotherapy or radiotherapy. In fact, through this combined modality, rituximab is the only agent that has markedly improved the progression-free survival (PFS) and/or OS of FL²⁴⁰⁻²⁴³ and DLBCL²⁴⁴⁻²⁴⁶ since the introduction of chemotherapy. Long-term analysis from the first randomised trial comparing rituximab-CHOP (RCHOP) versus CHOP in in 399 patients with DLBCL demonstrated a 10-year OS of 43.5% versus 27.6% in respective arms.²⁴⁷

In other diseases such as CLL and MCL, the efficacy of single agent rituximab is weaker and relatively more transient compared to DLBCL or FL.²⁴⁸⁻²⁵⁰ Results from combined chemo-immunotherapy in MCL were similarly unimpressive,²⁵¹ but appears more promising in CLL.²⁵²⁻²⁵⁴ Although randomised controlled trials are lacking for other subtypes of B-cell neoplasms, likely due to their lower incidence, there are small case series illustrating the benefit of rituximab in marginal zone lymphoma^{255,256} and primary mediastinal large B-cell lymphoma,²⁵⁷ amongst others.

The success of rituximab is now being transferred to the treatment of autoimmune disorders. Although rheumatoid arthritis is the only other licensed indication for rituximab at present, there is growing evidence of its efficacy in a diverse range of autoimmune disorders such as autoimmune cytopenias,²⁵⁸ myasthenia gravis²⁵⁹ and Wegener's granulomatosis.²⁶⁰

Despite the clinical success of rituximab, the function of the CD20 antigen and the mechanisms of action of anti-CD20 mAb are relatively less well-understood. The following sections discuss the current knowledge to date.

1.4.2 The CD20 antigen

CD20 was one of the first non-Ig related, B-cell specific antigens to be identified²⁶¹ hence its original designation as B1. B1 was shown to be expressed at a high density on >95% of normal and malignant B cells²⁶¹⁻²⁶³ and is expressed in B cells as early as the pre-B cell stage but is lost upon plasma cell differentiation.²⁶⁴ B1 was subsequently designated as CD20 in the 2nd International Workshop on Human Leucocyte Differentiation Antigens in Boston, in 1984.²⁶⁵

CD20 is a 33 kDa non-glycosylated phosphoprotein with a 297 amino acid polypeptide chain.²⁶⁶ Human CD20 is 73% homologous to murine CD20 with the most homology observed in the transmembrane regions.²⁶⁷ The polypeptide chain has 4 hydrophobic transmembrane regions, 2 extracellular loops and intracellular -NH₂ and -COOH termini.^{262,266,267} The larger extracellular loop is approximately 43 amino acid residues long and lies between the third and fourth transmembrane domain.²⁶⁸ Through site-directed mutagenesis, the alanine-x-proline motif at positions 170-172 in the larger extracellular loop has been shown to be critical for the binding and activity of most anti-CD20 mAb, including B1, rituximab and Bly1-the precursor of GA101, a new anti-CD20 in clinical development.²⁶⁸ Three known anti-CD20 mAb are excluded from this

general rule: ofatumumab, 1F5 and 2H7. Ofatumumab binds to two discontinuous epitopes in the smaller and larger extracellular loops. This will be discussed in further detail in **Section 1.5.2**. The specific epitope of 1F5 is still unknown, whereas 2H7 binding is dependent on isoleucine-asparagine-x-x-asparagine at positions 162-166 and the preservation of CD20 in an oligomeric complex.²⁶⁸ It is not yet known how these epitope differences translate into differences in biological effects. For example, whilst tositumomab shares most similarity with rituximab in terms of epitope reactivity, the in vitro effects of both Ab differ greatly, as will be discussed in **Section 1.5**.

CD20 exists as a hetero-oligomeric complex,^{269,270} and associates with other molecules such as MHC Class I, β 2M, MHC Class II-DR and -DG, CD53, CD81, CD82,²⁷¹ CD40²⁷² and the BCR.²⁷³⁻²⁷⁵ Of all the molecules investigated, the association between CD20 and BCR has been given the most attention. Deans' group demonstrated that the BCR and CD20 exist in close proximity in unstimulated cells but dissociate upon BCR stimulation.^{273,274} Similarly, recent evidence shows that CD20 provides the store-operated cation channel for the BCR through its association with this molecule and so presumably helps to regulate cytoplasmic calcium levels after antigen engagement.²⁷⁵ It was also demonstrated that the calcium flux, and ERK1/2, BLNK and SLP-76 activation elicited by the engagement and further cross-linking of CD20 is itself dependent on BCR expression, indicating that CD20 signals largely through its association with, and hijacking of the BCR. These findings are consistent with Uchida et al.'s work which demonstrated that CD20 -/- mice demonstrated reduced calcium flux upon either IgM or CD19 cross-linking.²⁷⁶ The latter receptor is known to act as a signalling molecule which transduces signals initiated through the BCR.²⁷⁷ Aside from physical coupling and calcium signalling, other similarities have also been reported between CD20 and BCR. Ligation of each receptor was found to induce expression of similar genes,^{278,279} and cytokine secretion produced by stimulation of either receptor could be abrogated by Syk inhibition in human cell lines.²⁷⁹ In another study using primary FL cells, Irish et al. observed that CD20 expression varied within individual cases, in a subset of

patients.²⁸⁰ Interestingly, the subset of low CD20-expressing cells also signalled poorly through the BCR. However this relationship was not exclusive as some high CD20-expressing cells also had defective BCR-signalling. Altogether, this data suggests a close connection between the CD20 and BCR, and further investigations to elucidate the link between the two molecules are ongoing.

Despite intensive study, no natural ligand for CD20 has been shown and CD20-deficient mice^{276,281} only manifest mild phenotypic changes such as lower IgM expression and CD19-induced calcium flux levels. Recently, a case report described the first CD20-deficient human being.²⁸² This patient presented at 4 years of age with recurrent bacterial infections and IgG deficiency. Upon further investigation, she was found to have a homozygous compound mutation affecting the 5' site of exon 5 of the CD20 gene. Normal circulating T, B and NK cell numbers were observed and BCL-6 and BCL-xL retroviral-transduced B cells from the patient demonstrated normal proliferation and calcium signalling on BCR cross-linking. Significantly, the authors found a reduction in TI Ab responses. The data also showed a reduction in class-switched memory B cells but the significance of this was not commented on. Although CD20 deficiency was clearly present, other causes of immune deficiency were not explored and therefore the abnormalities may not necessarily be solely due to CD20 deficiency. Perhaps more convincingly, the authors demonstrated that CD20 $-/-$ mice also demonstrated impaired TI Ab responses.

1.5 Effects of anti-CD20 mAb

Despite the uncertainty regarding CD20 function in vivo, ligation of CD20 with anti-CD20 mAb in vitro consistently produces a number of well-defined effects depending on the cells and mAb used.²⁸³⁻²⁸⁵ The main properties and mechanisms of action of anti-CD20 mAb are discussed in detail below but a variety of other features have also been reported. For instance, 1F5 has been shown to induce cell cycle transition from the G₀ to G₁ phase whilst

tositumomab causes cell cycle arrest at G₁²⁸⁶⁻²⁸⁸ and down-regulation of BCR²⁸⁹ and CD23 receptors.²⁹⁰

Work from our laboratory has indicated that anti-CD20 mAb can be grouped into two different classes depending on their in vitro activity in various assays.²⁸³⁻²⁸⁵ This distinction is based upon the ability of the mAb to redistribute CD20 into Triton-X 100 insoluble lipid rafts, induce homotypic adhesion, elicit CDC and/or direct cell death.^{283,285} Lipid rafts are areas of the cell membrane which are enriched in sphingolipid, cholesterol and GPI-anchored proteins, which allow organisation of the membrane into different functional compartments (reviewed in²⁹¹). Type I mAb such as rituximab and ofatumumab are more potent at translocating CD20 into lipid rafts and inducing CDC, whereas type II mAb such as tositumomab and GA101 are more effective at inducing homotypic adhesion and direct cell death induction.²⁹² As mentioned in the preceding section, early work by Polyak and Deans suggested that there were no differences in the epitope bound by type I and II mAb.²⁶⁸ More recent work has demonstrated that while both classes of mAb bind to overlapping epitopes, the epitope bound by type II mAb appear to be shifted to the carboxy terminus i.e. type I binds to amino acids at positions 162-176 and type II, 167-178.²⁹³ It is still uncertain if this minor difference in epitope binding can account for the distinction between type I and II mAb. Also discussed earlier, there are other type I mAb such as ofatumumab, which bind to entirely different regions. Klein's work was primarily focused on GA101, the first unconjugated type II mAb to be tested in clinical trials.²⁹³ GA101 is produced from murine mAb B-Ly1, which is further humanised by grafting the CDR regions of the murine mAb onto human light and heavy chain frameworks. Furthermore, the Fc region of GA101 has been defucosylated to increase its affinity for Fc receptors (discussed in further detail in Section 1.5.1). Interestingly, the type II nature of the mAb was strengthened by replacement of leucine in Kabat position 11 by valine, which occurred inadvertently during humanisation. Klein et al. showed that the valine replacement endowed a wider (30°) elbow angle to GA101, which may be a contributing factor the distinction of type I and II mAb. However, this is clearly

not the only determining factor as when the same mutation was generated in rituximab, no type II characteristics were observed.

Both type I and type II appear to have equal efficacy in inducing ADCC, with the exception of GA101 which has enhanced affinity to Fc receptors on innate immune effector cells.^{293,294} ADCC, CDC, induction of direct cell death, and to a much lesser extent, the induction of T-cell mediated immunity are the primary mechanisms thought to be responsible for the clinical efficacy of rituximab, and will therefore be discussed separately in the following sections (Fig. 5).

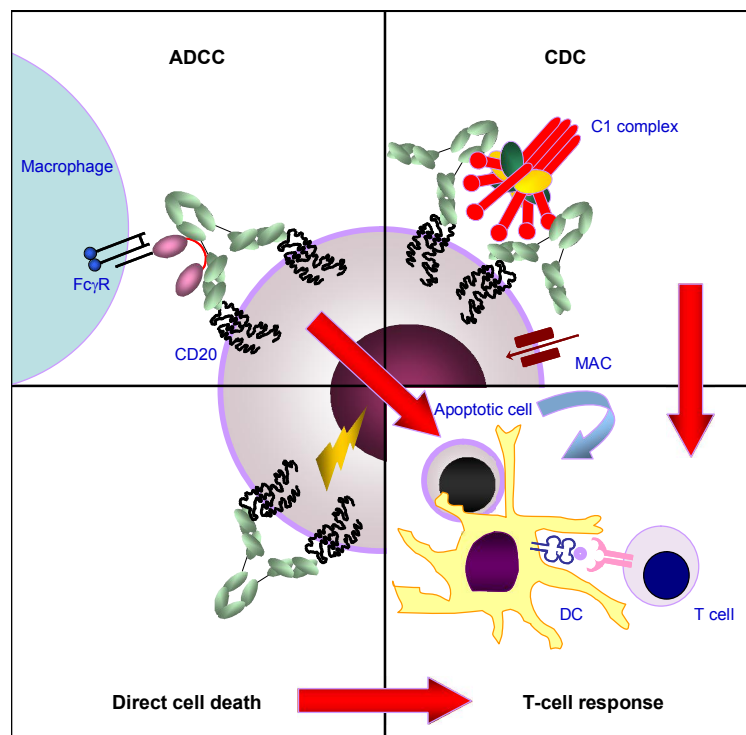


Figure 5: The effector mechanisms of anti-CD20 mAb

The figure illustrates the proposed mechanisms of action of anti-CD20 mAb. ADCC is mediated by Fc:FcγR interaction resulting in lysis or phagocytosis of opsonised target cells by immune effector cells such as macrophages, NK cells and possibly neutrophils. In CDC, the classical complement pathway is activated. C1q engages the glycan region on the C_H2 domain, leading to activation of the classical complement cascade and ultimately, formation of a membrane attack complex (MAC) on the target cell. Direct cell death induction is caused by the direct signal transduction induced by binding of anti-CD20 mAb to its target. Cell death from all three pathways promotes uptake of tumour antigen by DC and subsequent cross-presentation with MHC class I molecules to prime CTL.

1.5.1 Ab-dependent cellular cytotoxicity (ADCC)

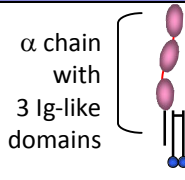
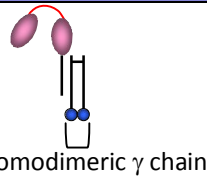
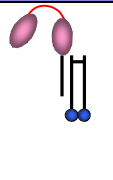

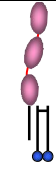





The interaction between the Fc domain of a bound Ab and Fc receptors (FcR) expressed on effector cells such as macrophages and NK cells allows Ab-directed killing of target cells. This process is termed ADCC and the specific pathway of cell-killing depends on the immune effector cell engaged e.g. NK cells and eosinophils kill cells via perforin-mediated membrane damage whereas macrophages have been shown to elicit ADCC via phagocytosis predominantly.^{295,296}

1.5.1.1 The role FcγR in immunotherapy

Prior to the discussion of anti-CD20 mAb mediated-ADCC, the human Fc gamma receptors (FcγR) will be reviewed since they play a crucial role in manipulating the outcomes of mAb therapy through ADCC.²⁹⁷ In both mice and humans, the FcγR family comprises three main classes of activatory receptors and a single inhibitory receptor (**Table 4**). Murine FcγRIII and FcγRIV are thought to represent homologues of human FcγRIIIa and FcγRIIIa, respectively, based on similarities in the sequences of their extracellular domains (reviewed in²⁹⁸). These receptors are jointly expressed in a variety of haematopoietic cells, with the exception of T cells, which typically do not express any FcγR, and NK cells which only express activatory FcγR.²⁹⁹ Human and murine B cells were originally shown to express only the inhibitory FcγRII (FcγRIIb),³⁰⁰ but some groups have also reported the expression of activatory FcγRII (FcγRIIIa) as well in human cells, although usually in low levels.^{301,302} Most of these later studies were performed using human B cell lines as opposed to primary cells, which may explain the disparate results. Furthermore, all the data has been generated from messenger RNA (mRNA) expression analyses due to the lack of specific anti-FcγRIIIa or anti-FcγRIIb mAb. Clearly, this does not equate to protein expression on the cell surface, which is more relevant functionally.

As a general rule, activatory FcγRs promote cellular activation whereas inhibitory receptors have the opposite effect. Thus, the balance of engagement

of inhibitory and activatory FcγRs on an immune effector cell by the Fc domain of Ab, determines the eventual response triggered, e.g. macrophage phagocytosis or neutrophil activation.

Mouse		Activatory FcγR			Inhibitory		
		FcγRI CD64	FcγRIII CD16	FcγRIV	FcγRIIb CD32b		
Structure							
		α chain with 3 Ig-like domains	Homodimeric γ chain containing ITAMs		α chain containing ITIM		
Affinity		High	Low/medium		Low		
Murine IgG subtype specificity ³⁰³		2a=2b>>1=3	2b>2a>1>>3	2a and 2b	1=2b>>2a=3		
Murine Cell	Mon	+	+	+	+		
	Neutrophil		+	+			
	NK		+				
	DC	+	+				
	B cells				+		
Human		Activatory FcγR					Inhibitory
		FcγRI CD64	FcγRIIa CD32a	FcγRIIc CD32c	FcγRIIIa CD16a	FcγRIIIb CD16b	FcγRIIb CD32b
Structure							
					GPI anchored (non-signalling)		
Affinity		High	Low/Medium			Low/Medium	
Human IgG subtype specificity ³⁰⁴		1>3>4	1>>3>2=4	4>3>1>2	3>>1>>4>2	1>3	
Human allelic variants (Affinity or activity)			131H (High) 131R		158V (High) 158F (Lower)	NA1 NA2 (similar affinity in both)	
						232T (impaired activity) 232I (normal activity)	
Human Cell	Mon	+	+		+	+	
	Neutrophil	+/-	+			+	
	NK			+	+		
	DC	+	+		+	+	
	B cells					+	

Mon=monocyte/macrophage

Table 4: Affinity, allelic variants and distribution of human and mouse FcγRs

The table describes the structure of human and mouse FcγRs, their affinity to IgG, preferential subtype specificity, common and significant allelic variants and their expression on haematopoietic cells.^{299,305,306}

In general, FcγRs are type I transmembrane glycoproteins and can be divided into an extracellular ligand-binding α subunit comprising two or three Ig-like domains and a homodimeric intracellular signal-transducing γ-chain,³⁰⁷ which serves to increase the binding affinity of the receptor for the ligand.^{307,308} The exceptions are the human neutrophil receptor, FcγRIIIb, which is glycosylphosphatidylinositol-anchored and does not possess an intracellular domain, and FcγRII receptors, where the signalling component lies within the α chain (reviewed in³⁰⁹). Activatory FcγRs are characterised by an immunoreceptor tyrosine-based activatory motif (ITAM)^{310,311} within the γ chain, or in the case of FcγRIIa/c, within the α chain. In contrast, FcγRIIb possesses an immunoreceptor tyrosine-based inhibitory motif (ITIM)³¹²⁻³¹⁴ within the cytoplasmic region of the α chain.

Ligation of the extracellular domain of ITAM-containing activatory FcγR leads to phosphorylation of tyrosine residues in the ITAM by Src family kinases (e.g. Lyn).³¹⁵ This leads to recruitment and activation of Syk family kinases. Syk phosphorylates adaptor molecules such as BLNK, LAT and SLP-76, thus facilitating signalling through PI3K and phosphatidylinositol 3,4,5 triphosphate (PIP₃) production.³¹⁶⁻³¹⁸ PIP₃ recruits phospholipase Cγ (PLCγ) which activates further downstream signalling molecules and finally, release of calcium from the endoplasmic reticulum.^{319,320} In addition to the calcium-dependent pathways, ITAM signalling also involves other signal-transduction molecules such as son of sevenless homologue (SOS) and Bruton's tyrosine kinase (BTK) which activates the Ras-Raf-Mitogen-activated protein kinase (MAPK)-ERK pathway (reviewed in³⁰⁶).

In order for FcγRIIb to deliver a dominant negative signal and inhibit an ITAM-containing activatory receptor (e.g. BCR), both receptors need to be co-ligated by an extracellular ligand (e.g. an immune complex) capable of binding the two receptors simultaneously.^{312,321} Co-aggregation of both molecules is followed

by selective phosphorylation of the ITIM at tyrosine residue 309.³¹³ The inhibitory activity of FcγRIIb is entirely dependent on this tyrosine residue and a point mutation at position 309 nullifies the inhibition.³¹³ Co-aggregation of FcγRIIb enables Src family protein kinase Lyn,³²² to phosphorylate and recruit SH2-containing inositol polyphosphate 5-phosphatase (SHIP), which hydrolyses 5-phosphate of inositol (1,3,4,5) phosphate thereby leading to dissociation of BTK and inhibition of calcium mobilisation.³²³

The inhibitory FcγR, FcγRIIb has been shown by many different groups to play an important role in the regulation of immune tolerance. As a result of alternative mRNA splicing, three human and mouse isoforms of FcγRIIb have been described.³⁰⁰ In humans, the IIb1 isoform has 19 amino acid residues less from the amino terminal end compared to the IIb2 isoform. The IIb3 isoform lacks 7 amino acids compared to IIb2, which contribute to the hydrophobic domain, rendering it a soluble receptor. Detailed knowledge concerning the function and relationships of the 3 isoforms is sparse, in particular with relation to the IIb3 isoform. The distribution of human IIb1 and IIb2 isoforms appear to differ in distribution when compared to murine isoforms. Mouse B cells only express the IIb1 isoform,³²⁴ whereas both IIb1 and IIb2 have been identified in human B cell lines.^{301,302} Both isoforms also appear to differ in their endocytic ability. Miettinen et al.³²⁴ first demonstrated that murine IIb2, but not IIb1 isoform, were capable of endocytosis. Similarly, another group demonstrated that the human IIb2 isoform was more efficient at endocytosis than the IIb1 isoform.^{302,325} To complicate matters, others have also not detected a difference in endocytosis between the murine isoforms.³²⁶

On B cells, co-ligation of FcγRIIb and the BCR results in inhibition of BCR-mediated signalling and thus, reduced cellular proliferation^{313,327} whereas isolated FcγRIIb homo-aggregation in B cells has been reported to cause apoptosis.³²⁸ In the GC, where selection of high affinity, somatically mutated, immunoglobulin-bearing B cells takes place, engagement of both BCR and

FcγRIIb by immune complexes on FDC, and recruitment of SHIP, is crucial for B cell survival.³²⁸ Isolated engagement of FcγRIIb results in failure to recruit SHIP and apoptosis of B cells.

On DC, the FcγR have two distinct roles, first to mediate antigen uptake and presentation, and the second to modulate DC maturation. Activatory FcγRI and FcγRIII endocytose IgG-opsonised particles via a proteolytic degradative pathway to facilitate T cell priming^{329,330} whereas FcγRIIb (IIb2 isoform) endocytoses opsonised antigen via a distinct non-degradative pathway to stimulate TI B-cell responses.³³¹ However, antigen uptake is in itself insufficient to initiate immune responses and a fully mature DC is required for optimal T-cell priming.³³² The activatory FcγRs promote maturation and activation of DCs through a Syk-dependent pathway, whilst FcγRIIb favours an immature or tolerogenic state.^{333,334}

Evidence from several different groups has indicated that reduced FcγRII expression is associated with increased autoimmune complications (e.g. glomerulonephritis, collagen-induced arthritis) in FcγRII -/- murine models,^{335,336} and FcγRIIb dysfunction has been directly linked to systemic lupus erythematosus (SLE)^{337,338} and rheumatoid arthritis (RA) in humans.³³⁹

Fc:FcγR interactions and activatory FcγR in particular, are crucial to the efficacy of anti-CD20 mAb immunotherapy.^{294,297,340,341} In contrast, the importance of the inhibitory FcγRIIb in regulating mAb immunotherapy is less certain, and its clinical impact still unproven in human studies. Published data so far hints that FcγRIIb may have two separate effects in malignancy. First, FcγRIIb over-expression has been shown to increase tumourgenicity (measured by tumour incidence and latency) in murine models injected with polyoma-virus transformed fibroblast (3T3) cells.³⁴² Moreover, evidence from other groups suggest that disease progression in melanoma³⁴³ and FL³⁴⁴ is associated with increased FcγRIIb expression. However, the mechanism by which FcγRIIb

increases tumourigenicity is unclear and definitive proof of FcγRIIb as a marker of disease progression is currently lacking. Second, Clynes and Ravetch demonstrated that in FcγRII -/- murine xenograft models, breast and lymphoid tumours were more sensitive to mAb therapy,²⁹⁷ an effect which was attributed to enhanced ADCC in the absence of inhibitory signalling. Among B-cell malignancies, FcγRIIb is expressed on CLL/SLL and MCL, and to a lesser extent on FL and DLBCL.³⁴⁴ Attempts have been made to correlate FcγRIIb expression with rituximab-CHOP chemotherapy in DLBCL without success.³⁴⁵ As with activatory FcγRs, polymorphisms influencing the activity of FcγRIIb have also been found^{346,347} with the 232I allele inhibiting BCR-mediated calcium flux more efficiently than the 232T allele. However, Weng and Levy³⁴⁸ also failed to establish a correlation between these polymorphisms and response to rituximab therapy in FL patients.

1.5.1.2 Anti-CD20 mAb mediated ADCC

The first evidence that Fc:FcγR interactions are critical for the efficacy of anti-CD20 mAb came from Clynes and Ravetch²⁹⁷ who showed that rituximab treatment of subcutaneous Raji xenografts was fully dependent upon the activatory FcγR. Supportive evidence in humans comes from clinical studies which demonstrated that patients with higher affinity allelic variants of FcγRIIIa responded better to treatment with rituximab than those with lower affinity alleles.³⁴⁹⁻³⁵¹ 131 histidine (H) or arginine (R) polymorphisms in FcγRIIIa have also been found to influence responses to rituximab in FL,³⁵⁰ but the reason for this is unclear as the improved affinity with 131 H/H is related to the IgG2a isotype and less so to the IgG1 isotype carried by rituximab. Interestingly, and in marked contrast to the above, no association was shown between FcγR polymorphic variation and response in CLL³⁵² or MCL patients.³⁵³ This indicates that either requirement for Fc:FcγR interaction may vary between diseases, as may the dominant effector mechanisms, or that the studies are statistically under-powered.

In syngeneic mouse model systems, using either murine anti-mouse CD20 mAb in wild-type mice³⁴⁰ or chimeric/murine anti-human CD20 mAb in human CD20 Tg mice,^{354,355} complete absence of normal B-cell depletion was observed in mice lacking the common γ chain, further supporting the absolute requirement for activatory Fc γ R interactions in vivo. Recently, the ability of anti-mouse CD20 mAb to deplete syngeneic E μ -Myc tumour cells was also shown to be dependent on activatory Fc γ R.³⁵⁶ However, it remains to be determined which of the Fc γ R-expressing immune effector cells are critical. In the mouse there is good agreement that monocytes/macrophages are the key effectors required for deleting either normal or malignant B-cells with anti-CD20 mAb.^{340,354-356} As such, depleting macrophages using liposomal clodronate^{355,357} resulted in decreased mAb efficacy^{340,354-356} whilst removal of neutrophils or NK cells had no impact.

In contrast most evidence from human in vitro experiments suggests that monocytes/macrophages are less important but that NK cells are the prominent effector cells in ADCC.³⁵⁸⁻³⁶⁰ Furthermore, there is a wealth of evidence from studies of other cancers suggesting that macrophages support tumour progression and metastases by releasing angiogenic factors and suppressing host anti-tumour responses (reviewed in³⁶¹). Different groups have also demonstrated an association between increased numbers of tumour-associated macrophages with poorer outcomes in a variety of cancers including FL.³⁶² However it should be noted that these initial clinical studies have been performed in patients treated by chemotherapy alone. In another study which assessed the prognostic value of tumour-associated macrophages in chemotherapy-treated patients with or without addition of rituximab, the macrophages only had predictive value in the chemotherapy-only arm.³⁶³ Altogether, these findings appear discordant, but may be reconciled as follows: First, macrophages are functionally plastic and can have both pro- and anti-tumour effects,³⁶¹ so the sum of their effects is likely to be dependent on

the specific subsets of macrophages present. Second, clinical studies of outcome measures do not only measure tumour pathogenesis or in this case, the contribution of macrophages to tumour growth, but are also complicated by response to therapy, which are distinct from each other.

Similarly, there is no evidence whether FcγRIIIb-expressing neutrophils, the predominant leucocytes in peripheral blood, play a role in providing therapy in vivo. Cartron et al.³⁶⁴ found no correlation between neutrophil phagocytosis (in patients with different FcγRIIIb polymorphisms) and response to rituximab. However, they did observe high response rates in FL patients given GM-CSF and rituximab, which could be attributed to increases in monocyte, granulocyte, and DC populations.³⁶⁵ Recently, Shibata-Koyama et al.³⁶⁶ demonstrated enhanced phagocytosis of lymphoma cells in human whole blood using a modified, non-fucosylated rituximab reagent with enhanced affinity for FcγRIIIb on neutrophils. Therefore, it is possible that neutrophils have a role in the functioning of rituximab in vivo, which may be boosted by additional manipulations, such as GCSF treatment or defucosylation of the mAb Fc domain,³⁶⁷ but definitive proof is currently lacking.

Gong et al.³⁵⁴ also investigated the relative importance of the various B-cell compartments in relation to B-cell depletion by anti-CD20 mAb in human CD20 Tg mice. For instance, despite treating mice by an intraperitoneal route, peritoneal B cells were slowest to deplete, compared to B cells in the lymph nodes (faster) and peripheral circulation (fastest). In addition, within secondary lymphoid organs, follicular B cells were more sensitive than MZ cells and GC B cells even more resistant. They also demonstrated that surgical limitation of hepatic blood supply correlated with lower B-cell depletion, underscoring the role of hepatic Kupffer cells and the reticuloendothelial system for maximal mAb efficacy. Altogether, they postulated that differences in depletion kinetics between different tissues were, for the most part, simply a reflection of the access of those B cells to the vasculature and that B-cell targets with slower recirculation kinetics were more resistant to depletion simply due to reduced

access to the reticuloendothelial system's effector cell populations. Similar studies are clearly impossible in humans, so it is not known whether the same systems operate. For this reason and the fact that there are relatively few macrophages in peripheral blood, the findings that NK cells are the key effector in human studies should be treated with caution. However, the need for lymphoma cells to traffic out of solid tumour deposits and pass over the reticuloendothelial system might help explain some of the slow and late responses to rituximab. This explanation is a feasible alternative to the vaccinal effect (discussed in **Section 1.5.4**) used to reason the delayed responses seen with rituximab.

Apart from circulatory kinetics, each B-cell compartment's sensitivity to depletion may be influenced by microenvironmental differences.³⁵⁴ To illustrate an example, BAFF, a member of the TNF superfamily, is secreted by myeloid cells and is critical for survival of B cells (reviewed in³⁶⁸ and also discussed in **Section 1.3.1**). As such, inhibition of the BAFF receptor on B cells in a human CD20 Tg mouse model promoted B-cell depletion with mAb over and above treatment by either agent alone.³⁵⁴ The clinical significance of BAFF is supported by a retrospective clinical study which demonstrated that in DLBCL, high serum BAFF levels were predictive of poorer responses and survival in patients treated with RCHOP.³⁶⁹ Other extrinsic factors that may also influence B-cell depletion are the complement defence molecules, which will be discussed in the following section.

1.5.2 Complement-dependent cytotoxicity

The classical pathway of the complement system is initiated when antigen-bound Ab of particular isotypes bind to the complement component, C1 (see **Fig. 6**). In humans, IgM, IgG1, IgG2 and IgG3, but not IgG4, are capable of activating the classical pathway, although to variable degrees.³³ The classical component C1, is a Ca²⁺ ion-stabilised macromolecular complex comprising C1q and two molecules of C1r and C1s. Activation of the pathway requires the

multiglobular C1q to bind a minimum of two juxtaposed Fc regions (C_H2 domain). Therefore, pentameric IgM is more effective at activating complement than monomeric IgG. Conformational change in C1 is followed by activation of a cascade of other components of the classical pathway such as C2, C4, C3, and C5, which ultimately leads to generation of a MAC which forms a pore in the membrane of the target cell, thus potentially causing lysis.

The complement cascade is closely regulated by a number of complement defence molecules, and some of which are shown in **Fig. 6**. For example, C1 inhibitor is a soluble protein which regulates C1, whilst the membrane protein CD55 inactivates C3 and C5 convertases by binding to C3b and C4b³⁷⁰ and CD59 binds to C8 and C9, thus preventing formation of a MAC.³⁷¹

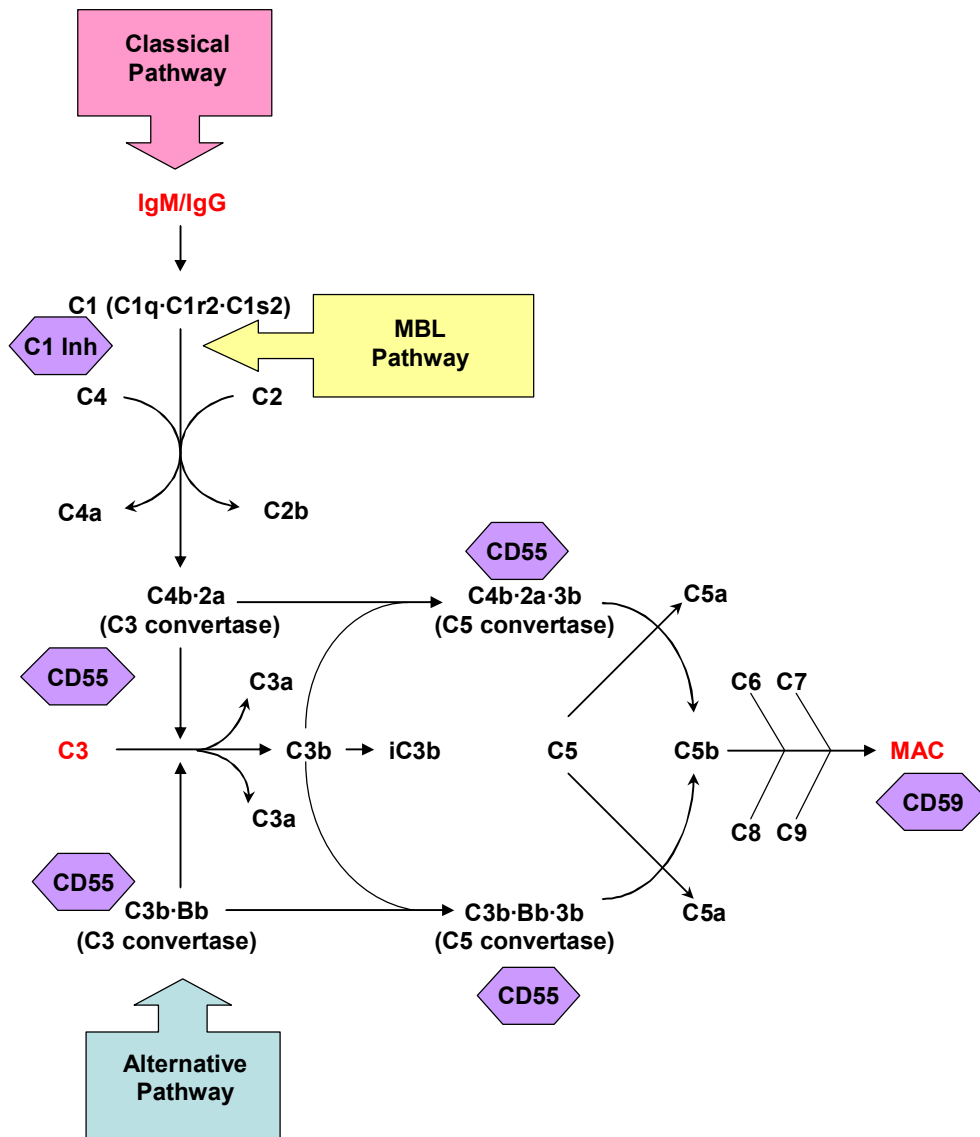


Figure 6: The classical complement pathway

The complement cascade comprises three distinct pathways; the classical, mannose-binding lectin (MBL) and alternative pathways. The classical pathway is initiated by the binding of C1q, a component of C1 complex, to the C_H2 region of the Fc domain of an antigen-bound Ab. Subsequently, C1s cleaves C4, then C2, resulting in the formation of C3 convertase. The MBL pathway is initiated when host MBL binds to mannose and fucose residues on a suitable surface such as a pathogen. The alternative pathway is constitutively activated at a low rate and is amplified on C3 cleavage. All three pathways converge at C3. C3 is cleaved by C3 convertase into C3a and C3b. C3b is an acceptor site for C5, which initiates formation of MAC. The complement cascade can be inhibited at various points by the C1 esterase inhibitor (C1 Inh), CD55 (decay accelerating factor) and CD59 (membrane inhibitor of reactive lysis). Illustration based upon^{372,373}.

Several different groups have shown that type I anti-CD20 mAb such as rituximab are capable of binding C1q and inducing potent CDC.^{284,359,374,375} It is clear that CD20 is an excellent target for CDC against numerous cell types in vitro probably at least in part because of its high expression and the proximity of the mAb binding epitope to the plasma membrane.³⁵⁹ Furthermore, type I mAb's ability to redistribute CD20 into Tx-100 insoluble lipid rafts allows clustering of the mAb and enhancement of its ability to capture C1q and elicit CDC.^{284,285} Support for CDC as a key effector mechanism comes from several lines of evidence. Firstly, high levels of complement defence molecules have been associated with rituximab resistance.^{376,377} Secondly complement is consumed in vivo following rituximab infusion, and replacement of the consumed components restores the activity of ex vivo rituximab in CDC assays,³⁷⁸ a process which may benefit patients.^{379,380} Similarly, a number of animal models have clearly shown that complement inactivation/deficiency results in reduced anti-CD20 mAb activity in vivo.^{285,381} However, it should be noted that syngeneic human CD20 Tg animal models of normal B cell depletion have shown little to no requirement for functional complement in the activity of rituximab.^{294,354,355} Furthermore, Weng and Levy³⁸² demonstrated that the level of expression of the complement defence molecules CD46, CD55 and CD59 on FL cells did not correlate with responses to rituximab.

To add a further layer of complexity, recent evidence suggests that complement may actually be disadvantageous to the efficacy of rituximab. Binding of rituximab to CD20 promotes complement activation and deposition of active complement components such as iC3b.³⁸³ C3b deposition has been shown to block the interaction between the Fc domain of rituximab and FcγRIIIa on NK cells, hence impairing ADCC.³⁸⁴ Further supportive evidence of the detrimental role of complement comes from a recent hypothesis-generating study,³⁸⁵ which investigated the impact of C1qA polymorphisms on the efficacy of rituximab. In this study of 133 patients, the A polymorphism which leads to low C1q levels was shown to correlate with enhanced rituximab responses in FL, whereas the G (high C1q expressing) allele correlated with a poorer prognosis. Although

suggestive, C1q and complement activation also has numerous other effects in vivo including a role in the phagocytosis of apoptotic bodies³⁸⁶ and effects on APC maturation and function^{387,388} that may contribute to the efficacy of rituximab. Furthermore, it is recognised that C5a is a potent chemo attractant of inflammatory cells³⁸⁹ and up-regulator of FcγRIIIa on monocytes and macrophages.³⁹⁰ On consideration of all of these data, there is little direct evidence to suggest that CDC provides a substantial positive effect on rituximab-mediated depletion of B cells in humans. However, its effects in vivo are clearly complex and although unproven, certain direct or indirect effects may be beneficial to rituximab therapy.

A fully human anti-CD20 mAb, ofatumumab, was recently approved for treatment of fludarabine and alemtuzumab-resistant CLL. Ofatumumab was generated by immunising human Ig Tg mice followed by splenocyte fusion and conventional hybridoma production. Like rituximab, it is a type I reagent but it differs in that it shows much higher affinity (slower off-rate) for CD20, recognises a distinct epitope and displays greater CDC activity.³⁵⁹ As a consequence, ofatumumab is able to lyse Raji cells, which are relatively resistant to CDC with rituximab.³⁵⁹ Others have also shown that ofatumumab has superior CDC activity when compared to rituximab in primary DLBCL cells isolated from chemotherapy-resistant patients and that it is also less sensitive to the actions of complement defence molecules.³⁹¹ It is proposed that the critical element involved in the potent CDC activity of ofatumumab is related to its unusual binding site on CD20.^{392,393} As previously mentioned in **Section 1.4.2**, ofatumumab recognises a region of the large extracellular loop of CD20 closer to the NH₂-terminal end of the molecule and also interacts with the smaller extracellular loop (**Fig. 7**). This proximal membrane binding, for reasons which are unclear³⁵⁹ allows ofatumumab (and other fully human CD20 mAb raised in this series) to bind 3 times more C1q at the cell surface than rituximab.³⁵⁹ Such an improvement could be due to the membrane-proximal epitope which promotes Ab:Ab interactions leading to IgG multimers at the cell surface which itself increases C1q binding. Other mAb which bind close to the cell membrane,

such as alemtuzumab (anti-CD52), are also potent in CDC against CLL.³⁹⁴ It is also possible that membrane-proximal epitopes enhance CDC activity because activated complement proteins, which are hydrolysed very rapidly, are more efficiently coated onto the target membrane. This proposition has recently been strengthened with evidence showing that ofatumumab binding is associated with higher C3b deposition and more rapid cell killing than rituximab.³⁹⁵ The clinical use of ofatumumab should assist us in the understanding of the contribution of CDC to the B-cell depleting capacity of anti-CD20 mAb.

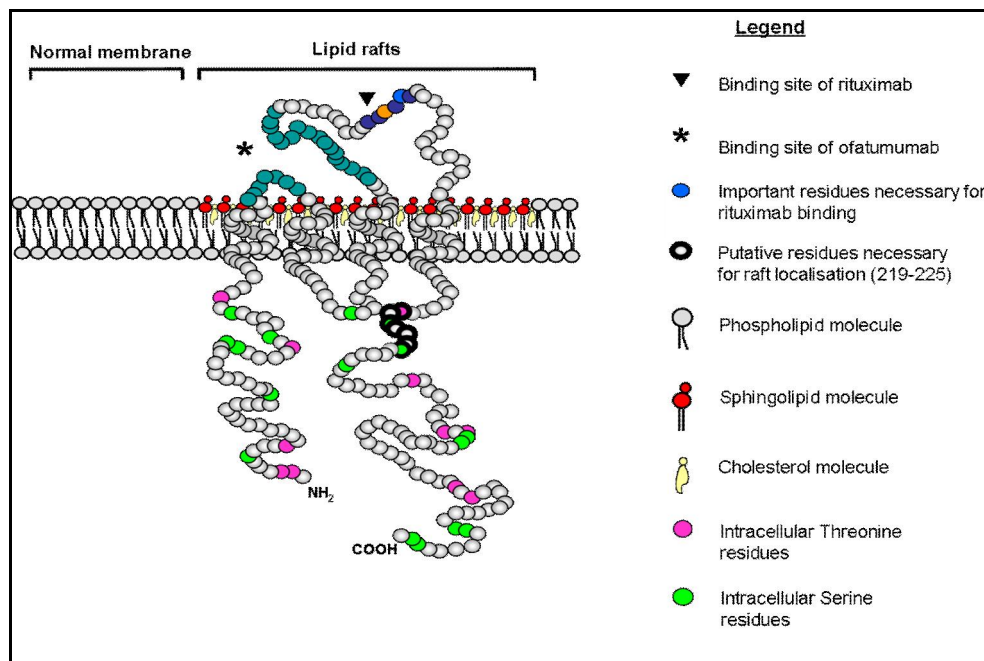


Figure 7: Illustration of the CD20 molecule and anti-CD20 mAb binding sites

The figure illustrates the structure of a CD20 molecule and the different epitopes bound by rituximab and ofatumumab (adapted from³⁹⁶). Ofatumumab binds to a more proximal extracellular loop than rituximab. Tositumomab and GA101 also bind to the same site as rituximab.

1.5.3 Direct cell death induction

Compared to ADCC and CDC, the ability of anti-CD20 mAb to induce direct cell death is still somewhat controversial. Cell death can be classified into 12 different types depending on a combination of features.³⁹⁷ For instance,

'apoptosis' morphologically describes cells that manifest a reduction in cell volume (pyknosis), cytoplasmic membrane blebbing, chromatin condensation, nuclear fragmentation (karyorrhexis) and phagocytosis by neighbouring phagocytes. This is in contrast to autophagy (no chromatin condensation but associated cytoplasmic vacuolisation), and necrosis (increased cell volume, plasma membrane rupture, loss of intracellular contents and associated inflammation), amongst others. Of interest, the Nomenclature on Cell Death 2009³⁹⁷ usefully emphasises that programmed cell death (PCD), a physiological phenomenon, and apoptosis are not synonymous as PCD can occur without apoptotic features.

The mechanism leading to apoptosis can itself be divided into extrinsic and intrinsic pathways. The extrinsic pathway is activated by death receptors on the cell surface whereas the intrinsic pathway is dependent on mitochondrial activation by loss of growth factor signals or as a response to intracellular stimuli. However, both pathways are interconnected and converge with proteolytic cleavage and activation of caspases which cleave critical cell targets necessary for survival.

It has been proposed that mAb binding of CD20 results in transmission of intracellular signals that lead to direct inhibition of cell growth, apoptosis induction and hence sensitisation to cytotoxic chemotherapy.^{283,398-404} These findings were based on early observations of changes in cell growth, including growth arrest with anti-CD20 mAb.^{286,405,406} Since then, direct cell death induction has been demonstrated with a range of lymphoma cell lines, but rarely on primary tumours and has generally been shown to depend on further cross-linking of anti-CD20 mAb with a secondary Ab or FcγR-expressing cells.⁴⁰⁶⁻⁴⁰⁸ In vivo, similar cross-linking of anti-CD20 mAb has yet to be shown, thus raising the uncertainty that the secondary cross-linking in these experiments may be artificial. Furthermore, not all B-cell lines are sensitive^{375,383} and the cell death pathways evoked appear cell line and stimulus dependent - apparently varying with both the mAb chosen and the degree of hyper-cross-linking

delivered. When rituximab is sufficiently cross-linked it is capable of eliciting potent apoptotic responses in sensitive cell lines via the intrinsic mitochondrial pathway.^{401,404} However, cell death induced by non-hyper-cross-linked anti-CD20 mAb appears to be non-apoptotic and varies considerably depending on the mAb used, rituximab being relatively weak and tositumomab strong at inducing direct cell death.²⁸³ By contrast, tositumomab (without further cross-linking) promotes a cytoplasmic form of death, involving lysosomes, which is able to bypass the apoptotic inhibition provided by high levels of BCL-2 both in the presence and absence of radiation^{409,410} perhaps explaining the efficacy of the I¹³¹-tositumomab (Bexxar), even in cases refractory to both chemotherapy and rituximab.⁴¹¹ Perhaps the best evidence that direct cell death induction may operate on primary tumour cells comes from an analysis of 10 rituximab-treated CLL patients.⁴¹² 5/10 patients demonstrated activation of caspases-9, signifying activation of the intrinsic death pathway. Furthermore, in correspondence with this, the anti-apoptotic protein MCL-1 was reduced in almost all of the patients. Whilst this evidence demonstrates the ability of rituximab to directly induce cell death, the sensitivity of CLL cells are clearly variable and the factors that govern this are presently unknown.

Stolz et al.⁴⁰⁴ demonstrated evidence of caspase activation and apoptosis in xenografted B-cell lymphomas in mice treated with rituximab. Rituximab insensitivity in this model was associated with increased expression of anti-apoptotic BCL-2 family proteins, which could be overcome with the BH3-mimetic ABT-737. Although interesting, these results only reflect effects in cell lines as opposed to bona fide tumour cells, and do not demonstrate that apoptosis is an important effector mechanism for in vivo depletion of primary human lymphoma cells.

Recently our laboratory investigated the ability of rituximab to deplete human CD20 Tg mouse B-cells in vivo in the presence or absence of a second transgene encoding high levels of BCL-2³⁵⁵ which blocks the intrinsic apoptosis pathway.⁴¹³ Although B cells expressing the BCL-2 transgene were highly relatively resistant

to apoptotic stimuli such as etoposide and dexamethasone in vitro, in vivo they were just as susceptible to rituximab depletion as B cells lacking the transgene. Therefore apoptosis was not a main route to B-cell depletion. Thus, as with CDC, the support for rituximab promoting cell death is apparent, but whether this mechanism is important for the depletion of CD20⁺ target cells in vivo remains to be proven.

1.5.4 Induction of T-cell mediated immunity

CDC, ADCC and induction of direct cell death are considered to be immediate and relatively short-acting effector mechanisms. The suggestion that rituximab can induce T-cell mediated immunity is a relatively new one compared to the initial mechanisms discussed.^{414,415} The notion that this may be true is supported by several clinical observations. Responses to rituximab in patients have been shown to be delayed to as many as 112 days (median 50 days) after administration⁴¹⁶ and could be explained by the time taken to induce T-cell immunity. Moreover, lymphoma patients who respond to rituximab the first time, appear to have a more durable response on re-treatment,⁴¹⁷ possibly accounted for by the presence of primed CTL. It is also possible that the durable responses seen with rituximab alone, and in FL patients on maintenance rituximab (given every 2-3 monthly)^{418,419} may be accounted for by involvement of the adaptive immune response through immunotolerance or immunoediting as discussed in **Section 1.1**.

Rituximab-induced cell-death, by the three main pathways described, potentially results in release of tumour antigens and changes in localised inflammation which promotes the uptake of tumour-associated antigens by APC particularly DC and macrophages.^{414,415,420-423} The APCs have the ability to present captured MHC class I associated peptide to CTL for priming. That this might occur during therapy was demonstrated recently in a small proof of principle study which showed an increase in idiotype-specific T cells after rituximab monotherapy of FL patients.⁴²⁴ However, due to the size of the study,

it is not known whether this so-called vaccinal effect correlates with clinical outcome⁴²⁵ and whether it is specific to therapeutic mAb in general or any cell-killing modality. More recently, another group demonstrated that anti-CD20 mAb therapy induced protection against tumour re-challenge in a mouse model.⁴²⁶ In this model, mouse thymoma EL4 cells expressing human CD20 were injected into C57Bl mice and treated with an anti-human CD20 mAb. They demonstrated that the protective immunity was dependent upon Fc interaction and the initial presence of CD4⁺ cells, and then CD4⁺ and CD8⁺ cells later. Addition of IL-2 also improved response rates to anti-CD20 mAb in this model. As IL-2 promotes T- and B-cell proliferation and NK cell activation, the benefits seen could be attributed to either augmentation of ADCC and/or T-cell dependent responses. However, the major flaw of the study was that human CD20 was expressed only on the transplanted tumour cells and not on the host itself. Hence, the model was effectively testing an anti-idiotypic Ab, and the findings are not specific for anti-CD20 treatment. Furthermore, therapy-induced immune responses observed in mouse models might not necessarily be representative of responses in humans since mice harbour active endogenous retroviruses that can modulate host immune responses.⁴²⁷ Moreover, if syngeneic models are not employed, differences in endogenous retroviral sequences between subspecies, might be account for the induction of immune responses, and not therapy itself.

Alternative explanations may also exist for the observed effects of rituximab, such as the general alteration of immunogenicity of tumour cells by chemotherapy and/or immunotherapy (reviewed in^{428, 429}). For instance, anthracyclines, often used in combination with rituximab in the treatment of DLBCL, have been shown to induce surface expression of calreticulin, a chaperone protein that can interact with CD91 on macrophages to promote phagocytosis of the tumour cell.^{430,431} Oxaliplatin, a platinum compound, and anthracyclines also promote secretion of high-mobility group box 1 protein (HMGB1), a nuclear protein released by apoptotic cells.⁴³² The interaction between HMGB1 and TLR4 is crucial for DC to present antigen from apoptotic

cells. Indeed the observed immunogenic and immunostimulatory effects on the tumour and host respectively, may account for the marked improvement seen with combined rituximab and CHOP or cyclophosphamide, vincristine and prednisolone (CVP) chemotherapy as opposed to rituximab alone.

1.6 Mechanisms of resistance to anti-CD20 therapy

Whilst rituximab has improved the survival of patients with B-NHL, an estimated 30% of patients either do not respond or relapse, and eventually become refractory to rituximab-containing regimens (reviewed in⁴³³). A number of explanations have been suggested for rituximab-refractory cases but because it is unclear as to how rituximab actually works, the molecular basis of rituximab resistance is largely unknown. The influence of complement defence molecules on patient outcome has been discussed earlier (**Section 1.5.2**). Another potential means of rituximab resistance is through the process of 'shaving'.^{434,435} Shaving or trogocytosis describes the process whereby phagocytic cells selectively remove bound antigen-IgG complexes (CD20:rituximab, in this case) from the surface of target cells rather than phagocytose them.⁴³⁶ Consequently, the target cells are no longer opsonised and are able to escape detection by immune effector cells. This process is thought to be mediated by localised deposition of antigen:IgG deposits, such as may occur due to translocation of rituximab into lipid rafts, and concomitant complement deposition, which aids Fc γ R binding.³⁷⁸ The evidence for trogocytosis with rituximab-treated patients stems from a series of comprehensive studies from Taylor's group. Taylor et al. first observed in CLL patients that the peripheral lymphocyte count fell rapidly after infusion of a fraction of a standard dose of rituximab (30 mg).³⁷⁸ However, upon completion of the entire 700 mg dose 7 hours' later, the lymphocyte count rapidly recovered, albeit usually to a level lower than pre-rituximab levels. These recovered lymphocytes expressed less CD20 which was not accounted for by epitope-masking from administered rituximab. Internalisation of CD20 was excluded as an explanation when immunoblotting showed reduced levels of

CD20 in recovered lymphocytes, although their conclusion is not necessarily correct since internalised CD20 could have been degraded. It was further shown that CD20:rituximab complexes were 'shaved' off by monocytes or macrophages in vitro⁴³⁴ and in vivo⁴³⁵ models. Distinction between phagocytosis and trogocytosis in these experiments were clearly difficult, and perhaps the most convincing evidence arose from confocal images demonstrating the latter.⁴³⁴ This process was largely independent of complement (addition of normal human serum did not alter the extent of shaving although heat-inactivated serum did), but was specifically Fc γ RI-dependent. As anticipated, addition of IVIg at normal serum concentrations (~10 mg/ml) in vitro or in vivo, blocked the high affinity Fc γ RI and reduced shaving. This in itself counters the clinical relevance of shaving, as whole blood would contain equivalent quantities of monomeric IgG that can continuously occupy Fc γ RI and hence inhibit shaving. Furthermore, as discussed in **Section 1.5.1**, evidence from different groups has demonstrated Fc γ RIII to be a determining factor in the efficacy of rituximab, yet it appears to be unimportant in shaving. In a proof-of-principle study to support the evidence for shaving, 12 CLL patients were treated with lower doses of rituximab (20 mg/m² or 60 mg/m² thrice a week for 2 initial weeks; as compared to conventional 375 mg/m² weekly for 4 weeks). The study demonstrated that even at doses as low as 20 mg/m², rituximab was able to effectively clear as much as 75% of the circulating CLL cells, and less shaving was seen in this group compared to the group given 60 mg/m².⁴³⁷ These results were however contradictory to another previous study in CLL which showed a direct dose-response relationship between rituximab and overall response rate.⁴³⁸ It is also not known if shaving would similarly apply to solid B-cell malignancies where the tumour cells are less accessible to the peripheral vasculature than circulating CLL cells.

Soluble CD20 has also been cited as a possible explanation for poor responses to rituximab in CLL.^{439,440} Higher levels of soluble CD20 have been detected in CLL compared to healthy individuals.⁴⁴⁰ More recently, in CLL patients treated with

FCR, higher serum CD20 levels in the peripheral blood had poorer PFS but not no significant association with OS.⁴⁴¹ It seems implausible that CD20 could be circulating freely since it contains four hydrophobic transmembrane domains. The authors hypothesise that soluble CD20 could arise from fragments of membrane of apoptotic cells, although this is yet to be proven.^{440,441} An alternative explanation is that soluble CD20 correspond to CD20-containing membrane microvesicles from CLL cell.⁴⁴² The finding that membrane microvesicles can be released from cells is not new and has been described as a normal physiologic phenomenon that is associated with cell activation and growth.⁴⁴³ However, the microvesicles identified by Ghosh et al. were CD19⁺/CD20^{low}, thus may explain the detection of apparently soluble, CD20.⁴⁴² Soluble CD20 has also been detected in smaller cohorts of other B-NHL patients, and furthermore, in vitro investigations indicate that binding of rituximab to CD20⁺ cells can be inhibited by soluble CD20.⁴³⁹ In view of the latter, it might have been more useful to correlate the levels of soluble CD20 with immediate response rates as well as PFS in FCR-treated CLL patients, but the study had too few patients with known pre-treatment values to do so. It might be that soluble CD20 is a surrogate marker for aggressive or advanced cases of CLL since is associated with advanced stage, CD38, as well as β 2M⁴⁴⁰ and furthermore, the number of CD20⁺ microvesicles also increased with advancing Rai stage. In terms of resistance to anti-CD20 mAb, these results are probably most relevant to tumours with relatively low CD20 expression or bulky tumours, where a saturating concentration of serum rituximab is not reached. In these cases, competition for rituximab by soluble and membrane-bound CD20 may affect the efficacy of the drug. Whilst interesting, a criticism of the group's work is that the published methodology for the ELISA used to measure the soluble CD20 is not uniform and lacks sufficient details for it to be validated. Furthermore, in the original paper, Manshouri et al. stated that a CD20 peptide (SP-B:SC-7703, Santa Cruz Biotechnology, US.) was used for standardisation, yet the company details the product as a pulmonary surfactant-associated protein.⁴⁴⁰

Another possible mechanism of resistance is the loss of surface CD20 expression after exposure to anti-CD20 mAb.⁴⁴⁴⁻⁴⁴⁶ Jilani et al. demonstrated loss of surface CD20 expression in cells derived from CLL patients treated with rituximab in vivo, using an anti-mouse Ig to detect the murine portion of rituximab to overcome masking of CD20 by rituximab. Internalisation was detected in some but not all of the cells, therefore the authors suggested that this was unlikely to be the major cause of loss of CD20 expression, but an alternative explanation was not provided. Michel et al.⁴⁴⁵ also demonstrated internalisation of CD20 into endosomes using type I mAb 1F5 and rituximab in Raji and Ramos (Burkitt's lymphoma) cell lines. Other groups suggested that CD20 loss post-rituximab was due to transcriptional down-regulation of CD20⁴⁴⁷ and/or selection of a CD20-negative clone.⁴⁴⁷⁻⁴⁵¹ All of these reports implied a reduction of surface CD20 as a cause of resistance but failed to provide satisfactory mechanistic support. Therefore it was widely assumed that CD20 did not internalise from the cell surface, and that this feature was critical to rituximab's success.^{452,453}

At the time of commencement of this project, data from yet unpublished investigations from our lab (Dr S. Beers and Mr S. Wijayaweera) suggested that rituximab did indeed internalise after binding. Initial in vivo experiments in human CD20 Tg mice indicated that Fc:FcR interactions were essential to B-cell depletion by anti-CD20 mAb. To elucidate the mechanism by which these mAb depleted B cells, carboxyfluorescein succinimidyl ester (CFSE) -labelled human CD20 Tg mouse B cells were adoptively transferred into γ -chain $-/-$ mice and different anti-CD20 mAb administered. Critically these experiments allowed analysis of target cells ex vivo after mAb binding in the absence of deletion. Surprisingly, surface expression of type I mAb had reduced by 80-90% within 16 hours of treatment whilst surface expression of type II mAb was relatively unchanged. Furthermore, γ chain $-/-$ mice lacked Fc γ R- bearing effector cells and so this phenomenon could not be explained by shaving. The findings observed were also not accounted for by transcriptional down-regulation of CD20, as mRNA levels from treated human CD20 Tg mouse B cells were unchanged compared to untreated cells. We postulated and demonstrated that

the reduction in surface CD20 was due to the internalisation of bound type I anti-CD20 mAbs:CD20 complexes. However, all these findings were based upon a single human CD20 Tg model. Therefore, to confirm the occurrence of internalisation of type I mAb, validation was required in primary human samples, and thus provided the basis of this project.

2 Project Outline

The aim of this project was to investigate the factors that determine the efficacy of anti-CD20 mAb therapy in B-cell malignancies. With the recent discovery that rituximab could internalise from the surface of human CD20 Tg mouse B cells, the project was specifically focused on whether this occurred in primary human cells and uncovering the mechanism behind internalisation. The project was therefore planned as described below:

- Investigation of the internalisation of rituximab and other anti-CD20 mAb in human cell lines and its comparison to primary human cells
- Characterisation of the internalisation of rituximab in different primary neoplastic B cells
- Elucidating the mechanism of internalisation of rituximab
- Confirmation of findings in a cohort of patients

3 Materials and Methods

3.1 Cell lines

Human Burkitt's lymphoma (Ramos, Raji and Daudi) and FL (DOHH2 and SUDHL4) cell lines were originally obtained from the European Collection of Cell Cultures (ECACC) or American Type Culture Collection (ATCC). Ramos FcγRIIb and FcγRIIIa transfectants were transfected by Dr S. Beers and Dr A. Vaughan respectively, using a recombinant expression plasmid (pcDNA3) encoding human FcγRIIb, or FcγRIIIa, respectively and Amaxa Cell Line Nucleofector Kit (Lonza), solution T, programme G16. Non-transfected cells were maintained in Roswell Park Memorial Institute 1640 medium (RPMI, Invitrogen, UK) supplemented with 10% foetal calf serum (FCS) (Lonza), 2.0 mM glutamine, 1.0 mM sodium pyruvate (both Invitrogen) and cultured at 37°C and 5% CO₂. Transfected cells were maintained in the same media with selection in 200 µg/ml Geneticin (Invitrogen).

3.2 Healthy human B cells and monocytes

Peripheral blood containing normal human B cells was obtained from healthy volunteers after informed consent. Peripheral blood was taken in either lithium heparin or ethylenediaminetetraacetic acid (EDTA)-containing Vacutainer blood collection tubes (BD, UK) to prevent samples from clotting. Where other collection methods were used, this is specified in the figure legends. Routinely, all samples were processed immediately after collection. Where this was not possible, samples were stored at room temperature (RT) and processed within 24 h.

3.2.1 Peripheral blood mononuclear cell isolation

Peripheral blood mononuclear cells (PBMC) were isolated using Lymphoprep (Axis-Shield, UK) and the protocol outlined below. Fresh blood was diluted at least two-fold with phosphate-buffered saline (PBS, Lonza) supplemented with 2 mM EDTA. Subsequently, 35 ml of diluted blood was layered carefully over 15

ml Lymphoprep in a 50 ml tube and then centrifuged at 400 *g* for 30 mins at RT with brakes off to allow gentle density gradient separation. The interphase containing the PBMC and platelets was then aspirated and transferred to a fresh 50 ml tube. Thereafter, the tube was topped up with PBS/EDTA and centrifuged at 300 *g* for 10 mins at RT. The supernatant was removed, cell pellet resuspended and topped up with PBS/EDTA before further centrifugation at 200 *g* for 10 mins at RT. This last step was repeated to ensure adequate platelet removal.

3.2.2 B cell isolation

B-cell isolation was performed as per the manufacturer's protocol (Miltenyi Biotec, Germany). The maximum number of total cells collected was usually less than 2×10^9 , therefore LS columns and the MidiMACS separators were used (all Miltenyi Biotec). First, the PBMC suspension was passed through a 40 μm filter to remove any cell clumps that might block the column. Cells were then centrifuged at 300 *g* for 5 mins at RT and supernatant aspirated completely to reduce unnecessary dilution of subsequent reagents. The cell pellet was resuspended in 40 μl of ice cold PBS/0.5% bovine serum albumin (BSA)/2 mM EDTA buffer per 10^7 cells. 10 μl biotin-Ab cocktail (comprising Ab against CD2, CD14, CD16, CD36, CD43 and glycoporphin A (CD235a)) was then added to bind non-B cells. The suspension was mixed and incubated for 10 mins at 4°C. 30 μl PBS/BSA/EDTA buffer was added followed by 20 μl anti-biotin microbeads to bind to the biotin-labelled Ab. After a further 15 mins of incubation at 4°C, cells were washed with ice cold 2 ml PBS/BSA/EDTA buffer and centrifuged at 300 *g* for 5 mins at 4°C. The supernatant was aspirated and cells resuspended in 500 μl buffer and passed through a magnetic column. The labelled cells were bound to the magnetic separator and column, allowing unlabelled B cells to pass through the column and be collected. Final B-cell purity was confirmed by flow cytometry by double staining with allophycocyanin (APC) labelled anti-CD19 and fluorescein isothiocyanate (FITC) labelled CD3 (described in **Section 3.9**).

3.2.3 Monocyte isolation

Peripheral blood monocytes were obtained from whole blood derived from healthy human volunteers or from leucocyte-rich fractions (via leucocyte reduction cones) from apheresis blood donors provided with consent from the National Blood Service, Southampton. Both products were prepared similarly, and PBMC isolated as described in **Section 3.2.1**.

Monocytes were then isolated using the human monocyte isolation kit II (Miltenyi Biotec) by negative selection. PBMC were divided into fractions so that the total cell count was less than 2×10^9 and LS columns and MidiMACS separators were used (all Miltenyi Biotec). Final monocyte cell purity was confirmed by flow cytometry, with phycoerythrin (PE) labelled anti-CD14 (described in **Section 3.9**).

3.3 Clinical samples

CLL/SLL, FL, DLBCL and MCL samples were obtained with informed consent in accordance with the Declaration of Helsinki, which comprises a set of principles aimed at safeguarding the best interests' of research participants and ensuring high quality research. Blood samples from CLL patients were collected in either lithium heparin or EDTA-containing tubes, and PBMC purified using Lymphoprep as detailed in **Section 3.2**. Where stated, fresh whole blood was also used, and was collected in either lithium heparin or preservative-free heparin (PFH). Routinely and unless otherwise stated, experiments were initiated within 24 hours (h) of venepuncture.

Solid tissue samples were processed and stored by staff from the Human Tissue Bank. The sample was first disaggregated through a sterile strainer placed in a Petri dish containing RPMI supplemented with 2 mM glutamine, 1 mM sodium pyruvate, 0.1 mM non-essential amino acids, penicillin 120 U/ml and streptomycin 120 µg/ml. The resultant cell suspension was then transferred to 50 ml tubes with a sterile Pasteur pipette. The Petri dish was washed with 5 ml

RPMI to remove any residual cells and transferred to the 50 ml tube. The cell suspension was centrifuged at 300 *g* for 5 mins at RT and supernatant discarded.

Resultant final cell pellets from both procedures were resuspended at 1×10^7 cells/ml in supplemented RPMI with 50% human AB serum and 10% dimethyl sulfoxide (DMSO) and transferred to vials in a Mr Frosty box (Nalgene, US) for storage at -80°C for a minimum of 4 h before subsequent transfer to liquid nitrogen storage. Clinical samples were stored in the University of Southampton's Cancer Sciences Division Tumour Bank under Human Tissue Authority licensing. Ethical approval for the use of clinical samples was obtained by the Southampton University Hospitals NHS Trust from the South West Hampshire Research Ethics Committee, REC reference 05/q1704/72.

Prior to use, clinical samples were rapidly thawed to reduce exposure to DMSO, using pre-warmed supplemented RPMI. The cell suspension was centrifuged at 300 *g* for 5 mins at RT and supernatant decanted. The pellet was then resuspended in supplemented RPMI to achieve an approximate concentration of 2×10^6 cells/ml unless otherwise stated. Cell viability was assessed as described in **Section 3.11**.

3.4 Cell quantitation

Cell numbers were determined using a Coulter Counter D Industrial model (Coulter Electronics, UK), which relies on changes in electrical impedance created by particles present in an electrolyte solution. Duplicate measurements were taken to ensure precision, and an average of both measurements was used.

3.5 Characterisation of prognostic markers in CLL samples

Most of the CLL clinical samples used were a kind gift from the CLL bank held by

Dr K. Potter and Professor F. Stevenson. The prognostic features for these samples had been determined and recorded by Dr I. Wheatley and Mr I. Mockridge. The mutation status of IgV_H genes,¹⁸⁹ ZAP70 expression^{195,196} and CD38 positivity²⁰¹ were determined as detailed previously. Briefly, for IgV_H analysis, a V_H leader primer mix and a C μ 100 primer were used to amplify heavy-chain genes from complementary DNA (cDNA). All nucleotide sequences were aligned to the V-base directory, and mutational status was determined using a 98% cut-off. For CD38 analysis, anti-CD38 PE (clone HB7; BD Biosciences) staining by flow cytometry was used. Determination of ZAP-70 status was carried out as described by Crespo et al.¹⁹⁵ Surface Ig expression of CLL cells was checked by flow cytometry as described previously.^{454,455}

CLL clinical samples characterised for del(11q) and del(17p) were kindly gifted by Professor D. Oscier. CLL samples were initially screened for 11q22-23 del status by FISH by Dr A. Gardiner at the Royal Bournemouth Hospital. FISH analysis was confirmed by genome wide screening using SNP array analysis by Dr J. Strefford from the Cancer Sciences Division, Southampton. ATM function was determined functionally following etoposide treatment⁴⁵⁶ (Dr A. Gardiner) and by mutation analysis of ATM coding exons by high performance liquid chromatography⁴⁵⁷ (Dr T. Stankovic, Birmingham). Del(17p) detection was performed by FISH, also by Dr A. Gardiner.

3.6 RT-PCR

The expression of Fc γ RIIIa and Fc γ RIIb1/b2 isoforms in primary human B cells was investigated by assessing mRNA expression of these genes. Total RNA was first extracted from these cells followed by synthesis of cDNA using the enzyme, reverse transcriptase. Finally, the resultant cDNA was amplified by PCR, and protein expression visualised using agarose gel electrophoresis. Details for each of these steps are detailed below.

3.6.1 RNA extraction

Cells were lysed and RNA extracted using RNEasy Mini kit (Qiagen, UK) as per the manufacturer's protocol. To ensure sufficient RNA was available, a minimum of 5×10^6 cells was used. Particular care was taken to ensure an RNase-free environment, and work was performed on ice to reduce RNA degradation. Resultant RNA was quantified using the Nanodrop ND-1000 (nuclei acid programme). The purity of RNA was indicated by an A260/280 absorbance ratio of ~ 2 . RNA was not used if the ratio was less than 1.8. RNA was used either used immediately or stored at -80°C .

3.6.2 cDNA synthesis

Superscript III first-strand synthesis system (Invitrogen, UK) was used for conversion of total RNA to cDNA as per the manufacturer's protocol. $1 \mu\text{g}$ RNA was combined with a deoxyribonucleotide triphosphate mix (dNTP) and oligo(dT) primers to prime the 3' poly(A) tails of mRNA. cDNA synthesis was catalysed by Superscript III reverse transcriptase and subsequent parent RNA digested by RNase H. The cDNA was stored at -20°C until use.

3.6.3 PCR and visualisation by agarose gel electrophoresis

cDNA generated was amplified using PCR by combining $1 \mu\text{l}$ cDNA ($\sim 40 \text{ ng}$), $10 \mu\text{l}$ GoTaq[®] Green master mix (Promega, UK), $1 \mu\text{l}$ forward primer, $1 \mu\text{l}$ reverse primer (see **Table 5**) and $7 \mu\text{l}$ dH_2O . Glyceraldehyde 3-phosphate dehydrogenase (GAPDH), a 'housekeeping gene' was utilised as a reaction control. The reaction was carried out in a C1000 thermal cycler (Bio-Rad Laboratories, UK), under the following conditions: 95°C for 180 s (denaturation and separation of strands), 95°C for 30 s, 55°C for 30 s (primers anneal), 72°C for 30 s (strand extension by DNA polymerase), repetition of preceding steps 24-29 times (amplification), 72°C for 300 s (final extension for gap-filling) and then cooled to 4°C until the next step.

20 µl of the amplified PCR product was then pipetted into individual wells of an agarose gel (2% agarose (w/v) in TAE buffer, 0.08% GelRed (v/v) (Biotium, US), a nucleic acid stain), immersed in TAE (tris(hydroxymethyl)aminomethane (TRIS) base, acetic acid and EDTA) buffer. A 100 base pair (bp) DNA ladder (Promega) was also assessed in the same gel to enable identification of the size of the final product. A voltage of ~150 v was applied to the gel and electrophoresis terminated when the bands reached the opposite end of the gel. The gel was then visualised using a Gel Doc™ XR molecular imager (Bio-Rad Laboratories).

Primers	Sequence	Product (bp)	Annealing temperature (°C)
FcγRIIb1/2 F (Invitrogen)	AAG CCT GTG ACC ATC ACT GTC	226 (CD32b1) 169 (CD32b2)	55
FcγRIIb1/2 R	TGT CAG CCT CAT CAG GAT TAG		
FcγRIIa F (Invitrogen)	AAG CCT GTG ACC ATC ACT GTC	235	55
FcγRIIa R	TTT CTT CAA GTT GTC TCT TTC TGA		
GAPDH F (Gibco)	CCA TCA CCA TCT TCC AGG AG	500	55
GAPDH R	CCT GCT TCA CCA CCT TCT TG		

F=forward, R=reverse

Table 5: The list of PCR primer pairs used in the investigations.

Primer sequences, expected PCR product sizes and annealing temperatures are also listed.

3.7 Ab and reagents

Table 6 describes Ab used in this study. In-house mAb were producing from secreting hybridoma lines expanded in tissue culture as per Köhler and Milstein's method, by Dr C. Chan, Ms A. Tutt and Mrs C. Penfold. Fused hybridoma cells were serially diluted to achieve a 1 cell/well concentration (in a 96-well plate, Nunc, Thermo Fisher Scientific, Denmark). After approximately 10 days, Ab secretion was checked by ELISA. Two separate single colonies were selected for expansion using Dulbecco's modified eagle medium (DMEM, Invitrogen) supplemented with 10% FCS (Lonza), 2.0 mM glutamine, 1.0 mM

sodium pyruvate (both Invitrogen) and cultured at 37°C, 5% CO₂. When approximately 7.5×10^7 cells were grown, the culture was centrifuged and the supernatant containing the secreted mAb collected. The supernatant was filtered using a 0.45 µm filter, concentrated (Amicon, Millipore, UK) and purified using either Protein A or G affinity chromatography (Amersham Biosciences, UK). Protein A, staphylococcal cell wall protein, binds mouse and human Ig Fc, but not rat Ig Fc, unlike streptococcal-derived Protein G, which binds all three species.⁴⁵⁸ The mAb attaches to the appropriate gel column, which is eluted off using an acidic (pH 3) elution buffer. The pH of eluted mAb was then rapidly neutralised to preserve mAb bond integrity. Concentration of purified mAb was checked by Nanodrop (Thermo Scientific), concentrated further to achieve a stock concentration of 2-4 mg/ml and purity assessed by gel electrophoresis (Beckman EP System, US). Where there was a high risk of aggregation, such as with anti-FcR, mAb was checked by high performance liquid chromatography (HPLC). All buffers were endotoxin-low and final mAb was also tested for endotoxin levels using Endosafe-PTS (Charles River, US) as per the manufacturer's protocol. Values of 10 endotoxin units/mg or less were considered to be endotoxin low.

Anti-human CD20 mAb were produced by Dr C. Chan. BHH2 and 2F2 were produced from published patented sequences of GA101 and ofatumumab, respectively. Variable light and heavy chain sequences were subcloned into expression vectors containing the constant regions (Invitrogen), and then transfected into 293F cells for transient expression. Chinese hamster ovary (CHO)-K1 cells were used for stable expression of protein. Protein produced was purified as above and checked for purity by gel electrophoresis and assessed for binding using flow cytometry.

Rituximab mouse IgG2a (Rit m2a) was produced with 1F5 heavy and light chain as a template and QuikChange Multi Site-Directed Mutagenesis kit (Stratagene, UK) as per the manufacturer's protocol. Mutagenic primers were designed and annealed to 1F5 template DNA to produce a single-stranded mutant DNA

template. The template DNA was then digested and resultant mutant DNA strand verified by DNA sequencing. The mutant DNA was then subcloned into an expression vector and transformed into ultracompetent *Escherichia coli* cells. Successfully transformed cells were selected by antibiotic-resistance conferred by the expression vector. Resultant DNA plasmids were isolated and transfected into 293F and CHO-K1 cells for protein expression as above.

The anti-human FcγRIIIa and FcγRIIb mAb used were produced by phage display technology by BioInvent (Sweden) and obtained under a material transfer agreement.

Alexa-488 and quenching anti-Alexa 488 reagents were purchased from Invitrogen. F(ab')₂ fragments were produced by Ms A. Tutt using a method previously described using pepsin digestion.⁴⁵⁹ The IgG mAb was prepared to a concentration of 10-15 mg/ml in 0.1 M sodium acetate at pH 4.2 and treated with 0.3 mg/ml pepsin for 18 h at 37°C. F(ab')₂ fragments were separated from IgG using size-exclusion chromatography. F(ab') fragments were generated by incubation with 20 mM 2-mercaptoethanol at 25°C, for 30 mins, followed by the addition of excess iodoacetamide (20 mM).⁴⁵⁹

Western blotting Ab used were anti-tubulin (Cell Signalling Technology, UK), anti-FcγRIIb (Abcam, UK), anti-phospho-FcγRIIb (Cell Signalling Technology) and anti-CD20 (AbD Serotec, UK) (**Table 7**).

Human AB serum was obtained from healthy volunteers. Freshly obtained peripheral blood venesected in the absence of anticoagulant was directly transferred into glass centrifuge tubes to prevent activation by plastic. The blood was stirred with a wooden stick and allowed to coagulate for 30 mins at RT. It was then centrifuged at 900 g for 20 mins at 4°C to separate serum from cells and preserve the stability of the complement components. The serum was then removed and if necessary, centrifuged a second time if erythrocyte contamination of serum was still visible. The serum was aliquoted into glass

vials at -80°C until use.

To inactivate the complement component within the serum, it was incubated at 56°C in a water bath for an hour, and then stored at -20°C.

Specificity	Ab/Clone	Isotype	Source
CD3	OKT3	mIgG2a	In-house/ATCC
CD4	C4	mIgG1	In-house/P. Beverley
CD5	OKT1	mIgG1	In-house/ATCC
CD16	3G8	mIgG1 and F(ab') ₂	In-house/ATCC
CD19	RFB9	mIgG1	In-house/Royal Free Hospital, UK
CD20	Rituximab	hu IgG1	Southampton General Hospital pharmacy, UK
	Rit m2a	mIgG2a	In-house/C. Chan
	Tositumomab	mIgG2a	In-house/C. Chan
	BHH2	hu IgG1	In-house/C. Chan
	2F2	hu IgG1	In-house/C. Chan
	GA101	Defucosylated hu IgG1	Prof T. Illidge, Manchester/Glycart
CD32	AT10	mIgG1 or F(ab') ₂	In-house/A. Tutt
	Anti-FcγRIIa (clone E05)	hu IgG1 (N297Q mutant)	BioInvent, Sweden
	Anti-FcγRIIb (clone E12)	hu IgG (N297Q mutant)	BioInvent, Sweden
CD38	HIT2	mIgG1	BD Biosciences
CD46	MCA2113	mIgG1	AbD Serotec, UK
CD52	Campath 1H	hu IgG1	Southampton General Hospital pharmacy, UK
CD55	MCA1614	mIgG1	AbD Serotec, UK
CD59	MCA1054	mIgG2a	AbD Serotec, UK
CD107a (LAMP-1)	EBioH4A3	mIgG1	Ebioscience, UK
IgG	SB2H2	mIgG1	In-house
IgG	Polyclonal (goat origin)	F(ab') ₂	Jackson Immunoresearch, US
IgM	M15/8	mIgG1	In-house
mIgG (Fc-specific)	Polyclonal (goat origin)	F(ab') ₂	Sigma-Aldrich
HLA Class II	F3.3	mIgG1	In-house

Table 6: List of Ab used in the investigations

The table describes the specificity, clone, isotype and source of the Ab used in this project. All Ab are anti-human unless otherwise specified. m denotes mouse Fc, and hu denotes human Fc region.

3.8 Labelling of mAb with fluorochromes

Labelled mAb were obtained from BD Biosciences or made in-house. FITC and PE-labelling was performed by Ms A. Tutt as previously described.⁴⁶⁰ Alexa 647 labelling was performed using the Alexa Fluor 647 labelling kit (Invitrogen) as per the manufacturer's protocol. Alexa 488 (Invitrogen), APC (Prozyme, US), Cy3 and Cy5 (both Amersham Biosciences, UK) labelling were also performed according to the manufacturer's recommendations, and the details are given below.

In general, the Ab was first concentrated to a range of 1 -10 mg/ml for efficient conjugation and then exchanged into an optimal buffer for the labelling reaction using either Slide-A-Lyzer dialysis cassettes or Zeba Desalt Spin Columns (all Thermo Scientific, Pierce Biotechnology). The Ab was then combined with the dye for 30-60 mins at RT in the dark, on a rotation platform. The conjugated Ab was then separated from the free dye by using a filtration column. For Alexa 488 labelling, a column was made in-house using a large Pasteur pipette, glass wool and Sephadex G-25 (Pharmacia Fine Chemicals, Sweden). Sephadex is a gel filtration media which separates labelled Ab from free dye by trapping the smaller molecules thus allowing free flow of larger molecules (e.g. labelled Ab). The size exclusion threshold is determined by the degree of cross-linking of the organic chains of the dextran beads which make up Sephadex. In addition, 0.5 ml 0.5 M NaOH was added to the column to remove the endotoxin in Sephadex prior to addition of the Ab mixture. The first fluorescent band to elute from the column is the labelled Ab and was collected. For APC, Cy3 and Cy5 labelling, endotoxin-low Zeba Desalt Spin Columns were used, again with the same size exclusion principle. The final concentration of the labelled Ab was determined using the Nanodrop (Thermo Scientific), which estimates the concentration based on a general reference that 1 mg/ml protein solution has an absorbance of 1.0 at 280 nm. The labelled mAb was tested by performing a serial dilution assay of labelled mAb with antigen-expressing human cell lines by flow cytometry (see next section).

3.9 Flow cytometry

Samples were assessed on either FACScan or FACSCalibur (both BD Biosciences), and data analysed with CellQuest Pro (BD Biosciences) or FCS Express (DeNovo Software, US).

To determine the level of surface antigen expression, cells were prepared to a concentration of $1-2 \times 10^6$ cells/ml (in supplemented RPMI) unless otherwise specified and labelled with the appropriate Ab as follows: For direct staining, fluorochrome-labelled mAb was added for 30 mins at 4°C and in the dark, to prevent antigenic modulation and bleaching of the fluorochrome. The cell suspension was then washed once with cold fluorescent-activated cell sorter (FACS) buffer (PBS, 1% w/v BSA, 0.1% w/v sodium azide) and then analysed by flow cytometry. An isotype-matched irrelevant mAb labelled with the same fluorochrome was used as a control to assess the proportion of non-specific binding.

For indirect staining, unless otherwise stated, 5-10 µg/ml primary mAb was added to the cells for 15 mins at RT, then excess mAb removed by washing twice with cold FACS buffer. Cells were then incubated with a fluorochrome-labelled secondary mAb (that binds to the primary mAb's Fc region) for 15 mins at RT in the dark before a final wash with cold FACS buffer and analysis by flow cytometry. Controls used were an isotype-matched irrelevant primary mAb, and cells incubated with the secondary mAb only.

In order to reduce inter-experimental variation due to differences in labelled-mAb batches and flow cytometer settings, comparison of the level of surface antigen expression between different samples were expressed as a ratio of the specific geographic mean fluorescence intensity (Geo MFI): isotype control Geo MFI.

3.10 Viability assay

Cell viability was assessed by flow cytometry using 1 µg/ml annexin V-FITC (in Annexin V binding buffer (10 mM 4-(2-hydroxyethyl)-1-piperazineethanesulfonic acid (HEPES), pH 7.4, 140 mM NaCl, 2.5 mM CaCl₂)) and 10 µg/ml propidium iodide (PI). Annexin V is a calcium-dependent phospholipid binding protein which binds with high affinity to phosphatidylserine.⁴⁶¹ Phosphatidylserine translocates from the inner to outer membrane of cells undergoing early apoptosis. PI is a nucleic acid dye which permeates late-stage apoptotic and apoptosed cells i.e. when the integrity of the plasma membrane is lost. Once it enters the cells, it binds to double-stranded DNA or RNA and fluoresces 20-30-fold more strongly.

Typically, cells were incubated with annexin V-FITC and PI for 15 mins, in the dark and at RT, and then immediately analysed by flow cytometry.

3.11 Quenching assay

This flow cytometry-based assay allows an estimation of the degree of mAb internalisation by surface fluorescence quenching.⁴⁶² Briefly, cells were cultured with different Alexa 488-labelled mAb. After a given period of incubation, the excess mAb was removed by washing, and the fluorescence of surface-bound mAb was quenched with anti-Alexa 488 mAb. Thus, residual fluorescence detected by flow cytometry represented the internalised mAb as illustrated in **Fig. 8**. The following equation was used to assess the % of surface mAb accessible for fluorescence quenching by anti-Alexa 488, which is inversely proportional to internalisation of Alexa 488-labelled mAb.

% Surface accessible CD20 =

$$\frac{\text{Pre-quench Geo MFI} - \text{Post-quench Geo MFI}}{\text{Pre-quench Geo MFI}} \times 100$$

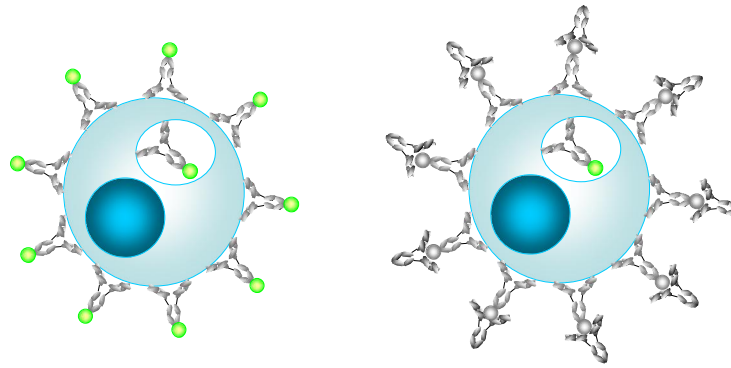


Figure 8: Illustration of the basic principle of the quenching assay

The cartoon on the left illustrates a cell with bound and internalised 488-labelled Ab. On the right, addition of anti-Alexa 488 results in quenching of surface fluorescence, thus residual fluorescence represents the amount of internalised Ab.

In detail, the assay was performed as follows: In 96-well plates, $2-4 \times 10^5$ cells per well were treated with Alexa-488 labelled mAb at a final concentration of 5 $\mu\text{g}/\text{ml}$ in supplemented RPMI, and incubated for 2, 6 and/or 24 h at 37°C and 5% CO_2 . Samples were then harvested into test tubes and excess mAb removed by washing twice with cold FACS buffer. Cells were then resuspended with supplemented RPMI to a total volume of 200-300 μl depending on whether bright field microscopy was performed or not. If microscopy was performed, 100 μl cells were removed and placed in 96-well plates. Cells were allowed to settle for a minimum of 30 mins at 4°C to reduce Brownian movement and to arrest any subsequent internalisation of mAb, and then examined by microscopy (see **Section 3.16**). To the remaining 200 μl cell suspension 2.5 $\mu\text{g}/\text{ml}$ anti-CD19-APC was added to identify B cells when primary tumour material was used. 100 μl cell suspension from each tube was then removed to another test tube containing 2.5 μl anti-Alexa-488. All samples were incubated at 4°C for 30 mins then washed once with cold FACS buffer and analysed on a flow cytometer.

Where whole blood was used as opposed to PBMC or purified B cells, red cell lysis solution (Erythrolyse, AbD Serotec, UK) was added after quenching. Cells were incubated for 10 mins at RT to allow osmotic lysis of red cells, then

centrifuged at 300 *g* for 5 mins at 4°C and washed once with FACS buffer before analysis.

3.12 Phagocytosis assay

Monocytes were isolated as described in **Section 3.2**. After a minimum of 2 h adherence to a 6-well plate (Nunc), the non-adherent cells were removed by washing with PBS and adherent cells were cultured with RPMI supplemented with GP, 2.5 % v/v autologous serum or FCS and penicillin and streptomycin. To stimulate monocyte differentiation into macrophages, human monocyte colony stimulating factor (M-CSF, Peprotech, UK) was added on alternate days at 50 ng/ml and the macrophages used after 6-9 days of culture.

B-cell targets (CLL cells were used) were thawed from liquid nitrogen storage in non-supplemented RPMI and resuspended at $1-2 \times 10^7$ cells/ml. B cells were then stained with 1 μ M CFSE, a stable cytoplasmic dye which covalently attaches to free amino groups of intracellular macromolecules and is visible when excited at 490 nm.⁴⁶³ After 15 mins incubation with CFSE, the reaction was stopped with addition of an equal volume of FCS for 1 min to bind and quench excess dye. Supplemented RPMI was then added up to a total volume of 10 ml and the cells centrifuged at 300 *g* for 5 mins at RT. This washing step was repeated twice more to ensure all excess dye was removed. The labelled cells were then resuspended in supplemented RPMI at $1-2 \times 10^6$ cells/ml and cultured with or without treatment with mAb for the times specified in the figure legends.

During this time, macrophages were harvested from 6-well plates, counted and resuspended at 0.5×10^6 cells/ml and added (100 μ l/well) to wells of a 96-well flat bottom plate (Nunc) to adhere for a minimum period of 2 h.

mAb-opsonised B cells were then harvested from the 48-well plates and excess mAb removed by washing with supplemented RPMI at 300 *g*, RT for 5 mins

before resuspension at 2.5×10^6 cells/ml. Untreated and treated B cells (100 μ l/well) were added to macrophages at \sim 2:1 ratio, in triplicate, for an hour to allow phagocytosis to take place. Subsequently, 5 μ g/ml CD16-APC (mIgG1 used initially, but F(ab')₂ in later stages to reduce non-specific binding via Fc region) was added to each well for 15 mins at RT to identify macrophages in subsequent analysis. Using a multichannel pipette, the wells were washed with 200 μ l FACS buffer (at RT) and then resuspended in 200 μ l ice cold FACS buffer and the plate incubated for a minimum of 10 mins on ice before harvesting for analysis by flow cytometry. The proportion of macrophages that had phagocytosed B cells was estimated from the number that were double-positive for CFSE and APC according to the following formula:

$$\% \text{ double-positive macrophages} = \frac{\% \text{ gated CD16}^+ \text{CFSE}^+ \text{ cell}}{(\% \text{ gated CD16}^+ \text{CFSE}^- \text{ cells} + \% \text{ gated CD16}^+ \text{CFSE}^+ \text{ cells})} \times 100\%$$

3.13 PKH26 cell labelling

PKH26-labelling was performed using PKH26 red fluorescent cell linker kit (Sigma Aldrich, US) to enable discrimination of specific cell populations in mixed cultures. Labelling was performed as per the manufacturer's protocol. Cells were initially washed in serum free media, then 2×10^7 cells pelleted through centrifugation at 300 g at RT for 5 mins. Supernatant was aspirated before 1 ml of Diluent C was added. Diluent C is an iso-osmotic aqueous solution which acts to maintain cell viability and maximise dye solubility. Cells were then mixed well with 1 ml PKH26 (2 μ M PKH26 in Diluent C) for 3 mins and the reaction terminated with the addition of an equal volume of serum supplemented RPMI. Excess PKH26 stain was removed by at least 3 washes using supplemented RPMI and transferring of cells to a new container after each wash. Labelling efficiency and cell viability was checked against unlabelled cells.

3.14 CDC assay

The ability of different anti-CD20 mAb to induce CDC was assessed using a CDC assay.³⁵⁹ Approximately 2×10^5 cells were incubated with a mAb a varying concentrations, typically at 2-fold dilutions for 15 minutes at RT. Thereafter, 10-20% (as specified in figure legends) human AB serum (complement source) was added to the cells for 30 mins at 37°C. Then, 10 µg/ml PI was added for 15 mins at RT, before analysis by flow cytometry. As controls, untreated cells with, and without serum were also stained with PI. % Cell lysis was calculated using the following formula:

$$a = \text{PI}^+ \text{ cells (\% of gated population)}$$

$$\text{Viable cells(\%)} = 100 - a = b$$

$$\text{Cell lysis(\%)} = 100 - [b(\text{treated sample})/b(\text{untreated sample}) * 100]$$

3.15 Western blotting

Western blotting was used to detect the expression of a range of proteins in unstimulated or stimulated cells, as described in the figure legends.

Typically, approximately $5-10 \times 10^6$ cells were treated as described in figure legends and then harvested into eppendorf tubes (Starlab, UK) to prepare protein lysates. This step was performed on ice to prevent further cell-signalling. Cells were washed with ice cold PBS and then lysed with Onyx lysis buffer (6 µl protease inhibitor, 50 mM NaF, 2 mM Na_3VO_4 , in 10 mM Tris-HCl pH 7.4, 67.5 mM NaCl, 0.5 mM MgCl_2 , 0.5 mM ethylene glycol tetraacetic acid (EGTA), 0.5% Triton X-100 (w/v) and 5% glycerol (w/v)) for 30 mins on ice. Samples were then centrifuged at 13,000 g at 4°C for 15 mins to precipitate unlysed components.

To allow accurate comparison between different samples on the gel, the protein content of the lysate was quantified prior to loading for electrophoresis.

Solubilised protein was quantified using a Bio-Rad protein assay (Bio-Rad, US) and standardised against a BSA standard curve of known protein concentration. The Bio-Rad protein assay relies on the use of acidic Coomassie brilliant blue dye, which shifts its absorbance from 465 to 595 nm in the presence of protein. A typical example is given in **Appendix 2**. After quantification, samples were stored at -20°C until use.

For optimal results 20 µg of protein was mixed with loading buffer (9% sodium dodecyl sulphate (SDS) (w/v), 0.03% bromophenol blue (w/v), 0.1875 M Tris-HCl, 30% glycerol (w/v), 10% (v/v) 2-mercaptoethanol (2-ME) in Milli-Q H₂O) in a 4:1 volume ratio. The solution was then boiled at 100°C for 5 mins, centrifuged and then loaded onto 10% Bis-Tris NuPage pre-cast polyacrylamide gels (Invitrogen), and immersed in 1 x 3-(N-morpholino) propanesulphonic acid (MOPS) buffer (50 mM MOPS, 3.5 M SDS, 50 mM Tris, 0.1 mM EDTA in dH₂O). Electrophoresis was performed using the XCell Surelock system (Invitrogen), applying 100 V for 1 h initially, before increasing to 150 V for an hour. Proteins were transferred using the XCell II Blot Module (Invitrogen) on to a methanol-activated polyvinylidene fluoride (PVDF) membrane (Immobilon-P, Millipore, UK).

After completion of protein transfer, the PVDF membrane was blocked with 5% low-fat dried milk (w/v), in Tris buffered saline (TBS) 0.05% Tween (v/v) (Sigma) (TBS-T) on a roller-mixer for 1 h at RT or 4°C overnight to prevent non-specific binding. After blocking, the membrane was rinsed twice with TBS-T.

Protein detection on the PVDF membrane was achieved using the primary Ab in **Table 7**. The primary mAb, diluted in TBS-T was incubated for 1 h at RT or overnight at 4°C on a roller mixer (Spiramix, Thermo Scientific). The membrane was then washed with TBS-T for 3 x 5 minute washes prior to incubation with a complementary secondary anti-rabbit, -rat or -mouse HRP-conjugated F(ab')₂ Ab (Sigma) (see **Table 7**) exactly as described for the primary Ab.

Following incubation, the membrane was visualised by SuperSignal West Pico Chemiluminescent Substrate (Pierce biotechnology) or Immobilon Western Chemiluminescent Horse Radish Peroxidase (HRP) Substrate (Millipore) and a UVP bioimager using VisionWorksLS software (UVP, UK).

Primary Ab	Origin	Source
Human anti-CD20	Mouse	Serotec
Anti-FcγRIIb	Rabbit	Abcam
Human anti-phosphoFcγRIIb (Tyr292)	Rabbit	Cell Signalling Technology, UK
Mouse anti-α-tubulin	Rabbit	Cell Signalling Technology, UK
Secondary HRP-linked Ab		
Anti-rabbit	Donkey	GE Healthcare, UK
Anti-mouse	Sheep	

Table 7: Primary and secondary Ab used in Western blots

The table shows the primary Ab, their origin and source used for Western blotting.

3.16 Light microscopy

All light microscopy was performed using an Olympus CKX41 microscope linked to a CC12 cooled camera and 100 W USH 1030L mercury lamp. Images were captured using CellB Software (Olympus, UK) and the magnification is shown in the figure legends.

3.17 Confocal microscopy

Confocal microscopy was used in these investigations to determine the intracellular trafficking of anti-CD20 mAb, FcγRIIb and the BCR, and assess phagocytosis in cells as detailed in **Section 3.12**. Assistance with confocal microscopy was provided by Drs S. Dixon and S. James.

Investigation of intracellular trafficking of anti-CD20:CD20 and FcγRIIb into lysosomes

Typically, B cells were incubated with the appropriate Alexa 488-labelled mAb

for various times as described in the figure legends and then harvested, washed and fixed with 2% paraformaldehyde. For concurrent detection of FcγRIIb, cells were then permeabilised with 300 µg/ml saponin and 10 µg/ml Alexa-647-labelled AT10 F(ab')₂. For detection of lysosomes, 5 µg/ml biotin conjugated anti-lysosomal-associated membrane protein 1 (LAMP-1, eBioscience) and 300 µg/ml saponin was added for 30 mins at 4°C. Cells were then washed with cold FACS buffer supplemented with 10 µg/ml saponin. Finally 10 µg/ml streptavidin-Alexa Fluor-546 (Invitrogen) and 300 µg/ml saponin was added, followed by further washing with FACS buffer (supplemented with 10 µg/ml saponin). Approximately 100 µl cells were then transferred onto slides and images captured using LAS-AF v2 software on a TCS-SP5 laser scanning confocal microscope (Leica Microsystems) (100x objective).

Investigation of the association between anti-CD20:CD20 and the BCR

To probe the association between CD20 and BCR, CLL cells were rested for a minimum of an hour to allow BCR re-expression,⁴⁵⁴ and then treated with Ritux-647 at 10 µg/ml for the time points specified in the figure legends. The cells were then harvested and washed once with cold FACS buffer, and fixed with PFH as above. The BCR was then identified with 10 µg/ml M15/8-488 and 300 µg/ml saponin for 30 mins at 4°C to stain for the BCR. The cells were washed with cold FACS buffer/10 µg/ml saponin and the cell pellet resuspended and transferred onto poly-L-lysine coated slides. The cells were allowed to settle then, excess fluid removed with a filter paper before mounting with coverslips using Vectashield hard set mounting medium for fluorescence (Vectashield, California, US).

Investigation of macrophage phagocytosis of anti-CD20-opsonised CLL cells

To assess phagocytosis of CLL cells by macrophages, a similar protocol was followed as in **Section 3.12**. Briefly, macrophages were harvested and transferred into plastic Lab Tek Chamber Slides (Nunc) for adherence for a

minimum of 2 h. CLL cells were CFSE-labelled and were left untreated or treated with mAb in 48-well plates. The CLL cells were then harvested, washed and added to the macrophages for an hour for phagocytosis to take place. After that, the media was aspirated, and chamber walls and gaskets of chamber slides removed. The slides were air-dried, then fixed in 100% dry acetone and coverslips mounted as above, before confocal microscopy.

3.18 May-Grünwald-Giemsa (MGG) staining

To enable better morphological characterisation of cells in the phagocytosis assay, an MGG stain was utilised. MGG consists of alkaline methylene blue and acidic eosin and stains the nucleus and cytoplasm of different cells characteristic blue or pink tones depending on their biochemical properties, thus allowing easier cellular recognition. The air-dried slides from above (**Section 3.17**) were stained with MGG using an automated slide stainer (Sysmex SP-1000i Milton Keynes, UK) and examined under light microscopy as detailed in **Section 3.16**.

3.19 Immunohistochemistry (IHC) and collection of clinical data

Ethical approval was obtained from the South West Hampshire Research Ethics Committee to study the correlation of FcγRIIb expression with clinical response in B-cell lymphoma patients treated with rituximab-containing regimens. The study protocol shown in **Appendix 3** details the specifics of the study. In brief, potential study subjects were identified from the pharmacy and clinical trials databases. The criteria for inclusion in the study was: 1) Diagnosis of a B-cell neoplasm, 2) treatment containing an anti-CD20 mAb, 3) available diagnostic tissue for IHC, and 4) accessible clinical data. Excess diagnostic paraffin-embedded tissue blocks were anonymised and prepared for IHC by technicians from the department of histopathology at Southampton General Hospital as per departmental protocols (**Appendix 4**). Briefly, tissue blocks were cut into 4 µm sections and stained using heat-mediated and enzyme antigen retrieval

techniques. The sections were stained with a specific anti-human Fc γ RIIb Ab (EP888Y, Abcam). The stained sections were then examined by consultant histopathologist Dr M. Ashton-Key, who was blinded to the clinical information. Clinical information was collected from Southampton General Hospital's electronic patient databases by Dr A. Davies, senior lecturer in medical oncology, using a case report form (**Appendix 5**). Dr A. Davies was also blinded to the IHC results. IHC and clinical data were then collated by Microsoft Excel and statistically analysed as described in **Section 3.20**.

3.20 Statistical analysis

Statistical analysis was performed using GraphPadPrism software (GraphPad Software, US) and assistance was provided by an in-house clinical trials unit statistician, Dr Sheila Barton. The distribution of each data set was first assessed using the D'Agostino-Pearson normality test. Non-parametric paired and unpaired data was analysed using the Wilcoxon's paired test and the Mann-Whitney test, respectively. Parametric data was analysed using either paired or unpaired student's t test. Where there are less than 12 data points per group, statistical analysis should be avoided. A p value of less than 0.05 was considered significant, and is marked with a single asterisk (*). Where the p value is less than 0.01, a double asterisk is used (**).

4 Internalisation of anti-CD20 mAb in different B cell-types

4.1 Introduction

Previous work in the laboratory indicated that B-cell depletion in human CD20 Tg mice was dependent on Fc:Fc γ R interaction, but not CDC or direct cell death.³⁵⁵ Furthermore, the investigations showed that type I anti-CD20 mAb were less effective at depleting B cells compared to type II mAb, i.e. B-cell clearance lasted for 20-30 days as opposed to 60 days, with type I and II, respectively. In order to investigate the reasons for the differences in B-cell depletion between type I and type II mAb, a human CD20 Tg x γ chain -/- mouse model was employed. γ chain -/- mice lack all activatory Fc γ R. Without any activatory Fc γ R, B cells were not deleted in this model, thus allowing the examination of cells that had been treated but not deleted in vivo. CD20 surface expression in type I-treated mice was observed to be 80-90% lower than type II-treated mice 16 h after mAb administration whereas the expression on type II-treated mice was relatively unchanged compared to isotype controls. The reduction in CD20 surface expression could be potentially explained by internalisation of CD20:mAb complexes into the cell. An in vitro surface fluorescence quenching assay was used to investigate this possibility (**Section 3.11**). When performed with human CD20 Tg mouse B cells, the assay demonstrated internalisation of type I but not type II mAb.³⁵⁵ The investigations presented in this section follow on from these findings, and aim to fully validate this methodology and characterise the internalisation of anti-CD20 in other cell-types such as human lymphoma cell lines, normal and malignant primary B cells.

4.2 Results

4.2.1 Internalisation of anti-CD20 mAb in human lymphoma cell lines

First, the surface fluorescence quenching assay (described in detail in **Section 3.11**) was performed on a panel of human B cell lymphoma lines. Rituximab and tositumomab were selected as the representative type I and type II mAb respectively, as they were the only clinically-approved anti-CD20 mAb at the time of investigation. These mAb carry different isotypes (rituximab-hulgG1, tositumomab-mIgG2a). Suitable controls were used to ensure that any variation seen in internalisation was not due to isotype differences where possible. However due to the unavailability of type II anti-CD20 mAb with hulgG1 isotype in the earlier experiments, isotype controls could not be employed.

Each cell line was resuspended at a concentration of $1-2 \times 10^6$ cells/ml in supplemented RPMI, with either 5 $\mu\text{g/ml}$ Alexa 488-labelled tositumomab (Tosit-488) or rituximab (Ritux-488) for 2, 6 and/or 24 h at 37°C, 5% CO₂. After each time point, the cells were harvested and washed twice with cold FACS buffer to remove excess unbound Ab. The washed cells were then resuspended in supplemented RPMI. A third of the total volume was removed and transferred into a 96-well plate for inspection by light microscopy. **Fig. 9A** demonstrates that the staining observed with Ritux-488 differed from that with Tosit-488. Tosit-488 remains evenly distributed on the surface of cells, whereas punctate staining compatible with internalisation was seen with Ritux-488, consistent with previous observations.³⁵⁵ Of the remaining cells, half was left untreated (unquenched sample reflecting the combined fluorescence from surface and internalised mAb) and the other half treated with 2.5 μl anti-Alexa 488 for 30 mins at 4°C to quench the surface fluorescence (quenched sample, reflecting internalised mAb only). Both samples were then examined by flow cytometry (**Fig. 9B**). The difference in Geo MFI values between unquenched and quenched samples represents the percentage of surface accessible anti-CD20 (**Fig. 9B**). **Fig. 9C** shows the surface accessible anti-CD20 levels of four different human lymphoma cell lines (SUDHL4, Daudi, DOHH2 and Raji cells) that were

treated with either Tosit-488 or Ritux-488 for 2, 6 or 24 h. In general, all 4 cell lines responded in a similar pattern. In each cell line, Ritux-488 internalised more than Tosit-488 at each time point (10-20% less surface accessible anti-CD20). Internalisation of anti-CD20 mAb increased over time (median 78% at 2 h, 76% at 6 h for and 40% at 24 h, for Ritux-488). Compared with human CD20 Tg mouse B cells, Ritux-488-treated cell lines internalised much less rapidly, i.e. median of 40% remaining on the surface by 24 h with human cell lines compared with 10-20% by 16 h with mouse cells. These results are consistent with those obtained by Mr S. Wijayaweera in the laboratory (data not shown). In summary, the human B-cell lymphoma cell lines appeared to internalise less rituximab than human CD20 Tg mouse B-cells, but consistent differences were observed between type I and type II mAb.

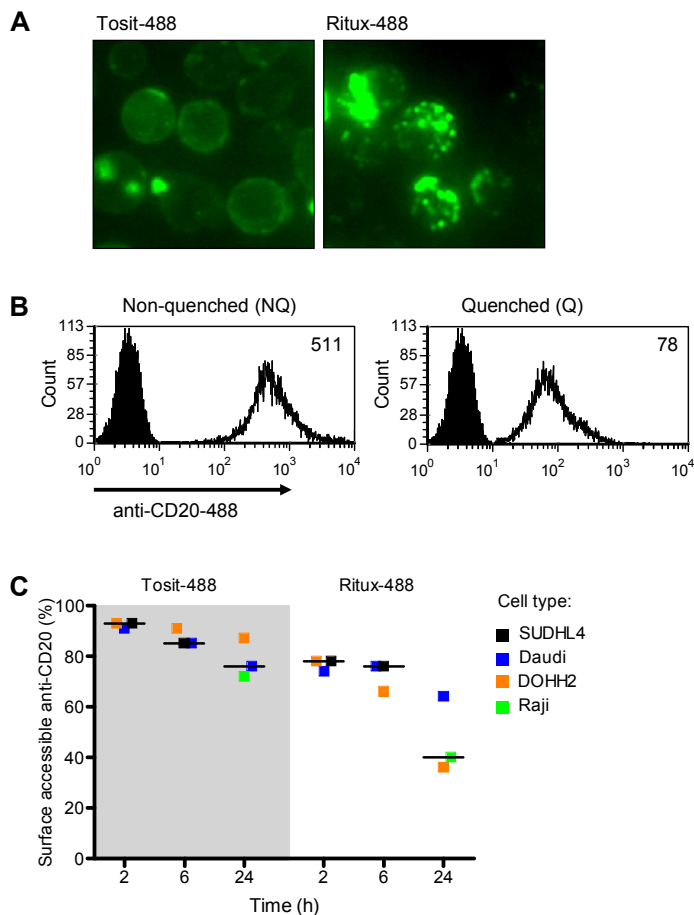


Figure 9: Internalisation of anti-CD20 mAb in human lymphoma cell lines

A) DOHH2 cells were treated with either Tosit-488 or Ritux-488 (both 5 $\mu\text{g}/\text{ml}$) for 24 h at 37°C and 5% CO_2 . The cells were then washed twice with cold FACS buffer and resuspended in 300 μl RPMI. 100 μl was transferred into a flat-bottomed 96-well plate for inspection by fluorescent light microscopy as described in **Section 3.16**. A 40x objective lens was used. The images shown are representative of other cell lines.

B) The remaining 200 μl of cells from A) was divided into two halves, and one half was treated with anti-Alexa 488 (quenched, Q) to quench surface fluorescence. The histograms show peaks for untreated cells (filled lines) and Ritux-488 treated cells (unfilled lines) of paired unquenched, and quenched samples. Geo MFI values are shown inset.

C) Human lymphoma cell lines, SUDHL4, Daudi, DOHH2 and Raji were treated with Tosit-488 or Ritux-488 for 2, 6, and 24 h. The quenching assay from B) was then performed. The % surface accessible anti-CD20 was calculated as $[\text{NQ Geo MFI} - (\text{NQ Geo MFI} - \text{Q Geo MFI})] / \text{NQ Geo MFI} * 100$ (**Section 3.11**). The quenching assay was repeated with each cell line up to 3 times, and representative results are shown. The lines shown represent the median.

4.2.2 Internalisation of anti-CD20 mAb in normal human B cells

Human cell lines are transformed and adapted to grow in tissue culture, and as a whole have been heavily passaged for generations. As such, like human CD20 Tg mouse B cells, they are not entirely representative of primary human cells. Therefore the quenching assay was repeated using whole blood extracted from healthy volunteers (which contained primary human B cells). The blood was directly treated with either Alexa 488-labelled type I or type II mAb for 2, 6 or 24 h at 5% CO₂ at 37°C. The quenching assay was then performed as described in the previous section. Harvested samples were washed twice with FACS buffer, then split for quenching with anti-Alexa 488 and concurrently stained with anti-CD19-APC or -PE to identify the B cell population. Red cells were then lysed and the samples analysed by flow cytometry.

Frequently, the raw data was difficult to interpret due to the presence of dual B-cell populations, both being CD19⁺ but with distinct CD20 expression (**Fig. 10A**). This feature was not observed when the same B cells were purified (discussed later). The presence of dual populations made identification of the correct populations in unquenched and quenched samples difficult. However, whether both populations were regarded as one or two distinct populations, time-dependent internalisation of both mAb was observed (**Fig. 10B**). As before, type I Ritux-488 internalised more than type II Tosit-488, but only to a statistically significant level after 24 h treatment. Internalisation of Tosit-488 was also far more heterogeneous than previously observed in human CD20 Tg mouse B cells and human B cell lines. As the mAb are of different isotypes (Tosit-488 mIgG2a and Ritux-488 huIgG1) the difference in mAb internalisation might also be due to variation in isotype and not type I/II differences.

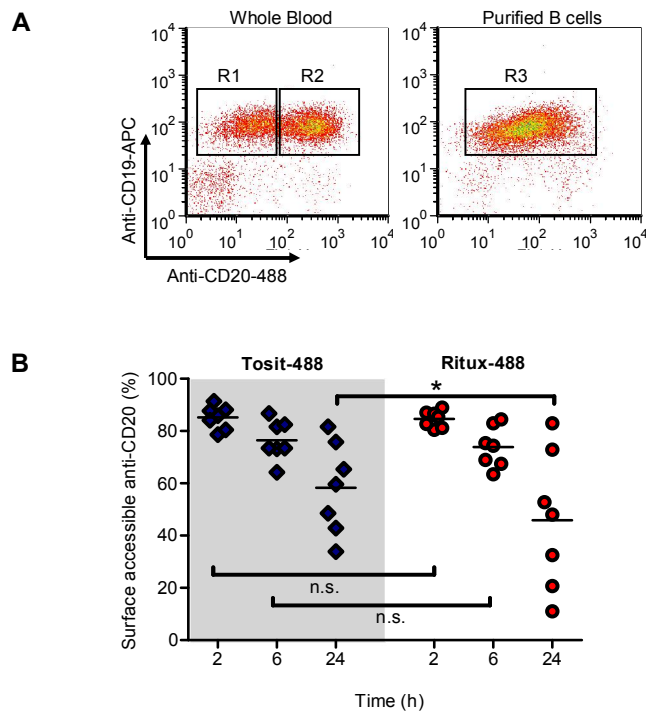


Figure 10: Internalisation of rituximab in whole blood and purified B cells

A) The FACS plots shown are derived from two quenching assays using whole blood (left) and purified B cells. Whilst a single, clearly-defined CD20⁺ population was seen when pure B cells were used, whole blood populations produced a bimodal CD20⁺ population which complicated gating of the correct cells in unquenched and quenched samples.

B) The graphs represent results obtained from the quenching assay using whole blood healthy volunteers. The whole blood samples were incubated with 5 µg/ml Tosit-488 or Ritux-488 for 2, 6 or 24 h. *p <0.05, medians are shown.

To address the difficulties encountered with whole blood, the quenching assay was repeated using purified human B cells negatively isolated by MACS magnetic beads as detailed in **Section 3.2.2**. A B-cell purity of 95% was achieved using this method (**Fig. 11A**). The quenching assay was repeated as described in **Section 4.2.1** and anti-CD19-PE/-APC was used to identify the B cells as before (**Fig. 11B**). **Fig. 11C** shows the results with B cells derived from 8 different healthy volunteers. In contrast to the results obtained with the whole blood experiments, the rates of internalisation of anti-CD20 were remarkably consistent despite the experiments being performed independently and on 8 different subjects of different ethnic origins (English, Irish, Indian and Japanese). As before, Ritux-488 internalised more than Tosit-488 at all time points (e.g. median 54% compared to 87% surface accessibility at 6 h, p values <0.01). As

before, this difference in mAb internalisation could be explained by either type I/II differences or the disparity in mAb isotype. Furthermore, a marked difference in the internalisation of Ritux-488 (after 6 h treatment) was observed between the cell lines (**Fig. 11C**) and primary B cells (**Fig. 9C**). 76% of mAb remained on the surface of cell lines compared to 54% on normal human B cells. At 24 h, the level of internalisation was equivalent on both primary cells and cell lines (33% and 40%, respectively). Altogether, these results indicate that Ritux-488 internalised in both cell lines and primary cells, but at a much slower rate in the former.

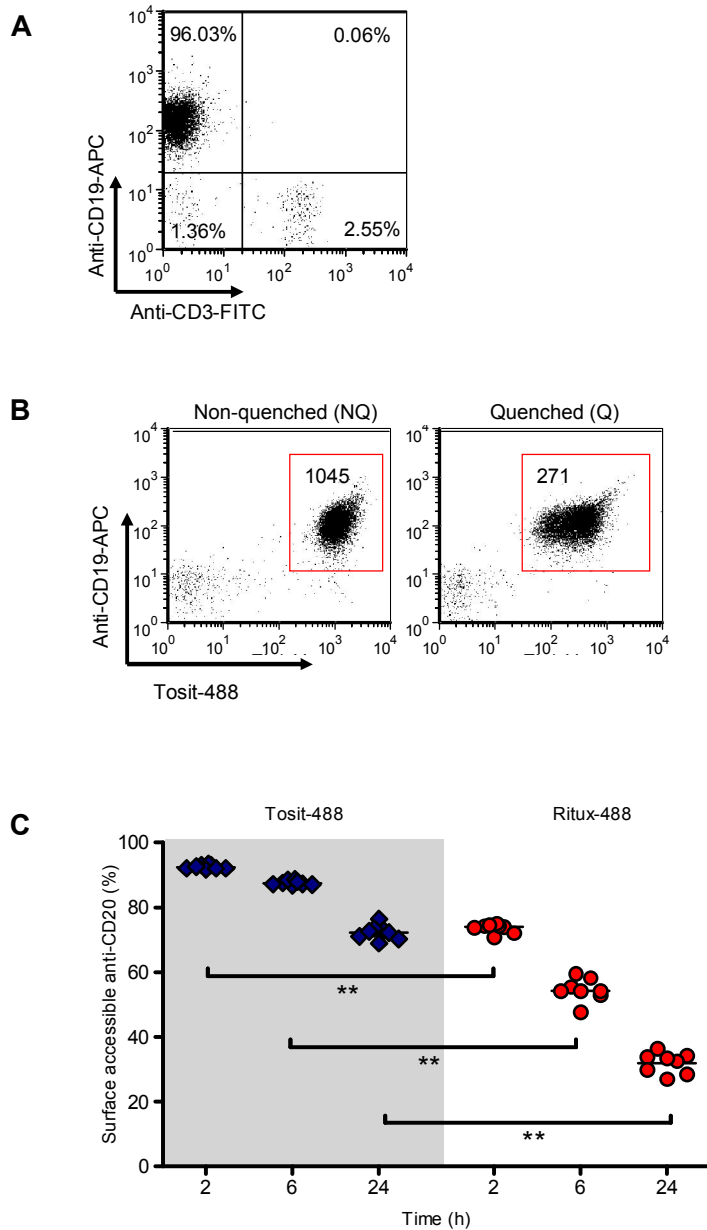


Figure 11: Internalisation of anti-CD20 in human B cells purified from healthy volunteers

A) The purity of B cells isolated by magnetic beads was checked by staining with anti-CD19-APC (5 µg/ml) and anti-CD3-FITC (10 µg/ml) for 30 mins at 4°C. The cells were washed once with cold FACS buffer and examined by flow cytometry. A representative FACS scatter plot is shown.

B) The quenching assay in **Fig. 9** was performed using purified normal B cells, after treatment with the specified mAb for 6 h. Anti-CD19-APC (5 µg/ml) was added during the quenching step to identify the B cells. Representative FACS plots show unquenched and quenched samples. Geo MFI values of the gated populations are shown inset.

C) The graph shows results of the quenching assay performed using Tosit-488 and Ritux-488 on purified normal B cells obtained from 8 different volunteers. **p < 0.001, medians shown.

4.2.3 Validation of the quenching assay

Prior to testing an extensive panel of precious primary tumour material, the quenching assay required further validation. To do this, the quenching assay was carried out at the same time as the direct cell surface assessment after 6 h incubation with the mAb (**Fig. 12A**). For direct cell surface assessment, anti-CD20 mAb with the same isotype were required, so GA101_{gly} and rituximab were used. As previously mentioned, GA101 is a new, clinically relevant type II anti-CD20 with a defucosylated Fc region.⁴⁶⁴ The unmodified Fc form, GA101_{gly} was used in these experiments. The surface-bound anti-CD20 mAb was detected by a secondary FITC labelled mAb, anti-huIgG SB2H2. To ensure that SB2H2 only bound to the mAb, non- IgG expressing cells were chosen.

In the direct cell surface assessment assay, baseline CD20 expression was determined using cells that were pre-incubated with 15 mM sodium azide and 25 mM 2-deoxyglucose to stop cellular metabolic activity and hence, endocytosis. These cells were then treated with unlabelled anti-CD20 mAb for an hour to enable maximal binding to surface CD20. This was followed by two washes using cold FACS buffer to remove excess unbound mAb and detection with SB2H2-FITC. After a further wash, the samples were analysed by flow cytometry. To analyse the extent of internalisation after 6 h, the cells were simultaneously treated with unlabelled mAb for an hour, then washed (to ensure similar levels of mAb was bound on the cell surface) and left to incubate for a further 5 h and then harvested and treated like the baseline cells. Internalised mAb will not be detectable by SB2H2-FITC thus the reduction in Geo MFI from the baseline cells represents the proportion of internalised mAb (**Fig. 12B**). **Fig. 12C** confirms that the percentage of surface accessible anti-CD20 obtained using both methods were comparable. These data also show the lack of internalisation of a second, different type II mAb.

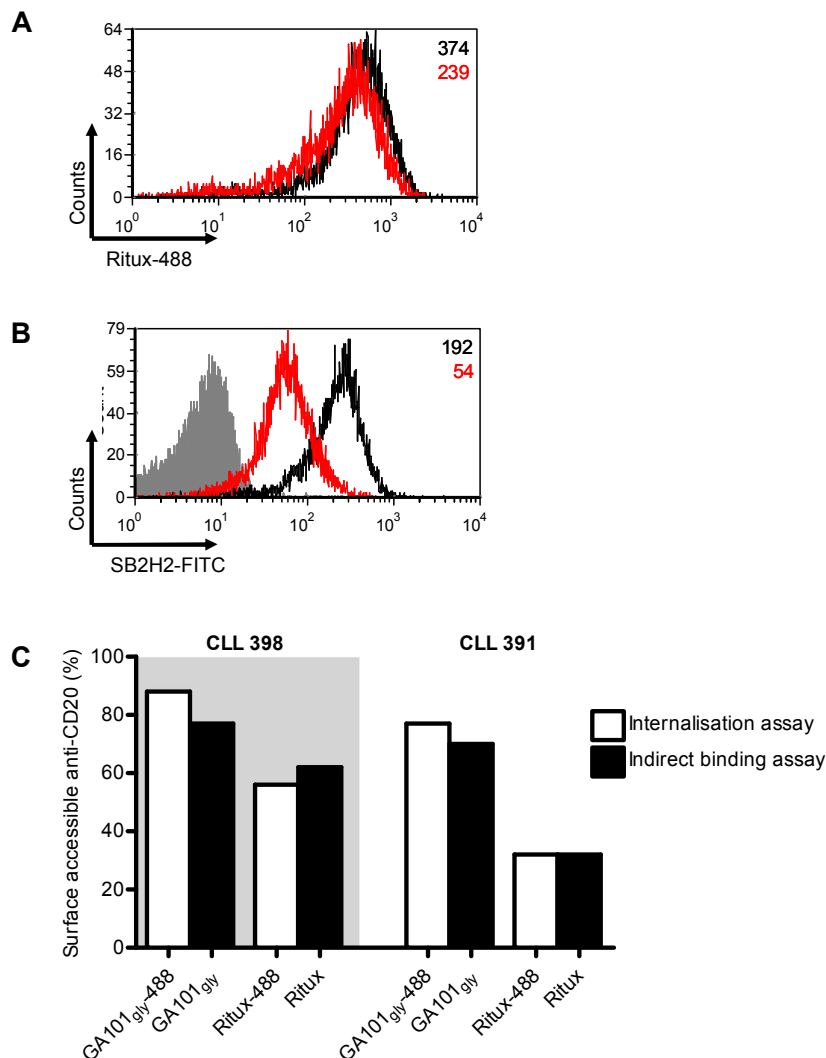


Figure 12: Validation of the quenching assay

A) CLL cells were treated with GA101_{gly}-488 or Ritux-488 (both 10 µg/ml) for 6 h and then the quenching assay performed as in Fig. 9. The histogram overlay shows an example of CD20 expression Ritux-488-treated cells. NQ (black), Q (red) samples and respective Geo MFI values are shown inset.

B) CLL cells were treated with 15 mM sodium azide and 25 mM 2-deoxyglucose for 30 mins and then further treated with GA101_{gly} or rituximab (both at 10 µg/ml) for 1 h at 4°C. The samples were then washed twice with cold FACS buffer and 10 µg/ml SB2H2-FITC added for 30 mins at 4°C. After a final wash, the samples were analysed by flow cytometry and the Geo MFI values obtained (black line) represented baseline surface CD20 expression. To measure residual surface CD20 expression after 6 h treatment, CLL cells were simultaneously incubated with GA101_{gly} or rituximab (both at 10 µg/ml) for 1 h at 37°C, then washed once in supplemented RPMI and returned for 5 h incubation at 37°C. Samples were then harvested and treated similarly to baseline CLL cells (red line). The grey line shows untreated CLL cells stained with SB2H2-FITC only. Geo MFI values are shown inset again.

C) The graph shows the % of surface accessible anti-CD20 obtained by the quenching assay in A), and by indirect staining in B) in 2 different CLLs.

4.2.4 Internalisation of anti-CD20 mAb in primary neoplastic B cells

Having validated the quenching assay with a more conventional assay and confirmed that primary human B cells do internalise rituximab from the cell surface, we undertook a comprehensive study of primary tumour cells. As before, clinically relevant rituximab and tositumomab were used in these assays to examine the differences in internalisation between type I and type II mAb. Isotype controls for rituximab were also included.

A total of 48 different CLL samples (**Fig. 13A**) were examined for internalisation of tositumomab and rituximab. The ability of tositumomab and rituximab to reduce the amount of surface accessible CD20 over 2, 6 and 24 h (**Fig. 13A**) is shown. As previously observed with normal human B cells, internalisation of anti-CD20 was time-dependent. Internalisation of each mAb was heterogeneous, and this was most marked with type I compared to type II mAb at 6 h (SD 11.8 compared to 6.9 respectively). However, despite the heterogeneity, type I mAb still clearly internalised more than type II mAb at all time points (median surface accessible anti-CD20 for tositumomab and rituximab 80% and 37% at 6 h, respectively). By 6 h, the internalisation of rituximab was near maximal, with medians of 37% and 20% of the mAb remaining accessible on the surface at 6 and 24 h, respectively. In view of this and the reduction in viability of CLL cells over time (data not shown), samples were treated for 6 h subsequently.

In order to confirm that the mAb isotype was not accountable for the difference in internalisation between type I and type II mAb, two other clinically relevant anti-CD20 mAb were generated in-house and tested. Ofatumumab (ofatum; type I) has recently been approved by the US FDA in relapsed/refractory CLL, and GA101_{gly} (**Fig. 13B**). Consistent with its type I nature, ofatumumab also resulted in a high degree of internalisation (median 26% accessible at 6 h). In contrast, GA101_{gly} showed far less internalisation, with a median of 70% (range 57-81%) of bound mAb accessible at 6 h, respectively. In summary, type I mAb internalised to a greater extent than type II mAb.

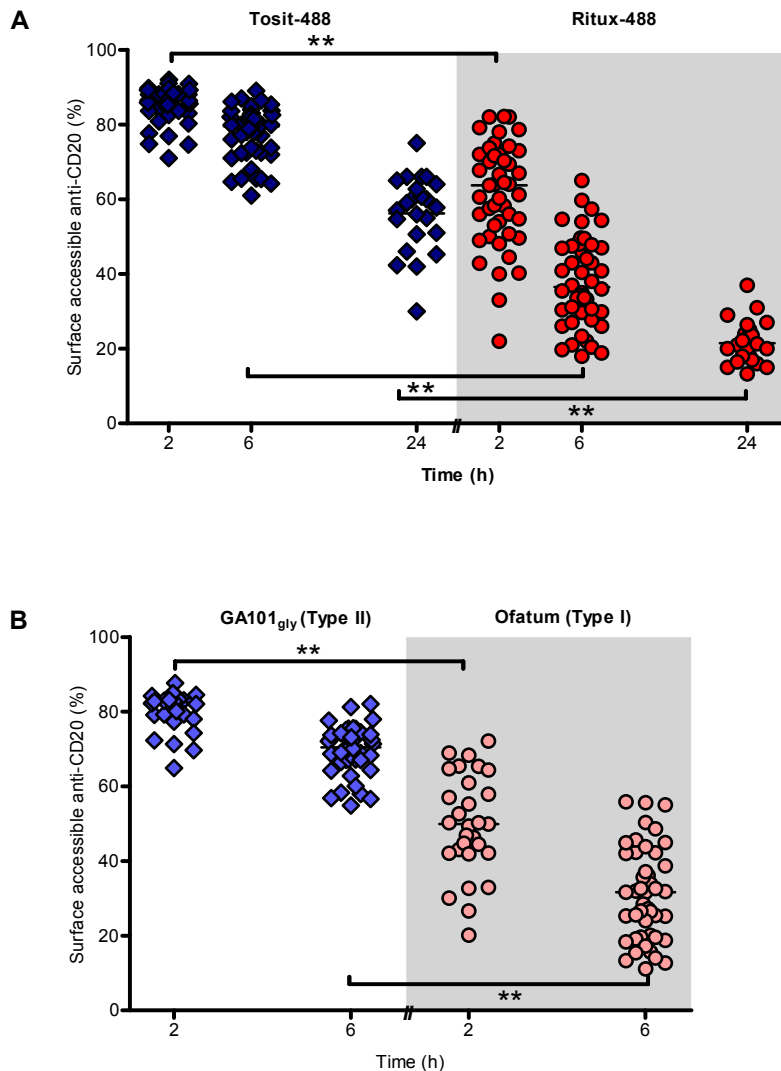


Figure 13: Type I mAb internalise from the cell surface of normal and malignant human B-cells

A) Primary CLL cells were cultured with Tosit-488 or Ritux-488 (all at 5 $\mu\text{g}/\text{ml}$) for 2, 6 or 24 h. The quenching assay in Fig. 9 was then performed. Each point represents a sample from a different CLL patient. ** p value < 0.001, and medians are shown.

B) As in A), the quenching assay was performed in primary CLL cells, but using GA101_{gly}-488 and Ofatum-488 (all at 5 $\mu\text{g}/\text{ml}$) for 2 or 6 h. ** p value < 0.001, and medians are shown.

Having shown rapid, yet heterogeneous internalisation of type I mAb in CLL, we wondered whether other primary B-cell tumours would demonstrate similar characteristics. Seven SLL and DLBCL patients each, 8 MCL and 14 FL patients were obtained with local ethical approval as detailed in Section 3.3, and also

examined by the quenching assay (**Fig. 14**). The results with the normal peripheral B cells shown in **Fig. 11C** were included for comparison. The difference in the ability of type I and II mAb to internalise persisted across all histological subtypes. Surprisingly, internalisation of rituximab on normal B cells was more uniform than in the malignant B cells, perhaps suggesting that factors associated with malignancy contributed to the observed heterogeneity. The rate of rituximab internalisation with SLL and MCL cells (**Fig. 14**) was similar to that with CLL (**Fig. 13A**). The similarity in the internalisation of rituximab between the SLL and CLL samples suggest that internalisation was not affected by compartmental differences (i.e. nodal compared to circulating B cells). For DLBCL and FL samples, the rate was somewhat slower (**Fig. 14**, $p < 0.0001$ and 0.0027 respectively, when compared to CLL from **Fig. 13A**). However, in FL 2/11 patient samples internalised rituximab extremely rapidly, leaving barely detectable levels of mAb or CD20 on the cell surface within 6 h of treatment. These two samples will be discussed further in **Section 5**.

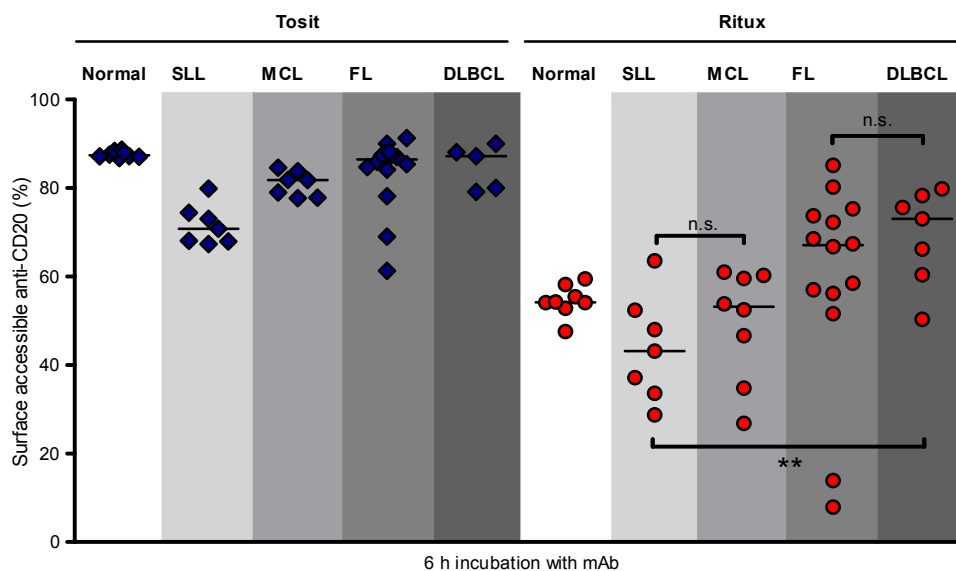


Figure 14: Type I mAb internalise from the cell surface of normal and malignant human B cells

Primary normal and malignant B cells were treated with either Tosit-488 or Ritux-488 (all at $5 \mu\text{g}/\text{ml}$) for 6 h and then the quenching assay performed as in **Fig. 9**. ** $p < 0.001$, medians are shown.

4.2.5 Potential modulators of internalisation of rituximab

4.2.5.1 The effect of CLL prognostic markers

The internalisation of type I anti-CD20 mAb within CLL cases was clearly heterogeneous (**Fig. 13**). It is recognised that CLL has well-established prognostic markers (**Section 1.3.3**), thus it is possible that one of these factors might be associated with some of the heterogeneity seen in CLL. Rituximab internalisation rates obtained by the quenching assay (Ritux-488 treatment for 6 h) were assessed in the context of IgV_H gene mutation status, ZAP-70 and CD38 expression levels between different samples. No correlation was found with any of these prognostic markers (**Figs. 15A-C**). In addition, other potential factors that might influence internalisation of anti-CD20 such as the degree of viability of the thawed cells and CD20 expression were also examined (**Figs. 15D-E**). We observed that although the cell viability of the samples was generally high, it did vary from 16 to 95% at the beginning of cell culture (median 81%, SD 15.5) (**Fig. 15D**). As energy is likely to be required for internalisation,³⁵⁵ the difference in viability could influence the degree of rituximab internalised. This relationship was not demonstrated to be statistically significant (**Fig. 15D**) but the p value was 0.055, i.e. close to the threshold for clinical significance. Therefore it is possible that a larger sample size may in fact demonstrate the proposed effect.

CLL classically has a lower surface CD20 expression^{465,466} than other B-cell lymphomas. Accordingly, 69% (30/45) of CLL samples demonstrated a CD20 Geo MFI of less than 500. The low level of CD20 expression has been presumed to be one of the causes for the poor response to rituximab, in comparison with DLBCL and FL which have higher CD20 expression, although this has never been proven.⁴⁶⁷ Nevertheless, the level of CD20 expression is predictive of survival in DLBCL.⁴⁶⁸ The surface density of CD20 could feasibly influence internalisation, perhaps through changes in antigen cross-linking. A significant but weak correlation was seen between CD20 expression and internalisation of rituximab

(p value 0.02, $r^2 = -0.12$) (Fig. 15E), and lower CD20 expression seemed to favour less internalisation.

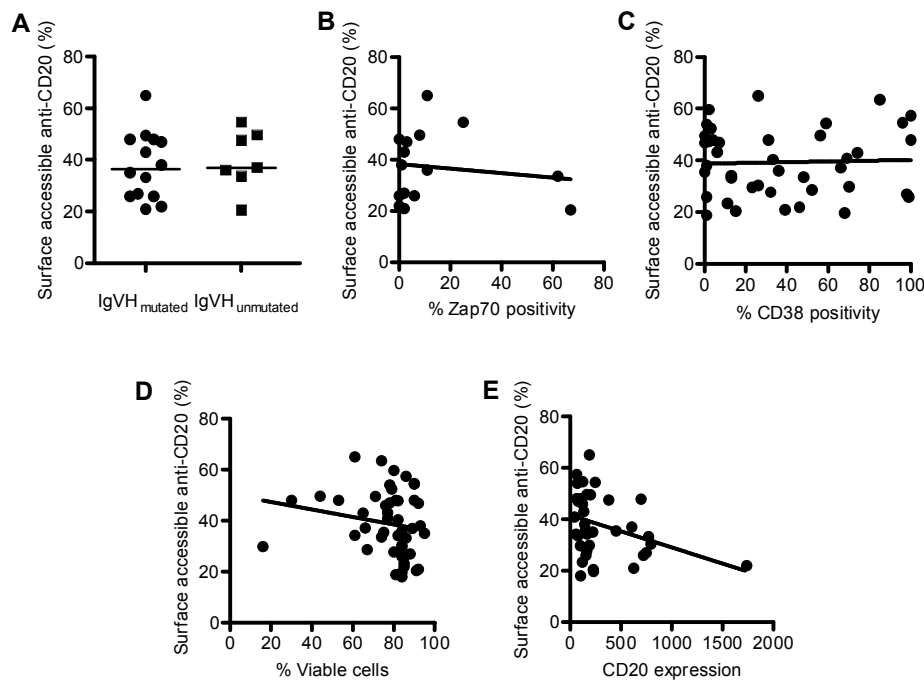


Figure 15: Correlation between internalisation of rituximab and CLL phenotypic and prognostic markers

A-E) CLL cases were phenotyped for IgV_H gene mutational status, Zap-70 and CD38 expression as described in **Section 3.5**. Viability was assessed using Annexin V/PI and CD20 expression was assessed using Ritux-488 staining for 2 h. The quenching assay was performed on these samples as described in **Fig. 9**. Correlation between each prognostic feature and internalisation of rituximab was performed by Spearman's correlation. Except CD20 expression, no correlation was seen with each prognostic factor ($p > 0.05$). A weak correlation was seen with CD20 expression (Spearman r value -0.34 , $p = 0.038$). Subsequent analysis using multivariate regression of CD20 and Fc γ RIIb expression (discussed later in **Section 5.2.3**) against rituximab internalisation showed that the weak correlation with CD20 was not significant ($p = 0.638$).

Although no correlation was demonstrated between CD38 expression and internalisation of rituximab (**Fig. 15C**), it is recognized that CD38 expression is variable throughout the course of disease.²⁰¹ Furthermore, even within an individual, expression on CLL cells can be variable.⁴⁶⁹ As an alternative means of

examining the influence of CD38 expression on internalisation of rituximab, and as a means of controlling the multiple biological variables that exist between different CLL cases, CD38 expression within individual CLL samples was analysed. Specifically, we explored whether internalisation of rituximab varied between CD38⁺ and CD38⁻ CLL cells in individual cases. To do this, the CLL cells were treated as with Ritux-488 for 2 or 6 h, and the quenching assay carried out as previously described. During the quenching step, the B cells were co-stained with anti-CD38 PE to identify CD38⁺ and CD38⁻ cells. The Geo MFI from Ritux-488 staining for each of CD38⁺ and CD38⁻ populations were used to calculate % surface accessible anti-CD20. No difference was observed between CD38⁺ or CD38⁻ cells in 3 different samples, and representative results are shown (**Figs. 16A-B**).

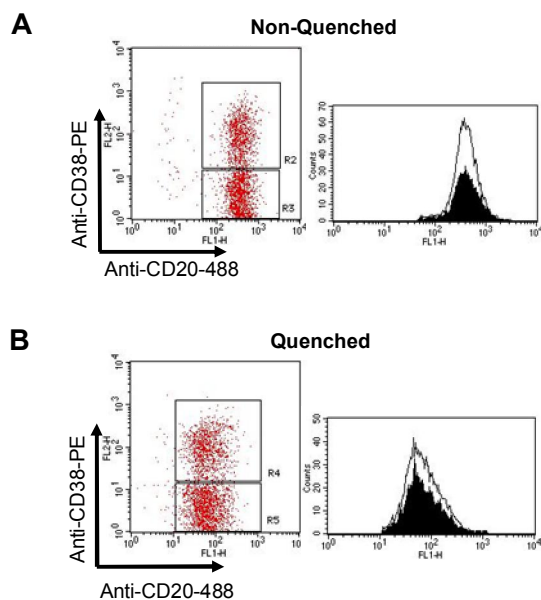


Figure 16: The effect of CD38 variability and rituximab internalisation

(A-B) Within a single CLL case, variation in CD38 expression was seen. The FACS plots show samples pre-quenching (A) and post-quenching (B). The corresponding histograms highlight that CD38⁺ and CD38⁻ cells within a single sample internalised rituximab at the same rate. CD38⁺ and CD38⁻ cells are represented by solid and hollow peaks respectively. These results are representative of 3 different cases.

4.2.5.2 Del(11q) and internalisation of anti-CD20

Recent evidence from clinical trials^{220,238} suggests that patients with del(11q) benefit from rituximab-incorporated chemoimmunotherapy (specifically FCR) more than other prognostic subgroups within CLL. The reason for this is unknown and seems counter-intuitive since del(11q) is associated with lower CD20 expression.²³⁵ We postulated that reduced internalisation of rituximab might account for the improved response seen in the del(11q) subgroup in CLL. As discussed in **Section 1.3.3.2**, the DNA repair protein, ATM, lies within this minimally deleted region. Therefore, the del(11q) CLL samples were specifically examined for ATM deletion and function as described in Material and Methods (**Section 3.5**).

We examined a cohort of 25 CLL samples with normal 11q region and normal ATM function, and 9 with ATM loss (**Fig. 17**). These samples were assessed in the quenching assay and phenotyped for CD20 expression and other markers (further discussed in **Section 5.2.3**). A statistically significant difference was observed wherein del(11q) samples had lower CD20 expression, consistent with published data (**Fig. 17A**).²³⁵ However, no significant difference was seen in the internalisation of rituximab between the two groups (**Fig. 17B**)

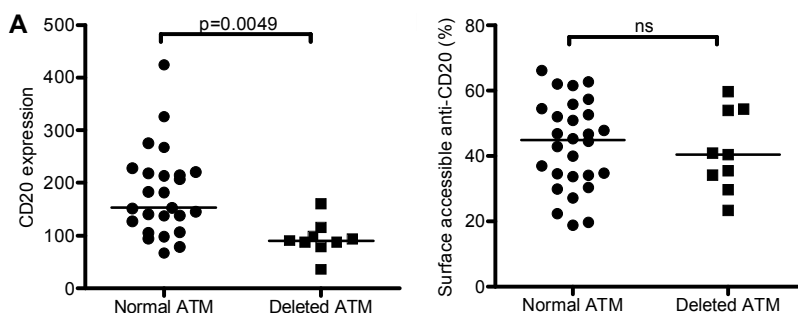


Figure 17: Correlation between internalisation of rituximab and ATM loss in CLL.

A) The 11q mutation status of CLL samples was determined by FISH and SNP and classified as normal ATM (other chromosomal abnormalities were not taken into account) or ATM loss. CD20 expression was determined by staining samples with Ritux-488 (5 µg/ml) for 2 h at 37°C, and then washed thrice with cold FACS buffer and analysed by flow cytometry. Medians are shown.

B) The same samples in A) were tested for internalisation of rituximab after 6 h treatment by the quenching assay in **Fig. 9**. Medians are shown.

4.2.5.3 The association of the BCR with the internalisation of anti-CD20

CD20 has been physically and functionally linked to the BCR e.g. oligomerisation of both molecules on the cell surface, and hijacking of BCR-mediated calcium signalling, as discussed in **Section 1.4.2**. Furthermore, the signalling ability of the BCR has been implicated in the survival of the tumour cells in CLL⁴⁷⁰ and other B-cell malignancies.²⁸⁰ Thus it was possible that the BCR may play a role in the internalisation of anti-CD20 mAb. First, we examined if the isotype of the BCR influenced internalisation of rituximab. We compared IgG⁺ and IgM⁺ CLL cases (n=7 and 39, respectively) and found no significant difference in internalisation after 6 h treatment with rituximab (**Fig. 18A**). Only 7 IgG⁺ CLL samples were tested owing to its low frequency.⁴⁷¹ We then went on to inspect if an association existed between the level of surface Ig expression and internalisation in the 39 IgM⁺ CLL cases. Again, no significant correlation was demonstrated (**Fig. 18B**). As a complementary approach, BCR-induced calcium flux levels (n=10) were compared with the internalisation of anti-CD20 (**Fig. 18C**), and no again correlation was seen.

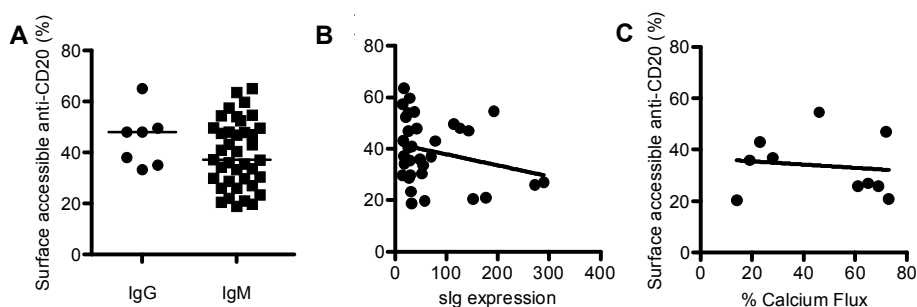


Figure 18: Correlation between internalisation of rituximab and del(11q) in CLL

A-C) CLL cases were phenotyped for sIg expression, sIgM expression level and % calcium flux on sIgM ligation as described in **Section 3.5**. The quenching assay was performed on these samples as described in **Fig. 9**. Correlation between each feature and internalisation of rituximab was performed by Spearman's correlation analysis. No correlation was seen ($p>0.05$).

As a more direct method of investigating the relationship between the BCR and CD20, the slg expression level at the cell surface of CLL cells was assessed after anti-CD20 mAb stimulation. Seven different CLL cases with known slg isotype/expression levels were selected and either cultured without treatment or treated with either GA101_{gly} or rituximab for 6 h (data not shown). 5 cases, including 2 IgG⁺ cases, showed minimal change in slg expression when compared to baseline, whether treated or untreated (**Fig. 19A**). Consistent with a previous report, 2 of the cases showed increased slg expression from just being cultured without stimulation (**Figs. 19B-C**).⁴⁵⁴ Treatment with either anti-CD20 mAb prevented this increase in slg expression. A similar observation was also previously noted in human lymphoma cell lines and normal B cells.²⁸⁹

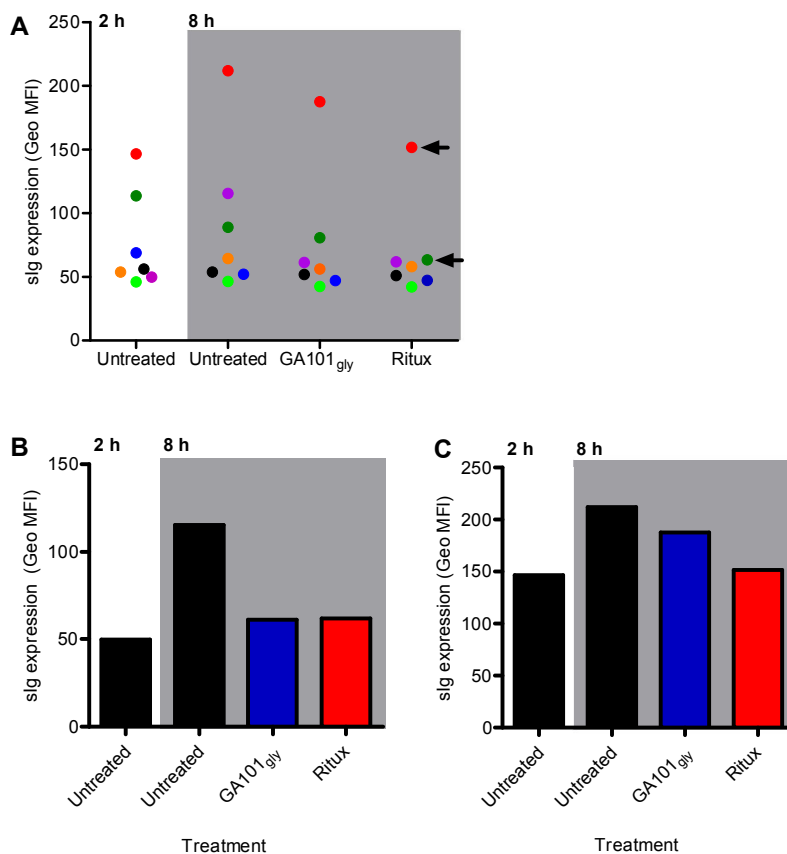


Figure 19: Changes in sIg expression of CLL cells after anti-CD20 cross-linking

A) The graph represents results from 7 different CLL patients. Each case is represented by a different colour. CLL cells were thawed from cryopreservation and rested for 2 h before treatment with the anti-CD20 mAb shown (10 $\mu\text{g}/\text{ml}$) or left untreated for a further 6 h (total 8 h) at 37°C and 5% CO₂. Surface Ig expression of the cells was assessed after resting (i.e. at 2 h) or after 8 h. For this, the cells were first washed, and then sIg expression assessed with M15/8-488 and SB2H2-FITC (all 10 $\mu\text{g}/\text{ml}$) for 30 mins at 4°C, for sIgM and sIgG positive cases, respectively. After a further wash, the samples were assessed by flow cytometry. The black arrows indicate the sIgG⁺ samples.

B-C) The two untreated samples from A) in which the sIg expression increased after 8 h compared 2 h is shown in isolation here. B) represents the purple (●), and C) the red (●) samples respectively.

In view of these findings, 4 further different cases of CLL were treated similarly and examined by confocal microscopy to explore whether a direct interaction could be visualised between the BCR and anti-CD20:CD20 complexes after anti-CD20 mAb treatment. The CLL cells were treated with Alexa 647-labelled rituximab (Ritux-647) or cultured without treatment for 2, 6 and 24 h (**Fig. 20**

and data not shown). The cells were then harvested and washed, and permeabilised with saponin and treated with M15/8-488 to detect IgM. In all 4 cases, minimal co-localisation was seen between the BCR and rituximab at all time points (**Fig. 20**). In all cases, BCR staining remained relatively uniform in comparison to the punctate staining seen with rituximab. In 2/4 cases, once again, BCR staining in Ritux-647 treated cells appeared less bright than untreated cells. However this is a subjective observation (data not shown).

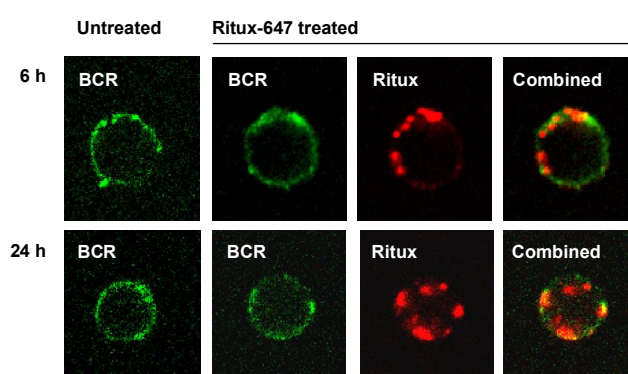


Figure 20: Investigation of co-localisation of BCR and rituximab

CLL cells were thawed from cryopreservation and rested for 2 h before treatment with Ritux-647 (10 $\mu\text{g/ml}$) or left untreated for 6 and 24 h at 37°C and 5% CO₂. The cells were then washed and permeabilised with saponin and stained M15/8-488 (10 $\mu\text{g/ml}$) for 30 mins at 4°C simultaneously. Then, the cells were washed with cold FACS buffer and saponin, and then fixed with 4% paraformaldehyde for 10 mins at RT. The cells were then washed again with cold FACS buffer and then transferred to poly-L-lysine coated slides and mounted for confocal microscopy. Different cases are shown at each time point, and are representative of 4 different cases.

4.3 Discussion

Here, we examined the relative ability of human cell lines and different subtypes of primary B cells to internalise type I and type II anti-CD20 mAb after validating the surface fluorescence quenching assay. Furthermore, within the CLL cases, we also examined whether there was an association between the established prognostic markers, and the BCR with internalisation of type I anti-CD20 mAb.

The method used to measure internalisation was validated objectively by an indirect binding assay, and subjectively by fluorescent light microscopy. Initially, B cells from whole blood were used for the quenching assay, but the existence of bimodal CD20-expressing B cells complicated the analysis. Previous reports of CD20 phenotyping in human whole blood only demonstrate a single population of CD20-expressing B cells.⁴⁷² Similarly, when we stain pure B cells, only single CD20-expressing populations are seen. We suggest that these disparate results are potentially due to the phagocytosis or trogocytosis of the anti-CD20 mAb opsonised B cells by the innate immune effector cells in the whole blood. In keeping with this, greater incubation times (e.g. 24 h compared to 2 h) and thus a greater period of interaction between the opsonised B cells and innate immune effector cells, increased CD20 bimodality (data not shown).

The findings also clearly show that type I anti-CD20 internalise to a greater extent than type II anti-CD20. Type I anti-CD20 internalises more rapidly in primary B cells compared to cell lines, hence rationalising the conclusions of earlier reports in human cell lines, which suggested that anti-CD20 mAb did not internalise from the surface of B cells using 1F5,^{452,473,474} 1H4^{452,473,474} (both type I) and tositumomab.^{452,473,474} This is in contrast to anti-CD22, which internalises very rapidly,⁴⁵² with 90% of the mAb internalised within an hour using the same surface fluorescence quenching assay (Dr A. Vaughan, personal communication). These earlier findings led to a general assumption that anti-CD20 mAb and its target CD20, did not internalise from the surface of B cells. Here, our findings highlight the importance of validating investigations of cell lines, in primary tumour material.

The internalisation of rituximab was markedly different between the various primary malignant B cell subtypes tested. CLL/SLL and MCL appeared to internalise more rituximab than FL or DLBCL at the same time points. The lack of difference between CLL and SLL hints that variation in internalisation of rituximab is probably not due to any intrinsic difference between the cells from different compartments. A similar conclusion cannot be made about the impact

of the microenvironment on the internalisation of rituximab seeing that the surrounding cells and cytokines which contribute to the microenvironmental influence is effectively removed when the cells transferred into a single cell suspension for testing. As previously discussed (**Section 1.4.1**), rituximab is of proven benefit in FL and DLBCL, but appears less so in CLL and MCL. This difference in clinical benefit appears to draw a parallel with the propensity of each disease subtype to internalise rituximab. Thus it is possible that internalisation might account for cases of rituximab resistance.

The internalisation of rituximab in normal B cells from healthy human volunteers was remarkably consistent despite the experiments being conducted independently. This observation, and other repeats on the same samples (data not shown) demonstrate the reproducibility of the quenching assay. Interestingly, the same consistency in the internalisation of rituximab was not observed in the primary tumour material tested. There were too few cases of MCL, FL and DLBCL to comment on heterogeneity, but heterogeneous internalisation of rituximab was evident within the cohort of CLL cases tested. An attempt was made to link the heterogeneous internalisation of rituximab with known prognostic markers in CLL, but no association was found. Admittedly, if a weak association does exist, the study is likely to be under-powered to detect it.

A recent clinical trial demonstrated that addition of rituximab to FC abrogated the poor prognosis implicated by del(11q) in CLL patients.²⁵⁴ Therefore, we explored whether internalisation of rituximab between non-11q and del(11q) groups could account for the difference in response between non-11q and del(11q) cohorts. No significant difference was demonstrable and again, the findings were impaired by the small sample size. Another interesting aspect noted in the examination of the del(11q) cases was the significantly weaker CD20 expression levels in this cohort, consistent with previous observations.²³⁶ This observation lends support to our argument that the historically assumed

poorer responses in CLL are unlikely to be due to its weaker CD20 expression, in comparison to other lymphomas.

The established links between the BCR and CD20 suggested that an association might exist with internalisation of rituximab. No correlation was observed in terms of BCR isotype, sIgM expression level, or the ability of the BCR to elicit calcium flux. A previous report demonstrated the re-expression of the BCR in unstimulated CLL cells in ex vivo culture.⁴⁵⁴ It was hypothesised that this re-expression could be due to removal of in vivo antigen-engagement when the cells were removed for ex vivo culture. In keeping with these findings, an increase in sIgM level was observed in untreated cells after 6 h in vitro culture in 2/7 cases. The expression level reported by Mockridge et al.⁴⁵⁴ was maximal by 48 h, and it is probable that most of the cases tested would exhibit the same change had we cultured it for the same period of time. However, due to concerns of viability and functionality, this was not undertaken. Interestingly, anti-CD20 mAb, regardless of type, appeared to prevent re-expression of the BCR. These results are consistent with a previous study whereby after 72 h treatment, tositumomab and another anti-CD20, L27 reduced sIgM expression of human cell lymphoma cell lines and normal human tonsil and peripheral blood B cells in comparison to untreated cells.²⁸⁹ The authors suggested that the observation was FcR-independent as tositumomab (mIgG2a) and the other type I mAb, L27 (hulgG1) are of different isotypes. It was also shown that the reduction in BCR expression by anti-CD20 mAb was inhibited by staurosporine. The authors therefore hypothesised that this effect by anti-CD20 mAb was dependent on the protein kinase C pathway. However, staurosporine is not a specific protein kinase C inhibitor,⁴⁷⁵ thus the conclusions are inaccurate. The reasons behind ex vivo BCR re-expression are poorly understood. However it is accepted that antigen-engagement of the BCR leads to internalisation of the receptor. Therefore it is possible that the anti-CD20 mAb are able to indirectly stimulate the BCR, thereby promoting BCR endocytosis. For type I anti-CD20, we explored whether the mAb was internalised together with the BCR using confocal microscopy. Minimal co-localisation was seen between type I anti-

CD20 and BCR in all four cases tested. However, a limitation of the confocal microscopy experiments is the need for sufficiently high sIgM CLL expressors to be selected to allow detection of the BCR, which may skew our findings.

In summary, this section demonstrates convincingly that type I anti-CD20 mAb internalise from the surface of primary B cells at a heterogeneous rate. No association was evident between the differing rates of internalisation and the known prognostic markers in CLL, or the BCR. In the next chapter, further work is focused on elucidating other factors that might be responsible for influencing internalisation of type I anti-CD20 mAb.

5 The role of Fc γ RIIb in the internalisation of anti-CD20 mAb

5.1 Introduction

The earlier investigations failed to clarify the reasons behind the heterogeneous internalisation of type I anti-CD20 mAb. This chapter sets out to explore whether internalisation of type I anti-CD20 mAb could be related to Fc:Fc:R interaction as many different groups have demonstrated this interaction to be important in the efficacy of anti-CD20 mAb in both mouse models and in patients (**Section 1.5.1**). Briefly, in γ chain knockout mice, B-cell depletion by anti-CD20 mAb was completely abrogated.^{297,340,367} Clinical observations in patients were also generally supportive. Patients with FL and Waldenstrom's macroglobulinaemia who bear the higher affinity Fc γ RIIIa 158V/V polymorphic variant in comparison to V/F or F/F variants, have better outcomes to rituximab.³⁴⁹⁻³⁵¹ The rationale behind the importance of the higher affinity activatory Fc γ RIIIa is that it allows improved engagement of the Fc domain of rituximab (bound to target B cells) to the activatory Fc γ RIIIa on immune effector cells. Although the quenching assay is performed with cell cultures comprising predominantly of B cells, we explored whether Fc:FcR interactions might also have an influence on internalisation. This interaction was first studied by comparing the internalisation of F(ab')₂ and IgG molecules of rituximab. Investigations were then undertaken to confirm the type of Fc γ RII, and the isoform of Fc γ RIIb present on the different subtypes of human B cells (**Section 1.5.1.1**). The latter sections then focus on elucidating the interaction between Fc γ RIIb and rituximab:anti-CD20 via variations of the quenching assay, confocal microscopy and phagocytosis assays.

5.2 Results

5.2.1 The influence of the Fc domain on the internalisation of rituximab

To investigate the necessity of Fc:FcR interaction for the internalisation of rituximab, the quenching assay was repeated with whole IgG and F(ab')₂ fragments of rituximab in CLL cells (**Fig. 21**). After 6 h treatment, the F(ab')₂ fragment had internalised markedly less (50% surface accessible anti-CD20) than the intact IgG molecule (37% surface accessible anti-CD20) despite similar binding levels (data not shown). Furthermore, the inter-sample heterogeneity seen with the intact IgG molecule was reduced with the F(ab')₂ fragment. Therefore these findings suggest that the internalisation of rituximab is at least partially dependent on Fc:FcR interaction, and that this interaction may be also responsible for the observed heterogeneity in rituximab internalisation.

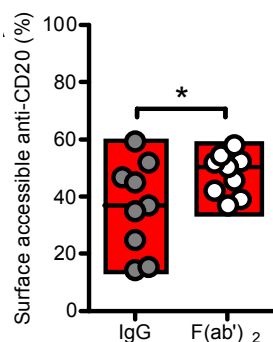


Figure 21: The Fc-dependency of internalisation of rituximab

The quenching assay was performed after culturing CLL cells for 6 h with Alexa-488-labelled F(ab')₂ or IgG molecules of rituximab. Data represent median +/- range. n=9, *p=0.0273

5.2.2 Characterisation of FcγR expression on B cells

The previous assays were performed with highly enriched (> 95% pure) B cells, so the predominant FcγR present should be the inhibitory FcγRIIb.³⁰⁰ However, as discussed in **Section 1.5.1.1**, there are some conflicting reports as to whether FcγRIIa is also expressed on B cells.^{300-301,302} Furthermore, at least two predominant isoforms of FcγRIIb exist, and it is not known which isoforms exist

on the different malignant subtypes of human B cells. Identification of the specific isoforms is especially relevant given that IIb2, but not IIb1 has been reported to mediate endocytosis of immune complexes. Due to the lack of availability of specific anti-FcγRIIIa/b mAb, RT-PCR was initially used to examine mRNA expression of these receptors. RT-PCR was performed on RNA extracted from purified B cells of normal healthy volunteers, CLL and MCL cells. FcγRIIIa and FcγRIIb1/2-specific primers were used to identify the mRNA expression levels of these molecules. FcγRII⁻ Ramos cells transfected with FcγRIIIa or FcγRIIb2 were used as controls. The RT-PCR gel demonstrates that only very low FcγRIIIa mRNA levels were expressed on all the subtypes of B cells tested (**Fig. 22a**). Ideally, quantitative PCR should have been used to compare the level of mRNA expression. Surprisingly, FcγRIIb was also detected in FcγRIIIa transfectants. However by flow cytometry, no FcγRII was detected on the surface of Ramos cells transfected by the empty vector control (**Fig. 22b**) indicating that this low level of transcription does not translate into protein on the cell surface.

With regards to the isoforms of FcγRIIb in the different B cell subtypes, both IIb1 and IIb2 isoforms were detectable. The RT-PCR gel shows that the proportion of each isoform expressed is dependent on the cell type (**Fig. 22a**). Normal B cells and MCL cells appear to demonstrate higher proportions of IIb1 whilst CLL cells express more IIb2. The rates of internalisation of rituximab previously characterised by the quenching assay were compared to the IIb1/IIb2 ratios in these and other samples tested, but no correlation was evident (data not shown). This suggests that the specific FcγRIIb isoform expressed was unimportant in mediating the internalisation of rituximab.

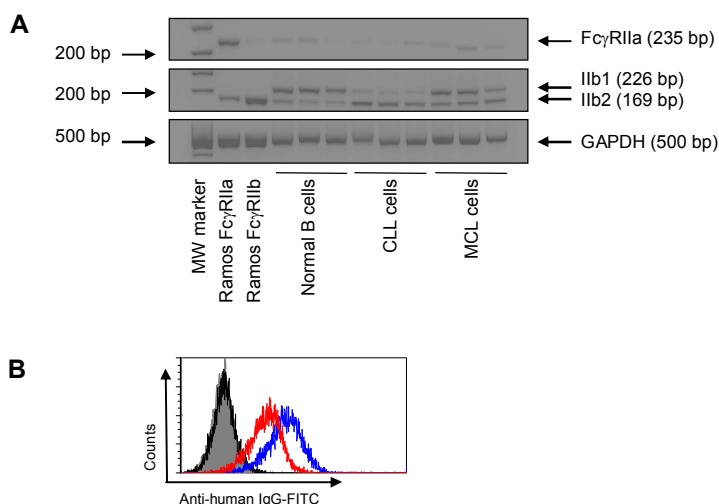


Figure 22: FcγRIIa and FcγRIIb1/2 expression on different primary B cell subtypes

A) RNA was extracted from Ramos FcγRIIa and FcγRIIb2 transfectants, purified normal B cells, CLL cells and MCL cells from 3 different individuals, in each case. cDNA was generated by reverse transcriptase and amplified for 35 cycles using FcγRIIa, FcγRIIb1/2 isoforms and GAPDH (control) primers. The RT-PCR products were visualised by 2% agarose gel electrophoresis. cDNA from FcγRIIa and FcγRIIb2 transfected Ramos cells acted as controls.

B) FcγRII⁻ cells (grey-filled), FcγRIIa (red line), FcγRIIb2 Ramos transfectants (blue line) were treated with unlabelled 10 µg/ml AT10 mIgG1 (N297Q mutated, to abrogate non-specific Fc:FcR binding) for 30 mins at 4°C, and then washed twice with cold FACS buffer. Anti-human IgG, SB2H2-FITC (10 µg/ml) was then added the cells to detect bound AT10, for 30 mins at 4°C. After a final wash, the samples were analysed by flow cytometry. The black line is representative of cells of all three types, stained with SB2H2-FITC only. Of note, although low levels of FcγRIIa (in Ramos FcγRIIb2 transfectant) and FcγRIIb mRNA (in Ramos FcγRIIa transfectant) were observed in A), no FcγRII expression was detected in vector control cells (grey-filled), thereby indicating that the mRNA was not translated into detectable surface protein.

Subsequent to this analysis, specific anti-FcγRIIa and anti-FcγRIIb mAb were then acquired through a material transfer agreement from a commercial company (Bioinvent), and were used to confirm the FcγRIIa/b expression on the B cells.

Fig. 23 demonstrates that the Ramos FcγRIIa/IIb2 transfectants express only FcγRIIa and FcγRIIb on the cell surface. Again, this confirms that the FcγRIIa detected in FcγRIIb2-transfected cells by RT-PCR has not been translated to protein expression (**Fig. 22A**). The same approach was used to confirm the

expression of FcγRIIIa/b on the normal primary B cells derived from healthy volunteers, and in addition, anti-CD19 was used to identify the B cells (**Fig. 24A**). A small population (6%) of cells were double-positive for CD19⁺ and FcγRIIIa⁺. The same population was also observed when the cells were stained with the isotype control. Thus, this population is probably due to the direct binding of anti-huIgG-PE to isotype-switched IgG⁺ B cells in the peripheral blood or non-specific binding by PE. The latter explanation is more likely since the same high background staining produced by PE was also observed in the malignant B cell subtypes tested (**Fig. 24B**), even though they were negative on sIgG staining by SB2H2-FITC (data not shown). Altogether, this confirms that FcγRIIb is the predominant FcR present on normal B cells, CLL, MCL and FL cells.

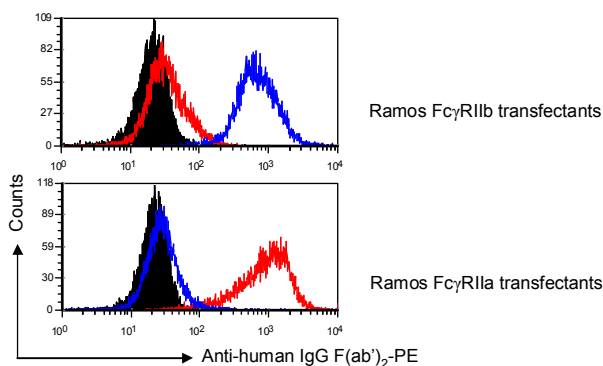


Figure 23: Confirmation of FcγRIIIa and FcγRIIb expression on Ramos transfectants by flow cytometry

The histograms represent the FcγRIIIa (red line) and FcγRIIb (blue line) expression in Ramos FcγRIIb2 (top) and FcγRIIIa transfectants (bottom). The cells were treated with unlabelled (10 μg/ml) specific anti-FcγRIIb, anti-FcγRIIIa mAb or an isotype control (all huIgG1, and carried N297Q mutations in the Fc domain to reduce non-specific FcR binding, as in previous figure) for 30 mins at 4°C, and then washed twice with cold FACS buffer. Anti-human IgG F(ab')₂-PE was then added to the cells to detect bound mAb, for 30 mins at 4°C. After a final wash, the samples were analysed by flow cytometry. The black filled line represents cells stained with the isotype control.

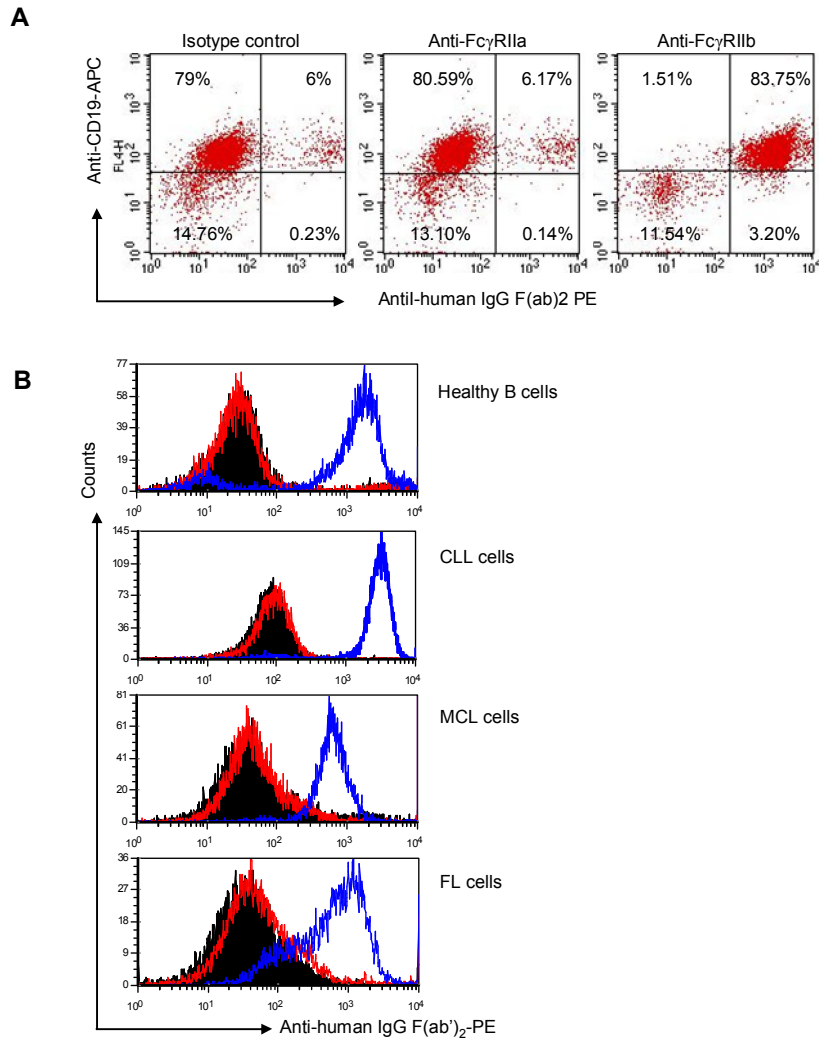


Figure 24: Fc γ RIIa and Fc γ RIIb expression on different primary B cell subtypes using specific mAb

A) Purified peripheral B cells were treated as in **Fig. 23** with the exception that the cells were co-stained with anti-CD19 APC during the incubation with the secondary mAb to identify B cells. The scatter plots show a representative example of the expression of the isotype control, Fc γ RIIa and Fc γ RIIb, in CD19⁺ B cells.

B) Purified normal B cells, CLL, MCL and FL cells were treated as in A). The lines are as follows: black-filled (isotype control), red (Fc γ RIIa) and blue (Fc γ RIIb). The histograms are gated on CD19⁺ cells and are representative of 3-4 examples in each B cell subtype.

5.2.3 The influence of target cell FcγRIIb expression on the internalisation of rituximab

Having confirmed that FcγRIIb is the predominant FcγR present on B cells and earlier demonstrated that internalisation of rituximab is dependent on FcR interaction, we explored the importance of FcγRIIb on internalisation. First, the pan-FcγRII mAb, AT10 was employed to block the interaction between anti-CD20 mAb and FcγRIIb (**Fig. 25**). Although AT10 is not specific for FcγRIIb, the previous experiments have demonstrated that only FcγRIIb is present on the surface of B cells. In the presence of the blocking mAb, the internalisation of rituximab was reduced, and comparable to that seen with rituximab F(ab')₂ fragments (**Fig. 21**).

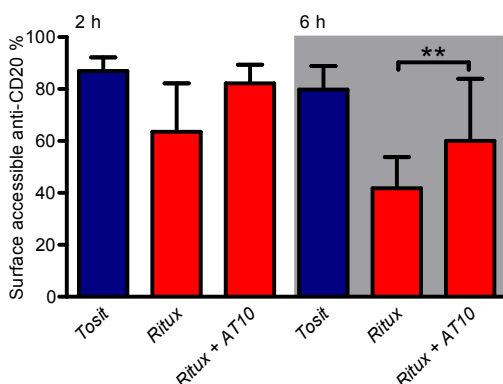


Figure 25: FcγRIIb inhibition reduces internalisation of rituximab

CLL cells were cultured with 5 µg/ml Tosit-488 or Ritux-488 +/- 10 µg/ml AT10 (added immediately prior to anti-CD20 mAb) for 2 and 6 h and the quenching assay performed as previously described. Median +/- range is shown for 6 different CLL samples. **p=0.0007

Given that FcγRIIb:Fc interaction could affect the rate of internalisation of rituximab, we went back and examined the expression of FcγRIIb on normal B cells and our panel of primary B-cell tumours by flow cytometry. As shown in **Fig. 26A-B**, there was marked heterogeneity of FcγRIIb expression within each group. However, expression was also broadly related to tumour type. As such, expression on CLL cells was relatively high, ranging from 20- to 300-fold over the

isotype control. In general, DLBCL and the majority of FL displayed lower FcγRIIb expression. Intriguingly two FL cases displayed very high FcγRIIb expression, and strikingly, these were the same two cases that we had previously observed to internalise rituximab extremely rapidly (**Fig. 14**). MCL and SLL expressed an intermediate albeit heterogeneous level of FcγRIIb.

The FcγRIIb expression of the normal and del(11q) cohort in **Fig. 17** was also re-examined. A small difference was seen whereby ATM deleted cases had weaker FcγRIIb expression levels than normal ATM cases, but this was not statistically significant (**Fig. 26C**). Although this cohort also had lower CD20 expression (**Fig. 17A**), no direct correlation was observed between CD20 and FcγRIIb expression, indicating that FcγRIIb expression levels were independent of CD20 expression (data not shown).

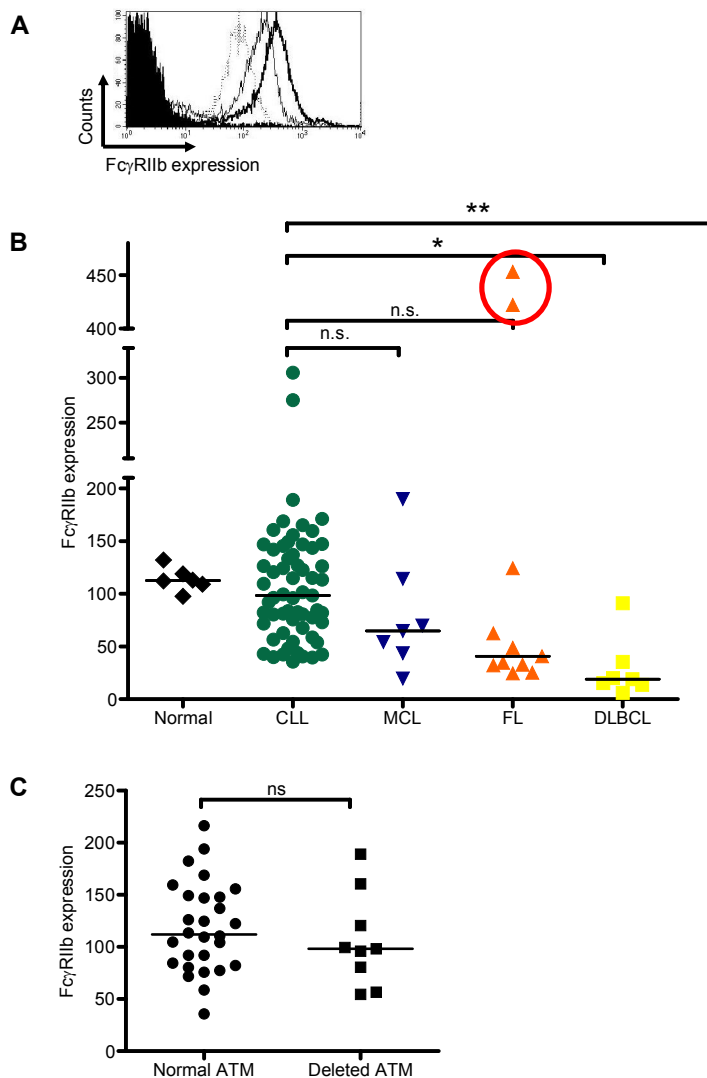


Figure 26: Fc γ RIIb expression on normal and malignant B cells

A-B) A variety of normal and malignant B cell samples were stained with 1:20 v/v AT10-PE for 30 mins at 4°C followed by one wash and analysis on the flow cytometer. The histogram (A) shows the diversity of Fc γ RIIb expression in 3 different CLL cases, representing nominal high (black line), medium (dark grey line) and low expressors (light grey line). The black filled line represents the isotype control. The scatter plot shows differences in Fc γ RIIb expression across healthy B cells, CLL, SLL, MCL, FL and DLBCL. Fc γ RIIb expression was expressed as a ratio of Fc γ RIIb:isotype control Geo MFI to control small differences due to inter-experimental variation. Median values are shown. Two outliers within the FL group are highlighted.

C) Similarly, Fc γ RIIb expression on CLL samples with known del(11q) status from Fig. 17 were examined. Median values are shown.

Altogether, these findings suggested that the expression level of FcγRIIb on the target B cells is a major participant in the internalisation of rituximab. To substantiate these findings, we compared FcγRIIb expression and internalisation of rituximab on the available normal B cell and primary NHL samples (**Fig. 27**). Spearman's correlation analysis revealed a strong relationship between these parameters (Spearman r value -0.7, with 95% confidence intervals between -0.8 and -0.6 and $p < 0.0001$). A multivariate analysis using Cox regression was also used to analyse the contribution of the weak CD20 expression discussed in **Section 4.2.5.1**. The strong association between FcγRIIb expression and rituximab internalisation persisted whereas the correlation between CD20 expression and internalisation became non-significant (data not shown). The data shows an inverse exponential curve with the majority of FL and DLBCL cases situated at the top and with the CLL and MCL samples showing a widespread distribution. This graph demonstrates that at low expression levels, small differences in FcγRIIb expression could lead to an greater, exponential change in the internalisation of rituximab, thereby underlining the capacity of this receptor in promoting the clearance of anti-CD20:CD20 complexes from the cell surface.

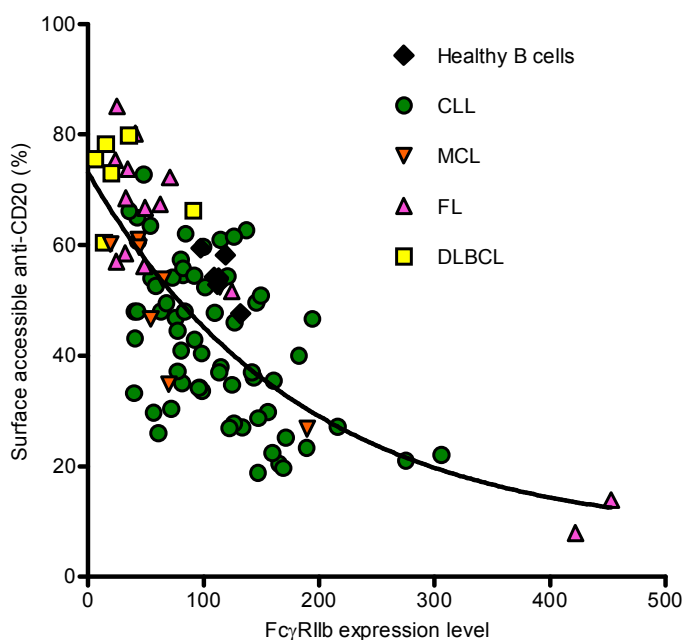


Figure 27: The correlation between FcγRIIb expression on B cell targets and the internalisation of rituximab

FcγRIIb expression (obtained in Fig. 26) was plotted against internalisation of rituximab (obtained in Figs. 13A-14) across all B-NHL subtypes and normal B cells. Analysis was performed using a Spearman's correlation assuming a non-parametric distribution. A strong correlation was demonstrated. Spearman r value = -0.7, 95% confidence interval between -0.8 and -0.6 and $p < 0.0001$. $N=109$.

As a complementary and more formal means of assessing the influence of FcγRIIb on the internalisation of rituximab, FcγRIIb2 transfected Ramos cells were sorted into sub-clones expressing low, medium and high levels of FcγRIIb. These cells, along with parental FcγRIIb⁻ Ramos cells were then assessed in the quenching assay. Internalisation of rituximab correlated directly with the expression level of FcγRIIb. Internalisation increased in the order of increasing FcγRIIb expression, i.e. FcγRIIb⁻ > FcγRIIb⁺ low > FcγRIIb⁺ medium > FcγRIIb⁺ high (Fig. 28). In contrast, FcγRIIb expression had minimal effect on the internalisation of tositumomab.

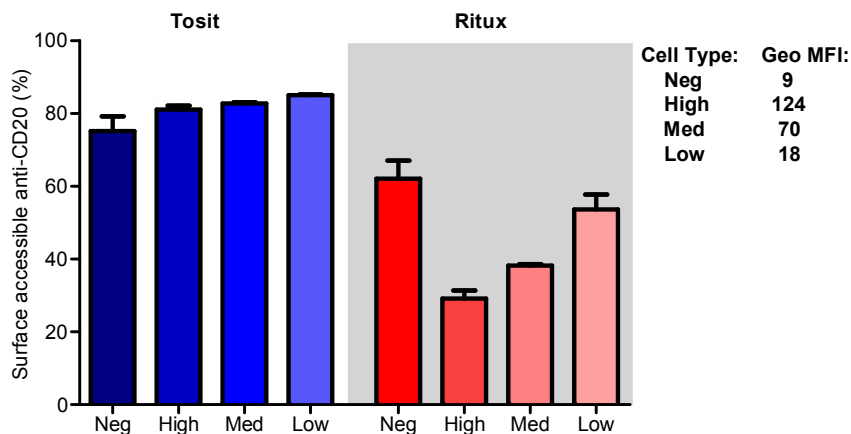


Figure 28: Effect of FcγRIIb expression level on internalisation of rituximab.

Ramos cells transfected with FcγRIIb2 were sorted to express low, medium and high levels of FcγRIIb and assessed in the quenching assay using Tosit-488 and Ritux-488 at the 6 h time-point alongside mock-transfected FcγRIIb⁻ Ramos cells. The bars represent median values +/- ranges from 3 experiments. Geo MFI values for FcγRIIb expression of the sorted cells are listed on the right. Statistical analysis was not performed due to the small sample size.

5.2.4 The binding orientation of rituximab to FcγRIIb

Thus far, the results suggest that rituximab co-ligated CD20 and FcγRIIb. Potentially, rituximab could co-ligate CD20 and FcγRIIb on either the same (cis) or adjacent (trans) cells. Identification of whether cis or trans binding occurs is important because if the latter predominates, then other FcγR-bearing cells are more likely to compete with FcγRIIb for binding, and hence also influence the internalisation of rituximab. To investigate this, high FcγRIIb-expressing Ramos transfectants were co-cultured with PKH26-labelled FcγRIIb⁻ Ramos cells (to enable identification of the different populations) (**Fig. 29A** scatter plot). The rate of internalisation of rituximab in each cell type when cultured together was compared with when cultured alone (**Fig. 29A**). As previously shown, when cultured alone, rituximab internalised to a greater extent in FcγRIIb⁺ cells compared to FcγRIIb⁻ Ramos cells (**Figs. 28-29A**). When co-cultured, the level of internalisation of rituximab in the FcγRIIb⁻ cells was slightly increased, but did not reach the level seen in the FcγRIIb⁺ cells. Similarly, FcγRIIb⁺ cells also

demonstrated less internalisation, but not to the extent of FcγRIIb⁻ cells. This suggests that while a trans interaction may occur, rituximab predominantly engages FcγRIIb on the surface of the same cell.

To demonstrate that this finding was not specific to the Ramos cell line, a CLL sample expressing low FcγRIIb was labelled with PKH26 as above and co-cultured with cells from 3 different CLL cases expressing high levels of FcγRIIb and the internalisation of rituximab assessed (**Fig. 29B**). As seen in the previous assay with Ramos cells, in the mixed co-cultures, the internalisation rates in low FcγRIIb-expressing CLL cells did not approach that seen in the high FcγRIIb-expressing population, again suggesting that engagement of FcγRIIb by rituximab occurs predominantly in a cis fashion. However, it is interesting to note that co-culture with the fastest internalisers resulted in the greatest increase in the internalisation of the low FcγRIIb-expressing CLL, but even here the increase was only modest (approximately 18% more internalisation, data not shown).

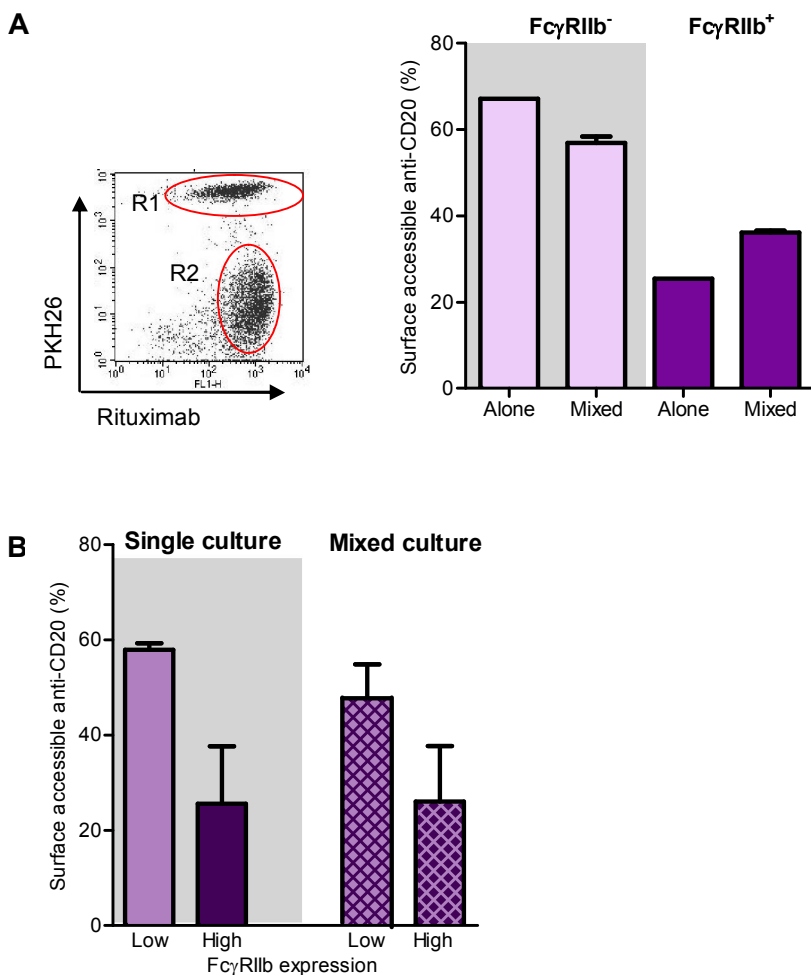


Figure 29: The effect of co-culturing with different FcγRIIb-expressing cells on rituximab internalisation

A) Left panel: PKH26-labelled Ramos cells (FcγRIIb⁻, R1) were mixed 1:1 with sorted high FcγRIIb-expressing Ramos transfectants (R2) (described in **Fig. 28**). Right panel: internalisation of rituximab on FcγRIIb⁺ and FcγRIIb⁻ cells after 6 h treatment. As controls, both populations were also cultured alone. Data represent the median +/- ranges from 3 independent experiments.

B) In a similar experiment, a low FcγRIIb-expressing CLL sample was PKH26-labelled then mixed 1:1 with a higher FcγRIIb-expressing CLL sample. The experiment was performed three times, each time with a different high FcγRIIb-expressing CLL. FcγRIIb levels (Geo MFI) were 42 (low) and 275, 306 and 165 for the high expressors. The quenching assay was then performed as in A). Data represent median +/- range.

In an additional experiment of this type, CLL cells were cultured at decreasing concentrations to reduce the potential for intercellular interaction (**Fig. 30**). Light microscopy images taken during this experiment demonstrate that the likelihood of intercellular interaction was much less at a concentration of 1×10^5

cells/ml compared to a concentration of 2×10^6 cells/ml. Moreover, no obvious stable interactions or cell adhesion were visualised at the lowest cell density at 6 h. A weak trend of less rituximab internalisation with decreasing cell concentration was observed (p values were not significant in all comparisons)

Altogether, these data indicate that Fc γ RIIb mediates its effects on rituximab internalisation predominantly through events on the same cell with less contribution from neighbouring Fc γ RIIb-expressing cells.

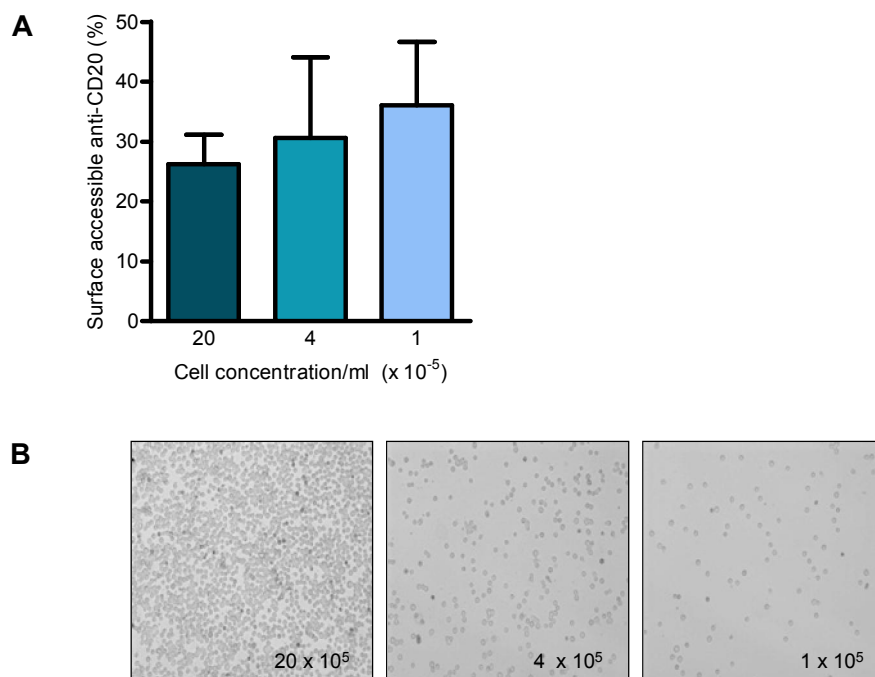


Figure 30: The effect of varying cell concentrations on rituximab internalisation

A-B) Different CLL samples were cultured with Ritux-488 for 6 h at concentrations of 20, 4 and 1×10^5 cells/ml, and the quenching assay performed at 6 h as before. Images were captured using a bright field microscope (10x objective lens) to demonstrate differences in cell proximity.

5.2.5 Activation of FcγRIIb by anti-CD20

The ability of FcγRIIb to promote internalisation of anti-CD20 appears unique to type I mAb, with little effect seen on type II mAb (**Fig. 28**). A plausible explanation might be that type I, but not type II mAb, binds to FcγRIIb. To explore this hypothesis, CLL cells were treated with rituximab or a variety of type II anti-CD20 (tositumomab, GA101_{gly} and GA101) for an hour, and then binding of FcγRIIb assessed indirectly by immunoblotting for receptor activation by assessing the phosphorylation of the tyrosine residue at position 292 (within the ITIM of FcγRIIb, **Section 1.5.1.1**). **Fig. 31** suggests that type I mAb, rituximab, phosphorylated FcγRIIb but not the type II mAb. This experiment suggests that the observed differences in mAb internalisation might be dependent on differences in binding to FcγRIIb.

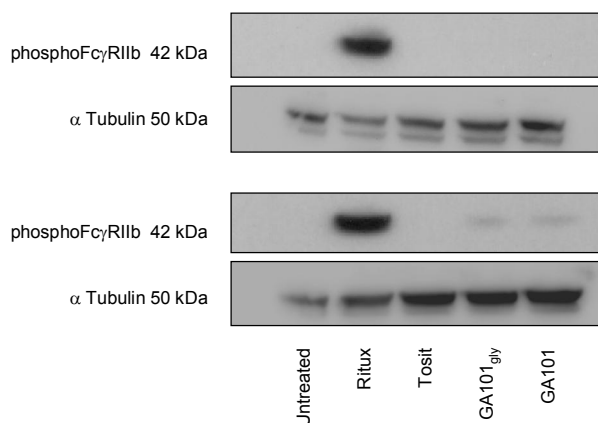


Figure 31: Type I and not type II anti-CD20 mAb phosphorylated FcγRIIb

CLL cells were cultured with the specified mAb (10 µg/ml) for 1 h at 37°C before harvesting, lysis and subsequent immunoblotting for phosphorylated FcγRIIb, and α-tubulin as a loading control. Two different CLL samples are demonstrated.

Having demonstrated the difference in FcγRIIb activation between type I and type II mAb, we explored whether an anti-FcγRII blocking mAb (AT10) was able to block FcγRIIb phosphorylation. CLL cells were cultured with tositumomab or rituximab for 2 or 6 h in the presence or absence of AT10, with immunoblotting performed to detect phosphorylated FcγRIIb. Again, phosphorylated FcγRIIb was readily detected in CLL cells treated by rituximab for 2 h, but much less so in

tositumomab-treated cells (**Fig. 32A**). Phosphorylation was at least partially inhibited by the addition of AT10 (**Fig. 32A**). Samples were also assessed for expression of total FcγRIIb after treatment with these mAb. The expression of FcγRIIb was not reduced after 2 or even 6 h cultures which suggest that it might be recycled after co-ligation (**Figs. 32A-B**). We previously observed that CD20 was degraded in type I but not type II mAb treated human CD20 Tg mouse B cells after 6 h in vitro culture, supporting internalisation of CD20 with type I mAb.³⁵⁵ Consistent with these previous findings, total CD20 was reduced in CLL cells cultured for 6 h with rituximab but not tositumomab (**Fig. 32B**). Loss in CD20 was reduced by addition of AT10, indicating that the results obtained were consistent with degradation of internalised CD20:rituximab complexes, which was prevented by FcγRIIb inhibition. Furthermore, no CD20 loss was observed after 2 h culture, supporting the time-dependent nature of internalisation (data not shown).

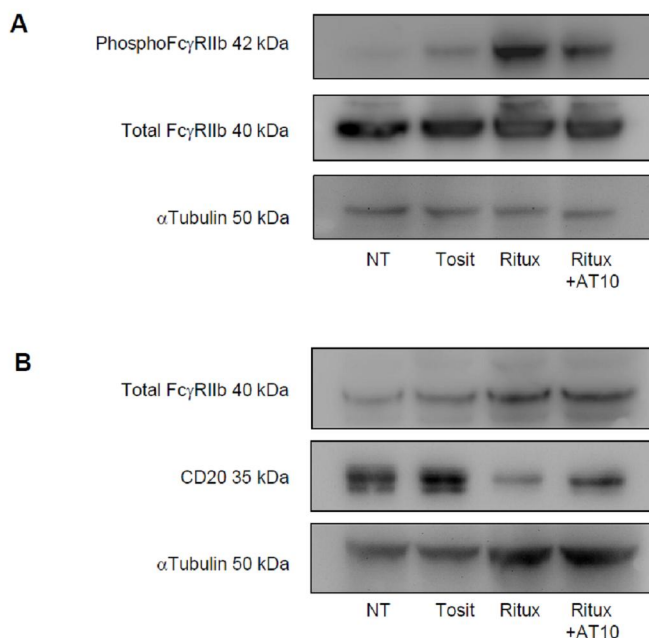


Figure 32: FcγRIIb phosphorylation and CD20 degradation following mAb stimulation of CLL cells

A) CLL cells were cultured with the specified mAb (10 μg/ml) for 2 h at 37°C before harvesting, lysis and subsequent immunoblotting for phosphoFcγRIIb, total FcγRIIb, and α-tubulin as a loading control.

B) As in A), a different CLL case was cultured under the exact same conditions except for 6 h before subsequent harvesting and immunoblotting for CD20, total FcγRIIb and α-tubulin.

5.2.6 Intracellular trafficking of anti-CD20:CD20:FcγRIIb complexes

Previous experiments using human lymphoma cells lines indicate that following internalisation, type I but not type II mAb are degraded in lysosomes.³⁵⁵ The trafficking of internalised anti-CD20 mAb or FcγRIIb in primary tumour material has not been investigated. The Western blot experiments detailed previously suggest that CD20 in type I, but not type II-treated CLL cells, are similarly degraded in lysosomes. The fate of FcγRIIb after engagement of type I mAb is less certain as no protein was lost after 6 h treatment (**Fig. 32B**). To ascertain the fate of FcγRIIb after engagement of rituximab at the cell surface, its expression and location was monitored by flow cytometry and confocal microscopy. First, it was ensured that rituximab binding to FcγRIIb did not impair subsequent detection by of FcγRIIb by AT10. For this experiment, FcγRIIb expression on untreated CLL cells were assessed using AT10-PE, and compared to FcγRIIb expression obtained after CLL cells were treated with rituximab (on ice to minimise internalisation). **Fig. 33A** demonstrates that minimal difference was seen between FcγRIIb expression of untreated and rituximab-bound cells, suggesting that the weak interaction between the Fc domain of rituximab and FcγRIIb is likely to be displaced by AT10. Alternatively, AT10 might bind to a different epitope on FcγRIIb from the Fc. Next, the cell surface expression of FcγRIIb was assessed from 6 different cases of CLL, and was observed to decline within 2 h of incubation with rituximab but not tositumomab (**Fig. 33B**). These findings suggest that FcγRIIb is internalised along with CD20 and rituximab (but not tositumomab) as part of a tri-partite complex.

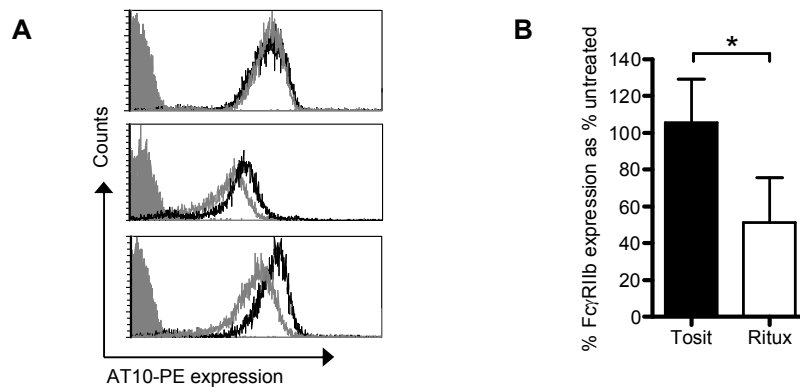


Figure 33: FcγRIIb expression is reduced over time in rituximab-treated CLL cells

A) CLL cells were untreated, or treated with 5 µg/ml unlabelled rituximab for 30 mins on ice, then washed with FACS buffer and stained with AT10-PE. Representative histograms from 3 patients are shown. (Grey-filled: isotype control; black line: AT10 expression of untreated cells; grey line: AT10 expression of rituximab treated cells).

B) CLL cells were incubated with Tosit-488 or Ritux-488 (5 µg/ml) for 2 h and then FcγRIIb expression detected using AT10-PE. Data are represented as medians ± ranges (n = 6; *p= 0.03).

It has previously been reported that type I anti-CD20 mAb are endocytosed and trafficked into early endosomes, then lysosomes.^{355,445} To address whether the same process occurred with FcγRIIb as part of an anti-CD20:CD20:FcγRIIb complex, CLL cells were cultured with either Tosit-488 or Ritux-488 before fixation and staining for FcγRIIb (using Alexa 647-labelled F(ab')₂ fragments of AT10) and the endosomal/lysosomal marker LAMP-1. Prior to stimulation with mAb, FcγRIIb staining was diffuse and evenly distributed (**Fig. 34A**). Following incubation with Ritux-488 for 30 mins, a distinct difference in staining was observed, whereby focal FcγRIIb staining was seen, and this co-localised with Ritux-488 staining (**Fig. 34B**). In cells stimulated with Tosit-488 for 6 h, CD20 expression remained evenly distributed on the surface and AT10-647 staining was unchanged from untreated cells (**Figs. 34A and 34C**). No co-localisation was seen between Tosit-488, AT10-647 and lysosomes (**Fig. 34C**). In contrast, over the same time course, Ritux-488 showed a distinct punctate pattern, indicative

of internalisation of the mAb, and consistent with previous observations in Raji cells (**Fig. 34D**).³⁵⁵ Furthermore, AT10-647 and LAMP-1-546 demonstrated a similar pattern of staining (**Fig. 34D**). Co-localisation between Ritux-488 and AT10-647 was observed in 58% of cells, whereas co-localisation of Ritux-488, AT10-647 and LAMP-1-546 was observed in 33% of cells. Presumably, the lower degree of co-localisation observed between all three stains reflects the fact that Ritux-488 and FcγRIIb internalise together and likely occupy other intracellular compartments prior to their appearance in endosomes/lysosomes. In summary, the confocal microscopy and earlier Western blot data suggest that rituximab: CD20: FcγRIIb complexes are localised predominantly to the endosomes/lysosomes where CD20 is likely to be degraded. The fate of FcγRIIb is less certain and will be discussed in the next section.

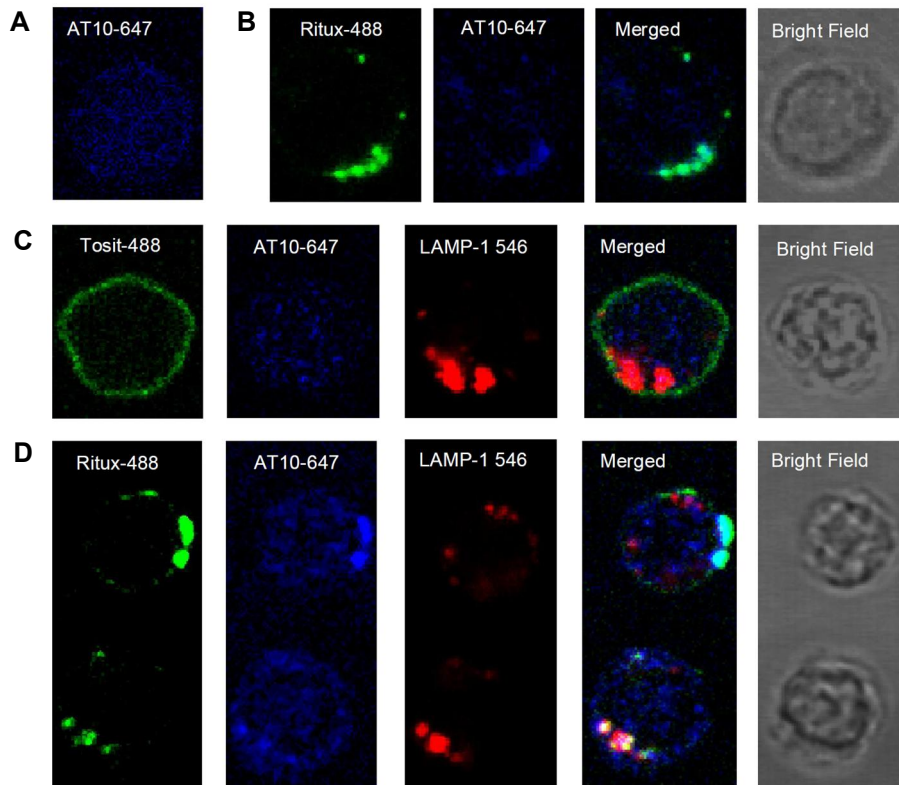


Figure 34: Rituximab: CD20: Fc γ RIIb complexes are internalised together into lysosomes

A) CLL cells were washed, fixed and permeabilised with before staining with AT10-647 (blue), further washing and inspection by confocal microscopy. This image represents the Fc γ RIIb staining pattern in unstimulated cells.

B) The same CLL sample was cultured with Ritux-488 for 30 mins and then treated as described in A).

C) CLL cells were incubated with Tosit-488 for 6 h before preparation for microscopy as in B). In addition, cells were also treated with biotinylated LAMP-1 and streptavidin-546 (red) to stain for lysosomes.

D) CLL cells were treated with Ritux-488 for 6 h and assessed as in C). Two representative cells are shown here. In each case the bright field (BF) image is shown from the same cell.

5.2.7 The effect of internalisation of anti-CD20 on engagement of immune effector cells

Internalisation of anti-CD20 mAb from the target cell surface would predictably reduce the engagement of FcR-bearing immune effector cells. To confirm that this indeed happened, a phagocytosis assay (see **Section 3.12**) was used. In this assay, CLL cells were identified by CFSE-labelling and then untreated, or exposed to with GA101_{gly} or rituximab for 6 h (to allow internalisation of mAb to occur) or 15 mins (no internalisation). The cells were then washed and 'fed' to human peripheral blood-derived macrophages to enable phagocytosis. After an hour, the mixed cell culture was washed with PBS to remove non-adherent (and non-phagocytosed) cells, and then further incubated on ice to detach adherent macrophages. This was followed by flow cytometry and microscopy. Both confocal and bright field microscopy were used to visualise the cells. **Fig. 35A** shows an example of the images obtained by confocal microscopy (left panel) and bright field microscopy (right). In both images, the CLL cells were treated with 6 h with GA101_{gly}. The confocal image is taken as a cross-section of the macrophages, and demonstrates green CFSE-labelled CLL cells within the macrophages, indicative of phagocytosis. The bright field image shows MGG-stained nuclei and cytoplasm of macrophages (large cells) and multiple small deeply basophilic-staining CLL cells within one of the macrophages (marked with red arrows). In general, less phagocytosis was observed in rituximab-treated cells, and even far less in untreated cells (data not shown). As a more objective measure of the phagocytosis, flow cytometry was used. Anti-CD16-APC was used to identify macrophages, and so CD16⁺ CFSE⁺ cells represented macrophages that had either phagocytosed CLL cells or had CLL cells rosetted on the surface (**Figs. 35B-C**). On inspection by confocal microscopy, the majority of the double-positive cells were seen to represent phagocytosed cells as opposed to CLL cells rosetted on the surface of the macrophages (**Fig. 35A**).

The effect of anti-CD20 mAb internalisation on macrophage-mediated phagocytosis was tested by comparing the change in phagocytosis of CLL cells

treated with a non-internalising mAb e.g. GA101_{gly} for 6 h in comparison to 15 mins. Similarly, CLL cells were also treated with rituximab for the same time periods (for 6 h and 15 mins). As anticipated, minimal or improved phagocytosis was seen after 6 h treatment with GA101_{gly} in comparison to 15 mins (**Fig. 35C**). In contrast, a reduction in phagocytosis was seen in CLL cells treated with rituximab for 6 h compared to 15 mins. To further demonstrate that the reduced phagocytosis seen in rituximab-opsonised CLL cells was due to internalisation of mAb, AT10 F(ab')₂ was added to block internalisation over the 6 h period (**Fig. 36**). The F(ab')₂ fragment of AT10 was employed to ensure that any observed change was not due to an interaction between the Fc domain of AT10 and FcγR on the macrophages. Furthermore excess AT10 was removed by washing to ensure that no mAb was free to bind to FcγRIIb on the macrophages, and inhibit their function. As anticipated, inhibition of FcγRIIb increased the phagocytosis of these target cells by at least 10%, and to levels equivalent to those seen without internalisation.

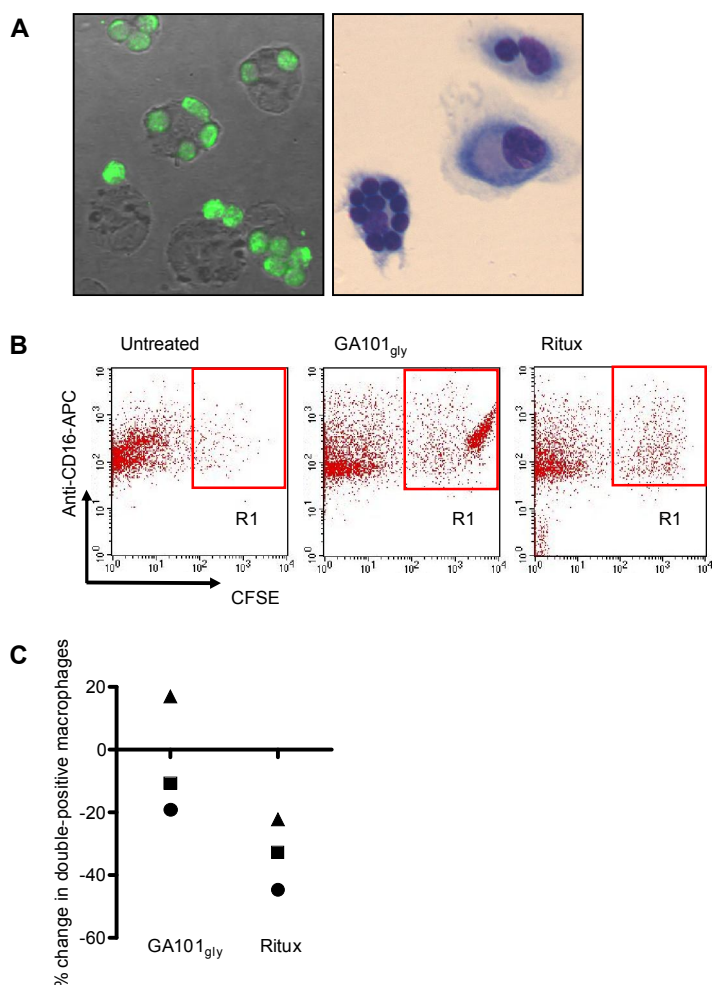


Figure 35: The effect of anti-CD20 internalisation on macrophage phagocytosis

A) CFSE-labelled CLL cells were fed to monocyte-derived macrophages as described in Section 3.12, and then examined by confocal microscopy (left panel) or MGG staining and light microscopy (right panel) as detailed in **Sections 3.17 and 3.18** respectively.

B) CFSE-labelled CLL cells were untreated or treated with 10 µg/ml GA101_{gly} or rituximab for 6 h before washing and incubation with macrophages for an hour. The mixed cell culture was then stained with CD16-APC 10 µg/ml to identify macrophages. After washing and incubation on ice, the cells were examined by flow cytometry. CD16⁺ CFSE⁺ cells indicate macrophages that have phagocytosed CLL cells (R1 gate). The scatter plots show representative examples.

C) The graph represents results of the phagocytosis assay in B) in 3 different CLL samples, as represented by the different symbols. CLL cells were opsonised with either GA101_{gly} or Ritux for 15 mins or 6 h, and the % change in phagocytosis at 6 h relative to 15 mins, is shown.

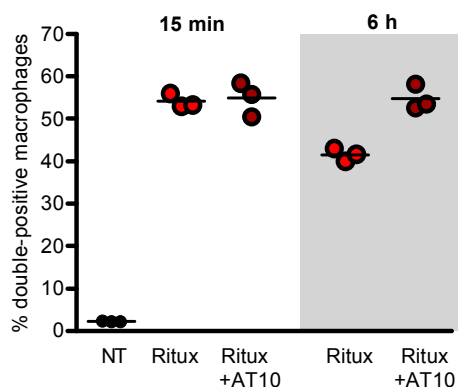


Figure 36: The effect of FcγRIIb inhibition on B cells on macrophage phagocytosis

The phagocytosis assay was repeated as described in Fig. 35B, except the CFSE-labelled CLL cells were treated either ritux or ritux and AT10 f(ab')₂ at 10 µg/ml, for 15 mins or 6 h. The CLL cells were then washed twice, and then incubated with macrophages for 30 mins, before staining with anti-CD16-APC. This was followed by further washing, incubation on ice and then analysis by flow cytometry. The medians of a single CLL sample done in triplicate are shown, and is representative of another separate CLL sample tested (data not shown).

5.3 Discussion

Here we examined influence of Fc:FcR interaction on the internalisation of rituximab. We demonstrate that the F(ab')₂ fragment of rituximab internalises markedly less than the whole IgG molecule in CLL cells. Next, we confirmed through mRNA expression and surface protein levels that FcγRIIb is the major FcR expressed on the surface of B cells, and that both FcγRIIb isoforms were expressed. The results also demonstrate that internalisation of rituximab was reduced by FcγRIIb inhibition, and that FcγRIIb expression on B cells correlated strongly and significantly with internalisation of rituximab. These findings were further supported by the data showing that FcγRIIb-transfected Ramos cells internalised rituximab in a dose-dependent manner. Rituximab predominantly bound to CD20 and FcγRIIb in a cis fashion, and unlike type II anti-CD20 mAb, was able to activate FcγRIIb. The rituximab:CD20:FcγRIIb complexes were then observed to internalise together into endosomal and lysosomal compartments.

Whilst we present evidence that supports FcγRIIb as the predominant FcγR on B cells, the current literature is inconsistent (**Section 1.5.1.1**). There is a general consensus that only FcγRIIb is expressed in B cells, and this is primarily based on the early work of Ravetch's group.³⁰⁰ Since then a handful of publications have reported the presence of FcγRIIa on B cells as well.^{301,476} This controversy is likely to have stemmed from the lack of available specific anti-FcγRIIa and anti-FcγRIIb mAb and the assumption that mRNA expression is entirely representative of expression of protein on the cell surface.⁴⁷⁷ Furthermore, some groups have regarded the anti-FcγRII mAb, IV.3 as a specific anti-FcγRIIa mAb^{476,478} despite the lack of data demonstrating its specificity, thus leading to anomalous conclusions. Our own work indicates that IV.3, whilst preferentially binds FcγRIIa over FcγRIIb, is not specific for it and also detects FcγRIIb (data not shown). Moreover, much of the published work has used cell lines,^{301,302} which for the reasons discussed previously, is not always representative of primary cells. Our RT-PCR and flow cytometry data demonstrates that FcγRIIb is indeed the predominant FcγR on the surface of primary human B cells.

As a further complication, two functionally different isoforms of FcγRIIb exist. The proportion of each isoform on the different B cell subtypes has not been previously characterised. Interestingly, we demonstrate that IIb1 predominates in normal human B cells and MCL cells whereas IIb2 is the main isoform in CLL cells. Clearly, more samples are required to confirm these findings. Since all the cells tested do internalise rituximab, it would suggest that the specific FcγRIIb isoform is irrelevant with respect to rituximab's internalisation. The relevance of the predominance of one isoform over the other in different diseases is interesting and is currently part of an ongoing study in the laboratory.

The internalisation of rituximab is dependent on FcγRIIb expression on target B cells in a dose-dependent manner. As such, higher FcγRIIb expression on target B cells increases the extent of internalisation of rituximab. However, despite this, F(ab')₂ fragments of rituximab, or concurrent FcγRIIb inhibition by AT10 does not reverse the process entirely. Therefore, although FcγRIIb is a major

participant in the internalisation of type I mAb, other factors are likely to be involved, such as the ability of type I, but not type II mAb to translocate CD20 into lipid rafts. This will be discussed further in the final discussion.

The effect of FcγRIIb on the internalisation of anti-CD20 mAb appears unique to type I and not type II mAb. The alternative explanation is that this difference in mAb internalisation might instead be due to a difference in binding to FcγRIIb. There is currently no published data on the ability of any of these different anti-CD20 mAb to bind to FcγRIIb. However as type I rituximab carries the same Fc domain (human IgG1) as type II GA101, thus should possess the same inherent ability to bind to FcγRIIb. However, rituximab but not GA101 was observed to activate FcγRIIb in Western blotting experiments. This suggests that either GA101 does not bind to FcγRIIb, or that it does so, but with insufficient affinity required for FcγRIIb activation. We propose that the ability to bind to FcγRIIb is related to the mAb's type I/II characterisation, i.e. we hypothesise that type I mAb bind to FcγRIIb and type II mAb do not. This hypothesis is based on recently published data (discussed in **Section 1.5**) which demonstrates that type II anti-CD20 mAb bind to an epitope which is right-shifted compared to the epitope bound by type I mAb.²⁹³ It is thought that this epitope shift, combined with the wider elbow angle of type II mAb such as GA101, causes the mAb to bind to CD20 in a different orientation from rituximab. It is possible that these differences in epitope and orientation of binding underpin the ability of type II mAb like GA101, and not type I rituximab to bind to FcγRIIb. Admittedly, further examples of type I and type II anti-CD20 mAb with comparable isotypes are required to ascertain that the difference in ability to bind to FcγRIIb can be generalised as a type I/II characteristic.

Using confocal microscopy, it was shown that rituximab:CD20:FcγRIIb is jointly internalised into the endosomal/lysosomal compartment. Western blot experiments further suggest that CD20 is degraded after 6 h in vitro culture with rituximab. No evidence of FcγRIIb loss was observed. There are various possible explanations for this. First, if there are proportionally greater FcγRIIb molecules

than CD20 molecules on the cell, then relatively low numbers of FcγRIIb molecules would have internalised into the cell with CD20:rituximab. Hence, the percentage of degraded FcγRIIb might be too small for detection by Western blot. Nonetheless, this first point is unlikely since there is usually twice as much CD20 compared to FcγRIIb on the B cells (data not shown). Second, recent evidence suggests that when bound by heat-aggregated IgG, internalised FcγRIIb2 dissociates from the immune complex before delivering it into lysosomes.⁴⁷⁹ Instead, FcγRIIb2 is transported to endosomes where it is recycled to the surface. LAMP-1 has been detected in both early and late endosomes, as well as lysosomes,⁴⁸⁰ so similarly, FcγRIIb might dissociate from the anti-CD20:CD20 complex in endosomes, prior to transport to acidic lysosomes for degradation. This would also account for the relatively low degree of co-localisation seen between all three stains. Whilst we have also demonstrated that the surface expression of FcγRIIb reduced over time when the cells were treated with rituximab for 2 h, thereby arguing against recycling of FcγRIIb, further incubation times are merited if the surface expression remains reduced after e.g. 6 h treatment with rituximab. A final explanation may be that there is compensatory up-regulation of FcγRIIb transcription by the cells.

We predicted that internalisation of anti-CD20 mAb from the target B cells would reduce the engagement of immune effector cells that mediate ADCC. The findings were consistent with this hypothesis in that the internalisation of rituximab, after 6 h treatment, resulted in a reduction in phagocytosis, in comparison to 15 mins treatment. The phagocytosis experiments also indicate two key points. First, GA101_{gly} mediates more phagocytosis than rituximab (data not shown, median 10%). This is especially interesting seeing that at least two-fold more type I mAb bind to the cell surface than type II mAb.²⁹⁴ Second, as predicted, internalisation of rituximab reduced phagocytosis, and that this reduction was restored by inhibition of FcγRIIb on the CLL cells. Potentially despite the higher number of type I mAb molecules bound to the surface, the binding of the Fc domain of the mAb to FcγRIIb on the same cells prevents the

engagement of the activatory Fc γ R on the macrophages. Therefore the benefit of type II mAb is two-fold, i.e. its Fc domain is freely available to bind to the activatory Fc γ R of immune effector cells, and it does not internalise into the target B cell. In vivo, one would therefore predict that cells in compartments less accessible to immune effector cells are likely to be more resistant to depletion, given that more time will be available for the internalisation of the mAb to occur.

6 Validation of FcγRIIb as a prognostic marker in patients

6.1 Introduction

Previous work in the laboratory had demonstrated that type I anti-CD20 mAb were five-fold more potent than type II mAb in a human CD20 Tg mouse model of B-cell depletion.³⁵⁵ Through the use of γ chain $-/-$ mice, it was shown that the difference in potency between type I and type II mAb could be attributed to the internalisation of type I mAb into target B cells. In the preceding chapters, the internalisation of type I, but not type II mAb, was confirmed in primary tumour material. Further investigations showed that FcγRIIb on B cells was a major participant in the internalisation of rituximab. Higher FcγRIIb expression levels on B cells were associated with increased internalisation of rituximab. Based on these findings, we hypothesised that internalisation of rituximab contributes to its resistance in patients with B-NHL. Given that FcγRIIb promotes internalisation of rituximab, we considered that it might act as a biomarker of response to rituximab. Up to now, most groups have concentrated on studying the association of the different polymorphic variants of the activatory FcγR, against responses to rituximab (**Section 1.5.1**). Only two clinical studies have analysed the importance of FcγRIIb on responses to rituximab in B-NHL.^{345,348} One study examined the FcγRIIb expression of tumour cells by immunohistochemistry in patients with DLBCL treated with RCHOP chemotherapy.³⁴⁵ The other examined the significance of the polymorphic variant, I232T in FcγRIIb on responses to rituximab in FL patients.³⁴⁸ Both studies yielded negative findings thereby down-playing the importance of FcγRIIb in predicting rituximab responses in lymphoma. Potential explanations for these negative findings will be discussed later in this chapter. As a proof-of-concept of our in vitro findings, we wanted to examine whether FcγRIIb expression in B-NHL cases could predict the responses in patients treated with regimens containing rituximab.

6.2 Results

6.2.1 FcγRIIb expression of B-NHL by immunohistochemistry (IHC)

To assess this we retrospectively examined the FcγRIIb expression levels of pre-rituximab tissue samples of a cohort of B-NHL patients who had received rituximab-containing regimens. For the retrospective study, we needed access to patient information and tissue samples for FcγRIIb staining. To do this, ethical approval was obtained from the local research ethics committee. The details of the study are outlined in the study protocol shown in **Appendix 5**. In essence, patients were identified using the local cancer trials network electronic database and Southampton General Hospital's oncology pharmacy database. The identified cohort encompassed patients over the last 10-year duration. Any patient diagnosed with a B-cell malignancy who had received treatment with a regimen containing rituximab was included in the study. Ideally, only patients treated with single-agent rituximab would have been included but that would have grossly limited the number of patients. Therefore, patients receiving any rituximab-containing regimen were included in the initial search. No viable tumour cells were stored for these patients and so consequently archival paraffin-embedded tissue was used for FcγRIIb staining by IHC instead. To facilitate this, we established a robust staining protocol for FcγRIIb expression in collaboration with Dr M. Ashton-Key, a consultant histopathologist. An IHC-compatible, commercial anti-FcγRIIb mAb (EP888Y, Abcam) was available and was confirmed by the company to be specific for FcγRIIb although no published data was obtainable. To confirm the specificity of the mAb for FcγRIIb, and not FcγRIIa, FcγRII⁻ Ramos cells transfected with FcγRIIa or FcγRIIb were cytospun, paraffin-embedded and then stained by IHC with the EP888Y mAb (**Fig. 37**). No staining was evident in FcγRIIa-transfected cells (left), but strong staining in a membranous pattern was observed in FcγRIIb-transfected cells (right).

Having validated the specificity of the mAb, we then assessed the expression of FcγRIIb in the clinical material. Initially we examined a set of FL samples

previously phenotyped for high or low FcγRIIb expression by flow cytometry (**Fig. 26**). The corresponding paraffin blocks of these FL samples were stained by IHC to ensure that the expression was concordant with the flow cytometry results (**Fig. 38**). The top panel demonstrates that the same pattern of membranous staining was seen in high-expressing FcγRIIb FL samples (Geo MFI values inset) and contrasted with the weaker granular cytoplasmic staining seen in FcγRIIb⁻ samples. In order to create a scoring system for FcγRIIb expression by IHC, samples with intermediate FcγRIIb expression by flow cytometry were also stained, but an objective distinction beyond positive (or membranous staining) and negative (or granular staining) was not readily achievable by IHC. Thus, on the whole, clinical samples were graded as either positive or negative for FcγRIIb. An example of FcγRIIb-positive/negative staining by IHC in MCL samples are also shown in **Fig. 38**.

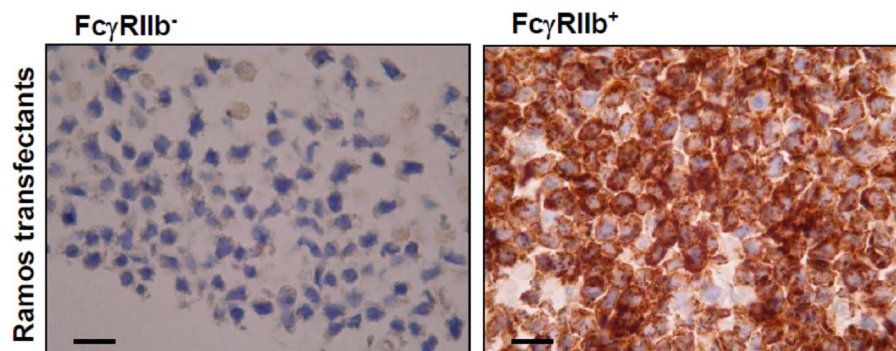


Figure 37: Confirmation of specificity of anti-FcγRIIb mAb used in IHC

Top panel: FcγRIIa (left) and FcγRIIb (right) transfected Ramos cells were cytospun and paraffin-embedded. IHC using mAb to human FcγRIIb demonstrated strong membrane staining in FcγRIIb but no staining in FcγRIIa. Scale bars represent 50 μm.

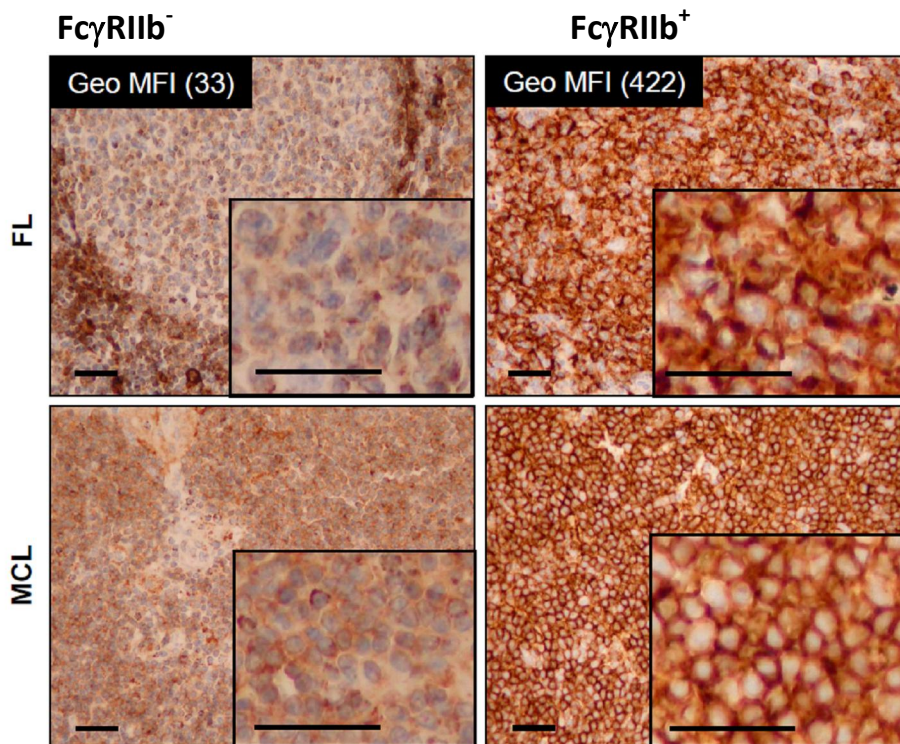


Figure 38: Anti-Fc γ RIIb staining of primary tumour material by IHC

IHC staining for Fc γ RIIb in FL (flow cytometric quantification of Fc γ RIIb expression of corresponding viable cells shown) and MCL samples are shown. Representative examples of negative (left) and positive membranous (right) staining are shown. The top left panel demonstrates Fc γ RIIb staining in the normal mantle region, which serves as an internal positive control for the staining. Scale bars represent 50 μ m.

6.2.2 Treatment outcomes of B-NHL patients according to Fc γ RIIb expression

In total, 72 patients were included in the study and the baseline clinical data for these patients are shown in **Table 8**. Within each disease subset, 8/17 (47%) MCL, 1/7 (14%) DLBCL, 0/6 (0%) transformed FL, 15/31 (48%) FL, 8/9 (89%) marginal zone lymphoma (MZL) and 1/2 (50%) lymphoplasmacytic lymphoma (LPL) cases were positive for Fc γ RIIb staining. The expression of Fc γ RIIb in the various B-NHL subsets has previously been published by another group.³⁴⁴ Similar to our study, IHC was performed, but using a polyclonal anti-Fc γ RIIb Ab directed at the first three intracytoplasmic sequences of Fc γ RIIb1. Their findings were comparable to ours, with a few exceptions. Notably, 7/12 cases

transformed FL cases examined by those authors were FcγRIIb⁺, whereas 0/6 cases were positive in our study. Potentially these differences can be explained by the relatively low number of cases of these subtypes in both studies. Furthermore, clinical features of high grade transformation of FL e.g. rapid nodal enlargement and hypercalcaemia, are not always supported by histological evidence, which is dependent on the area of biopsy (reviewed in⁴⁸¹). Thus, depending on whether the banked tissue was classed by clinical or histological diagnosis, a disparity may occur.

Patient ID	Diagnosis	FcyRIIb Status	Age	Sex	PF	Stage	Disease Bulk (Y/N)	LDH	Regimen compared (Line of therapy)	Total no of regimens
100	MCL	Neg	61	F	0	4	N	1669	FCR (1)	2
101	MCL	Neg	57	M	0	2	N	397	FCR (1)	1
102	MCL	Neg	54	M	0	2	N	624	FCR (1)	2
103	MCL	Neg	77	M	0	4	N	218	FCR (1)	1
106	MCL	Neg	51	M	1	4	N	690	FCR (1)	1
148	MCL	Neg	81	F	0	3	N	479	FCR (1)	1
151	MCL	Neg	77	M	2	4	N	269	Bendamustine Ritux (3)	3
158	MCL	Neg	78	M	1	3	N	515	Ritux-PMitCEBO x2 cycles only (4)	4
181	MCL	Neg	84	M	2	4	N	451	Ritux (1)	1
104	MCL	Pos	82	M	3	3	Y	1013	FCR (1)	1
119	MCL	Pos	69	M	1	4	N	114	Bortezomib/Ritux (3)	5
122	MCL	Pos	59	M	0	4	N	475	Bortezomib/Ritux (3)	4
123	MCL	Pos	54	M	0	4	N	463	Bortezomib/Ritux (2)	2
146	MCL	Pos	73	M	2	4	N	505	FCR (1)	1
149	MCL	Pos	62	M	0	4	N	1043	FCR (1)	1
188	MCL	Pos	52	M	1	4	N	501	Ritux (1)	1
204	MCL	Pos	73	M	0	4	N	431	FCR (1)	1
126	DLBCL	Neg	62	M	2	4	N	530	Ofatumumab (3)	3
128	DLBCL	Neg	55	F	0	2	Y	526	RCHOP (1)	1
134	DLBCL	Neg	79	M	1	4	N	379	Ritux -GCVP (1)	1
137	DLBCL	Neg	50	F	1	2	Y	1232	RCHOP (1)	1
141	DLBCL	Neg	63	M	0	3	N	1208	RCHOP-Bevacizumab (1)	1
164	DLBCL	Neg	84	M	2	1	N	454	Ritux-PMitCEBO+RT (1)	1
144	DLBCL	Pos	55	M	0	2	N	458	RCHOP (1)	1
129	tFL	Neg	61	M	0	3	N	479	Ritux-PMitCEBO (2)	2
133	tFL	Neg	60	F	3	3	N	909	RCHOP (4)	4
138	tFL	Neg	53	M	0	2	N	460	RCVP (1)	4
139	tFL	Neg	70	M	1	2	N	580	RCHOP (1)	1
140	tFL	Neg	82	M	4	2	Y	3181	RCHOP (1)	1
166	tFL	Neg	74	M	1	4	N	7078	Ritux-PACEBO (2)	2
113	FL	Pos	61	M	0	3	N	509	Bortezomib/Ritux (4)	6
114	FL	Pos	74	M	N/A	4	N	114	Ritux (2)	7
116	FL	Pos	64	M	0	4	N	94	Ritux (4)	4
120	FL	Pos	35	M	0	N/A	N/A	N/A	RCHOP (3)	6
125	FL	Pos	59	F	3	3	N	611	FCR maintenance Ritux (3)	3
156	FL	Pos	57	F	0	4	N	372	RCVP (1)	2
159	FL	Pos	71	M	2	2	N	282	RCVP (1)	1
170	FL	Pos	59	M	0	4	N	387	RCVP (1)	1
176	FL	Pos	77	F	1	2	N	519	RCVP (1)	1
178	FL	Pos	70	M	0	4	N	377	RCVP (1)	1
182	FL	Pos	60	F	1	3	N	501	RCVP (1)	1
185	FL	Pos	82	M	2	4	N	352	RCVP (1)	1
189	FL	Pos	81	M	2	4	N	321	Ritux (3)	3
193	FL	Pos	50	M	1	4	N	516	RCVP (1)	1
198	FL	Pos	79	F	2	3	Y	551	RCVP (1) (3 cycles)	1
186	FL	Neg	76	F	1	4	N	666	RCVP (1)	1

Patient ID	Diagnosis	FcγRIIb Status	Age	Sex	PF	Stage	Disease Bulk (Y/N)	LDH	Regimen compared (Line of therapy)	Total no of regimens
183	FL	Neg	55	F	0	4	N	440	RITUX (3)	3
174	FL	Neg	76	M	1	1	Y	458	RCVP (1)	1
163	FL	Neg	67	F	0	3	N	322	RCVP (2)	2
165	FL	Neg	58	F	0	3	N	474	RCVP (1)	1
167	FL	Neg	71	F	0	4	N	601	FCR (1)	1
169	FL	Neg	43	F	0	4	N	471	RCVP (1)	1
127	FL	Neg	70	F	1	4	N	496	Ritux (2)	4
131	FL	Neg	43	F	0	4	N	405	RCVP (1)	1
132	FL	Neg	80	M	1	3	N	732	RCVP (1)	1
135	FL	Neg	75	F	2	3	N	611	FCR (3)	4
136	FL	Neg	76	F	2	4	N	503	RCVP (1)	1
143	FL	Neg	60	M	0	2	Y	469	Ritux-PMitCEBO (2)	2
121	FL	Neg	59	M	0	3	N	N/A	RCHOP (4)	7
118	FL	Neg	56	M	0	4	N	N/A	Bortezomib/Ritux (5)	5
115	FL	Neg	52	F	0	3	N	438	RCHOP+autologous stem cell transplant(2)	2
154	SMZL	Pos	70	M	0	4	N	475	Ritux (5)	5
168	ENMZL	Pos	73	M	0	4	N	349	Ritux (1)	1
201	ENMZL	Pos	80	M	1	4	N	437	RCVP (1)	1
187	ENMZL	Pos	78	F	1	4	N	744	Cbl/Ritux (1)	1
162	MZL	Pos	73	F	0	4	N	326	Ritux-PMitCEBO (4)	4
200	ENMZL	Pos	66	M	0	4	N	1312	RCVPx2 (1) only then Ritux (2)	2
203	ENMZL	Pos	84	F	3	4	N	576	Cbl/Ritux (1)	1
173	ENMZL	Pos	75	F	1	2	N	352	Cbl/Ritux (2)	2
161	ENMZL	Neg	32	M	0	2	N	317	Cbl/Ritux (1)	1
153	LPL	Neg	87	M	2	4	N	435	Ritux (3)	4
179	LPL	Pos	74	M	1	4	N	452	RCVP (4)	4

SMZL=splenic MZL; ENMZL=extranodal MZL; tFL=transformed FL; PF=performance status; disease bulk (lymph node mass > 10 cm); PMitCEBO=prednisolone, mitoxantrone, cyclophosphamide, etoposide, bleomycin, vincristine; RT= radiotherapy; GCVP=gemcitabine, cyclophosphamide, vincristine, prednisolone; PACEBO=prednisolone, doxorubicin, cyclophosphamide, etoposide, bleomycin; Cbl=chlormbucil

Table 8: Demographic and clinical characteristics of FcγRIIb-phenotyped B-NHL patients

Details of the FcγRIIb expression status by IHC, diagnosis, demographic data and clinical characteristics of study patients are shown.

It is evident that the study patients were highly heterogeneous, even within the same diseases, particularly in terms of number and type of treatment regimens employed (**Table 8**). As highlighted above, the differences in FcγRIIb expression between disease types precluded a cumulative analysis of all patients. As an example, DLBCL tended to be FcγRIIb⁻ whereas MZL cases were mostly FcγRIIb⁺.

Thus all cases could not be grouped together simply as FcγRIIb⁺ or FcγRIIb⁻ since different diseases would make up the FcγRIIb^{-/+} groups, and the outcomes observed would be confounded by differences in disease. To reduce the heterogeneity due to different treatments, we chose to examine only FL patients who had received front-line RCVP chemotherapy. The baseline characteristics of FcγRIIb-positive and -negative groups within this cohort of patients are shown in **Table 9**. Although most of the factors studied were comparable, the median age and follow up was different between the two groups, in that FcγRIIb⁻ patients were older and had a shorter follow-up. Furthermore, although both groups had received front-line RCVP, we could not exclude the influence on survival caused by subsequent therapies. The PFS of the two groups were compared with the caveat of these potential confounding factors. Nonetheless, no statistical significance was demonstrated between PFS of FcγRIIb⁻ and FcγRIIb⁺ patients (**Fig. 39**).

	FcγRIIb⁻ patients	FcγRIIb⁺ patients
Number of patients	7	8
Median age, years (range)	76 (43-80)	65 (50-82)
Sex	5 females, 2 males	3 females, 5 males
Median ECOG performance status (range)	1 (0-3)	1 (0-2)
Median stage (range)	4 (2-4)	4 (2-4)
Median serum LDH, IU/ml (range)	474 (405-732)	382 (282-519)
Total number of lines of therapy, range	1	1-2
Responses	4 complete remission, 3 partial remission	4 complete remission, 4 partial remission
Median follow up, days (range)	434 (224-1004)	765 (170-878)

Table 9: Baseline characteristics of FcγRIIb^{+/-} FL patients treated with front-line RCVP

The table shows a summary of the baseline characteristics, median follow up and responses of FcγRIIb^{+/-} patients treated with front-line RCVP.

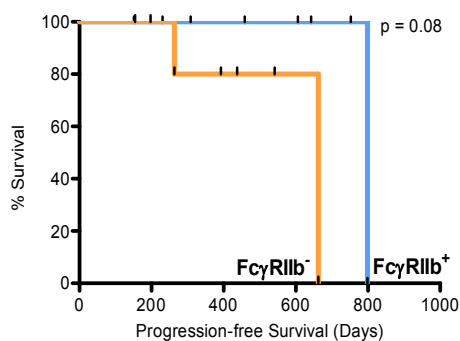


Figure 39: The role of FcγRIIb in predicting PFS of RCVP-treated FL patients

FcγRIIb status of FL patients who received initial therapy with RCVP chemotherapy obtained by IHC of diagnostic paraffin-embedded tissue as shown in **Fig. 38** and compared with PFS. PFS was measured from time of initiation of therapy until documentation of disease relapse/progression or death, whichever was earlier. Median survival in FcγRIIb⁺ and FcγRIIb⁻ groups were 798 and 662 days respectively, $p = ns$, $N = 15$ (7 FcγRIIb⁻ and 8 FcγRIIb⁺ patients).

The same analysis was performed on a cohort of MCL cases. One FcγRIIb⁻ patient was excluded from the analysis as he only received 2 of 6 intended cycles of rituximab-containing chemotherapy before showing evidence of disease progression (Patient ID 158, **Table 8**). Therefore, insufficient rituximab was given to enable adequate assessment of response. As before, the baseline characteristics were assessed (**Table 10**). Fortuitously, both FcγRIIb⁻ and FcγRIIb⁺ patients were comparable in terms of age and median follow-up. Furthermore, both groups also had an equivalent MCL international prognostic index (MIPI).⁴⁸² It was evident from assessment of the quality of responses that better overall responses were observed in FcγRIIb⁻ patients (6 patients with complete remissions compared to 2 complete remissions in FcγRIIb⁻ and FcγRIIb⁺ patients, respectively) (**Table 10**). Despite a small cohort of 16 MCL cases, patients with FcγRIIb⁻ disease had significantly better median PFS than those with FcγRIIb⁺ cells (median 852 and 189 days, respectively, $p=0.0127$) (**Fig. 40A**). However, there was heterogeneity in chemotherapy types used. To address this, we examined the results of those patients treated with either single-agent rituximab or FCR for initial therapy. The PFS curves showed the same trend but the p value was not statistically significant due to the low sample numbers (**Fig.**

40B). In summary, this preliminary clinical data supports the in vitro findings and substantiates the role of FcγRIIb as a biomarker of response to rituximab at least in MCL.

	FcγRIIb⁻ patients	FcγRIIb⁺ patients
Number of patients	8	8
Median age, years (range)	61 (51-84)	65.5 (52-82)
Sex	2 females, 6 males	8 males
Median ECOG performance status (range)	0 (0-2)	1 (1-3)
Median stage (range)	4 (2-4)	4 (3-4)
Median serum LDH, IU/ml (range)	465 (218-1889)	475 (114-1043)
Median WBC, 10 ⁹ /L (range)	5.2 (1.6-9.5)	16.3 (1.4-209.8)
Median MIPI score (range)	4 (3-7)	5 (3-8)
Total number of lines of therapy, range	1-3	1-3
Median line of therapy compared (range)	1(1-3)	1(1-3)
Quality of responses	6 complete remission, 1 partial remission, 1 progressive disease	2 complete remission, 1 partial remission, 1 stable disease, 3 progressive disease, 1 died before formal assessment
Median PFS, days (range)	609 (36-2287)	144 (0-336)
Median follow-up, days (range)	1049.5 (234-2714)	904.5 (175-2546)

Bortez=bortezomib; *Patient died of pneumonia prior to formal assessment

Table 10: Baseline characteristics of MCL patients

The baseline characteristics and data used to calculate MIPI for the MCL patients are shown.

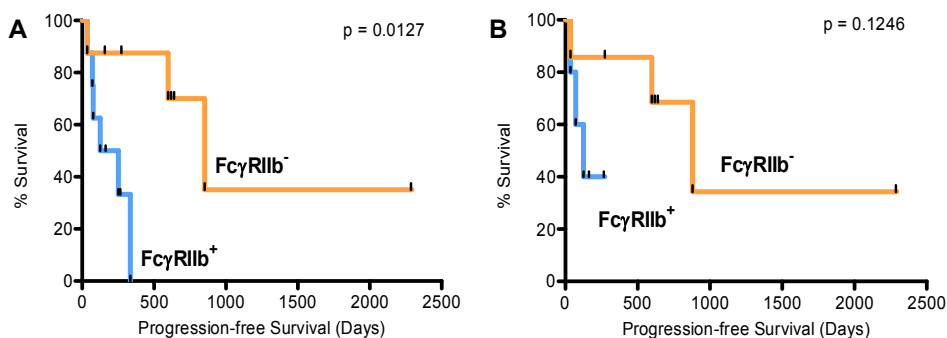


Figure 40: Stratification of FcγRIIb as a biomarker of response in rituximab-treated MCL patients

A) Correlation between FcγRIIb expression and PFS in MCL patients treated with rituximab-containing regimens, $p = 0.0127$ (median survival in FcγRIIb⁺ and FcγRIIb⁻ groups were 189 and 852 days respectively), $n = 8$ per group.

B) From A), only MCL patients treated with FCR or single agent rituximab first line were included for analysis. Median survival in FcγRIIb⁺ and FcγRIIb⁻ groups were 125 and 880 days respectively, $p = ns$, $n = 6$ per group.

6.2.3 The correlation between FcγRIIb expression by IHC and flow cytometry

Having assessed FcγRIIb expression in primary tumour material using two different techniques, we wanted to assess the correlation between the results obtained by IHC and flow cytometry. As mentioned earlier, some of the viable tumour cells analysed by flow cytometry had corresponding paraffin-embedded tissue stored. Therefore, the paraffin blocks were stained for FcγRIIb expression by IHC as before, and then the results directly compared with FcγRIIb Geo MFI expression by flow cytometry. **Fig. 41** is a composite of IHC and flow cytometry data (from **Fig. 27**), from the available samples and demonstrates that the cut-off value between positive and negative FcγRIIb expression by IHC approximated to a FcγRIIb Geo MFI expression of 40 by flow cytometry, indicating that the IHC protocol employed was highly sensitive in detecting FcγRIIb. Using this cut-off value, the number of FcγRIIb⁺ samples obtained by flow cytometry previously, were compared to the results obtained by IHC (**Table 11**). The percentage of FcγRIIb⁺ cases for each disease was similar with the exception of transformed FL and MCL, where a greater proportion of cases were positive by flow cytometry. This disparity is again likely to be due to the small sample size.

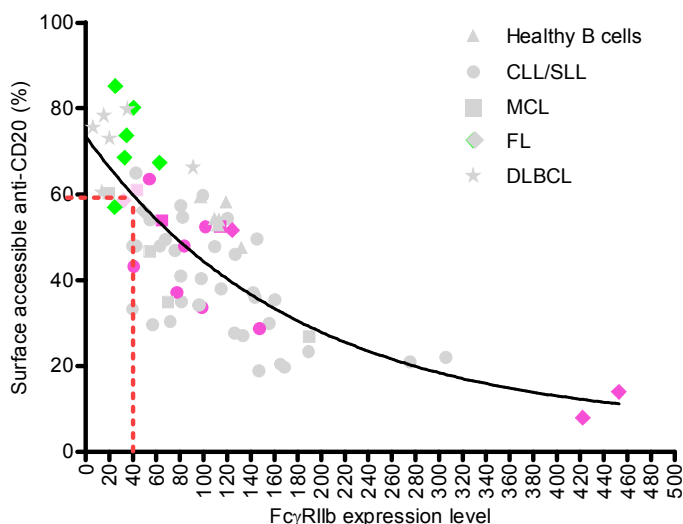


Figure 41: Comparison of FcγRIIb expression by IHC and flow cytometry

The flow cytometry data in Fig. 27 was re-analysed and coloured to indicate results based on IHC. The samples in pink and green were tested by IHC. Green denotes FcγRIIb-negative staining by IHC, and pink, FcγRIIb-positive. Some samples had distinctively weaker membranous staining than others, and are shown in light pink. The distinction between positive and negative staining by IHC approximately correlates with a cut-off of 40 by flow cytometry.

Disease	FcγRIIb+ cases by:	
	Flow cytometry	IHC
DLBCL	14% (1/7)	14% (1/7)
Transformed FL	100% (1/1)	0% (0/6)
FL	40% (4/10)	48% (15/31)
MCL	86% (6/7)	47% (8/17)
CLL	91% (42/46)	N/A
MZL	N/A	89% (8/9)
LPL	N/A	50% (1/2)

Table 11: FcγRIIb expression in different subtypes of B-cell malignancies

The table describes the proportion of FcγRIIb⁺ cases found by flow cytometry using (AT10-PE) and IHC. FcγRIIb⁺ cases were defined as an FcγRIIb expression level < 40, as shown in Fig. 41.

6.3 Discussion

We suggest here that the FcγRIIb expression on tumour cells in MCL patients can predict responses to treatment with rituximab-containing regimens. No significant difference was observed with FL cases treated with front-line RCVP chemotherapy, but the two groups compared were not equivalent in terms of median age or follow-up, thus complicating analysis. Furthermore, the disparity

in the results between FL and MCL may be due to the difference in the variance of FcγRIIb expression levels between both diseases. For instance, when measured by flow cytometry (**Fig. 26**) the distribution of FcγRIIb expression within FL is skewed to the left, with most cases having low FcγRIIb levels whilst MCL cases display a normal distribution. Furthermore, our in vitro data does not take into account the effect of chemotherapeutic agents on the internalisation of rituximab. While the link established in MCL suggests that FcγRIIb-mediated internalisation of rituximab is still important despite co-administration of chemotherapy, these results may be dependent on the specific chemotherapy combinations employed.

As yet, no other studies have investigated the role of FcγRIIb expression as a biomarker of response to rituximab in MCL or FL. In DLBCL, an approach similar to ours has been used. Camilleri-Broet et al. analysed patients with DLBCL treated with RCHOP chemotherapy as part of a randomised controlled study comparing first-line RCHOP against CHOP alone using a specific polyclonal anti-FcγRIIb mAb by IHC.³⁴⁴ 31/129 FcγRIIb⁺ cases were found. No correlation was seen between FcγRIIb expression and survival after RCHOP but the level of expression of the positive cases was not known. This aspect may be of particular importance as our data indicates that a wide spectrum of FcγRIIb expression level exists. For the same reason, this may have contributed to a lack of difference in the PFS of our cohort of FL patients treated with RCVP. When FcγRIIb expression by IHC was directly compared to flow cytometric quantification, positive IHC staining correlated with flow cytometric values as low as 40. This corresponds to 60% of surface accessible rituximab in a 6 h in vitro culture (**Fig. 41**). A higher cut-off value for FcγRIIb expression level may be required to stratify FcγRIIb as a prognostic marker more effectively. At present, with the assistance of Dr M. Ashton-Key, ongoing efforts are being undertaken to reduce the sensitivity of the mAb. This is being achieved by performing 5-fold dilutions of the mAb compared to the 1/200 dilution currently used. The mAb dilutions are then tested on primary tumour sections that are known to be positive for FcγRIIb by IHC, and that have corresponding viable cells tested by

flow cytometry. An arbitrary FcγRIIb expression (by flow cytometry) of 110 (~40% surface accessible anti-CD20) has been selected as the new target cut-off value. Thus using this method, previous IHC-positive samples with Geo MFI values of 100 should be IHC-negative, but samples with values >110, to remain IHC-positive. Evidently, the cut-off value selected is arbitrary and might still not be able to stratify with survival. As discussed earlier, flow cytometry would be a far more sensitive method, but is limited by the lack of storage of viable cells.

In another study examining the clinical importance of FcγRIIb, Weng and Levy³⁴⁸ investigated whether two alleles of FcγRIIb influenced responses to rituximab. The 232I allele was previously shown to be more efficient at BCR-mediated calcium regulation than the 232T allele in autoimmune disease.^{346,347} No correlation was found between this polymorphism and response to single-agent rituximab therapy in FL patients. The main concern, raised by the authors themselves, was that in this study, only 17 patients possessed the 232T allele, thereby limiting the statistical power of the study. In addition, the polymorphisms studied reflected efficiency of BCR inhibition in autoimmune disease, and there are no published observations indicating that these polymorphisms are relevant in lymphoma or influence Fc binding of human IgG1 or internalisation of rituximab.

Altogether, this clinical data is supportive of the in vitro findings. However, the study of MCL patients is small and retrospective, and the patients groups heterogeneous. Thus, these preliminary findings require validation with a larger prospective cohort. Ongoing efforts are being made to obtain further patient material from two trials, the first in FL patients treated with first line, single-agent rituximab and the other, in MCL patients treated with first line FCR chemotherapy. If substantiated, we predict that FcγRIIb is also likely to be a biomarker for response to other type I anti-CD20 mAb, such as ofatumumab.

7 The activity of new anti-CD20 mAb in CLL with del(17p)

7.1 Introduction

Despite mounting evidence that rituximab augments the efficacy of standard FC chemotherapy in CLL, the dismal prognosis of patients with del(17p) remains unaltered.²⁵⁴ This group of patients is characterised by resistance to purine analogues such as fludarabine (**Section 1.3.3.2**), although this relationship is not exclusive as half of fludarabine-refractory patients do not carry del(17p).²¹⁷ Fludarabine resistance in del(17p) CLL patients occurs because p53-mediated cell death triggered by purine analogue-induced DNA breaks is disrupted (reviewed in⁴⁸³). Although as indicated above, fludarabine resistance can also occur through p53-independent mechanisms. The anti-CD52 mAb alemtuzumab has been adopted as the first line therapy for this group of patients. CD52 is highly expressed on many haematopoietic mononuclear cells, such as T cells, B cells, monocytes and macrophages.⁴⁸⁴ Alemtuzumab has activity in CLL regardless of del(17p) but its clinical use is hampered by allergic reactions and immunosuppression, especially when used in combination with standard chemotherapy.⁴⁸⁵ Thus, there remains an unfilled niche for treatment of del(17p) CLL patients.

With the approval of the new type I anti-CD20 mAb ofatumumab, in fludarabine and/or alemtuzumab-resistant CLL cases, and the entry of the first unconjugated type II mAb, GA101, into phase III clinical trials, this chapter examines whether these new mAb will be superior to rituximab in del(17p) CLL patients. This is achieved through investigation of their in vitro activity such as mAb internalisation, induction of direct cell death and CDC.

7.2 Results

7.2.1 The effect of del(17p) on anti-CD20 mAb-mediated direct cell death in CLL

The CLL cases were kindly provided by Professor D. Oscier and were phenotyped for del(17p) by FISH (**Section 3.5**). These were compared to CLL cases bearing both normal 17p and 11q regions (hereafter referred to as normal 17p), so as to rule out an indirect route for p53 dysfunction through ATM dysfunction (**Section 1.3.3.2**). A total of 9 del(17p) and 20 normal 17p cases were obtained. As a means of double-checking the function of the p53 status of the CLL cases provided, an in vitro death assay was performed. Previous work from different groups had documented that del(17p) CLL cases were resistant to fludarabine-induced direct cell death in an in vitro setting.^{486,487} A similar methodology was adopted for the assay performed here. CLL cells were treated with type I or type II anti-CD20 and other clinically relevant reagents such as alemtuzumab, fludarabine and mafosfamide (a stable and active metabolite of the prodrug cyclophosphamide⁴⁸⁸) for a 48 h duration at 37°C and 5% CO₂. The viability of the cells was then measured with Annexin V-FITC/PI staining and flow cytometry (**Section 3.10**).

An example of Annexin V-FITC/PI staining in an untreated sample, and a sample treated with fludarabine chemotherapy is shown in **Fig. 42A**. As reported by Pettitt et al.,⁴⁸⁷ when treated by fludarabine, less cell death was observed in the del(17p) cases compared to the normal 17p cases (median 10% against 46%, respectively, $p < 0.05$), thereby giving confidence that the del(17p) cases are indeed dysfunctional for p53 (**Fig. 42B**). When the cells were treated with anti-CD20 mAb alone, an observable but low level of cell death was observed in either normal or del(17p) groups (medians in the normal 17p group are GA101_{gly} 6%, GA101 6%, rituximab 1.5% and ofatumumab 0.4%; for del(17p) group, GA101_{gly} 4.7%, GA101 -1.8%, rituximab 3.7% and ofatumumab 1.2%) (**Fig. 43**). The small difference in cell death between the type II and type I mAb were not statistically significant in either groups. These results are consistent with

previously published data using anti-CD20 mAb without secondary cross-linking with an anti-Fc Ab.⁴⁸⁹ In contrast, alemtuzumab was able to induce substantial direct cell death without the need for cross-linking (median 42% and 25% in normal 17p and del(17p) cases, respectively, $p > 0.05$) (Fig. 43). The exact mechanism by which alemtuzumab induces in vitro apoptosis is unknown, but has been suggested to be both caspase-dependent⁴⁹⁰ and -independent.⁴⁹¹

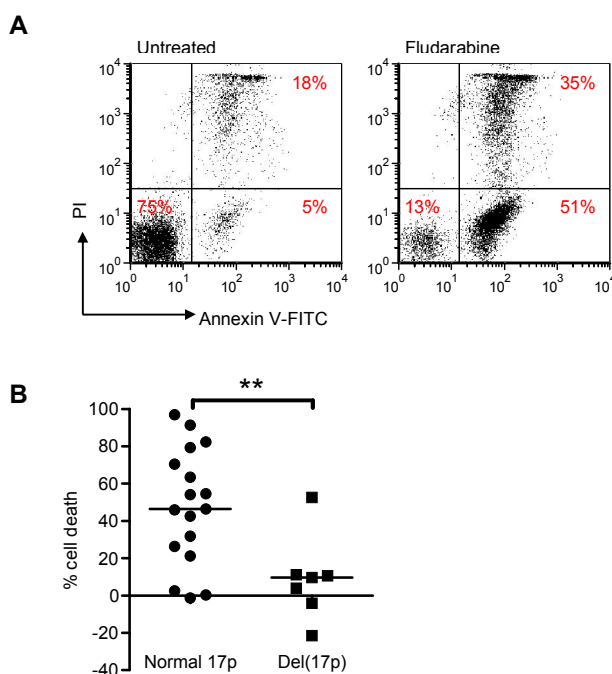


Figure 42: Fludarabine-induced cell death in normal and del(17p) CLL

A) CLL cells were either untreated, or treated with the specified reagent(s) for 48 h at 37°C and 5% CO₂, in a 96-well plate. The cell culture was then harvested into test tubes and treated with Annexin V-FITC/PI for 15 mins at RT, in the dark. The sample was then analysed by flow cytometry. The scatter plots show examples of Annexin V-FITC/PI staining in untreated, and fludarabine-treated cells. The % of Annexin V-FITC⁺ and PI⁺ cells are shown inset.

B) The graph presents the % cell death for normal and del(17p) cells when treated by 1 µg/ml fludarabine for 48 h at 37°C. % Cell lysis was calculated as follows; $100 - [(100 - \% \text{ Annexin V-FITC}^+/\text{PI}^+ \text{ treated cells}) / (100 - \% \text{ Annexin V-FITC}^+/\text{PI}^+)] * 100$. Medians are shown, $p < 0.05$, $n = 17$ (normal 17p) and 7 (del(17p)).

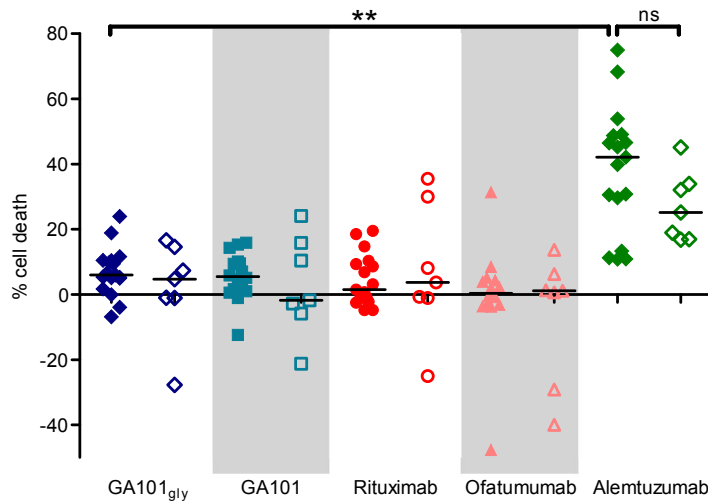


Figure 43: mAb-mediated direct cell death in normal and del(17p) CLL

The graph presents the % cell death for normal and del(17p) cells when treated with either anti-CD20 mAb (GA101_{gly}, GA101, rituximab and ofatumumab) or alemtuzumab (all 10 µg/ml) 48 h at 37°C. Cell death was assessed and calculated as described in Fig. 42. Normal 17p samples are represented by filled dots, and del(17p) by unfilled dots (n=17 and 7, respectively). **p<0.001.

It was observed that the expression of CD52 on the CLL cells was in general four-fold higher than CD20 (median 141 against 804, respectively) (Fig. 44A). Thus, alemtuzumab could be far more effective than anti-CD20 at inducing direct cell death by virtue of the higher expression of CD52, compared to CD20, on the cell surface. Therefore, we examined if CD52 expression correlated with cell death in all the cases. Indeed, high CD52 expression levels were significantly associated with higher % cell death (p=0.0417, r²=0.2, Pearson's correlation) (Fig. 44B). As a further example, a single case of CLL which exhibited similarly high levels of MHC Class II (Geo MFI 1419) was also susceptible to direct cell death induction by the anti-Class MHC II mAb, F3.3 (44% cell death after 48 h treatment).

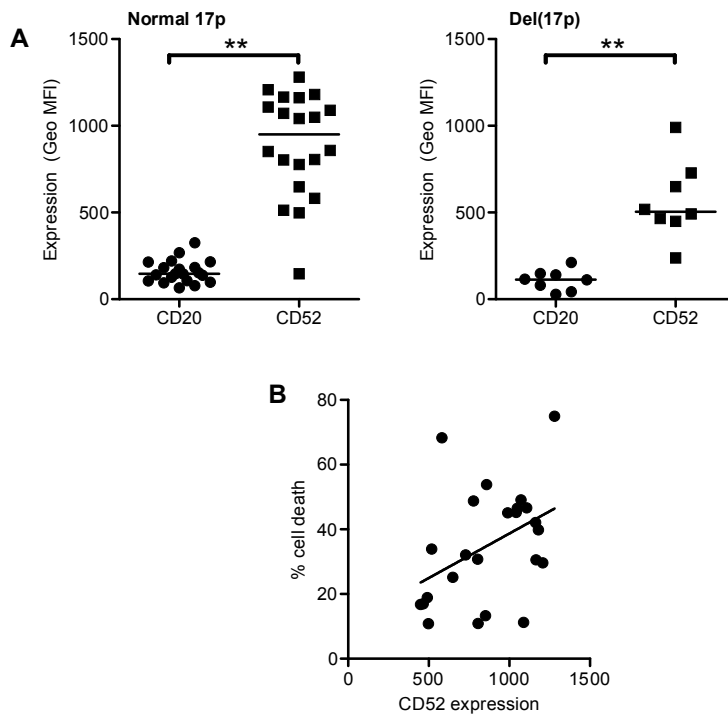


Figure 44: Correlation between CD52 expression and sensitivity to mAb-induced cell death

A) CD20 expression levels were obtained from concurrently performed quenching assays. Briefly, the cells were treated by 5 $\mu\text{g}/\text{ml}$ Ritux-488 for 2 h at 37°C, then washed twice before co-staining with anti-CD19-APC for 30 mins at 4°C. After a final wash, the samples were examined by flow cytometry. CD52 expression was obtained by treating the cells with 10 $\mu\text{g}/\text{ml}$ alemtuzumab-488 for 30 mins at 4°C, followed by one wash with cold FACS buffer and flow cytometry. Results for normal and del(17p) patients are shown (medians are shown, ** $p < 0.01$).

B) CD52 expression of normal and del(17p) cases obtained from A) was compared to % cell death in **Fig. 43**. $n=24$, Pearson's correlation, $p=0.04$, r^2 0.2.

Next, we explored to what extent did the chemoimmunotherapy combinations used in the clinic, mediated direct cell death. Mafosfamide was more effective than fludarabine at inducing cell death in both groups and addition of mafosfamide to fludarabine further improved the % of cell death in both groups significantly (medians 71% and 84% in del(17p) and non-deleted groups, respectively) (**Fig. 45**). However, the addition of either type I, or type II anti-CD20 mAb did not improve on the proportion of cell death. Apart from fludarabine, the observed proportion of cell death in normal and del(17p) groups were not statistically significant for all the other reagents tested.

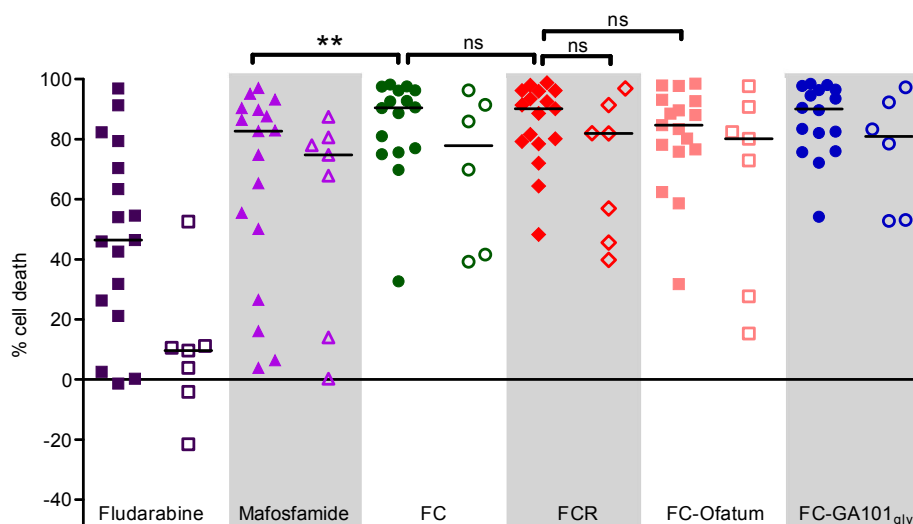


Figure 45: Induction of direct cell death in normal and del(17p) CLL

CLL cells were treated with the specified reagent(s) for 48 h at 37°C and 5% CO₂, in a 96-well plate. The concentrations used were 10 µg/ml for all mAb and 1 µg/ml for fludarabine and mafosfamide, respectively. The abbreviation FC here denotes fludarabine and mafosfamide together. % Cell death was assessed by Annexin V-FITC/PI as before. **p<0.01

7.2.2 Internalisation of anti-CD20 mAb in normal 17p and del(17p) CLL cases

Building on the data presented in the previous chapters which suggests that internalisation of rituximab is a plausible mechanism of treatment resistance, we explored if cases with or without del(17p) internalised rituximab at different rates. As before, the CD20 and FcγRIIb expression of both groups were compared by flow cytometry. Del(17p) demonstrated marginally lower CD20 expression levels than normal 17p but this was not statistically significant (**Fig. 46A**). Similarly, no difference was observed in FcγRIIb expression levels between both groups (**Fig. 46B**). The quenching assay was then performed after treating the cells with Alexa-488 labelled type II (GA101_{gly} and GA101) and type I (rituximab and ofatumumab) mAb for 6 h (**Fig. 46C**). No difference was observed between the internalisation of respective mAb between normal and

del(17p) groups. As previously noted, type I mAb internalised significantly more than type II mAb. Interestingly, GA101, with its defucosylated Fc domain internalised slightly but consistently more (median 4% in both groups, $p < 0.05$) than parental GA101_{gly}. The defucosylated Fc domain has been shown to bind with increased affinity to FcγRIIIa, but as far as we are aware, there is no published data on its affinity to FcγRIIb.⁴⁹² These results would suggest that the internalisation of anti-CD20 is not just dependent on type I/II differences, but the optimal isotype. **Fig. 46C** also demonstrates that the newly-approved ofatumumab, internalises consistently more than rituximab (median 10%, $p < 0.05$) in both normal and del(17p) cohorts.

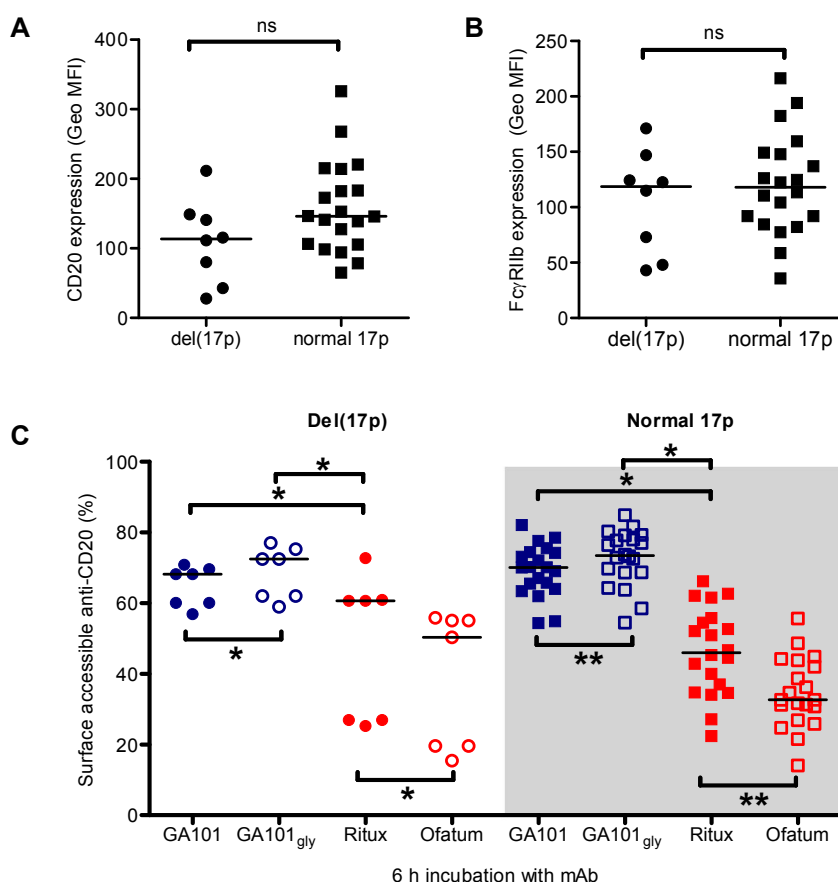


Figure 46: Internalisation of anti-CD20 mAb in del(17p) and normal 17p patients

A-B) CD20 and FcγRIIb expression was assessed by flow cytometry as previously described in **Section 5.2.2**. Medians are shown.

C) The quenching assay as in **Fig. 9** was performed after treating the CLL cells with either GA101_{gly}-488, GA101-488, Ritux-488 or Ofatum-488 (all 5 μg/ml) for 6 h at 37°C and 5% CO₂. Medians are shown. * $p < 0.05$, ** $p < 0.01$.

7.2.3 The impact of del(17p) on anti-CD20 mediated CDC in CLL

The results show that del(17p) does not confer any further resistance to CLL cells in terms of induction of direct cell death or internalisation of type I anti-CD20 mAb. The other two widely reported modes of action of anti-CD20 mAb are ADCC and CDC (**Section 1.5**). In CLL, alemtuzumab and ofatumumab, both of which have stronger in vitro CDC activity than rituximab, are more clinically active than rituximab. This led us to hypothesise that anti-CD20 mediated CDC may be relatively more important in the treatment of CLL than in other B-cell malignancies. Therefore we proceeded to characterise the in vitro CDC activity of the new anti-CD20 mAb, and examine whether del(17p) conferred any resistance to CDC.

First, to ensure that the in-house produced GA101_{gly} and ofatumumab (from published patented sequences) were comparable to the clinically approved reagents, the CDC activity of both mAb was compared to rituximab in Daudi cells. Daudi cells were treated with the anti-CD20 mAb at a range of concentrations for 15 mins at RT, or untreated. Then, complement (20% v/v human AB serum) was added to the cells for 30 mins and incubated at 37°C. The proportion of cells undergoing lysis (CDC) was detected using PI exclusion and flow cytometry. The typical PI staining observed from treated and untreated cells is shown in **Fig. 47A**. Consistent with previous data,³⁵⁹ ofatumumab showed appreciable lysis of Daudi cells, and was more effective than either GA101_{gly} (**Fig. 47B**).

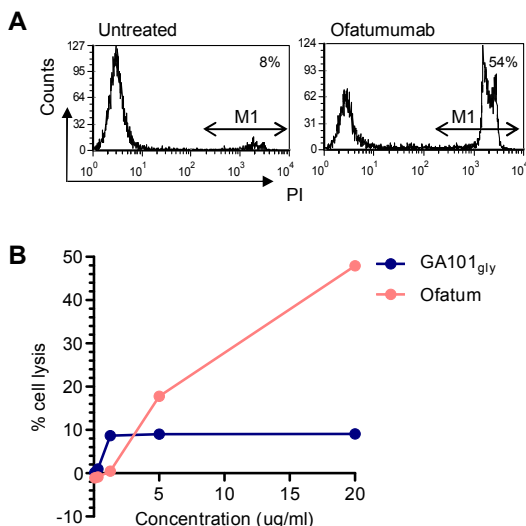


Figure 47: Confirmation of CDC activity of in-house produced GA101_{gly} and ofatumumab.

A) Daudi cells were treated with the specified mAb (0.31-20 $\mu\text{g/ml}$, 4-fold dilutions) for 15 mins at RT. 20% normal human AB serum was added for 30 mins at 37°C, and then cell lysis detected by adding 10 $\mu\text{g/ml}$ PI for 15 mins at RT, in the dark. The histogram shows an example of an untreated, and an ofatumumab-treated case. M1 denotes lysed, PI+ cells. % of cells in the M1 gate are shown inset.

B) The dose-response curves from A) using Daudi cells are shown. The cells were treated with either GA101_{gly} or ofatumumab as described. % Cell lysis was calculated as described in **Section 3.14**.

Prior to characterisation of the CDC activity of the various anti-CD20 mAb in primary CLL cells, we compared the expression of the complement defence molecules of the two cohorts. As mentioned earlier, complement defence molecules have been previously linked to in vitro CDC susceptibility and in vivo responses, although results are conflicting. The expression of three complement defence molecules, CD46, CD55 and CD59 were measured by flow cytometry and expression levels between the normal 17p cases were compared to del(17p) cases (**Fig. 48**). No difference was seen in the expression of these molecules between normal and del(17p) cases. CD46 and CD59 expression in the normal 17p cases appeared more heterogeneous than CD55, but this could simply be explained by the larger number of normal 17p cases.

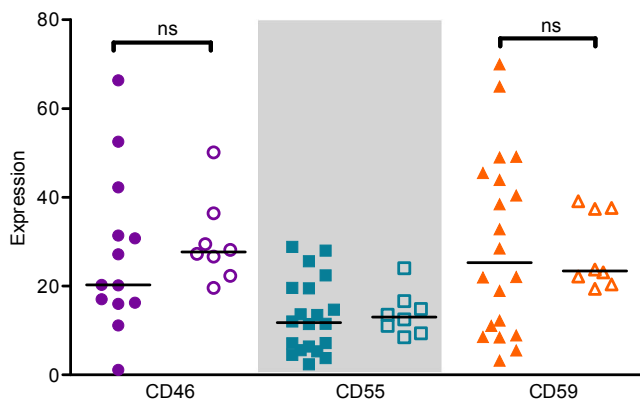


Figure 48: Expression of complement defence molecules in CLL cases with or without del(17p)

Del(17p) and non-17p deleted CLL cases were examined for CD46, CD55 and CD59 expression using clones MCA2113, MCA1614 and MCA1054, respectively. Appropriate isotype controls were used in each case. 10 µg/ml mAb (unlabelled) was added for 30 mins at 4°C, then washed twice before detection of bound primary mAb with anti-mouse Fc F(ab')₂-PE.

We then went on to examine the CDC activity of rituximab, GA101_{gly} and ofatumumab in the CLL cases. Alemtuzumab is known to elicit strong CDC activity, and was used as a positive control. The assay was performed as described in the Daudi cells but the percentage of AB human serum was reduced from 20 to 10% as no increase in CDC activity was observed with the higher concentration, for each mAb tested. The cumulative results of the CDC assays are shown in **Fig. 49**. Eight (del)17p cases were compared with 20 normal 17p cases. No difference was seen between the maximal % cell lysis or IC₅₀ (mAb concentration required to kill 50% of the cells) for any of the mAb, between normal and del(17p) cohorts. Alemtuzumab induced the highest level of CDC activity as anticipated. Amongst the anti-CD20 mAb, ofatumumab was most potent, but this was still six-fold less than alemtuzumab at an equivalent concentration of 10 µg/ml. Negligible CDC was evoked by GA101_{gly} and rituximab. The latter observation might appear surprising, but it is consistent with previous reports demonstrating the lack of CDC activity in primary CLL cells in contrast to results in cell lines.³⁹⁴ Again, this point emphasises the importance of interpreting results in cell lines with caution.

It was observed that the CDC activity of each mAb was somewhat variable between CLL samples. As such, the CD20 and complement defence molecule levels of each case were compared with the CDC activity of each mAb. No correlation was seen between CD20 or CD55 expression with any of the mAb. CLL cases with lower CD59 expression did appear more sensitive to ofatumumab-induced cell death but this was not statistically significant (**Fig. 50**).

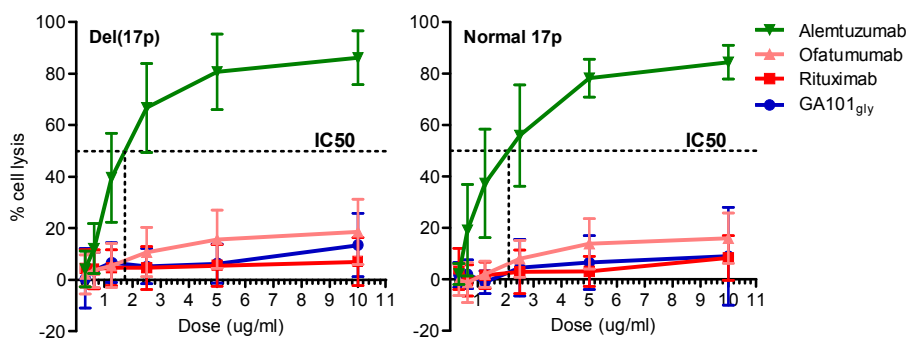


Figure 49: mAb-mediated CDC activity in CLL with or without del(17p)

The results of the CDC assay as described in Fig. 43 for anti-CD20 (GA101_{gly}, rituximab and ofatumumab) and alemtuzumab-treated normal and del(17p) CLL cells are shown above. The median and SD for each concentration is shown. The IC₅₀ for alemtuzumab in normal and del(17p) cohorts are 1.8 and 2.1 µg/ml respectively. n=20 (normal 17p) and 8 (del(17p))

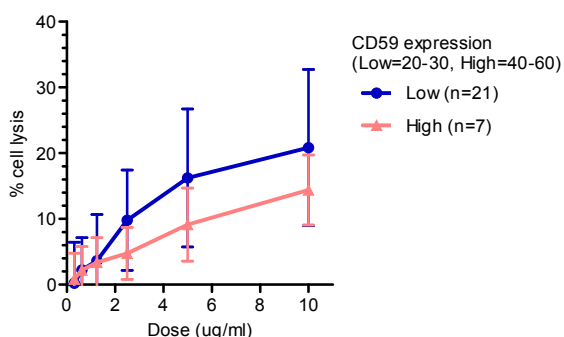


Figure 50: Correlation between CD59 expression and ofatumumab-mediated CDC

Within the normal 17p cohort, the CD59 expression of the CLL cases were grouped into low (20-30) or high (40-60) expression levels. The CDC activity from **Fig. 49** of these groups were compared (p=ns).

7.3 Discussion

The addition of rituximab to FC chemotherapy has resulted in an improved 3-year PFS, but not OS, in the del(17p) group.²⁵⁴ However this group of patients still has the shortest survival when compared to other cytogenetic groups (38% median OS at 3 years, compared to 87% in all patients). Here, using in vitro assays, we examined if the new anti-CD20 mAb ofatumumab and GA101, will achieve better response rates than rituximab. First we studied the ability of anti-CD20 mAb to induce direct cell death, which as discussed in **Section 1.5.3**, appears to be model-dependent. However, this assay was useful for verifying p53 dysfunction in the del(17p) cases, which tend to be more resistant to fludarabine than normal 17p cases.⁵⁰⁰ In contrast, the majority of these cases were sensitive to mafosfamide regardless of 17p status, thus suggesting that mafosfamide is able to induce cell death in a p53-independent manner. Previous studies have suggested in vitro resistance of del(17p) cases to alkylating agents, although this is dependent on the precise agent used, i.e. more resistance is observed with chlorambucil than mafosfamide.⁴⁹³ Consistent with clinical observations, the FC combination is more effective than fludarabine alone in CLL patients.⁴⁹⁴ Minimal cell death was observed with the anti-CD20 mAb, consistent with previous data when used without mAb cross-linking. The combination of anti-CD20 mAb to FC also failed to improve the proportion of FC-mediated death. It is interesting to note that whilst alemtuzumab is primarily known for its CDC activity, it also demonstrated a clear ability to induce direct cell death in the absence of complement, as previously reported.⁴⁹⁰ This ability was at least partly dependent on the CD52 expression levels on the CLL cells. Likewise, in a CLL sample that expressed high levels of MHC class II, we also observed a high level of direct cell killing by an anti- MHC class II mAb. Altogether, apart from a difference in sensitivity to fludarabine-induced cell death, no other differences were observed between the normal and del(17p) cohorts. Furthermore, no improvement in cell death was observed with any of the new anti-CD20 mAb in our model, and that the findings suggest

that the anti-CD20 mAb are unlikely to add to the direct cell-killing effects of currently used chemotherapy agents.

There is evidence that CLL cells are deficient in a variety of complement components^{495,496} and that replenishing these components through infusion of fresh frozen plasma may improve responses to rituximab^{380,497} (**Section 1.5.2**). Furthermore, inhibition of the complement defence molecules, CD55 and CD59 increased rituximab-mediated CDC of primary CLL cells⁴⁹⁸ and lymphoma cell lines.³⁷⁶ However, CD55 and CD59 expression levels did not predict clinical outcomes to rituximab in CLL³⁷⁷ or FL,³⁸² but in the CLL study, CLL cells that resisted depletion by rituximab appeared to express more CD59.³⁷⁷ For these reasons, we chose to investigate the CDC activity of the anti-CD20 mAb in the CLL samples. However, no difference was observed in the CDC ability of anti-CD20 mAb or alemtuzumab between the normal and del(17p) cohorts. Unlike findings in cell lines, ofatumumab appeared far less potent in primary cells, albeit still more active than the type II GA101_{gly}. A non-statistically significant trend was observed between CD59 expression and the ability of ofatumumab to induce CDC, in that lower CD59 levels increased the sensitivity to this mAb. As we only had 28 samples, a larger cohort is required to confirm if this is a genuine effect. Unlike previous reports which documented a trend between CD20 expression levels and CDC activity,⁴⁹⁸ we failed to establish a correlation, again possibly due to the low sample numbers.

We also examined the ability of anti-CD20 mAb to internalise in the normal and del(17p) cohorts. As in the preceding chapters, the type II anti-CD20 mAb appeared to internalise markedly less than the type I anti-CD20. Within the type I mAb, ofatumumab internalised consistently more than rituximab. The underlying reason for this is unknown and will be discussed further in the next section. No difference was observed with FcγRIIb expression levels between the normal and del(17p) cohorts, and similarly no difference in internalisation of the respective mAb.

In conclusion, the normal and del(17p) CLL cases appear to demonstrate similar rates of anti-CD20-mediated cell death, CDC activity and rates of internalisation of anti-CD20 mAb. Based on these assays, ofatumumab would not be predicted to improve upon the response rates achieved by rituximab. It is interesting to note that in the clinical trial of ofatumumab in fludarabine and/or alemtuzumab-resistant CLL patients, ofatumumab demonstrated activity in rituximab-refractory patients. However it should be noted that this was achieved in nearly four times the usual dose of rituximab, and the OS was still in the region of 14 to 15 months.⁴⁹⁹ More recently, preliminary findings on the use of first line FC-ofatumumab have been reported.⁵⁰⁰ Whilst results from different trials are difficult to compare, the best overall response rate seen with FC-ofatumumab was 77%, in contrast to the 90% achieved with FCR,²⁵⁴ and patients from both trials had comparable baseline factors. Thus, this potentially supports our suggestion that ofatumumab would be clinically less active than rituximab. With respect to GA101, it internalises less than rituximab in both normal and del(17p) cohorts, and so would be expected to achieve better initial response rates. However it is likely GA101 will require augmentation with other therapeutic agents, for reasons that will be discussed in the next section.

8 Final discussion and future work

Since the approval of rituximab for the treatment of relapsed B-cell neoplasms over a decade ago, its use in malignant and non-malignant B-cell diseases has increased almost exponentially. Many in the field have now focused on understanding how anti-CD20 mAb deplete B cells and how their efficacy can be improved. Recently, our group observed that type I mAb like rituximab internalise from the surface of human CD20 Tg mouse B cells (in vitro and in vivo) thereby limiting their capacity to recruit effectors and deplete target cells.³⁵⁵ In this thesis, the internalisation of type I anti-CD20 such as rituximab and ofatumumab, was also clearly demonstrated in primary human B cells. Further, a mechanism behind the internalisation of these mAb was proposed and data supporting this presented.

When primary CLL/SLL cells were cultured with type I anti-CD20 mAb, significant but heterogeneous internalisation was observed, and this heterogeneity could not be linked to currently used disease prognostic markers. Analysis of other B cell neoplasm subtypes showed that MCL displayed similar levels of internalisation to CLL, but that FL and notably DLBCL showed significantly less internalisation. Likewise in patients, rituximab is of most proven benefit in DLBCL and FL, where it is established first-line therapy in combination with chemotherapy. By contrast, higher doses of rituximab is required in CLL,²⁵³ and its benefits in MCL are modest.²⁵¹ It therefore seemed a reasonable hypothesis to propose that mAb internalisation could explain some of the heterogeneity observed in the responses to rituximab in these diseases.

We subsequently showed that internalisation of rituximab in a 6 h in vitro culture correlated strongly with FcγRIIb expression levels on the target cells. As a general finding, B-cell malignancies that express high levels of FcγRIIb such as CLL and MCL, were more likely to internalise rituximab and tend to benefit less from rituximab treatment. Internalisation of rituximab showed a strong correlation with FcγRIIb expression level regardless of disease subtype. It was

previously suggested that FcγRIIb could inhibit therapeutic mAb efficacy by competing with activatory Fc receptors on effector cells, thereby inhibiting cytotoxic signalling.⁵⁰¹ Our in vitro investigations suggest an alternative mechanism that is independent of effector cells. Rituximab co-ligates CD20 and FcγRIIb on the same cell, resulting in activation of FcγRIIb, and rapid paired internalisation of both surface antigens together with bound mAb into endosomal and lysosomal compartments. The Western blot data suggest that CD20 is then degraded within the lysosomes of CLL cells as it was in the huCD20 Tg mouse B cells.³⁵⁵ Internalisation resulted in decreased effector-cell recruitment through down-regulation of the surface expression of the mAb on the target cell. Correspondingly, inhibiting internalisation with a blocking FcγRIIb mAb restored phagocytosis of tumour cells. Whilst a direct correlation was not demonstrated between the proportion of reduction in phagocytosis and the FcγRIIb expression levels on target B cells, inhibition of FcγRIIb did increase the phagocytic potential of rituximab-opsonised cells. The difference in phagocytosis between type I and type II mAb observed was smaller than anticipated, and may be accounted for by several factors. First, type I mAb bind twice as much CD20 than type II,²⁹⁴ therefore despite internalisation of type I mAb, residual surface type I mAb at 6 h, may still be relatively high compared to surface type II mAb levels. We only examined 6 h incubations of mAb treatment but it is clear that extended incubations may produce a more marked difference between both mAb in the phagocytosis assay. The cells were only incubated for 6 h to restrict the extent of cell death, as macrophages will also engulf dead cells. However, since those experiments were performed, it has come to our attention that the viability of ex vivo CLL cells can be extended by using an alternative medium such as AIM-V (Invitrogen), which maintains better cell viability than standard 10% FCS in RPMI.⁵⁰² Potentially then, experiments might be performed in this media to examine the consequence of extended incubation times. Furthermore, some groups have demonstrated that CD20 expression does not affect the efficiency of in vitro ADCC^{503,504} although this may be dependent on the baseline surface CD20 expression of the target cells. For

instance, in CLL where the CD20 expression is already weak, further reduction in bound-rituximab as a result of internalisation, might have a clinically significant effect.

The experiments we performed are somewhat non-physiological as they are performed in the absence of other FcγR-bearing cells. In vivo, the Fc domain of rituximab would also encounter FcγR on other haematopoietic cells such as FcγRI and FcγRIIIa on monocytes, and not only FcγRIIb on B cells, as in these experiments. It is not known whether other FcγR (such as the high affinity FcγRI) would out-compete binding of FcγRIIb, and therefore inhibit FcγRIIb binding and activation at the target cell surface and subsequent internalisation of rituximab. The whole blood experiments are more representative of the in vivo environment, but do not allow us to study the influence of each variable (such as the influence of the different effector cells, complement, serum, immunoglobulin) separately. It would therefore have been informative to have introduced these separate variables, one at a time e.g. by adding complement or monocytes, then both.

FcγRIIb is a low-affinity Fc receptor and thus able to bind immune complexes, but almost undetectable amounts of monomeric IgG.³⁰⁶ At the cell membrane where there is a high local concentration of mAb and FcγRIIb, anti-CD20 mAb bound to CD20 would strongly favour engagement with FcγRIIb located on the same cell, as indicated by the cis/trans experiments. Clearly, to facilitate this interaction the Fc of the mAb also needs to be in an appropriate orientation to bind to FcγRIIb. Together, our Western blot data and the work of Klein's group²⁹³ suggest that the differences in orientation between type I and type II anti-CD20 mAb binding may explain why type I and not type II mAb bind to engage and activate FcγRIIb.

The main difference between type I and II mAb is the ability of type I mAb to translocate CD20 into lipid rafts. Likewise, it has been previously reported that

a small fraction of FcγRIIb is present constitutively in lipid rafts, and this is increased upon BCR-FcγRIIb cross-linking.⁵⁰⁵ It is not known whether CD20-FcγRIIb cross-linking results in translocation into lipid rafts as well. However, it should be noted that type I (but not type II) local mAb concentrations are likely to be greatly augmented in the plasma membrane by the redistribution of CD20 into lipid rafts, a property linked to their superior ability to bind C1q and elicit potent CDC.²⁸⁴ In this context, it is possible that the high concentration of Ab allows immune complex formation and subsequent co-engagement of FcγRIIb at the cell surface, analogous to the situation with the BCR and FcγRIIb (commented in⁵⁰⁶). As discussed earlier, a single-nucleotide polymorphism of FcγRIIb in the transmembrane region has been associated with a two-fold increased risk of SLE,⁵⁰⁷ and more recently, protection against malaria.³³⁸ In transfection experiments, 232T/T resulted in exclusion of FcγRIIb from redistribution into lipid raft regions unlike the alternate FcγRIIb (232I/I or 232I/T) alleles.⁵⁰⁸ Therefore, it will be interesting to see if these polymorphic variants of FcγRIIb will have different abilities in mediating internalisation of rituximab. Further, it is interesting that amongst the type II mAb, tositumomab, which does not induce CD20 redistribution and carries the mouse IgG2a isotype and consequently has a low affinity for FcγRIIb, does not activate FcγRIIb and shows the least internalisation of all mAb assessed. In comparison, GA101, with its glycomodified Fc affinity internalises more than non-Fc modified GA101_{gly}. Within the type I mAb, Rit m2a, which redistributes CD20 and shares the mouse IgG2a isotype is only able to activate FcγRIIb weakly, compared to the human IgG1 isotype carried by rituximab (data not shown). Co-incubation with a blocking anti-FcγRIIb mAb was able to prevent both FcγRIIb activation and rapid internalisation of rituximab. Altogether, these data confirm the direct link between activation of FcγRIIb and rapid internalisation of mAb from the cell surface and indicate that both a type I mAb (presumably through raft redistribution) and optimal isotype are required for maximal internalisation. Other members of our team are currently investigating the requirement of lipid rafts for internalisation of type I mAb.

Whilst we have demonstrated that FcγRIIb is phosphorylated by rituximab and not GA101 and its non-FC modified version, GA101_{gly}, it is not known if this difference can be extended to other type I/II mAb as yet. Furthermore, it is not known if activation of FcγRIIb is required for internalisation of anti-CD20 to take place. There are at least two approaches for examining whether FcγRIIb activation is required for anti-CD20 internalisation. The first is to block the FcγRIIb signalling pathway with a tyrosine kinase inhibitor and second, to generate and transfect cells with FcγRIIb molecules deficient for specific regions such as the transmembrane domain or ITIM, and examine if cells bearing these constructs are able to internalise rituximab like wild type FcγRIIb. A drawback of the first approach is the availability of an inhibitor capable of targeting the FcγRIIb signalling pathway without affecting other cell-signalling pathways. Thus, the second approach is more favourable, and ongoing work of this nature is being carried out in the laboratory. As an extension of the hypothesis, it is possible that the internalisation of type I anti-CD20 mAb might not require the specific expression of the inhibitory FcγR on the target tumour cell. Seeing that all FcγRs are capable of binding Fc, and endocytosing immune complexes, any FcγR on the target cell may mediate the same phenomenon. This point, if true, would indicate that FcγR of any type might have the ability to impair the efficacy of type I mAb therapy. To address this, each FcγR can be transfected into CD20⁺ FcγR⁻ cells to explore the influence of the different FcγR in mediating the internalisation of type I anti-CD20 mAb.

Given that FcγRIIb is a negative regulator of BCR activation, and CD20 associates with the BCR after type I binding, it seemed likely that that BCR could be linked to internalisation of anti-CD20 in some respect. However, CLL cells, which characteristically express low levels of BCR, displayed amongst the highest levels of internalisation and BCR expression levels on these cells were not predictive of rapid rituximab internalisation. As an interesting observation, experiments were also carried out to investigate whether the BCR internalised alongside rituximab in CLL and MCL samples, but no change was seen in the surface

expression of the BCR in these conditions. However, treatment of the CLL cells with either type I or type II anti-CD20 mAb, seemed to prevent the re-expression of the BCR. Since FcγRIIb and BCR are co-aggregated by immune complex binding to the cognate antigen, and CD20 also associates with BCR, we used confocal microscopy to examine if the BCR co-localised with anti-CD20:CD20 complexes, but this was not observed. Another means of excluding the involvement of the BCR in the internalisation of type I anti-CD20 mAb would be through inhibition of the BCR signalling pathway e.g. using a Syk inhibitor, and this work is underway. Furthermore, complementary work from Dr A. Vaughan has demonstrated that Ramos cells lacking BCR expression (Rx3) display modestly impaired internalisation of rituximab but that this defect is overcome by over-expression of FcγRIIb in these cells (Rx3 cells lacking BCR⁻ and FcγRIIb⁺) (data not shown). Therefore, whilst BCR may have a role in internalisation of rituximab, FcγRIIb remains the main participant of this process.

In vitro and xenograft models have shown that FcγRIIb on effector cells can reduce the efficacy of monoclonal Ab efficacy by competing with activatory FcγR, and hence reducing ADCC.²⁹⁷ However, the ability of FcγRIIb to influence the efficacy of mAb therapy has never been clinically proven. Two different groups attempted to evaluate the role of FcγRIIb in lymphoma patients treated with rituximab through different means. One group examined if FcγRIIb expression by IHC would predict survival in patients with DLBCL treated with RCHOP chemotherapy,³⁴⁵ and a second examined the influence of the 232T/T polymorphism of FcγRIIb, in FL patients treated with rituximab.³⁴⁸ Both studies yielded negative results, and the underlying reasons for these findings have been discussed in detail in the previous sections.

We also explored whether underlying cytogenetic abnormalities in CLL cells, for example del(11q) or del(17p) influenced rituximab internalisation, but no difference was observed. Equally, no significant difference was observed

between the ability of anti-CD20 mAb to induce direct cell death or CDC in the normal and del(17p) patients. Evidently, any minor differences that existed would not be detectable by the small number of samples used, and to examine this more fully, larger cohorts of patients are required. It is interesting to note that although both deletions affect p53 function, albeit in a different manner, present clinical data suggests that del(11p) patients derive more benefit from FCR than del(17p) patients.²⁵⁴ This implies that it is an over-simplification to attribute the dismal outcome of del(17p) patients to p53 alone. As previously reported, del(17p) produces a host of differentially expression genes,⁵⁰⁹ all of which may contribute to the aggressive nature of this cohort of CLL cases. Furthermore, CLL cases harbouring del(17p) tend to have an unstable genome,⁵¹⁰ with a propensity to develop further mutations capable of driving disease progression. It is likely that standard chemotherapy combinations have reached their therapeutic benefit, and that further manipulation of these regimens will simply increase toxicity without extra benefit. Thus, combinations of novel therapeutic agents, each capable of targeting a p53-independent pathway, for example employed by mAb, is required. One of the limitations of mAb therapy, is that of access to the tumour. As an example, despite being active in CLL regardless of p53, alemtuzumab is notably less efficacious for patients with bulky lymphadenopathy.⁵¹¹ Similarly, for the anti-CD20 mAb, B-cell depletion is partly dependent on access to the different compartments.³⁵⁴ Interestingly, several different new agents such as a CXCR4 antagonist (plerixafor), a Btk inhibitor (PCI32765) and PI3K inhibitor (CAL-101) are able to promote the migration of CLL cells from the tissues into the peripheral blood.⁵¹² Indeed, a small phase 1 study of CAL-101 with rituximab in indolent B-NHL and CLL showed very promising response rates (11/12 patients responded).⁵¹³ Thus the addition of any of these agents with anti-CD20 mAb and/or alemtuzumab may prove to be a sensible combination for treatment of B-cell malignancies.

Despite the fact that rituximab has activity against B-cell tumours as a single agent, it is now well-established that far better results are achieved when it is combined with chemotherapy. However, rituximab is no longer the only

clinically available anti-CD20 mAb. With the potential availability of at least 7 other new anti-CD20 mAb,⁵⁴ the intriguing question is whether any of these mAb will be superior to rituximab. Amongst the new mAb, only type I ofatumumab has been approved for clinical use so far. The clinical testing of many of the other mAb, such as ocrelizumab, AME-133v, PRO131921 and TRU015 appear to have waned after phase I/II trials, presumably because of a lack of clear advantage over rituximab. The first three mAb are type I and humanised, and in addition AME-133v and PRO131921 also have a modified Fc region for enhanced binding to FcγRIIIa. The fourth, TR015 is a fusion protein comprising a single CD20 binding domain, a hinge region and C_H2 and C_H3 domains of IgG1. The rationale of developing a smaller molecule than rituximab was to improve the penetration of the anti-CD20 into solid tumours. As such, TRU015 demonstrated better responses than rituximab in lymphoma xenograft models with bulky tumours, although this is yet to be confirmed in syngeneic models or clinical trials.⁵¹⁴ Veltuzumab is another type I humanised anti-CD20 mAb still undergoing active clinical trial testing. It is very similar to rituximab in terms of the CDR varying only by one amino acid (Asp instead of Asn at residue 101).⁵¹⁵ However this single amino acid change has apparently assisted in improving its binding avidity and CDC activity in comparison to rituximab.⁵¹⁵ Furthermore, as a humanised mAb, it is better tolerated than chimeric rituximab thus allowing shorter drug infusion times and subcutaneous administration.

GA101 is the only type II anti-CD20 mAb in clinical trials. The results so far have demonstrated that it has significant activity as a single agent in lymphoma patients, including rituximab-refractory patients.⁵¹⁶ A trial to directly compare the activity of rituximab against GA101 is underway and should inform us if type II mAb are better than type I as anticipated.⁵¹⁷ However, the caveat with the planned trial is that equivalent doses have not been chosen so final analysis will be confounded by this dose difference. Despite this difference, our in vitro data suggests that as a type II anti-CD20 mAb, GA101 internalises significantly less than rituximab and is also better at mediating ADCC, thus should demonstrate improved response rates over rituximab. Albeit, our in vitro data also indicate

that despite the lack of activation of FcγRIIb by Western blot, GA101 appears to internalise marginally more than GA101_{gly} in in vitro experiments. Shields et al.⁴⁹² previously demonstrated that defucosylation of IgG1 improved binding to FcγRIIb, albeit only to a minor extent. We presume this similarly improves binding of GA101 to FcγRIIb, but this requires investigation. As a type II mAb, the CDC activity of GA101 has also been shown to be weaker than rituximab in in vitro assays in human lymphoma cell lines, thus the lower CDC activity of GA101 should translate into a better side effect profile than rituximab. Certainly, GA101 has been reported to be well-tolerated in phase I/II studies.⁵¹⁶

In summary, the findings of this project have two major implications. First, response to anti-CD20 mAb therapy may be optimised by using type II anti-CD20 mAb such as GA101, which circumvent the limitations of internalisation, regardless of FcγRIIb expression. Alternatively, concurrent administration of an FcγRIIb inhibitor with rituximab may potentiate its therapeutic efficacy in cases of high FcγRIIb expression. The benefit of this latter approach over the former would be that FcγRIIb on immune effector cells could also be simultaneously blocked by the FcγRIIb inhibitor, thus potentially augmenting ADCC activity. Finally, this work uncovers a previously unrecognised means by which FcγRIIb may reduce the efficacy of anti-CD20 mAb immunotherapy. Although it is well-established that internalisation of a mAb and its target is detrimental to therapy, the events surrounding internalisation is not as well-understood. This concept of internalisation of anti-CD20 mAb through engagement of FcγRIIb might be relevant to mAb treatment of other tumours. Our laboratory is still in the process of investigating whether other FcγR are capable of mediating mAb internalisation, and if proven to do so, the findings will be especially important to other FcγR-expressing tumours such as the monocytic leukaemias. For the time being, the findings in this thesis give further impetus to investigate the association between FcγRIIb expression and response to mAb immunotherapy in B-cell neoplasms and other FcγRIIb-expressing tumours such as metastatic malignant melanoma.

9 References

1. Dunn, G.P., Bruce, A.T., Ikeda, H., Old, L.J. & Schreiber, R.D. Cancer immunoediting: from immunosurveillance to tumor escape. *Nat Immunol* 3, 991-998 (2002).
2. Old, L.J. & Boyse, E.A. Immunology of Experimental Tumors. *Annu Rev Med* 15, 167-186 (1964).
3. Shinkai, Y., *et al.* RAG-2-deficient mice lack mature lymphocytes owing to inability to initiate V(D)J rearrangement. *Cell* 68, 855-867 (1992).
4. Shankaran, V., *et al.* IFN γ and lymphocytes prevent primary tumour development and shape tumour immunogenicity. *Nature* 410, 1107-1111 (2001).
5. Delorme, E.J. & Alexander, P. Treatment of Primary Fibrosarcoma in the Rat with Immune Lymphocytes. *Lancet* 2, 117-120 (1964).
6. Fefer, A. Immunotherapy and chemotherapy of Moloney sarcoma virus-induced tumors in mice. *Cancer Res* 29, 2177-2183 (1969).
7. Woodruff, M.F. & Nolan, B. Preliminary Observations on Treatment of Advanced Cancer by Injection of Allogeneic Spleen Cells. *Lancet* 2, 426-429 (1963).
8. Andrews, G.A., *et al.* Preliminary trials of clinical immunotherapy. *Cancer Res* 27, 2535-2541 (1967).
9. Westwood, J.A., *et al.* Enhancing adoptive immunotherapy of cancer. *Expert Opin Biol Ther* 10, 531-545 (2010).
10. Yee, C., *et al.* Adoptive T cell therapy using antigen-specific CD8⁺ T cell clones for the treatment of patients with metastatic melanoma: in vivo persistence, migration, and antitumor effect of transferred T cells. *Proc Natl Acad Sci U S A* 99, 16168-16173 (2002).
11. Dudley, M.E., *et al.* Cancer regression and autoimmunity in patients after clonal repopulation with antitumor lymphocytes. *Science* 298, 850-854 (2002).
12. Mackensen, A., *et al.* Phase I study of adoptive T-cell therapy using antigen-specific CD8⁺ T cells for the treatment of patients with metastatic melanoma. *J Clin Oncol* 24, 5060-5069 (2006).
13. Dudley, M.E., *et al.* Adoptive cell therapy for patients with metastatic melanoma: evaluation of intensive myeloablative chemoradiation preparative regimens. *J Clin Oncol* 26, 5233-5239 (2008).
14. Heslop, H.E., *et al.* Long-term restoration of immunity against Epstein-Barr virus infection by adoptive transfer of gene-modified virus-specific T lymphocytes. *Nat Med* 2, 551-555 (1996).
15. Rice, J., Ottensmeier, C.H. & Stevenson, F.K. DNA vaccines: precision tools for activating effective immunity against cancer. *Nat Rev Cancer* 8, 108-120 (2008).
16. Stevenson, G.T. & Stevenson, F.K. Antibody to a molecularly-defined antigen confined to a tumour cell surface. *Nature* 254, 714-716 (1975).
17. Kwak, L.W., *et al.* Induction of immune responses in patients with B-cell lymphoma against the surface-immunoglobulin idiotype expressed by their tumors. *N Engl J Med* 327, 1209-1215 (1992).

18. Hsu, F.J., *et al.* Tumor-specific idiotype vaccines in the treatment of patients with B-cell lymphoma--long-term results of a clinical trial. *Blood* 89, 3129-3135 (1997).
19. Bendandi, M. Idiotype vaccines for lymphoma: proof-of-principles and clinical trial failures. *Nat Rev Cancer* 9, 675-681 (2009).
20. Curiel, T.J. Tregs and rethinking cancer immunotherapy. *J Clin Invest* 117, 1167-1174 (2007).
21. Munn, D.H. & Mellor, A.L. Indoleamine 2,3-dioxygenase and tumor-induced tolerance. *J Clin Invest* 117, 1147-1154 (2007).
22. Aihara, H. & Miyazaki, J. Gene transfer into muscle by electroporation in vivo. *Nat Biotechnol* 16, 867-870 (1998).
23. Ahlen, G., *et al.* In vivo electroporation enhances the immunogenicity of hepatitis C virus nonstructural 3/4A DNA by increased local DNA uptake, protein expression, inflammation, and infiltration of CD3+ T cells. *J Immunol* 179, 4741-4753 (2007).
24. Rosenberg, S.A., *et al.* Inability to immunize patients with metastatic melanoma using plasmid DNA encoding the gp100 melanoma-melanocyte antigen. *Hum Gene Ther* 14, 709-714 (2003).
25. Wolchok, J.D., *et al.* Safety and immunogenicity of tyrosinase DNA vaccines in patients with melanoma. *Mol Ther* 15, 2044-2050 (2007).
26. Low, L., *et al.* DNA vaccination with electroporation induces increased antibody responses in patients with prostate cancer. *Hum Gene Ther* 20, 1269-1278 (2009).
27. Timmerman, J.M., *et al.* Immunogenicity of a plasmid DNA vaccine encoding chimeric idiotype in patients with B-cell lymphoma. *Cancer Res* 62, 5845-5852 (2002).
28. Banchereau, J. & Steinman, R.M. Dendritic cells and the control of immunity. *Nature* 392, 245-252 (1998).
29. Tacken, P.J., de Vries, I.J., Torensma, R. & Figdor, C.G. Dendritic-cell immunotherapy: from ex vivo loading to in vivo targeting. *Nat Rev Immunol* 7, 790-802 (2007).
30. Higano, C.S., *et al.* Integrated data from 2 randomized, double-blind, placebo-controlled, phase 3 trials of active cellular immunotherapy with sipuleucel-T in advanced prostate cancer. *Cancer* 115, 3670-3679 (2009).
31. Fagraeus, A. The plasma cellular reaction and its relation to the formation of antibodies in vitro. *J Immunol* 58, 1-13 (1948).
32. Arnold, J.N., Wormald, M.R., Sim, R.B., Rudd, P.M. & Dwek, R.A. The impact of glycosylation on the biological function and structure of human immunoglobulins. *Annu Rev Immunol* 25, 21-50 (2007).
33. Kindt, T.J., Goldsby, R.A. & Osborne, B.A. *Kuby Immunology*, (W.H. Freeman and Company, New York, 2007).
34. Chothia, C., *et al.* Conformations of immunoglobulin hypervariable regions. *Nature* 342, 877-883 (1989).
35. Davis, M.M. & Bjorkman, P.J. T-cell antigen receptor genes and T-cell recognition. *Nature* 334, 395-402 (1988).
36. Xu, J.L. & Davis, M.M. Diversity in the CDR3 region of V(H) is sufficient for most antibody specificities. *Immunity* 13, 37-45 (2000).

37. Amzel, L.M. & Poljak, R.J. Three-dimensional structure of immunoglobulins. *Annu Rev Biochem* 48, 961-997 (1979).
38. Porter, R.R. The hydrolysis of rabbit γ -globulin and antibodies with crystalline papain. *Biochem J* 73, 119-126 (1959).
39. Duncan, A.R. & Winter, G. The binding site for C1q on IgG. *Nature* 332, 738-740 (1988).
40. Mimura, Y., *et al.* Role of oligosaccharide residues of IgG1-Fc in Fc gamma RIIb binding. *J Biol Chem* 276, 45539-45547 (2001).
41. Mimura, Y., *et al.* The influence of glycosylation on the thermal stability and effector function expression of human IgG1-Fc: properties of a series of truncated glycoforms. *Mol Immunol* 37, 697-706 (2000).
42. Okazaki, A., *et al.* Fucose depletion from human IgG1 oligosaccharide enhances binding enthalpy and association rate between IgG1 and Fc gamma RIIIa. *J Mol Biol* 336, 1239-1249 (2004).
43. Kohler, G. & Milstein, C. Continuous cultures of fused cells secreting antibody of predefined specificity. *Nature* 256, 495-497 (1975).
44. Fjermedal, G. *Magic Bullets*, (Macmillan, New York, 1984).
45. Emmons, C. & Hunsicker, L.G. Muromonab-CD3 (Orthoclone OKT3): the first monoclonal antibody approved for therapeutic use. *Iowa Med* 77, 78-82 (1987).
46. Gay, W.A., Jr., *et al.* OKT3 monoclonal antibody in cardiac transplantation. Experience with 102 patients. *Ann Surg* 208, 287-290 (1988).
47. Goldstein, G., *et al.* OKT3 monoclonal antibody plasma levels during therapy and the subsequent development of host antibodies to OKT3. *Transplantation* 42, 507-511 (1986).
48. Van Kroonenburgh, M.J. & Pauwels, E.K. Human immunological response to mouse monoclonal antibodies in the treatment or diagnosis of malignant diseases. *Nucl Med Commun* 9, 919-930 (1988).
49. Mirick, G.R., Bradt, B.M., Denardo, S.J. & Denardo, G.L. A review of human anti-globulin antibody (HAGA, HAMA, HACA, HAHA) responses to monoclonal antibodies. Not four letter words. *Q J Nucl Med Mol Imaging* 48, 251-257 (2004).
50. Boulianne, G.L., Hozumi, N. & Shulman, M.J. Production of functional chimaeric mouse/human antibody. *Nature* 312, 643-646 (1984).
51. Jones, P.T., Dear, P.H., Foote, J., Neuberger, M.S. & Winter, G. Replacing the complementarity-determining regions in a human antibody with those from a mouse. *Nature* 321, 522-525 (1986).
52. McCafferty, J., Griffiths, A.D., Winter, G. & Chiswell, D.J. Phage antibodies: filamentous phage displaying antibody variable domains. *Nature* 348, 552-554 (1990).
53. Lonberg, N., *et al.* Antigen-specific human antibodies from mice comprising four distinct genetic modifications. *Nature* 368, 856-859 (1994).
54. Lim, S.H., *et al.* Anti-CD20 monoclonal antibodies: historical and future perspectives. *Haematologica* 95, 135-143 (2010).

55. French, R.R., Chan, H.T., Tutt, A.L. & Glennie, M.J. CD40 antibody evokes a cytotoxic T-cell response that eradicates lymphoma and bypasses T-cell help. *Nat Med* 5, 548-553 (1999).
56. Advani, R., *et al.* Phase I study of the humanized anti-CD40 monoclonal antibody dacetuzumab in refractory or recurrent non-Hodgkin's lymphoma. *J Clin Oncol* 27, 4371-4377 (2009).
57. Fong, L. & Small, E.J. Anti-cytotoxic T-lymphocyte antigen-4 antibody: the first in an emerging class of immunomodulatory antibodies for cancer treatment. *J Clin Oncol* 26, 5275-5283 (2008).
58. Hodi, F.S., *et al.* Improved survival with ipilimumab in patients with metastatic melanoma. *N Engl J Med* 363, 711-723 (2010).
59. Pai, L.H., *et al.* Clinical evaluation of intraperitoneal *Pseudomonas* exotoxin immunoconjugate OVB3-PE in patients with ovarian cancer. *J Clin Oncol* 9, 2095-2103 (1991).
60. Larson, R.A., *et al.* Antibody-targeted chemotherapy of older patients with acute myeloid leukemia in first relapse using Mylotarg (gemtuzumab ozogamicin). *Leukemia* 16, 1627-1636 (2002).
61. DiJoseph, J.F., *et al.* Antibody-targeted chemotherapy with CMC-544: a CD22-targeted immunoconjugate of calicheamicin for the treatment of B-lymphoid malignancies. *Blood* 103, 1807-1814 (2004).
62. Younes, A., *et al.* Brentuximab vedotin (SGN-35) for relapsed CD30-positive lymphomas. *N Engl J Med* 363, 1812-1821.
63. Francisco, J.A., *et al.* cAC10-vcMMAE, an anti-CD30-monomethyl auristatin E conjugate with potent and selective antitumor activity. *Blood* 102, 1458-1465 (2003).
64. Chen, R., *et al.* Results of a Pivotal Phase 2 Study of Brentuximab Vedotin (SGN-35) in Patients with Relapsed or Refractory Hodgkin Lymphoma. *Blood* 116, 283 (2010).
65. Gordon, L.I., *et al.* Durable responses after ibritumomab tiuxetan radioimmunotherapy for CD20+ B-cell lymphoma: long-term follow-up of a phase 1/2 study. *Blood* 103, 4429-4431 (2004).
66. Fisher, R.I., *et al.* Tositumomab and iodine-131 tositumomab produces durable complete remissions in a subset of heavily pretreated patients with low-grade and transformed non-Hodgkin's lymphomas. *J Clin Oncol* 23, 7565-7573 (2005).
67. Gisselbrecht, C., Vose, J., Nademanee, A., Gianni, A.M. & Nagler, A. Radioimmunotherapy for stem cell transplantation in non-Hodgkin's lymphoma: in pursuit of a complete response. *Oncologist* 14 Suppl 2, 41-51 (2009).
68. Illidge, T.M., *et al.* Phase 1/2 study of fractionated (131)I-rituximab in low-grade B-cell lymphoma: the effect of prior rituximab dosing and tumor burden on subsequent radioimmunotherapy. *Blood* 113, 1412-1421 (2009).
69. Goldsmith, S.J. Radioimmunotherapy of lymphoma: Bexxar and Zevalin. *Semin Nucl Med* 40, 122-135 (2010).

70. Mack, M., Riethmuller, G. & Kufer, P. A small bispecific antibody construct expressed as a functional single-chain molecule with high tumor cell cytotoxicity. *Proc Natl Acad Sci U S A* 92, 7021-7025 (1995).
71. d'Argouges, S., et al. Combination of rituximab with blinatumomab (MT103/MEDI-538), a T cell-engaging CD19-/CD3-bispecific antibody, for highly efficient lysis of human B lymphoma cells. *Leuk Res* 33, 465-473 (2009).
72. Bargou, R., et al. Tumor regression in cancer patients by very low doses of a T cell-engaging antibody. *Science* 321, 974-977 (2008).
73. Topp, M.S., et al. Report of a Phase II Trial of Single-Agent BiTE Antibody Blinatumomab in Patients with Minimal Residual Disease (MRD) Positive B-Precursor Acute Lymphoblastic Leukemia (ALL). *Blood* 114, Abstract 840 (2009).
74. Leonard, J.P., et al. Durable complete responses from therapy with combined epratuzumab and rituximab: final results from an international multicenter, phase 2 study in recurrent, indolent, non-Hodgkin lymphoma. *Cancer* 113, 2714-2723 (2008).
75. Advani, A., et al. Safety, pharmacokinetics, and preliminary clinical activity of inotuzumab ozogamicin, a novel immunoconjugate for the treatment of B-cell non-Hodgkin's lymphoma: results of a phase I study. *J Clin Oncol* 28, 2085-2093 (2010).
76. Byrd, J.C., et al. Phase 1/2 study of lumiliximab combined with fludarabine, cyclophosphamide, and rituximab in patients with relapsed or refractory chronic lymphocytic leukemia. *Blood* 115, 489-495 (2010).
77. Furman, R.R., Forero-Torres, A., Shustov, A. & Drachman, J.G. A phase I study of dacetuzumab (SGN-40, a humanized anti-CD40 monoclonal antibody) in patients with chronic lymphocytic leukemia. *Leuk Lymphoma* 51, 228-235 (2010).
78. ClinicalTrials.gov. Study of HCD122 in Adults With Non-Hodgkin's or Hodgkin's Lymphoma Who Have Progressed After at Least Two Prior Therapies. (2009).
79. McEarchern, J.A., et al. Preclinical characterization of SGN-70, a humanized antibody directed against CD70. *Clin Cancer Res* 14, 7763-7772 (2008).
80. Leonard, J.P., et al. A phase I/II study of galiximab (an anti-CD80 monoclonal antibody) in combination with rituximab for relapsed or refractory, follicular lymphoma. *Ann Oncol* 18, 1216-1223 (2007).
81. Statistics., O.f.N. Cancer Registration Statistics England 2007. Vol. 2010 (Office for National Statistics, 2007).
82. Swerdlow SH, et al. *WHO Classification of Tumours of Haematopoietic and Lymphoid Tissues (IARC WHO Classification of Tumours)*, (WHO Press, Geneva, 2008).
83. Hardy, R.R., Kincade, P.W. & Dorshkind, K. The protean nature of cells in the B lymphocyte lineage. *Immunity* 26, 703-714 (2007).
84. Till, J.E. & Mc, C.E. A direct measurement of the radiation sensitivity of normal mouse bone marrow cells. *Radiat Res* 14, 213-222 (1961).

85. Spangrude, G.J., Heimfeld, S. & Weissman, I.L. Purification and characterization of mouse hematopoietic stem cells. *Science* 241, 58-62 (1988).
86. Kondo, M., Weissman, I.L. & Akashi, K. Identification of clonogenic common lymphoid progenitors in mouse bone marrow. *Cell* 91, 661-672 (1997).
87. Akashi, K., Traver, D., Miyamoto, T. & Weissman, I.L. A clonogenic common myeloid progenitor that gives rise to all myeloid lineages. *Nature* 404, 193-197 (2000).
88. Busslinger, M. Transcriptional control of early B cell development. *Annu Rev Immunol* 22, 55-79 (2004).
89. Sitnicka, E., *et al.* Complementary signaling through flt3 and interleukin-7 receptor alpha is indispensable for fetal and adult B cell genesis. *J Exp Med* 198, 1495-1506 (2003).
90. Giliani, S., *et al.* Interleukin-7 receptor alpha (IL-7Ralpha) deficiency: cellular and molecular bases. Analysis of clinical, immunological, and molecular features in 16 novel patients. *Immunol Rev* 203, 110-126 (2005).
91. LeBien, T.W. Fates of human B-cell precursors. *Blood* 96, 9-23 (2000).
92. Ghia, P., *et al.* Ordering of human bone marrow B lymphocyte precursors by single-cell polymerase chain reaction analyses of the rearrangement status of the immunoglobulin H and L chain gene loci. *J Exp Med* 184, 2217-2229 (1996).
93. Schatz, D.G., Oettinger, M.A. & Baltimore, D. The V(D)J recombination activating gene, RAG-1. *Cell* 59, 1035-1048 (1989).
94. Oettinger, M.A., Schatz, D.G., Gorka, C. & Baltimore, D. RAG-1 and RAG-2, adjacent genes that synergistically activate V(D)J recombination. *Science* 248, 1517-1523 (1990).
95. Dudley, D.D., Chaudhuri, J., Bassing, C.H. & Alt, F.W. Mechanism and control of V(D)J recombination versus class switch recombination: similarities and differences. *Adv Immunol* 86, 43-112 (2005).
96. Komori, T., Okada, A., Stewart, V. & Alt, F.W. Lack of N regions in antigen receptor variable region genes of TdT-deficient lymphocytes. *Science* 261, 1171-1175 (1993).
97. Minegishi, Y., *et al.* Mutations in the human lambda5/14.1 gene result in B cell deficiency and agammaglobulinemia. *J Exp Med* 187, 71-77 (1998).
98. Lam, K.P., Kuhn, R. & Rajewsky, K. In vivo ablation of surface immunoglobulin on mature B cells by inducible gene targeting results in rapid cell death. *Cell* 90, 1073-1083 (1997).
99. Campbell, K.S., Hager, E.J., Friedrich, R.J. & Cambier, J.C. IgM antigen receptor complex contains phosphoprotein products of B29 and mb-1 genes. *Proc Natl Acad Sci U S A* 88, 3982-3986 (1991).
100. Weiner, H.L., Moorhead, J.W., Yamaga, K. & Kubo, R.T. Anti-immunoglobulin stimulation of murine lymphocytes. II. Identification of cell surface target molecules and requirements for cross-linkage. *J Immunol* 117, 1527-1531 (1976).

101. Nossal, G.J. Immunologic tolerance: collaboration between antigen and lymphokines. *Science* 245, 147-153 (1989).
102. Gay, D., Saunders, T., Camper, S. & Weigert, M. Receptor editing: an approach by autoreactive B cells to escape tolerance. *J Exp Med* 177, 999-1008 (1993).
103. Hertz, M. & Nemazee, D. BCR ligation induces receptor editing in IgM+IgD- bone marrow B cells in vitro. *Immunity* 6, 429-436 (1997).
104. Buhl, A.M., Nemazee, D., Cambier, J.C., Rickert, R. & Hertz, M. B-cell antigen receptor competence regulates B-lymphocyte selection and survival. *Immunol Rev* 176, 141-153 (2000).
105. Kraus, M., Alimzhanov, M.B., Rajewsky, N. & Rajewsky, K. Survival of resting mature B lymphocytes depends on BCR signaling via the Igalphabeta heterodimer. *Cell* 117, 787-800 (2004).
106. Mackay, F., Figgett, W.A., Saulep, D., Lepage, M. & Hibbs, M.L. B-cell stage and context-dependent requirements for survival signals from BAFF and the B-cell receptor. *Immunol Rev* 237, 205-225 (2010).
107. Hardy, R.R. & Hayakawa, K. B cell development pathways. *Annu Rev Immunol* 19, 595-621 (2001).
108. Hayakawa, K., Hardy, R.R., Parks, D.R. & Herzenberg, L.A. The "Ly-1 B" cell subpopulation in normal immunodeficient, and autoimmune mice. *J Exp Med* 157, 202-218 (1983).
109. Griffin, D.O., Holodick, N.E. & Rothstein, T.L. Human B1 cells in umbilical cord and adult peripheral blood express the novel phenotype CD20+ CD27+ CD43+ CD70. *J Exp Med* 208, 67-80 (2011).
110. Oracki, S.A., Walker, J.A., Hibbs, M.L., Corcoran, L.M. & Tarlinton, D.M. Plasma cell development and survival. *Immunol Rev* 237, 140-159 (2010).
111. Carrasco, Y.R. & Batista, F.D. B-cell activation by membrane-bound antigens is facilitated by the interaction of VLA-4 with VCAM-1. *EMBO J* 25, 889-899 (2006).
112. Lane, P.J., Gray, D., Oldfield, S. & MacLennan, I.C. Differences in the recruitment of virgin B cells into antibody responses to thymus-dependent and thymus-independent type-2 antigens. *Eur J Immunol* 16, 1569-1575 (1986).
113. Weill, J.C., Weller, S. & Reynaud, C.A. Human marginal zone B cells. *Annu Rev Immunol* 27, 267-285 (2009).
114. Martin, F., Oliver, A.M. & Kearney, J.F. Marginal zone and B1 B cells unite in the early response against T-independent blood-borne particulate antigens. *Immunity* 14, 617-629 (2001).
115. Smith, K.G., Hewitson, T.D., Nossal, G.J. & Tarlinton, D.M. The phenotype and fate of the antibody-forming cells of the splenic foci. *Eur J Immunol* 26, 444-448 (1996).
116. Hsu, M.C., Toellner, K.M., Vinuesa, C.G. & MacLennan, I.C. B cell clones that sustain long-term plasmablast growth in T-independent extrafollicular antibody responses. *Proc Natl Acad Sci U S A* 103, 5905-5910 (2006).
117. Jacob, J., Kelsoe, G., Rajewsky, K. & Weiss, U. Intraclonal generation of antibody mutants in germinal centres. *Nature* 354, 389-392 (1991).

118. Vieira, P. & Rajewsky, K. Persistence of memory B cells in mice deprived of T cell help. *Int Immunol* 2, 487-494 (1990).
119. de Vinuesa, C.G., *et al.* Germinal centers without T cells. *J Exp Med* 191, 485-494 (2000).
120. Delker, R.K., Fugmann, S.D. & Papavasiliou, F.N. A coming-of-age story: activation-induced cytidine deaminase turns 10. *Nat Immunol* 10, 1147-1153 (2009).
121. Muramatsu, M., *et al.* Class switch recombination and hypermutation require activation-induced cytidine deaminase (AID), a potential RNA editing enzyme. *Cell* 102, 553-563 (2000).
122. Revy, P., *et al.* Activation-induced cytidine deaminase (AID) deficiency causes the autosomal recessive form of the Hyper-IgM syndrome (HIGM2). *Cell* 102, 565-575 (2000).
123. Petersen-Mahrt, S.K., Harris, R.S. & Neuberger, M.S. AID mutates E. coli suggesting a DNA deamination mechanism for antibody diversification. *Nature* 418, 99-103 (2002).
124. Kuppers, R. Mechanisms of B-cell lymphoma pathogenesis. *Nat Rev Cancer* 5, 251-262 (2005).
125. Pasqualucci, L., *et al.* BCL-6 mutations in normal germinal center B cells: evidence of somatic hypermutation acting outside Ig loci. *Proc Natl Acad Sci U S A* 95, 11816-11821 (1998).
126. Muschen, M., *et al.* Somatic mutation of the CD95 gene in human B cells as a side-effect of the germinal center reaction. *J Exp Med* 192, 1833-1840 (2000).
127. Vinuesa, C.G., Linterman, M.A., Goodnow, C.C. & Randall, K.L. T cells and follicular dendritic cells in germinal center B-cell formation and selection. *Immunol Rev* 237, 72-89 (2010).
128. Roozendaal, R. & Carroll, M.C. Complement receptors CD21 and CD35 in humoral immunity. *Immunol Rev* 219, 157-166 (2007).
129. Gaspal, F.M., *et al.* The generation of thymus-independent germinal centers depends on CD40 but not on CD154, the T cell-derived CD40-ligand. *Eur J Immunol* 36, 1665-1673 (2006).
130. Qin, D., *et al.* Fc gamma receptor IIB on follicular dendritic cells regulates the B cell recall response. *J Immunol* 164, 6268-6275 (2000).
131. Nurieva, R.I., *et al.* Bcl6 mediates the development of T follicular helper cells. *Science* 325, 1001-1005 (2009).
132. Johnston, R.J., *et al.* Bcl6 and Blimp-1 are reciprocal and antagonistic regulators of T follicular helper cell differentiation. *Science* 325, 1006-1010 (2009).
133. Crotty, S. Follicular Helper CD4 T Cells (TFH). *Annu Rev Immunol* 29, 621-663.
134. Kuo, T.C., *et al.* Repression of BCL-6 is required for the formation of human memory B cells in vitro. *J Exp Med* 204, 819-830 (2007).
135. Ehrhardt, G.R., *et al.* Discriminating gene expression profiles of memory B cell subpopulations. *J Exp Med* 205, 1807-1817 (2008).

136. Noelle, R.J., *et al.* A 39-kDa protein on activated helper T cells binds CD40 and transduces the signal for cognate activation of B cells. *Proc Natl Acad Sci U S A* 89, 6550-6554 (1992).
137. Han, S., *et al.* Cellular interaction in germinal centers. Roles of CD40 ligand and B7-2 in established germinal centers. *J Immunol* 155, 556-567 (1995).
138. Facchetti, F., Appiani, C., Salvi, L., Levy, J. & Notarangelo, L.D. Immunohistologic analysis of ineffective CD40-CD40 ligand interaction in lymphoid tissues from patients with X-linked immunodeficiency with hyper-IgM. Abortive germinal center cell reaction and severe depletion of follicular dendritic cells. *J Immunol* 154, 6624-6633 (1995).
139. Oprea, M. & Perelson, A.S. Somatic mutation leads to efficient affinity maturation when centrocytes recycle back to centroblasts. *J Immunol* 158, 5155-5162 (1997).
140. McAdam, A.J., *et al.* ICOS is critical for CD40-mediated antibody class switching. *Nature* 409, 102-105 (2001).
141. McAdam, A.J., *et al.* Mouse inducible costimulatory molecule (ICOS) expression is enhanced by CD28 costimulation and regulates differentiation of CD4+ T cells. *J Immunol* 165, 5035-5040 (2000).
142. Dong, C., *et al.* ICOS co-stimulatory receptor is essential for T-cell activation and function. *Nature* 409, 97-101 (2001).
143. Tafuri, A., *et al.* ICOS is essential for effective T-helper-cell responses. *Nature* 409, 105-109 (2001).
144. Kaminski, D.A., Lee, B.O., Eaton, S.M., Haynes, L. & Randall, T.D. CD28 and inducible costimulator (ICOS) signalling can sustain CD154 expression on activated T cells. *Immunology* 127, 373-385 (2009).
145. Neuberger, M.S., *et al.* Memory in the B-cell compartment: antibody affinity maturation. *Philos Trans R Soc Lond B Biol Sci* 355, 357-360 (2000).
146. Defrance, T., *et al.* Interleukin 10 and transforming growth factor beta cooperate to induce anti-CD40-activated naive human B cells to secrete immunoglobulin A. *J Exp Med* 175, 671-682 (1992).
147. Punnonen, J., *et al.* Interleukin 13 induces interleukin 4-independent IgG4 and IgE synthesis and CD23 expression by human B cells. *Proc Natl Acad Sci U S A* 90, 3730-3734 (1993).
148. Schitteck, B. & Rajewsky, K. Maintenance of B-cell memory by long-lived cells generated from proliferating precursors. *Nature* 346, 749-751 (1990).
149. Shaffer, A.L., *et al.* Blimp-1 orchestrates plasma cell differentiation by extinguishing the mature B cell gene expression program. *Immunity* 17, 51-62 (2002).
150. Ye, B.H., *et al.* The BCL-6 proto-oncogene controls germinal-centre formation and Th2-type inflammation. *Nat Genet* 16, 161-170 (1997).
151. Jackson, N., *et al.* An analysis of myeloma plasma cell phenotype using antibodies defined at the IIIrd International Workshop on Human Leucocyte Differentiation Antigens. *Clin Exp Immunol* 72, 351-356 (1988).

152. Pascual, V., *et al.* Analysis of somatic mutation in five B cell subsets of human tonsil. *J Exp Med* 180, 329-339 (1994).
153. Maruyama, M., Lam, K.P. & Rajewsky, K. Memory B-cell persistence is independent of persisting immunizing antigen. *Nature* 407, 636-642 (2000).
154. McHeyzer-Williams, M.G. & Ahmed, R. B cell memory and the long-lived plasma cell. *Curr Opin Immunol* 11, 172-179 (1999).
155. A clinical evaluation of the International Lymphoma Study Group classification of non-Hodgkin's lymphoma. The Non-Hodgkin's Lymphoma Classification Project. *Blood* 89, 3909-3918 (1997).
156. Miller, T.P., *et al.* Prognostic significance of the Ki-67-associated proliferative antigen in aggressive non-Hodgkin's lymphomas: a prospective Southwest Oncology Group trial. *Blood* 83, 1460-1466 (1994).
157. Alizadeh, A.A., *et al.* Distinct types of diffuse large B-cell lymphoma identified by gene expression profiling. *Nature* 403, 503-511 (2000).
158. Lenz, G., *et al.* Stromal gene signatures in large-B-cell lymphomas. *N Engl J Med* 359, 2313-2323 (2008).
159. Shipp, M.A., *et al.* Diffuse large B-cell lymphoma outcome prediction by gene-expression profiling and supervised machine learning. *Nat Med* 8, 68-74 (2002).
160. Ott, G., *et al.* Immunoblastic morphology but not the immunohistochemical GCB/nonGCB classifier predicts outcome in diffuse large B-cell lymphoma in the RICOVER-60 trial of the DSHNHL. *Blood* 116, 4916-4925 (2010).
161. de Jong, D., *et al.* Immunohistochemical prognostic markers in diffuse large B-cell lymphoma: validation of tissue microarray as a prerequisite for broad clinical applications--a study from the Lunenburg Lymphoma Biomarker Consortium. *J Clin Oncol* 25, 805-812 (2007).
162. Tsujimoto, Y., Cossman, J., Jaffe, E. & Croce, C.M. Involvement of the bcl-2 gene in human follicular lymphoma. *Science* 228, 1440-1443 (1985).
163. Limpens, J., *et al.* Lymphoma-associated translocation t(14;18) in blood B cells of normal individuals. *Blood* 85, 2528-2536 (1995).
164. Strasser, A., Harris, A.W., Bath, M.L. & Cory, S. Novel primitive lymphoid tumours induced in transgenic mice by cooperation between myc and bcl-2. *Nature* 348, 331-333 (1990).
165. Gallagher, C.J., *et al.* Follicular lymphoma: prognostic factors for response and survival. *J Clin Oncol* 4, 1470-1480 (1986).
166. Bosch, F., *et al.* Mantle cell lymphoma: presenting features, response to therapy, and prognostic factors. *Cancer* 82, 567-575 (1998).
167. Martin, P., *et al.* Outcome of deferred initial therapy in mantle-cell lymphoma. *J Clin Oncol* 27, 1209-1213 (2009).
168. Vandenberghe, E., *et al.* Translocation (11;14): a cytogenetic anomaly associated with B-cell lymphomas of non-follicle centre cell lineage. *J Pathol* 163, 13-18 (1991).
169. Jares, P., *et al.* Expression of retinoblastoma gene product (pRb) in mantle cell lymphomas. Correlation with cyclin D1 (PRAD1/CCND1)

- mRNA levels and proliferative activity. *Am J Pathol* 148, 1591-1600 (1996).
170. Camacho, E., *et al.* ATM gene inactivation in mantle cell lymphoma mainly occurs by truncating mutations and missense mutations involving the phosphatidylinositol-3 kinase domain and is associated with increasing numbers of chromosomal imbalances. *Blood* 99, 238-244 (2002).
 171. Inghirami, G., *et al.* Differential expression of LFA-1 molecules in non-Hodgkin's lymphoma and lymphoid leukemia. *Blood* 72, 1431-1434 (1988).
 172. Angelopoulou, M.K., Kontopidou, F.N. & Pangalis, G.A. Adhesion molecules in B-chronic lymphoproliferative disorders. *Semin Hematol* 36, 178-197 (1999).
 173. Tsimberidou, A.M., *et al.* Assessment of chronic lymphocytic leukemia and small lymphocytic lymphoma by absolute lymphocyte counts in 2,126 patients: 20 years of experience at the University of Texas M.D. Anderson Cancer Center. *J Clin Oncol* 25, 4648-4656 (2007).
 174. Matutes, E., *et al.* The immunological profile of B-cell disorders and proposal of a scoring system for the diagnosis of CLL. *Leukemia* 8, 1640-1645 (1994).
 175. Gribben, J.G. How I treat CLL up front. *Blood* 115, 187-197.
 176. Rai, K.R., *et al.* Clinical staging of chronic lymphocytic leukemia. *Blood* 46, 219-234 (1975).
 177. Binet, J.L., *et al.* A new prognostic classification of chronic lymphocytic leukemia derived from a multivariate survival analysis. *Cancer* 48, 198-206 (1981).
 178. Butler, T. & Gribben, J.G. Biologic and clinical significance of molecular profiling in Chronic Lymphocytic Leukemia. *Blood Rev* 24, 135-141 (2010).
 179. Molica, S. & Alberti, A. Prognostic value of the lymphocyte doubling time in chronic lymphocytic leukemia. *Cancer* 60, 2712-2716 (1987).
 180. Simonsson, B., Wibell, L. & Nilsson, K. Beta 2-microglobulin in chronic lymphocytic leukaemia. *Scand J Haematol* 24, 174-180 (1980).
 181. Sarfati, M., *et al.* Prognostic importance of serum soluble CD23 level in chronic lymphocytic leukemia. *Blood* 88, 4259-4264 (1996).
 182. Stilgenbauer, S., Bullinger, L., Lichter, P. & Dohner, H. Genetics of chronic lymphocytic leukemia: genomic aberrations and V(H) gene mutation status in pathogenesis and clinical course. *Leukemia* 16, 993-1007 (2002).
 183. Calin, G.A., *et al.* Frequent deletions and down-regulation of micro-RNA genes miR15 and miR16 at 13q14 in chronic lymphocytic leukemia. *Proc Natl Acad Sci U S A* 99, 15524-15529 (2002).
 184. Cimmino, A., *et al.* miR-15 and miR-16 induce apoptosis by targeting BCL2. *Proc Natl Acad Sci U S A* 102, 13944-13949 (2005).
 185. Fulci, V., *et al.* Quantitative technologies establish a novel microRNA profile of chronic lymphocytic leukemia. *Blood* 109, 4944-4951 (2007).

186. Dohner, H., *et al.* Genomic aberrations and survival in chronic lymphocytic leukemia. *N Engl J Med* 343, 1910-1916 (2000).
187. Porpaczy, E., *et al.* Gene expression signature of chronic lymphocytic leukaemia with Trisomy 12. *Eur J Clin Invest* 39, 568-575 (2009).
188. Damle, R.N., *et al.* Ig V gene mutation status and CD38 expression as novel prognostic indicators in chronic lymphocytic leukemia. *Blood* 94, 1840-1847 (1999).
189. Hamblin, T.J., Davis, Z., Gardiner, A., Oscier, D.G. & Stevenson, F.K. Unmutated Ig V(H) genes are associated with a more aggressive form of chronic lymphocytic leukemia. *Blood* 94, 1848-1854 (1999).
190. Kipps, T.J., *et al.* Developmentally restricted immunoglobulin heavy chain variable region gene expressed at high frequency in chronic lymphocytic leukemia. *Proc Natl Acad Sci U S A* 86, 5913-5917 (1989).
191. Deane, M. & Norton, J.D. Preferential rearrangement of developmentally regulated immunoglobulin VH1 genes in human B-lineage leukaemias. *Leukemia* 5, 646-650 (1991).
192. Schroeder, H.W., Jr. & Dighiero, G. The pathogenesis of chronic lymphocytic leukemia: analysis of the antibody repertoire. *Immunol Today* 15, 288-294 (1994).
193. Matsuda, F., *et al.* Structure and physical map of 64 variable segments in the 3'0.8-megabase region of the human immunoglobulin heavy-chain locus. *Nat Genet* 3, 88-94 (1993).
194. Wiestner, A., *et al.* ZAP-70 expression identifies a chronic lymphocytic leukemia subtype with unmutated immunoglobulin genes, inferior clinical outcome, and distinct gene expression profile. *Blood* 101, 4944-4951 (2003).
195. Crespo, M., *et al.* ZAP-70 expression as a surrogate for immunoglobulin-variable-region mutations in chronic lymphocytic leukemia. *N Engl J Med* 348, 1764-1775 (2003).
196. Orchard, J.A., *et al.* ZAP-70 expression and prognosis in chronic lymphocytic leukaemia. *Lancet* 363, 105-111 (2004).
197. Deaglio, S., Vaisitti, T., Aydin, S., Ferrero, E. & Malavasi, F. In-tandem insight from basic science combined with clinical research: CD38 as both marker and key component of the pathogenetic network underlying chronic lymphocytic leukemia. *Blood* 108, 1135-1144 (2006).
198. Hamblin, T.J., *et al.* Immunoglobulin V genes and CD38 expression in CLL. *Blood* 95, 2455-2457 (2000).
199. Thunberg, U., *et al.* CD38 expression is a poor predictor for VH gene mutational status and prognosis in chronic lymphocytic leukemia. *Blood* 97, 1892-1894 (2001).
200. Krober, A., *et al.* V(H) mutation status, CD38 expression level, genomic aberrations, and survival in chronic lymphocytic leukemia. *Blood* 100, 1410-1416 (2002).
201. Hamblin, T.J., *et al.* CD38 expression and immunoglobulin variable region mutations are independent prognostic variables in chronic lymphocytic leukemia, but CD38 expression may vary during the course of the disease. *Blood* 99, 1023-1029 (2002).

202. Juliusson, G., *et al.* Prognostic subgroups in B-cell chronic lymphocytic leukemia defined by specific chromosomal abnormalities. *N Engl J Med* 323, 720-724 (1990).
203. Hollstein, M., Sidransky, D., Vogelstein, B. & Harris, C.C. p53 mutations in human cancers. *Science* 253, 49-53 (1991).
204. Gaidano, G., *et al.* p53 mutations in human lymphoid malignancies: association with Burkitt lymphoma and chronic lymphocytic leukemia. *Proc Natl Acad Sci U S A* 88, 5413-5417 (1991).
205. Fenaux, P., *et al.* Mutations of the p53 gene in B-cell lymphoblastic acute leukemia: a report on 60 cases. *Leukemia* 6, 42-46 (1992).
206. Sander, C.A., *et al.* p53 mutation is associated with progression in follicular lymphomas. *Blood* 82, 1994-2004 (1993).
207. Malcikova, J., *et al.* Monoallelic and biallelic inactivation of TP53 gene in chronic lymphocytic leukemia: selection, impact on survival, and response to DNA damage. *Blood* 114, 5307-5314 (2009).
208. Zenz, T., *et al.* Monoallelic TP53 inactivation is associated with poor prognosis in chronic lymphocytic leukemia: results from a detailed genetic characterization with long-term follow-up. *Blood* 112, 3322-3329 (2008).
209. Levine, A.J. p53, the cellular gatekeeper for growth and division. *Cell* 88, 323-331 (1997).
210. Bates, S., *et al.* p14ARF links the tumour suppressors RB and p53. *Nature* 395, 124-125 (1998).
211. el-Deiry, W.S., *et al.* WAF1, a potential mediator of p53 tumor suppression. *Cell* 75, 817-825 (1993).
212. Miyashita, T., Harigai, M., Hanada, M. & Reed, J.C. Identification of a p53-dependent negative response element in the bcl-2 gene. *Cancer Res* 54, 3131-3135 (1994).
213. Miyashita, T. & Reed, J.C. Tumor suppressor p53 is a direct transcriptional activator of the human bax gene. *Cell* 80, 293-299 (1995).
214. Wattel, E., *et al.* p53 mutations are associated with resistance to chemotherapy and short survival in hematologic malignancies. *Blood* 84, 3148-3157 (1994).
215. Dohner, H., *et al.* p53 gene deletion predicts for poor survival and non-response to therapy with purine analogs in chronic B-cell leukemias. *Blood* 85, 1580-1589 (1995).
216. Boyd, K. & Dearden, C.E. Alemtuzumab in the treatment of chronic lymphocytic lymphoma. *Expert Rev Anticancer Ther* 8, 525-533 (2008).
217. Zenz, T., *et al.* Detailed analysis of p53 pathway defects in fludarabine-refractory chronic lymphocytic leukemia (CLL): dissecting the contribution of 17p deletion, TP53 mutation, p53-p21 dysfunction, and miR34a in a prospective clinical trial. *Blood* 114, 2589-2597 (2009).
218. Dohner, H., *et al.* 11q deletions identify a new subset of B-cell chronic lymphocytic leukemia characterized by extensive nodal involvement and inferior prognosis. *Blood* 89, 2516-2522 (1997).

219. Austen, B., *et al.* Mutations in the ATM gene lead to impaired overall and treatment-free survival that is independent of IGVH mutation status in patients with B-CLL. *Blood* 106, 3175-3182 (2005).
220. Stilgenbauer, S., *et al.* Genomic Aberrations, VH Mutation Status and Outcome after Fludarabine and Cyclophosphamide (FC) or FC Plus Rituximab (FCR) in the CLL8 Trial. *Blood* 112(2008).
221. Stilgenbauer, S., *et al.* Molecular characterization of 11q deletions points to a pathogenic role of the ATM gene in mantle cell lymphoma. *Blood* 94, 3262-3264 (1999).
222. Fang, N.Y., *et al.* Oligonucleotide microarrays demonstrate the highest frequency of ATM mutations in the mantle cell subtype of lymphoma. *Proc Natl Acad Sci U S A* 100, 5372-5377 (2003).
223. Stilgenbauer, S., *et al.* Molecular cytogenetic delineation of a novel critical genomic region in chromosome bands 11q22.3-923.1 in lymphoproliferative disorders. *Proc Natl Acad Sci U S A* 93, 11837-11841 (1996).
224. Tsukita, S. & Yonemura, S. Cortical actin organization: lessons from ERM (ezrin/radixin/moesin) proteins. *J Biol Chem* 274, 34507-34510 (1999).
225. Coghlan, V.M. & Vickery, L.E. Site-specific mutations in human ferredoxin that affect binding to ferredoxin reductase and cytochrome P450_{scc}. *J Biol Chem* 266, 18606-18612 (1991).
226. Xu, Y., *et al.* Targeted disruption of ATM leads to growth retardation, chromosomal fragmentation during meiosis, immune defects, and thymic lymphoma. *Genes Dev* 10, 2411-2422 (1996).
227. Vorechovsky, I., *et al.* Clustering of missense mutations in the ataxia-telangiectasia gene in a sporadic T-cell leukaemia. *Nat Genet* 17, 96-99 (1997).
228. Taylor, A.M., Metcalfe, J.A., Thick, J. & Mak, Y.F. Leukemia and lymphoma in ataxia telangiectasia. *Blood* 87, 423-438 (1996).
229. Savitsky, K., *et al.* A single ataxia telangiectasia gene with a product similar to PI-3 kinase. *Science* 268, 1749-1753 (1995).
230. Savitsky, K., *et al.* The complete sequence of the coding region of the ATM gene reveals similarity to cell cycle regulators in different species. *Hum Mol Genet* 4, 2025-2032 (1995).
231. Zakian, V.A. ATM-related genes: what do they tell us about functions of the human gene? *Cell* 82, 685-687 (1995).
232. Banin, S., *et al.* Enhanced phosphorylation of p53 by ATM in response to DNA damage. *Science* 281, 1674-1677 (1998).
233. Canman, C.E., *et al.* Activation of the ATM kinase by ionizing radiation and phosphorylation of p53. *Science* 281, 1677-1679 (1998).
234. Pettitt, A.R., *et al.* p53 dysfunction in B-cell chronic lymphocytic leukemia: inactivation of ATM as an alternative to TP53 mutation. *Blood* 98, 814-822 (2001).
235. Sembries, S., Pahl, H., Stilgenbauer, S., Dohner, H. & Schriever, F. Reduced expression of adhesion molecules and cell signaling receptors by chronic lymphocytic leukemia cells with 11q deletion. *Blood* 93, 624-631 (1999).

236. Tam, C.S., *et al.* Chronic lymphocytic leukaemia CD20 expression is dependent on the genetic subtype: a study of quantitative flow cytometry and fluorescent in-situ hybridization in 510 patients. *Br J Haematol* 141, 36-40 (2008).
237. Tedder, T.F., *et al.* The gene that encodes the human CD20 (B1) differentiation antigen is located on chromosome 11 near the t(11;14)(q13;q32) translocation site. *J Immunol* 142, 2555-2559 (1989).
238. Tsimberidou, A.M., *et al.* Chemoimmunotherapy may overcome the adverse prognostic significance of 11q deletion in previously untreated patients with chronic lymphocytic leukemia. *Cancer* 115, 373-380 (2009).
239. Maloney, D.G., *et al.* Phase I clinical trial using escalating single-dose infusion of chimeric anti-CD20 monoclonal antibody (IDEC-C2B8) in patients with recurrent B-cell lymphoma. *Blood* 84, 2457-2466 (1994).
240. Czuczman, M.S., Weaver, R., Alkuzweny, B., Berlfein, J. & Grillo-Lopez, A.J. Prolonged clinical and molecular remission in patients with low-grade or follicular non-Hodgkin's lymphoma treated with rituximab plus CHOP chemotherapy: 9-year follow-up. *J Clin Oncol* 22, 4711-4716 (2004).
241. Marcus, R., *et al.* CVP chemotherapy plus rituximab compared with CVP as first-line treatment for advanced follicular lymphoma. *Blood* 105, 1417-1423 (2005).
242. Hiddemann, W., *et al.* Frontline therapy with rituximab added to the combination of cyclophosphamide, doxorubicin, vincristine, and prednisone (CHOP) significantly improves the outcome for patients with advanced-stage follicular lymphoma compared with therapy with CHOP alone: results of a prospective randomized study of the German Low-Grade Lymphoma Study Group. *Blood* 106, 3725-3732 (2005).
243. Marcus, R., *et al.* Phase III study of R-CVP compared with cyclophosphamide, vincristine, and prednisone alone in patients with previously untreated advanced follicular lymphoma. *J Clin Oncol* 26, 4579-4586 (2008).
244. Feugier, P., *et al.* Long-term results of the R-CHOP study in the treatment of elderly patients with diffuse large B-cell lymphoma: a study by the Groupe d'Etude des Lymphomes de l'Adulte. *J Clin Oncol* 23, 4117-4126 (2005).
245. Habermann, T.M., *et al.* Rituximab-CHOP versus CHOP alone or with maintenance rituximab in older patients with diffuse large B-cell lymphoma. *J Clin Oncol* 24, 3121-3127 (2006).
246. Pfreundschuh, M., *et al.* Six versus eight cycles of bi-weekly CHOP-14 with or without rituximab in elderly patients with aggressive CD20+ B-cell lymphomas: a randomised controlled trial (RICOVER-60). *Lancet Oncol* 9, 105-116 (2008).
247. Coiffier, B., *et al.* Long-term outcome of patients in the LNH-98.5 trial, the first randomized study comparing rituximab-CHOP to standard CHOP chemotherapy in DLBCL patients: a study by the Groupe d'Etudes des Lymphomes de l'Adulte. *Blood* 116, 2040-2045 (2010).

248. Foran, J.M., *et al.* European phase II study of rituximab (chimeric anti-CD20 monoclonal antibody) for patients with newly diagnosed mantle-cell lymphoma and previously treated mantle-cell lymphoma, immunocytoma, and small B-cell lymphocytic lymphoma. *J Clin Oncol* 18, 317-324 (2000).
249. Hainsworth, J.D., *et al.* Single-agent rituximab as first-line and maintenance treatment for patients with chronic lymphocytic leukemia or small lymphocytic lymphoma: a phase II trial of the Minnie Pearl Cancer Research Network. *J Clin Oncol* 21, 1746-1751 (2003).
250. Ghilmini, M., *et al.* Effect of single-agent rituximab given at the standard schedule or as prolonged treatment in patients with mantle cell lymphoma: a study of the Swiss Group for Clinical Cancer Research (SAKK). *J Clin Oncol* 23, 705-711 (2005).
251. Lenz, G., *et al.* Immunochemotherapy with rituximab and cyclophosphamide, doxorubicin, vincristine, and prednisone significantly improves response and time to treatment failure, but not long-term outcome in patients with previously untreated mantle cell lymphoma: results of a prospective randomized trial of the German Low Grade Lymphoma Study Group (GLSG). *J Clin Oncol* 23, 1984-1992 (2005).
252. Lamanna, N., *et al.* Sequential therapy with fludarabine, high-dose cyclophosphamide, and rituximab in previously untreated patients with chronic lymphocytic leukemia produces high-quality responses: molecular remissions predict for durable complete responses. *J Clin Oncol* 27, 491-497 (2009).
253. Robak, T., *et al.* Rituximab plus fludarabine and cyclophosphamide prolongs progression-free survival compared with fludarabine and cyclophosphamide alone in previously treated chronic lymphocytic leukemia. *J Clin Oncol* 28, 1756-1765 (2010).
254. Hallek, M., *et al.* Addition of rituximab to fludarabine and cyclophosphamide in patients with chronic lymphocytic leukaemia: a randomised, open-label, phase 3 trial. *Lancet* 376, 1164-1174 (2010).
255. Seker, M., *et al.* Eight-cycle rituximab therapy resulted in complete remission in primary cutaneous marginal zone lymphoma. *Leuk Res* 34, 160-163 (2010).
256. Levy, M., *et al.* Treatment of t(11;18)-positive gastric mucosa-associated lymphoid tissue lymphoma with rituximab and chlorambucil: clinical, histological, and molecular follow-up. *Leuk Lymphoma* 51, 284-290 (2010).
257. Ahn, H.K., *et al.* Improved treatment outcome of primary mediastinal large B-cell lymphoma after introduction of rituximab in Korean patients. *Int J Hematol* 91, 456-463 (2010).
258. Zecca, M., *et al.* Rituximab for the treatment of refractory autoimmune hemolytic anemia in children. *Blood* 101, 3857-3861 (2003).
259. Lebrun, C., Bourg, V., Tieulie, N. & Thomas, P. Successful treatment of refractory generalized myasthenia gravis with rituximab. *Eur J Neurol* 16, 246-250 (2009).

260. Seo, P., Specks, U. & Keogh, K.A. Efficacy of rituximab in limited Wegener's granulomatosis with refractory granulomatous manifestations. *J Rheumatol* 35, 2017-2023 (2008).
261. Stashenko, P., Nadler, L.M., Hardy, R. & Schlossman, S.F. Characterization of a human B lymphocyte-specific antigen. *J Immunol* 125, 1678-1685 (1980).
262. Oettgen, H.C., Bayard, P.J., Van Ewijk, W., Nadler, L.M. & Terhorst, C.P. Further biochemical studies of the human B-cell differentiation antigens B1 and B2. *Hybridoma* 2, 17-28 (1983).
263. Ledbetter, J.A. & Clark, E.A. Surface phenotype and function of tonsillar germinal center and mantle zone B cell subsets. *Hum Immunol* 15, 30-43 (1986).
264. Nadler, L.M., *et al.* B cell origin of non-T cell acute lymphoblastic leukemia. A model for discrete stages of neoplastic and normal pre-B cell differentiation. *J Clin Invest* 74, 332-340 (1984).
265. Clark, E.A. & Yokochi, F. Human B cell and B cell blast-associated surface molecules defined by monoclonal antibodies. in *Leucocyte Typing* (eds. A. Bernard, Boumsell, A.L., Dausset, J., Milstein, C. & Schlossman, S.F.) 339 (Springer Verlag, Berlin, 1984).
266. Einfeld, D.A., Brown, J.P., Valentine, M.A., Clark, E.A. & Ledbetter, J.A. Molecular cloning of the human B cell CD20 receptor predicts a hydrophobic protein with multiple transmembrane domains. *EMBO J* 7, 711-717 (1988).
267. Tedder, T.F., *et al.* Cloning of a complementary DNA encoding a new mouse B lymphocyte differentiation antigen, homologous to the human B1 (CD20) antigen, and localization of the gene to chromosome 19. *J Immunol* 141, 4388-4394 (1988).
268. Polyak, M.J. & Deans, J.P. Alanine-170 and proline-172 are critical determinants for extracellular CD20 epitopes; heterogeneity in the fine specificity of CD20 monoclonal antibodies is defined by additional requirements imposed by both amino acid sequence and quaternary structure. *Blood* 99, 3256-3262 (2002).
269. Tedder, T.F. & Schlossman, S.F. Phosphorylation of the B1 (CD20) molecule by normal and malignant human B lymphocytes. *J Biol Chem* 263, 10009-10015 (1988).
270. Bubien, J.K., Zhou, L.J., Bell, P.D., Frizzell, R.A. & Tedder, T.F. Transfection of the CD20 cell surface molecule into ectopic cell types generates a Ca²⁺ conductance found constitutively in B lymphocytes. *J Cell Biol* 121, 1121-1132 (1993).
271. Szollosi, J., Horejsi, V., Bene, L., Angelisova, P. & Damjanovich, S. Supramolecular complexes of MHC class I, MHC class II, CD20, and tetraspan molecules (CD53, CD81, and CD82) at the surface of a B cell line JY. *J Immunol* 157, 2939-2946 (1996).
272. Leveille, C., R, A.L.-D. & Mourad, W. CD20 is physically and functionally coupled to MHC class II and CD40 on human B cell lines. *Eur J Immunol* 29, 65-74 (1999).

273. Petrie, R.J. & Deans, J.P. Colocalization of the B cell receptor and CD20 followed by activation-dependent dissociation in distinct lipid rafts. *J Immunol* 169, 2886-2891 (2002).
274. Polyak, M.J., Li, H., Shariat, N. & Deans, J.P. CD20 homo-oligomers physically associate with the B cell antigen receptor. Dissociation upon receptor engagement and recruitment of phosphoproteins and calmodulin-binding proteins. *J Biol Chem* 283, 18545-18552 (2008).
275. Walshe, C.A., *et al.* Induction of cytosolic calcium flux by CD20 is dependent upon B Cell antigen receptor signaling. *J Biol Chem* 283, 16971-16984 (2008).
276. Uchida, J., *et al.* Mouse CD20 expression and function. *Int Immunol* 16, 119-129 (2004).
277. Lankester, A.C., *et al.* Alteration of B-cell antigen receptor signaling by CD19 co-ligation. A study with bispecific antibodies. *J Biol Chem* 271, 22326-22330 (1996).
278. Mathas, S., Rickers, A., Bommert, K., Dorken, B. & Mapara, M.Y. Anti-CD20- and B-cell receptor-mediated apoptosis: evidence for shared intracellular signaling pathways. *Cancer Res* 60, 7170-7176 (2000).
279. Franke, A., Niederfellner, G.J., Klein, C. & Burtscher, H. Antibodies against CD20 or B-cell receptor induce similar transcription patterns in human lymphoma cell lines. *PLoS ONE* 6, e16596 (2010).
280. Irish, J.M., *et al.* B-cell signaling networks reveal a negative prognostic human lymphoma cell subset that emerges during tumor progression. *Proc Natl Acad Sci U S A* 107, 12747-12754 (2010).
281. O'Keefe, T.L., Williams, G.T., Davies, S.L. & Neuberger, M.S. Mice carrying a CD20 gene disruption. *Immunogenetics* 48, 125-132 (1998).
282. Kuijpers, T.W., *et al.* CD20 deficiency in humans results in impaired T cell-independent antibody responses. *J Clin Invest* 120, 214-222 (2010).
283. Chan, H.T., *et al.* CD20-induced lymphoma cell death is independent of both caspases and its redistribution into triton X-100 insoluble membrane rafts. *Cancer Res* 63, 5480-5489 (2003).
284. Cragg, M.S., *et al.* Complement-mediated lysis by anti-CD20 mAb correlates with segregation into lipid rafts. *Blood* 101, 1045-1052 (2003).
285. Cragg, M.S. & Glennie, M.J. Antibody specificity controls in vivo effector mechanisms of anti-CD20 reagents. *Blood* 103, 2738-2743 (2004).
286. Golay, J.T., Clark, E.A. & Beverley, P.C. The CD20 (Bp35) antigen is involved in activation of B cells from the G0 to the G1 phase of the cell cycle. *J Immunol* 135, 3795-3801 (1985).
287. Smeland, E., *et al.* The specific induction of myc protooncogene expression in normal human B cells is not a sufficient event for acquisition of competence to proliferate. *Proc Natl Acad Sci U S A* 82, 6255-6259 (1985).
288. Clark, E.A. & Shu, G. Activation of human B cell proliferation through surface Bp35 (CD20) polypeptides or immunoglobulin receptors. *J Immunol* 138, 720-725 (1987).

289. Bourget, I., Breitmayer, J.P., Grenier-Brossette, N. & Cousin, J.L. CD20 monoclonal antibodies down-regulate IgM at the surface of B cells. *Eur J Immunol* 23, 768-771 (1993).
290. Bourget, I., *et al.* CD20 monoclonal antibodies stimulate extracellular cleavage of the low affinity receptor for IgE (Fc epsilon RII/CD23) in Epstein-Barr-transformed B cells. *J Biol Chem* 269, 6927-6930 (1994).
291. Lingwood, D. & Simons, K. Lipid rafts as a membrane-organizing principle. *Science* 327, 46-50 (2010).
292. Ivanov, A., *et al.* Monoclonal antibodies directed to CD20 and HLA-DR can elicit homotypic adhesion followed by lysosome-mediated cell death in human lymphoma and leukemia cells. *J Clin Invest* 119, 2143-2159 (2009).
293. Niederfellner, G., *et al.* Epitope characterization and crystal structure of GA101 provide insights into the molecular basis for type I/II distinction of CD20 antibodies. *Blood* 118, 358-367 (2011).
294. Beers, S.A., *et al.* Type II (tositumomab) anti-CD20 monoclonal antibody out performs type I (rituximab-like) reagents in B-cell depletion regardless of complement activation. *Blood* 112, 4170-4177 (2008).
295. Munn, D.H. & Cheung, N.K. Phagocytosis of tumor cells by human monocytes cultured in recombinant macrophage colony-stimulating factor. *J Exp Med* 172, 231-237 (1990).
296. Lefebvre, M.L., Krause, S.W., Salcedo, M. & Nardin, A. Ex vivo-activated human macrophages kill chronic lymphocytic leukemia cells in the presence of rituximab: mechanism of antibody-dependent cellular cytotoxicity and impact of human serum. *J Immunother* 29, 388-397 (2006).
297. Clynes, R.A., Towers, T.L., Presta, L.G. & Ravetch, J.V. Inhibitory Fc receptors modulate in vivo cytotoxicity against tumor targets. *Nat Med* 6, 443-446 (2000).
298. Nimmerjahn, F. & Ravetch, J.V. Fc gamma receptors: old friends and new family members. *Immunity* 24, 19-28 (2006).
299. Ravetch, J.V. & Bolland, S. IgG Fc receptors. *Annu Rev Immunol* 19, 275-290 (2001).
300. Brooks, D.G., Qiu, W.Q., Luster, A.D. & Ravetch, J.V. Structure and expression of human IgG FcRII(CD32). Functional heterogeneity is encoded by the alternatively spliced products of multiple genes. *J Exp Med* 170, 1369-1385 (1989).
301. Cassel, D.L., *et al.* Differential expression of Fc gamma RIIA, Fc gamma RIIB and Fc gamma RIIC in hematopoietic cells: analysis of transcripts. *Mol Immunol* 30, 451-460 (1993).
302. Van Den Herik-Oudijk, I.E., Westerdaal, N.A., Henriquez, N.V., Capel, P.J. & Van De Winkel, J.G. Functional analysis of human Fc gamma RII (CD32) isoforms expressed in B lymphocytes. *J Immunol* 152, 574-585 (1994).
303. Nimmerjahn, F., Bruhns, P., Horiuchi, K. & Ravetch, J.V. Fc gamma RIV: a novel FcR with distinct IgG subclass specificity. *Immunity* 23, 41-51 (2005).

304. Bruhns, P., *et al.* Specificity and affinity of human Fc γ receptors and their polymorphic variants for human IgG subclasses. *Blood* 113, 3716-3725 (2009).
305. Warmerdam, P.A., van de Winkel, J.G., Gosselin, E.J. & Capel, P.J. Molecular basis for a polymorphism of human Fc γ receptor II (CD32). *J Exp Med* 172, 19-25 (1990).
306. Nimmerjahn, F. & Ravetch, J.V. Fc γ receptors as regulators of immune responses. *Nat Rev Immunol* 8, 34-47 (2008).
307. Ravetch, J.V. & Kinet, J.P. Fc receptors. *Annu Rev Immunol* 9, 457-492 (1991).
308. Miller, K.L., Duchemin, A.M. & Anderson, C.L. A novel role for the Fc receptor gamma subunit: enhancement of Fc γ R ligand affinity. *J Exp Med* 183, 2227-2233 (1996).
309. Nimmerjahn, F. & Ravetch, J.V. Fc-receptors as regulators of immunity. *Adv Immunol* 96, 179-204 (2007).
310. Reth, M.G., Ammirati, P., Jackson, S. & Alt, F.W. Regulated progression of a cultured pre-B-cell line to the B-cell stage. *Nature* 317, 353-355 (1985).
311. Cambier, J.C. New nomenclature for the Reth motif (or ARH1/TAM/ARAM/YXXL). *Immunol Today* 16, 110 (1995).
312. Sinclair, N.R. & Chan, P.L. Relationship between antibody-mediated immunosuppression and tolerance induction. *Nature* 234, 104-105 (1971).
313. Muta, T., *et al.* A 13-amino-acid motif in the cytoplasmic domain of Fc γ RIIb modulates B-cell receptor signalling. *Nature* 368, 70-73 (1994).
314. Daron, M., *et al.* The same tyrosine-based inhibition motif, in the intracytoplasmic domain of Fc γ RIIb, regulates negatively BCR-, TCR-, and FcR-dependent cell activation. *Immunity* 3, 635-646 (1995).
315. Crowley, M.T., *et al.* A critical role for Syk in signal transduction and phagocytosis mediated by Fc γ receptors on macrophages. *J Exp Med* 186, 1027-1039 (1997).
316. Odin, J.A., Edberg, J.C., Painter, C.J., Kimberly, R.P. & Unkeless, J.C. Regulation of phagocytosis and [Ca²⁺]_i flux by distinct regions of an Fc receptor. *Science* 254, 1785-1788 (1991).
317. Kiener, P.A., *et al.* Cross-linking of Fc γ receptor I (Fc γ RI) and receptor II (Fc γ RII) on monocytic cells activates a signal transduction pathway common to both Fc receptors that involves the stimulation of p72 Syk protein tyrosine kinase. *J Biol Chem* 268, 24442-24448 (1993).
318. Rankin, B.M., Yocum, S.A., Mittler, R.S. & Kiener, P.A. Stimulation of tyrosine phosphorylation and calcium mobilization by Fc γ receptor cross-linking. Regulation by the phosphotyrosine phosphatase CD45. *J Immunol* 150, 605-616 (1993).
319. Liao, F., Shin, H.S. & Rhee, S.G. Tyrosine phosphorylation of phospholipase C- γ 1 induced by cross-linking of the high-affinity or low-affinity Fc receptor for IgG in U937 cells. *Proc Natl Acad Sci U S A* 89, 3659-3663 (1992).

320. Cambier, J.C. Antigen and Fc receptor signaling. The awesome power of the immunoreceptor tyrosine-based activation motif (ITAM). *J Immunol* 155, 3281-3285 (1995).
321. Daron, M., Malbec, O., Latour, S., Arock, M. & Fridman, W.H. Regulation of high-affinity IgE receptor-mediated mast cell activation by murine low-affinity IgG receptors. *J Clin Invest* 95, 577-585 (1995).
322. Malbec, O., et al. Fc epsilon receptor I-associated lyn-dependent phosphorylation of Fc gamma receptor IIB during negative regulation of mast cell activation. *J Immunol* 160, 1647-1658 (1998).
323. Ono, M., Bolland, S., Tempst, P. & Ravetch, J.V. Role of the inositol phosphatase SHIP in negative regulation of the immune system by the receptor Fc(gamma)RIIB. *Nature* 383, 263-266 (1996).
324. Miettinen, H.M., Rose, J.K. & Mellman, I. Fc receptor isoforms exhibit distinct abilities for coated pit localization as a result of cytoplasmic domain heterogeneity. *Cell* 58, 317-327 (1989).
325. Budde, P., Bewarder, N., Weinrich, V., Schulzeck, O. & Frey, J. Tyrosine-containing sequence motifs of the human immunoglobulin G receptors FcRIIb1 and FcRIIb2 essential for endocytosis and regulation of calcium flux in B cells. *J Biol Chem* 269, 30636-30644 (1994).
326. Indik, Z.K., Park, J.G., Hunter, S. & Schreiber, A.D. Structure/function relationships of Fc gamma receptors in phagocytosis. *Semin Immunol* 7, 45-54 (1995).
327. Amigorena, S., et al. Cytoplasmic domain heterogeneity and functions of IgG Fc receptors in B lymphocytes. *Science* 256, 1808-1812 (1992).
328. Pearse, R.N., et al. SHIP recruitment attenuates Fc gamma RIIB-induced B cell apoptosis. *Immunity* 10, 753-760 (1999).
329. Amigorena, S., et al. Type II and III receptors for immunoglobulin G (IgG) control the presentation of different T cell epitopes from single IgG-complexed antigens. *J Exp Med* 187, 505-515 (1998).
330. Bonnerot, C., et al. syk protein tyrosine kinase regulates Fc receptor gamma-chain-mediated transport to lysosomes. *EMBO J* 17, 4606-4616 (1998).
331. Bergtold, A., Desai, D.D., Gavhane, A. & Clynes, R. Cell surface recycling of internalized antigen permits dendritic cell priming of B cells. *Immunity* 23, 503-514 (2005).
332. Matzinger, P. Tolerance, danger, and the extended family. *Annu Rev Immunol* 12, 991-1045 (1994).
333. Sedlik, C., et al. A critical role for Syk protein tyrosine kinase in Fc receptor-mediated antigen presentation and induction of dendritic cell maturation. *J Immunol* 170, 846-852 (2003).
334. Boruchov, A.M., et al. Activating and inhibitory IgG Fc receptors on human DCs mediate opposing functions. *J Clin Invest* 115, 2914-2923 (2005).
335. Yuasa, T., et al. Deletion of fcgamma receptor IIB renders H-2(b) mice susceptible to collagen-induced arthritis. *J Exp Med* 189, 187-194 (1999).

336. Bolland, S. & Ravetch, J.V. Spontaneous autoimmune disease in Fc(gamma)RIIB-deficient mice results from strain-specific epistasis. *Immunity* 13, 277-285 (2000).
337. Su, K., *et al.* Expression profile of FcgammaRIIb on leukocytes and its dysregulation in systemic lupus erythematosus. *J Immunol* 178, 3272-3280 (2007).
338. Willcocks, L.C., *et al.* A defuncting polymorphism in FCGR2B is associated with protection against malaria but susceptibility to systemic lupus erythematosus. *Proc Natl Acad Sci U S A* 107, 7881-7885.
339. Radstake, T.R., *et al.* The functional variant of the inhibitory Fcgamma receptor IIb (CD32B) is associated with the rate of radiologic joint damage and dendritic cell function in rheumatoid arthritis. *Arthritis Rheum* 54, 3828-3837 (2006).
340. Uchida, J., *et al.* The innate mononuclear phagocyte network depletes B lymphocytes through Fc receptor-dependent mechanisms during anti-CD20 antibody immunotherapy. *J Exp Med* 199, 1659-1669 (2004).
341. Nimmerjahn, F. & Ravetch, J.V. Antibodies, Fc receptors and cancer. *Curr Opin Immunol* 19, 239-245 (2007).
342. Zusman, T., *et al.* The murine Fc-gamma (Fc gamma) receptor type II B1 is a tumorigenicity-enhancing factor in polyoma-virus-transformed 3T3 cells. *Int J Cancer* 65, 221-229 (1996).
343. Cassard, L., *et al.* Selective expression of inhibitory Fcgamma receptor by metastatic melanoma impairs tumor susceptibility to IgG-dependent cellular response. *Int J Cancer* 123, 2832-2839 (2008).
344. Camilleri-Broet, S., *et al.* FcgammaRIIB is differentially expressed during B cell maturation and in B-cell lymphomas. *Br J Haematol* 124, 55-62 (2004).
345. Camilleri-Broet, S., *et al.* FcgammaRIIB expression in diffuse large B-cell lymphomas does not alter the response to CHOP+rituximab (R-CHOP). *Leukemia* 18, 2038-2040 (2004).
346. Li, X., *et al.* A novel polymorphism in the Fcgamma receptor IIB (CD32B) transmembrane region alters receptor signaling. *Arthritis Rheum* 48, 3242-3252 (2003).
347. Kono, H., *et al.* FcgammaRIIB Ile232Thr transmembrane polymorphism associated with human systemic lupus erythematosus decreases affinity to lipid rafts and attenuates inhibitory effects on B cell receptor signaling. *Hum Mol Genet* 14, 2881-2892 (2005).
348. Weng, W.K. & Levy, R. Genetic polymorphism of the inhibitory IgG Fc receptor FcgammaRIIb is not associated with clinical outcome in patients with follicular lymphoma treated with rituximab. *Leuk Lymphoma* 50, 723-727 (2009).
349. Cartron, G., *et al.* Therapeutic activity of humanized anti-CD20 monoclonal antibody and polymorphism in IgG Fc receptor FcgammaRIIIa gene. *Blood* 99, 754-758 (2002).
350. Weng, W.K. & Levy, R. Two immunoglobulin G fragment C receptor polymorphisms independently predict response to rituximab in patients with follicular lymphoma. *J Clin Oncol* 21, 3940-3947 (2003).

351. Treon, S.P., *et al.* Polymorphisms in FcγRIIIA (CD16) receptor expression are associated with clinical response to rituximab in Waldenström's macroglobulinemia. *J Clin Oncol* 23, 474-481 (2005).
352. Farag, S.S., *et al.* Fc γRIIIa and Fc γRIIa polymorphisms do not predict response to rituximab in B-cell chronic lymphocytic leukemia. *Blood* 103, 1472-1474 (2004).
353. Ghielmini, M., *et al.* Single agent rituximab in patients with follicular or mantle cell lymphoma: clinical and biological factors that are predictive of response and event-free survival as well as the effect of rituximab on the immune system: a study of the Swiss Group for Clinical Cancer Research (SAKK). *Ann Oncol* 16, 1675-1682 (2005).
354. Gong, Q., *et al.* Importance of cellular microenvironment and circulatory dynamics in B cell immunotherapy. *J Immunol* 174, 817-826 (2005).
355. Beers, S.A., *et al.* Antigenic modulation limits the efficacy of anti-CD20 antibodies. *Blood* 115, 5191-5201 (2010).
356. Minard-Colin, V., *et al.* Lymphoma depletion during CD20 immunotherapy in mice is mediated by macrophage FcγRI, FcγRIII, and FcγRIV. *Blood* 112, 1205-1213 (2008).
357. Van Rooijen, N. & Sanders, A. Liposome mediated depletion of macrophages: mechanism of action, preparation of liposomes and applications. *J Immunol Methods* 174, 83-93 (1994).
358. Golay, J., *et al.* Rituximab-mediated antibody-dependent cellular cytotoxicity against neoplastic B cells is stimulated strongly by interleukin-2. *Haematologica* 88, 1002-1012 (2003).
359. Teeling, J.L., *et al.* Characterization of new human CD20 monoclonal antibodies with potent cytolytic activity against non-Hodgkin lymphomas. *Blood* 104, 1793-1800 (2004).
360. Bologna, L., *et al.* Mechanism of action of type II, glycoengineered, anti-CD20 monoclonal antibody GA101 in B-chronic lymphocytic leukemia whole blood assays in comparison with rituximab and alemtuzumab. *J Immunol* 186, 3762-3769 (2011).
361. Qian, B.Z. & Pollard, J.W. Macrophage diversity enhances tumor progression and metastasis. *Cell* 141, 39-51.
362. Farinha, P., *et al.* Analysis of multiple biomarkers shows that lymphoma-associated macrophage (LAM) content is an independent predictor of survival in follicular lymphoma (FL). *Blood* 106, 2169-2174 (2005).
363. Canioni, D., *et al.* High numbers of tumor-associated macrophages have an adverse prognostic value that can be circumvented by rituximab in patients with follicular lymphoma enrolled onto the GELA-GOELAMS FL-2000 trial. *J Clin Oncol* 26, 440-446 (2008).
364. Cartron, G., *et al.* Neutrophil role in in vivo anti-lymphoma activity of rituximab: FCGR3B-NA1/NA2 polymorphism does not influence response and survival after rituximab treatment. *Ann Oncol* 19, 1485-1487 (2008).
365. Cartron, G., *et al.* Granulocyte-macrophage colony-stimulating factor potentiates rituximab in patients with relapsed follicular lymphoma: results of a phase II study. *J Clin Oncol* 26, 2725-2731 (2008).

366. Shibata-Koyama, M., *et al.* Nonfucosylated rituximab potentiates human neutrophil phagocytosis through its high binding for FcγRIIIb and MHC class II expression on the phagocytotic neutrophils. *Exp Hematol* 37, 309-321 (2009).
367. Shibata-Koyama, M., *et al.* The N-linked oligosaccharide at Fc γRIIIa Asn-45: an inhibitory element for high Fc γRIIIa binding affinity to IgG glycoforms lacking core fucosylation. *Glycobiology* 19, 126-134 (2009).
368. Mackay, F., Schneider, P., Rennert, P. & Browning, J. BAFF AND APRIL: a tutorial on B cell survival. *Annu Rev Immunol* 21, 231-264 (2003).
369. Kim, S.J., *et al.* Serum BAFF predicts prognosis better than APRIL in diffuse large B-cell lymphoma patients treated with rituximab plus CHOP chemotherapy. *Eur J Haematol* 81, 177-184 (2008).
370. Lublin, D.M. & Atkinson, J.P. Decay-accelerating factor: biochemistry, molecular biology, and function. *Annu Rev Immunol* 7, 35-58 (1989).
371. Davies, A., *et al.* CD59, an LY-6-like protein expressed in human lymphoid cells, regulates the action of the complement membrane attack complex on homologous cells. *J Exp Med* 170, 637-654 (1989).
372. Walport, M.J. Complement. Second of two parts. *N Engl J Med* 344, 1140-1144 (2001).
373. Walport, M.J. Complement. First of two parts. *N Engl J Med* 344, 1058-1066 (2001).
374. Reff, M.E., *et al.* Depletion of B cells in vivo by a chimeric mouse human monoclonal antibody to CD20. *Blood* 83, 435-445 (1994).
375. Golay, J., *et al.* Biologic response of B lymphoma cells to anti-CD20 monoclonal antibody rituximab in vitro: CD55 and CD59 regulate complement-mediated cell lysis. *Blood* 95, 3900-3908 (2000).
376. Treon, S.P., *et al.* Tumor cell expression of CD59 is associated with resistance to CD20 serotherapy in patients with B-cell malignancies. *J Immunother* 24, 263-271 (2001).
377. Bannerji, R., *et al.* Apoptotic-regulatory and complement-protecting protein expression in chronic lymphocytic leukemia: relationship to in vivo rituximab resistance. *J Clin Oncol* 21, 1466-1471 (2003).
378. Kennedy, A.D., *et al.* Rituximab infusion promotes rapid complement depletion and acute CD20 loss in chronic lymphocytic leukemia. *J Immunol* 172, 3280-3288 (2004).
379. Takami, A., *et al.* Treatment of primary central nervous system lymphoma with induction of complement-dependent cytotoxicity by intraventricular administration of autologous-serum-supplemented rituximab. *Cancer Sci* 97, 80-83 (2006).
380. Klepfish, A., Schattner, A., Ghoti, H. & Rachmilewitz, E.A. Addition of fresh frozen plasma as a source of complement to rituximab in advanced chronic lymphocytic leukaemia. *Lancet Oncol* 8, 361-362 (2007).
381. Golay, J., *et al.* The role of complement in the therapeutic activity of rituximab in a murine B lymphoma model homing in lymph nodes. *Haematologica* 91, 176-183 (2006).

382. Weng, W.K. & Levy, R. Expression of complement inhibitors CD46, CD55, and CD59 on tumor cells does not predict clinical outcome after rituximab treatment in follicular non-Hodgkin lymphoma. *Blood* 98, 1352-1357 (2001).
383. Kennedy, A.D., et al. An anti-C3b(i) mAb enhances complement activation, C3b(i) deposition, and killing of CD20+ cells by rituximab. *Blood* 101, 1071-1079 (2003).
384. Wang, S.Y., Racila, E., Taylor, R.P. & Weiner, G.J. NK-cell activation and antibody-dependent cellular cytotoxicity induced by rituximab-coated target cells is inhibited by the C3b component of complement. *Blood* 111, 1456-1463 (2008).
385. Racila, E., et al. A polymorphism in the complement component C1qA correlates with prolonged response following rituximab therapy of follicular lymphoma. *Clin Cancer Res* 14, 6697-6703 (2008).
386. Ogden, C.A., et al. C1q and mannose binding lectin engagement of cell surface calreticulin and CD91 initiates macropinocytosis and uptake of apoptotic cells. *J Exp Med* 194, 781-795 (2001).
387. Nauta, A.J., et al. Opsonization with C1q and mannose-binding lectin targets apoptotic cells to dendritic cells. *J Immunol* 173, 3044-3050 (2004).
388. Castellano, G., et al. Immune modulation of human dendritic cells by complement. *Eur J Immunol* 37, 2803-2811 (2007).
389. Godau, J., et al. C5a initiates the inflammatory cascade in immune complex peritonitis. *J Immunol* 173, 3437-3445 (2004).
390. Shushakova, N., et al. C5a anaphylatoxin is a major regulator of activating versus inhibitory FcγR3s in immune complex-induced lung disease. *J Clin Invest* 110, 1823-1830 (2002).
391. Cilleßen, S., et al. Chemotherapy-Refractory Diffuse Large B-Cell Lymphomas (DLBCL) Are Effectively Killed by Ofatumumab-Induced Complement-Mediated Cytotoxicity. *Blood* 110(2007).
392. Teeling, J.L., et al. The biological activity of human CD20 monoclonal antibodies is linked to unique epitopes on CD20. *J Immunol* 177, 362-371 (2006).
393. Du, J., Yang, H., Guo, Y. & Ding, J. Structure of the Fab fragment of therapeutic antibody Ofatumumab provides insights into the recognition mechanism with CD20. *Mol Immunol* 46, 2419-2423 (2009).
394. Zent, C.S., et al. Direct and complement dependent cytotoxicity in CLL cells from patients with high-risk early-intermediate stage chronic lymphocytic leukemia (CLL) treated with alemtuzumab and rituximab. *Leuk Res* 32, 1849-1856 (2008).
395. Pawluczko-wycz, A.W., et al. Binding of submaximal C1q promotes complement-dependent cytotoxicity (CDC) of B cells opsonized with anti-CD20 mAbs ofatumumab (OFA) or rituximab (RTX): considerably higher levels of CDC are induced by OFA than by RTX. *J Immunol* 183, 749-758 (2009).

396. Cragg, M.S., Walshe, C.A., Ivanov, A.O. & Glennie, M.J. The biology of CD20 and its potential as a target for mAb therapy. *Curr Dir Autoimmun* 8, 140-174 (2005).
397. Kroemer, G., *et al.* Classification of cell death: recommendations of the Nomenclature Committee on Cell Death 2009. *Cell Death Differ* 16, 3-11 (2009).
398. Alas, S. & Bonavida, B. Rituximab inactivates signal transducer and activation of transcription 3 (STAT3) activity in B-non-Hodgkin's lymphoma through inhibition of the interleukin 10 autocrine/paracrine loop and results in down-regulation of Bcl-2 and sensitization to cytotoxic drugs. *Cancer Res* 61, 5137-5144 (2001).
399. Jazirehi, A.R., Gan, X.H., De Vos, S., Emmanouilides, C. & Bonavida, B. Rituximab (anti-CD20) selectively modifies Bcl-xL and apoptosis protease activating factor-1 (Apaf-1) expression and sensitizes human non-Hodgkin's lymphoma B cell lines to paclitaxel-induced apoptosis. *Mol Cancer Ther* 2, 1183-1193 (2003).
400. Bezombes, C., *et al.* Rituximab antiproliferative effect in B-lymphoma cells is associated with acid-sphingomyelinase activation in raft microdomains. *Blood* 104, 1166-1173 (2004).
401. Janas, E., Priest, R., Wilde, J.I., White, J.H. & Malhotra, R. Rituxan (anti-CD20 antibody)-induced translocation of CD20 into lipid rafts is crucial for calcium influx and apoptosis. *Clin Exp Immunol* 139, 439-446 (2005).
402. Suzuki, E., Umezawa, K. & Bonavida, B. Rituximab inhibits the constitutively activated PI3K-Akt pathway in B-NHL cell lines: involvement in chemosensitization to drug-induced apoptosis. *Oncogene* 26, 6184-6193 (2007).
403. Leseux, L., *et al.* PKC zeta mTOR pathway: a new target for rituximab therapy in follicular lymphoma. *Blood* 111, 285-291 (2008).
404. Stolz, C., *et al.* Targeting Bcl-2 family proteins modulates the sensitivity of B-cell lymphoma to rituximab-induced apoptosis. *Blood* 112, 3312-3321 (2008).
405. Tedder, T.F., Forsgren, A., Boyd, A.W., Nadler, L.M. & Schlossman, S.F. Antibodies reactive with the B1 molecule inhibit cell cycle progression but not activation of human B lymphocytes. *Eur J Immunol* 16, 881-887 (1986).
406. Shan, D., Ledbetter, J.A. & Press, O.W. Apoptosis of malignant human B cells by ligation of CD20 with monoclonal antibodies. *Blood* 91, 1644-1652 (1998).
407. Hofmeister, J.K., Cooney, D. & Coggeshall, K.M. Clustered CD20 induced apoptosis: src-family kinase, the proximal regulator of tyrosine phosphorylation, calcium influx, and caspase 3-dependent apoptosis. *Blood Cells Mol Dis* 26, 133-143 (2000).
408. Pedersen, I.M., Buhl, A.M., Klausen, P., Geisler, C.H. & Jurlander, J. The chimeric anti-CD20 antibody rituximab induces apoptosis in B-cell chronic lymphocytic leukemia cells through a p38 mitogen activated protein-kinase-dependent mechanism. *Blood* 99, 1314-1319 (2002).

409. Ivanov, A., Krysov, S., Cragg, M.S. & Illidge, T. Radiation therapy with tositumomab (B1) anti-CD20 monoclonal antibody initiates extracellular signal-regulated kinase/mitogen-activated protein kinase-dependent cell death that overcomes resistance to apoptosis. *Clin Cancer Res* 14, 4925-4934 (2008).
410. Ivanov A, *et al.* CD20 (Tositumomab) and HLA DR monoclonal antibodies induce homotypic adhesion and lysosomal cell death. *Journal of Clinical Investigation* (2009).
411. Horning, S.J., *et al.* Efficacy and safety of tositumomab and iodine-131 tositumomab (Bexxar) in B-cell lymphoma, progressive after rituximab. *J Clin Oncol* 23, 712-719 (2005).
412. Byrd, J.C., *et al.* The mechanism of tumor cell clearance by rituximab in vivo in patients with B-cell chronic lymphocytic leukemia: evidence of caspase activation and apoptosis induction. *Blood* 99, 1038-1043 (2002).
413. Egle, A., Harris, A.W., Bath, M.L., O'Reilly, L. & Cory, S. VavP-Bcl2 transgenic mice develop follicular lymphoma preceded by germinal center hyperplasia. *Blood* 103, 2276-2283 (2004).
414. Selenko, N., *et al.* CD20 antibody (C2B8)-induced apoptosis of lymphoma cells promotes phagocytosis by dendritic cells and cross-priming of CD8+ cytotoxic T cells. *Leukemia* 15, 1619-1626 (2001).
415. Selenko, N., *et al.* Cross-priming of cytotoxic T cells promoted by apoptosis-inducing tumor cell reactive antibodies? *J Clin Immunol* 22, 124-130 (2002).
416. Maloney, D.G., *et al.* IDEC-C2B8 (Rituximab) anti-CD20 monoclonal antibody therapy in patients with relapsed low-grade non-Hodgkin's lymphoma. *Blood* 90, 2188-2195 (1997).
417. Davis, T.A., *et al.* Rituximab anti-CD20 monoclonal antibody therapy in non-Hodgkin's lymphoma: safety and efficacy of re-treatment. *J Clin Oncol* 18, 3135-3143 (2000).
418. Hainsworth, J.D., *et al.* Rituximab as first-line and maintenance therapy for patients with indolent non-hodgkin's lymphoma. *J Clin Oncol* 20, 4261-4267 (2002).
419. van Oers, M.H., *et al.* Rituximab maintenance treatment of relapsed/resistant follicular non-Hodgkin's lymphoma: long-term outcome of the EORTC 20981 phase III randomized intergroup study. *J Clin Oncol* 28, 2853-2858 (2010).
420. Fadok, V.A., *et al.* Exposure of phosphatidylserine on the surface of apoptotic lymphocytes triggers specific recognition and removal by macrophages. *J Immunol* 148, 2207-2216 (1992).
421. Albert, M.L., *et al.* Immature dendritic cells phagocytose apoptotic cells via alphavbeta5 and CD36, and cross-present antigens to cytotoxic T lymphocytes. *J Exp Med* 188, 1359-1368 (1998).
422. Rafiq, K., Bergtold, A. & Clynes, R. Immune complex-mediated antigen presentation induces tumor immunity. *J Clin Invest* 110, 71-79 (2002).
423. Kalergis, A.M. & Ravetch, J.V. Inducing tumor immunity through the selective engagement of activating Fcgamma receptors on dendritic cells. *J Exp Med* 195, 1653-1659 (2002).

424. Hilchey, S.P., *et al.* Rituximab immunotherapy results in the induction of a lymphoma idiotype-specific T-cell response in patients with follicular lymphoma: support for a "vaccinal effect" of rituximab. *Blood* 113, 3809-3812 (2009).
425. Taylor, C., *et al.* Augmented HER-2 specific immunity during treatment with trastuzumab and chemotherapy. *Clin Cancer Res* 13, 5133-5143 (2007).
426. Abes, R., Gelize, E., Fridman, W.H. & Teillaud, J.L. Long-lasting antitumor protection by anti-CD20 antibody through cellular immune response. *Blood* 116, 926-934 (2010).
427. Gifford, R. & Tristem, M. The evolution, distribution and diversity of endogenous retroviruses. *Virus Genes* 26, 291-315 (2003).
428. Zitvogel, L., Apetoh, L., Ghiringhelli, F. & Kroemer, G. Immunological aspects of cancer chemotherapy. *Nat Rev Immunol* 8, 59-73 (2008).
429. Haynes, N.M., van der Most, R.G., Lake, R.A. & Smyth, M.J. Immunogenic anti-cancer chemotherapy as an emerging concept. *Curr Opin Immunol* 20, 545-557 (2008).
430. Gardai, S.J., *et al.* Cell-surface calreticulin initiates clearance of viable or apoptotic cells through trans-activation of LRP on the phagocyte. *Cell* 123, 321-334 (2005).
431. Obeid, M., *et al.* Calreticulin exposure dictates the immunogenicity of cancer cell death. *Nat Med* 13, 54-61 (2007).
432. Apetoh, L., *et al.* The interaction between HMGB1 and TLR4 dictates the outcome of anticancer chemotherapy and radiotherapy. *Immunol Rev* 220, 47-59 (2007).
433. Stolz, C. & Schuler, M. Molecular mechanisms of resistance to Rituximab and pharmacologic strategies for its circumvention. *Leuk Lymphoma* 50, 873-885 (2009).
434. Beum, P.V., Kennedy, A.D., Williams, M.E., Lindorfer, M.A. & Taylor, R.P. The shaving reaction: rituximab/CD20 complexes are removed from mantle cell lymphoma and chronic lymphocytic leukemia cells by THP-1 monocytes. *J Immunol* 176, 2600-2609 (2006).
435. Li, Y., *et al.* Rituximab-CD20 complexes are shaved from Z138 mantle cell lymphoma cells in intravenous and subcutaneous SCID mouse models. *J Immunol* 179, 4263-4271 (2007).
436. Griffin, F.M., Jr., Griffin, J.A. & Silverstein, S.C. Studies on the mechanism of phagocytosis. II. The interaction of macrophages with anti-immunoglobulin IgG-coated bone marrow-derived lymphocytes. *J Exp Med* 144, 788-809 (1976).
437. Williams, M.E., *et al.* Thrice-weekly low-dose rituximab decreases CD20 loss via shaving and promotes enhanced targeting in chronic lymphocytic leukemia. *J Immunol* 177, 7435-7443 (2006).
438. O'Brien, S.M., *et al.* Rituximab dose-escalation trial in chronic lymphocytic leukemia. *J Clin Oncol* 19, 2165-2170 (2001).
439. Giles, F.J., *et al.* Circulating CD20 and CD52 in patients with non-Hodgkin's lymphoma or Hodgkin's disease. *Br J Haematol* 123, 850-857 (2003).

440. Manshouri, T., *et al.* Circulating CD20 is detectable in the plasma of patients with chronic lymphocytic leukemia and is of prognostic significance. *Blood* 101, 2507-2513 (2003).
441. Alatrash, G., *et al.* Circulating CD52 and CD20 levels at end of treatment predict for progression and survival in patients with chronic lymphocytic leukaemia treated with fludarabine, cyclophosphamide and rituximab (FCR). *Br J Haematol* 148, 386-393.
442. Ghosh, A.K., *et al.* Circulating microvesicles in B-cell chronic lymphocytic leukemia can stimulate marrow stromal cells: implications for disease progression. *Blood* 115, 1755-1764 (2010).
443. Ratajczak, J., Wysoczynski, M., Hayek, F., Janowska-Wieczorek, A. & Ratajczak, M.Z. Membrane-derived microvesicles: important and underappreciated mediators of cell-to-cell communication. *Leukemia* 20, 1487-1495 (2006).
444. Pulczynski, S., Boesen, A.M. & Jensen, O.M. Modulation and intracellular transport of CD20 and CD21 antigens induced by B1 and B2 monoclonal antibodies in RAJI and JOK-1 cells--an immunofluorescence and immunoelectron microscopy study. *Leuk Res* 18, 541-552 (1994).
445. Michel, R.B. & Mattes, M.J. Intracellular accumulation of the anti-CD20 antibody 1F5 in B-lymphoma cells. *Clin Cancer Res* 8, 2701-2713 (2002).
446. Jilani, I., *et al.* Transient down-modulation of CD20 by rituximab in patients with chronic lymphocytic leukemia. *Blood* 102, 3514-3520 (2003).
447. Takei, K., Yamazaki, T., Sawada, U., Ishizuka, H. & Aizawa, S. Analysis of changes in CD20, CD55, and CD59 expression on established rituximab-resistant B-lymphoma cell lines. *Leuk Res* 30, 625-631 (2006).
448. Kinoshita, T., Nagai, H., Murate, T. & Saito, H. CD20-negative relapse in B-cell lymphoma after treatment with Rituximab. *J Clin Oncol* 16, 3916 (1998).
449. Davis, T.A., Czerwinski, D.K. & Levy, R. Therapy of B-cell lymphoma with anti-CD20 antibodies can result in the loss of CD20 antigen expression. *Clin Cancer Res* 5, 611-615 (1999).
450. Schmitz, K., Brugger, W., Weiss, B., Kaiserling, E. & Kanz, L. Clonal selection of CD20-negative non-Hodgkin's lymphoma cells after treatment with anti-CD20 antibody rituximab. *Br J Haematol* 106, 571-572 (1999).
451. Massengale, W.T., McBurney, E. & Gurtler, J. CD20-negative relapse of cutaneous B-cell lymphoma after anti-CD20 monoclonal antibody therapy. *J Am Acad Dermatol* 46, 441-443 (2002).
452. Press, O.W., Farr, A.G., Borroz, K.I., Anderson, S.K. & Martin, P.J. Endocytosis and degradation of monoclonal antibodies targeting human B-cell malignancies. *Cancer Res* 49, 4906-4912 (1989).
453. Glennie, M.J., French, R.R., Cragg, M.S. & Taylor, R.P. Mechanisms of killing by anti-CD20 monoclonal antibodies. *Mol Immunol* 44, 3823-3837 (2007).

454. Mockridge, C.I., *et al.* Reversible anergy of sIgM-mediated signaling in the two subsets of CLL defined by VH-gene mutational status. *Blood* 109, 4424-4431 (2007).
455. Potter, K.N., *et al.* Structural and functional features of the B-cell receptor in IgG-positive chronic lymphocytic leukemia. *Clin Cancer Res* 12, 1672-1679 (2006).
456. Best, O.G., *et al.* A novel functional assay using etoposide plus nutlin-3a detects and distinguishes between ATM and TP53 mutations in CLL. *Leukemia* 22, 1456-1459 (2008).
457. Premstaller, A. & Oefner, P.J. Denaturing high-performance liquid chromatography. *Methods Mol Biol* 212, 15-35 (2003).
458. Akerstrom, B., Brodin, T., Reis, K. & Bjorck, L. Protein G: a powerful tool for binding and detection of monoclonal and polyclonal antibodies. *J Immunol* 135, 2589-2592 (1985).
459. Glennie, M.J., McBride, H.M., Worth, A.T. & Stevenson, G.T. Preparation and performance of bispecific F(ab' gamma)2 antibody containing thioether-linked Fab' gamma fragments. *J Immunol* 139, 2367-2375 (1987).
460. Tutt, A.L., Reid, R., Wilkins, B.S. & Glennie, M.J. Activation and preferential expansion of rat cytotoxic (CD8) T cells in vitro and in vivo with a bispecific (anti-TCR alpha/beta x anti-CD2) F(ab')2 antibody. *J Immunol* 155, 2960-2971 (1995).
461. Zhang, G., Gurtu, V., Kain, S.R. & Yan, G. Early detection of apoptosis using a fluorescent conjugate of annexin V. *Biotechniques* 23, 525-531 (1997).
462. Austin, C.D., *et al.* Endocytosis and sorting of ErbB2 and the site of action of cancer therapeutics trastuzumab and geldanamycin. *Mol Biol Cell* 15, 5268-5282 (2004).
463. Weston, S.A. & Parish, C.R. New fluorescent dyes for lymphocyte migration studies. Analysis by flow cytometry and fluorescence microscopy. *J Immunol Methods* 133, 87-97 (1990).
464. Mossner, E., *et al.* Increasing the efficacy of CD20 antibody therapy through the engineering of a new type II anti-CD20 antibody with enhanced direct- and immune effector cell-mediated B-cell cytotoxicity. *Blood* 115, 4393-4402 (2010).
465. Almasri, N.M., Duque, R.E., Iturraspe, J., Everett, E. & Braylan, R.C. Reduced expression of CD20 antigen as a characteristic marker for chronic lymphocytic leukemia. *Am J Hematol* 40, 259-263 (1992).
466. Ginaldi, L., *et al.* Levels of expression of CD19 and CD20 in chronic B cell leukaemias. *J Clin Pathol* 51, 364-369 (1998).
467. Perz, J., Topaly, J., Fruehauf, S., Hensel, M. & Ho, A.D. Level of CD 20-expression and efficacy of rituximab treatment in patients with resistant or relapsing B-cell prolymphocytic leukemia and B-cell chronic lymphocytic leukemia. *Leuk Lymphoma* 43, 149-151 (2002).
468. Johnson, N.A., *et al.* Diffuse large B-cell lymphoma: reduced CD20 expression is associated with an inferior survival. *Blood* 113, 3773-3780 (2009).

469. Pittner, B.T., Jelinek, D.F. & Kay, N.E. CLL B cells with a bimodal CD38 expression pattern: persistence of bimodal populations despite effective therapy for B-CLL. *Leukemia* 18, 180-182 (2004).
470. Stevenson, F.K. & Caligaris-Cappio, F. Chronic lymphocytic leukemia: revelations from the B-cell receptor. *Blood* 103, 4389-4395 (2004).
471. Dighiero, G., Bodega, E., Mayzner, R. & Binet, J.L. Individual cell-by-cell quantitation of lymphocyte surface membrane Ig in normal and CLL lymphocyte and during ontogeny of mouse B lymphocytes by immunoperoxidase assay. *Blood* 55, 93-100 (1980).
472. Vugmeyster, Y., Howell, K., Bakshi, A., Flores, C. & Canova-Davis, E. Effect of anti-CD20 monoclonal antibody, Rituxan, on cynomolgus monkey and human B cells in a whole blood matrix. *Cytometry A* 52, 101-109 (2003).
473. Press, O.W., Howell-Clark, J., Anderson, S. & Bernstein, I. Retention of B-cell-specific monoclonal antibodies by human lymphoma cells. *Blood* 83, 1390-1397 (1994).
474. Vervoordeldonk, S.F., Merle, P.A., van Leeuwen, E.F., von dem Borne, A.E. & Slaper-Cortenbach, I.C. Preclinical studies with radiolabeled monoclonal antibodies for treatment of patients with B-cell malignancies. *Cancer* 73, 1006-1011 (1994).
475. Smith, C.D., Glickman, J.F. & Chang, K.J. The antiproliferative effects of staurosporine are not exclusively mediated by inhibition of protein kinase C. *Biochem Biophys Res Commun* 156, 1250-1256 (1988).
476. Gamberale, R., *et al.* Signaling capacity of FcγRII isoforms in B-CLL cells. *Leuk Res* 29, 1277-1284 (2005).
477. van Vugt, M.J., *et al.* The alternatively spliced CD64 transcript FcγRIIb2 does not specify a surface-expressed isoform. *Eur J Immunol* 29, 143-149 (1999).
478. Rabinovitch, N. & Gelfand, E.W. Expression of functional activating and inhibitory Fcγ receptors on human B cells. *Int Arch Allergy Immunol* 133, 285-294 (2004).
479. Zhang, C.Y. & Booth, J.W. Divergent intracellular sorting of FcγRIIA and FcγRIIb2. *J Biol Chem* 285, 34250-34258 (2010).
480. Ebrahim, R. & Thilo, L. Kinetic evidence that newly-synthesized endogenous lysosome-associated membrane protein-1 (LAMP-1) first transits early endosomes before it is delivered to lysosomes. *Mol Membr Biol* 28, 227-242 (2011).
481. Bernstein, S.H. & Burack, W.R. The incidence, natural history, biology, and treatment of transformed lymphomas. *Hematology Am Soc Hematol Educ Program*, 532-541 (2009).
482. Hoster, E., *et al.* A new prognostic index (MIPI) for patients with advanced-stage mantle cell lymphoma. *Blood* 111, 558-565 (2008).
483. Pettitt, A.R., Sherrington, P.D. & Cawley, J.C. Role of poly(ADP-ribosylation) in the killing of chronic lymphocytic leukemia cells by purine analogues. *Cancer Res* 60, 4187-4193 (2000).

484. Ginaldi, L., *et al.* Levels of expression of CD52 in normal and leukemic B and T cells: correlation with in vivo therapeutic responses to Campath-1H. *Leuk Res* 22, 185-191 (1998).
485. Hainsworth, J.D., *et al.* Combination therapy with fludarabine and rituximab followed by alemtuzumab in the first-line treatment of patients with chronic lymphocytic leukemia or small lymphocytic lymphoma: a phase 2 trial of the Minnie Pearl Cancer Research Network. *Cancer* 112, 1288-1295 (2008).
486. Silber, R., *et al.* Chemosensitivity of lymphocytes from patients with B-cell chronic lymphocytic leukemia to chlorambucil, fludarabine, and camptothecin analogs. *Blood* 84, 3440-3446 (1994).
487. Pettitt, A.R., Sherrington, P.D. & Cawley, J.C. The effect of p53 dysfunction on purine analogue cytotoxicity in chronic lymphocytic leukaemia. *Br J Haematol* 106, 1049-1051 (1999).
488. Gorski, A. & Korczak-Kowalska, G. Inhibition of human B lymphocyte differentiation by a stable metabolite of cyclophosphamide (ASTA Z 7557, INN mafosfamide). *Invest New Drugs* 2, 227-229 (1984).
489. Alduaij, W., *et al.* Novel type II anti-CD20 monoclonal antibody (GA101) evokes homotypic adhesion and actin-dependent, lysosome-mediated cell death in B-cell malignancies. *Blood* 117, 4519-4529.
490. Smolewski, P., *et al.* Proapoptotic activity of alemtuzumab alone and in combination with rituximab or purine nucleoside analogues in chronic lymphocytic leukemia cells. *Leuk Lymphoma* 46, 87-100 (2005).
491. Mone, A.P., *et al.* Alemtuzumab induces caspase-independent cell death in human chronic lymphocytic leukemia cells through a lipid raft-dependent mechanism. *Leukemia* 20, 272-279 (2006).
492. Shields, R.L., *et al.* Lack of fucose on human IgG1 N-linked oligosaccharide improves binding to human Fcγ3 and antibody-dependent cellular toxicity. *J Biol Chem* 277, 26733-26740 (2002).
493. Sturm, I., *et al.* Mutation of p53 and consecutive selective drug resistance in B-CLL occurs as a consequence of prior DNA-damaging chemotherapy. *Cell Death Differ* 10, 477-484 (2003).
494. Flinn, I.W., *et al.* Phase III trial of fludarabine plus cyclophosphamide compared with fludarabine for patients with previously untreated chronic lymphocytic leukemia: US Intergroup Trial E2997. *J Clin Oncol* 25, 793-798 (2007).
495. Marquart, H.V., Gronbaek, K., Christensen, B.E., Svehag, S.E. & Leslie, R.G. Complement activation by malignant B cells from patients with chronic lymphocytic leukaemia (CLL). *Clin Exp Immunol* 102, 575-581 (1995).
496. Schlesinger, M., Broman, I. & Lugassy, G. The complement system is defective in chronic lymphatic leukemia patients and in their healthy relatives. *Leukemia* 10, 1509-1513 (1996).
497. Xu, W., *et al.* Enhancing the action of rituximab by adding fresh frozen plasma for the treatment of fludarabine refractory chronic lymphocytic leukemia. *Int J Cancer* 128, 2192-2201 (2011).

498. Golay, J., *et al.* CD20 levels determine the in vitro susceptibility to rituximab and complement of B-cell chronic lymphocytic leukemia: further regulation by CD55 and CD59. *Blood* 98, 3383-3389 (2001).
499. Wierda, W.G., *et al.* Ofatumumab as single-agent CD20 immunotherapy in fludarabine-refractory chronic lymphocytic leukemia. *J Clin Oncol* 28, 1749-1755(2010).
500. Wierda, W.G., *et al.* Chemoimmunotherapy with O-FC in previously untreated patients with chronic lymphocytic leukemia. *Blood* 117, 6450-6458 (2011).
501. Fridman, W.H., *et al.* Soluble Fc gamma receptors. *J Leukoc Biol* 54, 504-512 (1993).
502. Levesque, M.C., O'Loughlin, C.W. & Weinberg, J.B. Use of serum-free media to minimize apoptosis of chronic lymphocytic leukemia cells during in vitro culture. *Leukemia* 15, 1305-1307 (2001).
503. van Meerten, T., van Rijn, R.S., Hol, S., Hagenbeek, A. & Ebeling, S.B. Complement-induced cell death by rituximab depends on CD20 expression level and acts complementary to antibody-dependent cellular cytotoxicity. *Clin Cancer Res* 12, 4027-4035 (2006).
504. Leidi, M., *et al.* M2 macrophages phagocytose rituximab-opsonized leukemic targets more efficiently than m1 cells in vitro. *J Immunol* 182, 4415-4422 (2009).
505. Aman, M.J., Tosello-Tramont, A.C. & Ravichandran, K. Fc gamma RIIB1/SHIP-mediated inhibitory signaling in B cells involves lipid rafts. *J Biol Chem* 276, 46371-46378 (2001).
506. Heyman, B. Feedback regulation by IgG antibodies. *Immunol Lett* 88, 157-161 (2003).
507. Kyogoku, C., *et al.* Fc gamma receptor gene polymorphisms in Japanese patients with systemic lupus erythematosus: contribution of FCGR2B to genetic susceptibility. *Arthritis Rheum* 46, 1242-1254 (2002).
508. Floto, R.A., *et al.* Loss of function of a lupus-associated Fc gamma RIIB polymorphism through exclusion from lipid rafts. *Nat Med* 11, 1056-1058 (2005).
509. Fabris, S., *et al.* Molecular and transcriptional characterization of 17p loss in B-cell chronic lymphocytic leukemia. *Genes Chromosomes Cancer* 47, 781-793 (2008).
510. Forconi, F., *et al.* Genome-wide DNA analysis identifies recurrent imbalances predicting outcome in chronic lymphocytic leukaemia with 17p deletion. *Br J Haematol* 143, 532-536 (2008).
511. Fiegl, M., *et al.* Routine clinical use of alemtuzumab in patients with heavily pretreated B-cell chronic lymphocytic leukemia: a nation-wide retrospective study in Austria. *Cancer* 107, 2408-2416 (2006).
512. Burger, J. Mechanisms of homing and tissue invasion in CLL. in *16th Congress of the European Hematology Association* (London, 2011).
513. Leonard, J., *et al.* A Phase 1 Study of CAL-101, an isoform-selective inhibitor of phosphatidylinositol 3-kinase P110D, in combination with anti-CD20 monoclonal antibody therapy and/or bendamustine in

- patients with previously treated B-cell malignancies. *Annals of Oncology* 22, 37 (2011).
514. Hayden-Ledbetter, M.S., *et al.* CD20-directed small modular immunopharmaceutical, TRU-015, depletes normal and malignant B cells. *Clin Cancer Res* 15, 2739-2746 (2009).
 515. Goldenberg, D.M., *et al.* Properties and structure-function relationships of veltuzumab (hA20), a humanized anti-CD20 monoclonal antibody. *Blood* 113, 1062-1070 (2009).
 516. Salles, G.A., *et al.* Results from a phase I/II study (BO20999) of RO5072759 (GA101) monotherapy in relapsed/refractory non-Hodgkin's Lymphom. *Annals of Oncology* 22, 104; Abstract 066 (2011).
 517. ClinicalTrials.gov. A Study of RO5072759 (GA101) Plus Chemotherapy in Comparison With MabThera/Rituxan (Rituximab) Plus Chemotherapy Followed by GA101 or MabThera/Rituxan Maintenance in Patients With Untreated Advanced Indolent Non-Hodgkin's Lymphoma. Vol. 2011 (2011).

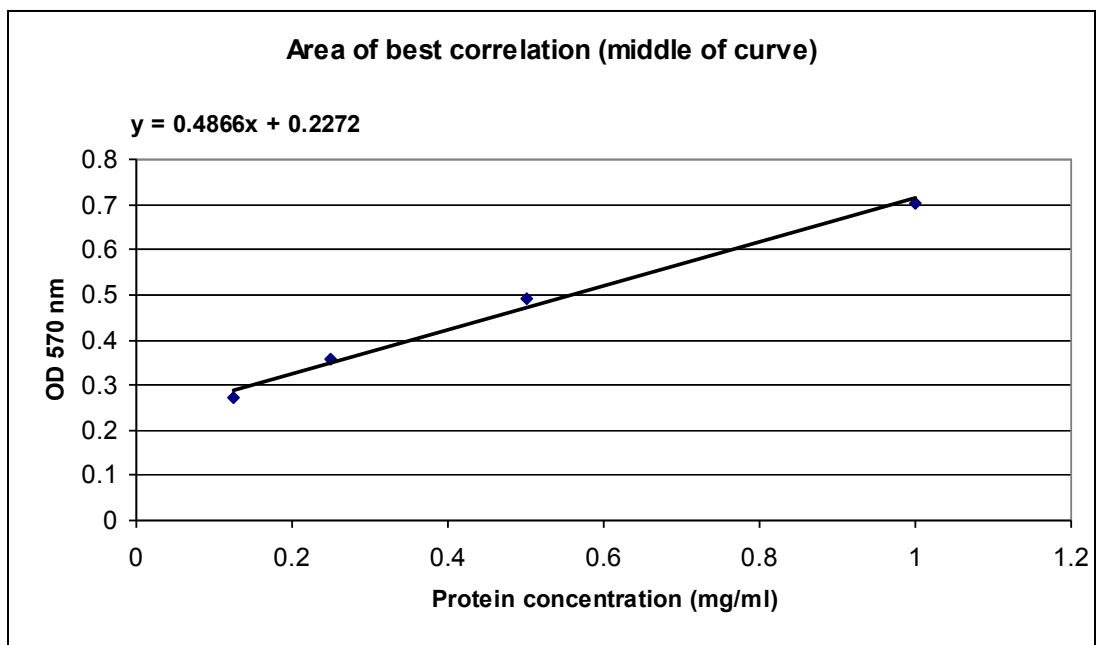
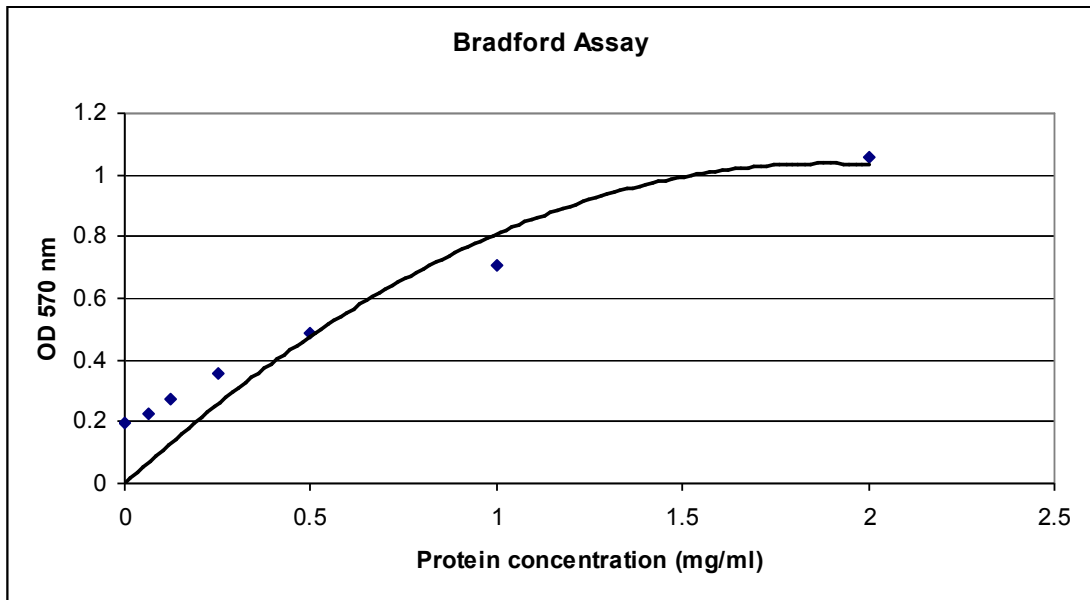
Appendix 1

WHO Classification of Tumours of Haematopoietic and Lymphoid Tissues

Mature B-cell Neoplasms

Chronic lymphocytic leukaemia/ small lymphocytic lymphoma
B-cell prolymphocytic leukaemia
Splenic marginal zone lymphoma
Hairy cell leukaemia
Lymphoplasmacytic lymphoma
Heavy chain diseases
Plasma cell myeloma
Solitary plasmacytoma of bone
Extraosseous plasmacytoma
Extranodal marginal zone lymphoma of mucosa-associated lymphoid tissue (MALT lymphoma)
Nodal marginal zone lymphoma
Follicular lymphoma
Primary cutaneous follicle centre lymphoma
Mantle cell lymphoma
Diffuse large B cell lymphoma (DLBCL), not otherwise specified
 T-cell/histiocyte rich large B cell lymphoma
 Primary DLBCL of the CNS
 Primary cutaneous DLBCL, leg type
 EBV positive DLBCL of the elderly
DLBCL associated with chronic inflammation
Lymphomatoid granulomatosis
Primary mediastinal (thymic) large B cell lymphoma
Intravascular large B cell lymphoma
ALK positive large B cell lymphoma
Plasmablastic lymphoma
Large B cell lymphoma arising in HHV8-associated multicentric Castleman disease
Primary effusion lymphoma
Burkitt lymphoma
B-cell lymphoma, unclassifiable, with features intermediate between DLBCL and Burkitt lymphoma
B-cell lymphoma, unclassifiable, with features intermediate between DLBCL and Classical Hodgkin lymphoma

Appendix 2



Appendix 3

Investigation of biomarkers of response to antibody therapy in lymphoproliferative disorders

Short Title: Biomarkers of Response in Lymphoma Study

REC Reference Number: 10/H0502/21

Chief investigator Professor Peter Johnson

Co-Investigators Dr Sean Lim

CRUK Clinical Centre
Cancer Sciences Division
Somers Cancer Research Building
MP824
Southampton General Hospital
Tremona Road
Southampton
SO16 6YD
Tel: 023 8079 6186

(Study related medical decisions should be addressed to Professor Johnson in the first instance.)

Study Sponsor Southampton University Hospitals Trust, R&D Office, Mailpoint 18,
Southampton General Hospital, Tremona Road, Southampton, SO16 6YD.
Tel: 023 8079 4245. Fax: 023 8079 8678.
Email: R&Doffice@suht.swest.nhs.uk.

Study Sites Southampton General Hospital, Tremona Road, Southampton, SO16 6YD
Tel: 023 8077 7222

Departments CRUK Clinical Centre, Cancer Sciences Division, Somers Cancer Research
Building, MP824, Southampton General Hospital, Tremona Road,
Southampton, SO16 6YD

Tenovus Research Laboratory, School of Medicine, Mailpoint 88,
Southampton General Hospital, Tremona Road, Southampton, SO16 6YD

Abbreviations

CR	complete remission
CRF	case report form
ECOG	Eastern Cooperative Oncology Group
NCIWG	National Cancer Institute Working Group
PR	partial remission
REC	research ethics committee
SUHT	Southampton University Hospitals NHS Trust
TTP	time to progression

Contents

Background	5
Objective	5
Study Design	5
Patient Identification	6
Inclusion Criteria	6
Study Procedures	6
Archival Samples	7
Data Collection	7
Sample Storage	7
Clinical Data Collection	7
Data Storage	7
Statistics and Sample Size	8
Monitoring and Audit	9
Ethics and R&D Approval	9
Research Governance	9
Indemnity	9
Funding	9
Appendix	10
References	13

Background

Although antibodies in combination with chemotherapy have improved the treatment of many lymphoid cancers, a sizeable proportion of patients still fail to respond to this combination (reviewed in ¹). Furthermore, despite their undoubted success, the mechanism of action of antibodies is still poorly understood. Identification of biomarkers serves to promote both understanding of disease pathology as well as the mechanism of action of antibodies. Our main interest and expertise lie in the latter.

The anti-CD20 monoclonal antibody, rituximab is the most successful antibody used in the field of lymphoma. It is now incorporated into standard frontline therapy in combination with chemotherapy in the treatment of diffuse large B-cell lymphoma (DLBCL) and follicular lymphoma (FL). However, it is still uncertain as to how rituximab actually works and whether identical mechanisms are critical in different diseases¹. However, of the main potential mechanisms, those involving engagement of immune effector cells have the strongest support. In addition, despite its synergy with chemotherapy, approximately 30% of patients are either refractory, or eventually become unresponsive to rituximab, and understanding of how resistance occurs, is even less well known.²

Identification of biomarkers which correlate with response to rituximab-containing regimens will assist in the understanding of how rituximab and newer, next-generation monoclonal antibodies currently entering the clinic function. For example, our in-vitro investigations (manuscript in preparation) using primary tumour material derived from lymphoma patients, indicate that Fc gamma receptor (Fc γ R) expression can be correlated to down-modulation of CD20 expression from the surface of the tumour cells. When rituximab binds CD20, the resulting complex becomes modulated from the surface of tumour cells and is trafficked to the lysosomes for degradation. As such, rituximab is unable to recruit effector mechanisms that result in tumour clearance, hence resulting in tumour resistance.

Objective

To identify biomarkers of response to antibody therapy in patients with lymphoproliferative disorders.

Study Design

Firstly patients will be identified by a member of the patient's clinical team (i.e. lymphoma clinical team) from established clinical, pharmacy and histopathology databases.

Samples will be obtained from the Southampton General Hospital Histopathology Department by a histology biomedical scientist (BMS). The BMS will be given a list with patients' hospital identification numbers and a linked-anonymisation code. Adhesive labels containing the anonymisation code will

be given to the BMS who will remove the original label where possible and replace it with the coded labels, prior to immunohistochemistry staining and analysis by a histopathologist. The original list containing the patient details and anonymisation code will be held by the original clinical team member.

Clinical data will be collected by a member of the lymphoma clinical team from electronic databases and recorded in a linked anonymised manner. If information is inadequate, then information will be obtained from medical notes.

Patient Identification

Patients treated with a monoclonal antibody containing regimen (eg rituximab, ofatumumab) are identified from pharmacy and electronic clinical trials databases by a member of the lymphoma clinical team.

Inclusion Criteria

All participants must meet the following criteria

1. Diagnosed with a B-cell lymphoproliferative disorder
2. Received any treatment containing a monoclonal antibody (eg rituximab and ofatumumab) for new, relapsed or progressive disease
3. Relevant disease site must have been biopsied prior to receiving the treatment in (2)
4. Surplus diagnostic material must be available from paraffin- or plastic-embedded tissue samples.
5. Age 16 years or older

Study Procedures

No specific consent will be obtained for this study. Prior consent has been given by all patients prior to collection of diagnostic material, which states that excess diagnostic material can be used for research purposes. Identification of patients and subsequent collection of clinical data are performed by members of the lymphoma clinical team who are involved directly in the care of these patients, to preserve their confidentiality. Every attempt will also be made to anonymise archival material and clinical data.

In the identification of study subjects, the following data is collected in a linked anonymised manner by members of the lymphoma clinical team:

- Hospital number

- Treatment regimen
- Date treatment commenced

Archival Samples

Sample Processing and Analysis

The list containing patients' details and linked-anonymisation code will be given to histopathology BMS with authorisation to access samples. The histopathology BMS will locate archival material and link anonymise samples with coded adhesive labels provided. Samples will then be processed by immunohistochemistry by qualified histopathology laboratory staff as per validated protocols, for relevant biomarkers. The original list will be returned to a member of the lymphoma clinical team who will act as custodian of the list.

Anonymised samples will be interpreted by an independent histopathologist who is blinded to the clinical data. Data will be recorded in a linked anonymous manner. All identifying information on the data sheet will be removed. Data recorded will include:

- Tumour type
- Tumour grade where relevant
- Biopsy site
- Expression of individual biomarkers

Sample Storage

Tissue samples obtained within this study will be stored within a secure facility within the Southampton CRUK Clinical Centre. Samples will be held as linked anonymised samples and labelled by a study specific number. The Chief Investigator and Co-Investigators will have access to the samples for analyses relating to this study.

Clinical Data Collection

Clinical data for study subjects will be collected by members of the lymphoma clinical team who are involved in the care of these patients, and are also blinded to the laboratory results. Most data will be

obtainable through Southampton University Hospital Trust electronic databases by authorised clinicians. Clinical data will be recorded onto specific Case report forms (CRFs) in a linked anonymised manner to allow eventual correlation to histopathology data, but no patient identifiable data will be recorded. CRF data will include:

- Age
- Sex
- Baseline ECOG Performance Status score where available
- Disease subtype
- IPI and previous line of treatment
- Treatment details:
 - Regimen
 - Commencement and completion date
 - Number of cycles
- Response:
 - Remission status (CR or PR as defined by NCIWG for individual disease subtypes)
 - Remission duration (TTP)

CRFs will be stored within a secure facility within the Southampton CRUK Clinical Centre. The Chief Investigator will retain overall responsibility for the recording and quality of the data.

Data Storage

All essential documents including source documents will be retained for a minimum period of 15 years following the end of the study. Analytical data from this study will be stored electronically on password protected data files on workstations within the Southampton CRUK Clinical Centre by the investigators. The Chief Investigator and Co-Investigators will have access to the data for analyses.

Patient confidentiality will be maintained by removing patient identifiable labels other than an assigned study specific number to create linked anonymised samples. No personally identifying information will be released in any report or publication relating to this work.

Data will be collected and retained in accordance with the Data Protection Act 1998.

Statistics and Sample Size

Analysis endpoints will be exploratory in nature. We are planning a study of a continuous response variable from independent control and experimental subjects with 5 controls per experimental subject.

In *in vitro* studies, "response" within each subject group was normally distributed with standard deviation of 18. If the true difference in the experimental and control means is 20, we will need to study 8 experimental subjects and 40 control subjects to be able to reject the null hypothesis that the population means of the experimental and control groups are equal with probability (power) 0.8. The Type 1 error probability associated with the test of this null hypothesis is 0.05.

Experimental subjects are expressors of biomarkers of response, and *in vitro* studies suggest a population frequency of 28%, therefore analysis of approximately 30 subjects will give 8 required experimental subjects, making total minimum samples necessary 80. However greater numbers will be analysed depending on ongoing results, such as discovery of new biomarkers and availability. We anticipate a total estimated recruitment of 200 subjects over 5 years.

Monitoring and Audit

The study will be monitored and audited in accordance with SUHT procedures. All trial related documents will be made available on request for monitoring and audit by SUHT, the relevant REC and other licensing bodies.

Ethics and R&D Approval

The study will be performed subject to Research Ethics Committee (REC) approval, including any provision for Site Specific Assessment (SSA), and local Research and Development (R&D) approval.

Research Governance

This study will be conducted in accordance with The Medicine for Human Use (Clinical Trial) Amendment Regulations 2006 and subsequent amendments; the International Conference for Harmonisation of Good Clinical Practice (ICH GCP) guidelines; and the Research Governance Framework for Health and Social Care.

Indemnity

This is an NHS-sponsored research study. For NHS sponsored research HSG(96)48 reference no. 2 refers. If there is negligent harm during the clinical trial when the NHS body owes a duty of care to the person harmed, NHS Indemnity covers NHS staff, medical academic staff with honorary contracts, and those conducting the trial. NHS Indemnity does not offer no-fault compensation and is unable to

agree in advance to pay compensation for non-negligent harm. Ex-gratia payments may be considered in the case of a claim.

Funding

This study is funded through research grants held by Dr Lim.

Appendix:

Table 1: Response Criteria for Lymphoma³

Response	Definition	Nodal Masses	Spleen,Liver	Bone Marrow
CR	Disappearance of all evidence of disease	(a) FDG-avid or PET positive prior to therapy; mass of any size permitted if PET negative (b) Variably FDG-avid or PET negative; regression to normal size on CT	Not palpable, nodules disappeared	Infiltrate cleared on repeat biopsy; if indeterminate by morphology, immunohistochemistry should be negative
PR	Regression of measurable disease and no new sites	≥ 50% decrease in SPD of up to 6 largest dominant masses; no increase in size of other nodes (a) FDG-avid or PET positive prior to therapy; one or more PET positive at previously involved site (b) Variably FDG-avid or PET negative; regression on CT	≥ 50% decrease in SPD of nodules (for single nodule in greatest transverse diameter); no increase in size of liver or spleen	Irrelevant if positive prior to therapy; cell type should be specified
SD	Failure to attain CR/PR or PD	(a) FDG-avid or PET positive prior to therapy; PET positive at prior sites of disease and no new sites on CT or PET (b) Variably FDG-avid or PET negative; no change in size of previous lesions on CT		
Relapsed disease or PD	Any new lesion or increase by ≥ 50% of previously involved sites from nadir	Appearance of a new lesion(s) >1.5 cm in any axis, ≥50% increase in SPD of more than one node, or ≥50% increase in longest diameter of a previously identified node >1 cm in short axis Lesions PET positive if FDG-avid lymphoma or PET positive prior to therapy	>50% increase from nadir in the SPD of any previous lesions	New or recurrent involvement

Abbreviations: CR, complete remission; FDG, [18F]fluorodeoxyglucose; PET, positron emission tomography; CT, computed tomography; PR, partial remission; SPD, sum of the product of the diameters; SD, stable disease; PD, progressive disease.

Table 2: IWG Response definition after treatment for CLL patients⁴

Parameter	CR	PR	PD	SD
Lymphadenopathy*	None above 1.5 cm	Decrease \geq 50%	Increase \geq 50%	Change of -49% to +49%
Liver and/or spleen size	Normal size	Decrease \geq 50%	Increase \geq 50%	Change of -49% to +49%
Constitutional symptoms	None	Any	Any	Any
Polymorphonuclear leukocytes	> 1500/ul	> 1500/ul or > 50% improvement over baseline	Any	Any
Circulating clonal B-lymphocytes	Nil	Decrease \geq 50% from baseline	Increase \geq 50% over baseline	Change of -49% to +49%
Platelet count	> 100,000/ul	> 100,000/ul or increase \geq 50% over baseline	Decrease of 50% from baseline secondary to CLL	Change of -49% to +49%
Haemoglobin	> 11.0 g/dl	> 11 g/dl or increase \geq 50% over baseline	Decrease of > 2g/dl from baseline secondary to CLL	Increase < 11.0 g/dl or < 50% over baseline, or decrease <2g/dl
Marrow	Normocellular, < 30% lymphocytes, no B-lymphoid nodules. Hypocellular marrow defines CRi	\geq 30% lymphocytes, or B-lymphoid nodules, or not done	Increase of lymphocytes to more than 30% from normal	No change in marrow infiltrate

* sum of the products of multiple lymph nodes (as evaluated by CT scans in clinical trials, or by physical exam or ultrasound in general practice)

Immunohistochemistry

The antibodies will be titrated using paraffin embedded cell lines known to express various Fc receptors. The staining will be performed using heat mediated and enzyme antigen retrieval techniques. Once optimal staining has been achieved the tumour sections will be stained using the same protocol.

Tissue sections will be cut from the tumours to be investigated and will be stained for Fc receptors. Automated immunohistochemistry will be performed using the Bond-maX (Leica Microsystems, Milton Keynes) automated immunostaining machine. The appropriate epitope retrieval method will be used. The mouse monoclonal antibody will be incubated with the sections for 20 minutes at room temperature at the optimal concentration. A biotin-free, polymeric horseradish peroxidase-linker antibody conjugate system (Bond™ Polymer Refine Detection System, Leica Microsystems, Milton Keynes) and DAB-chromogen will be applied and the slides will be counterstained with haematoxylin.

Immunohistochemistry analysis

An H&E section of the tumour will be examined by light microscopy to assess the presence of tumour. Tumour expression of Fc receptors will be assessed by light microscopy. The degree of expression of Fc receptors will be assessed within the tumour cells. Tumours will be assessed as negative or positive and positive staining as strong or weak depending on intensity of staining of tumour cells and focal or diffuse.

References

1. Lim SH, Beers SA, French RR, et al. Anti-CD20 monoclonal antibodies - historical and future perspectives. *Haematologica*. 2009. [Epub ahead of print]
2. Stolz C, Schuler M. Molecular mechanisms of resistance to Rituximab and pharmacologic strategies for its circumvention. *Leuk Lymphoma*. 2009;50 (6):873-85.
3. Cheson BD, Horning SJ, Coiffier B, et al. Report of an international workshop to standardize response criteria for non-Hodgkin's lymphomas. NCI Sponsored International Working Group. *J Clin Oncol*. 1999;17(4):1244.
4. Hallek M, Cheson BD, Catovsky D, et al. Guidelines for the Diagnosis and Treatment of Chronic Lymphocytic Leukemia: A Report from the International Workshop on Chronic Lymphocytic Leukemia (IWCLL) updating the National Cancer Institute-Working Group (NCI-WG) 1996 guidelines. *Blood*. 2008 Jun 15;111(12):5446-56.

Appendix 4

Immunohistochemistry

The staining was performed using standard heat-mediated and enzyme antigen retrieval techniques as follows. 4 µm thick tissue sections were cut from paraffin-embedded tissue blocks using a Microm HM 325 microtome (GMI Inc., US) and mounted onto Superfrost® Plus coated slides (Thermo Scientific). Immunohistochemical staining was performed using the fully automated Bond-Max™ (Leica Microsystems) immunostaining machine with Bond reagents as per the manufacturer's protocol. Briefly, the sections were first deparaffinised, and then pretreated by heat-induced epitope retrieval using the Bond ER2 protocol to uncover antigenic determinants masked by paraffin-embedding. The primary Ab was then applied and incubated for 20 mins. A peroxidase blocking step was included after the primary Ab incubation to block endogenous peroxidase which is resistant to heat destruction unlike other endogenous enzymes. To visualise the primary Ab, a biotin-free, polymeric horseradish peroxidase-linked Ab conjugate detection system was used (Bond™ Polymer Refine Detection System) with 3,3' Diaminobenzidine (DAB) as a chromogen substrate. The slides were then counterstained with haematoxylin and mounted with Pertex (Histolab®, Germany) and glass coverslips (Surgipath Europe Limited, UK) applied using a Leica CV5330 machine.

For FcγRIIb staining, a specific anti-FcγRIIb mAb (clone EP888Y, Abcam) at 1:300 dilution was used as the primary Ab.

Appendix 5

Biomarkers of Lymphoma Study : Case Report Form v1		
Trial ID		
<u>Patient Details (Pre-first anti-CD20 containing therapy)</u>		
Age		
Sex		M / F
ECOG PF if documented		
Stage		
Bulky disease (LN mass > 10cm)		Y / N
LDH level		
IPI score (nb use FLIPI for FL and MIPI for MCL)		
<u>Disease Details</u>		
Disease Subtype (circle)		DLBCL de novo
		FL Grade <input type="text"/>
		Transformed FL
		MCL
		Other
Baseline histology results 1.		Date:
Histology pre-anti-CD20 therapy if different 2.		Date:
<u>Therapy Details</u>		
No of lines of therapy		1 / 2 / 3 / 4 / 5 /
Regimen details		1 <input type="text"/>
		2 <input type="text"/>
		3 <input type="text"/>
		4 <input type="text"/>
		5 <input type="text"/>
<u>Details of anti-CD20 antibody-containing therapy</u>		
1. Regimen		
Date commenced therapy		
Date of last therapy		
Number of cycles		
Response on completion of therapy (circle)		Method:
		CR
		CRu
		PR
		NR
		PD
		CT
		Clinical
		Other
Date of disease progression/relapse		
2. Regimen		
Date commenced therapy		
Date of last therapy		
Number of cycles		
Response on completion of therapy		Method:
		CR
		CRu
		PR
		NR
		PD
		CT
		Clinical
		Other
Date of disease progression/relapse		
Date of death		